INVESTIGATIONS OF MIXING IN PIPELINES WITH SIDE-, OPPOSED-, AND MULTIPLE-TEES

BY

Zahid Hafeez Khokhar

A Thesis Presented to the

DEANSHIP OF GRADUATE STUDIES

KING FAHD UNIVERSITY OF PETROLEUM & MINERALS

DHAHRAN, SAUDI ARABIA

In Partial Fulfillment of the
Requirements for the Degree of

MASTER OF SCIENCE

In

CHEMICAL ENGINEERING

November 2002

King Fahd University of Petroleum & Minerals
DHAHRAN 31261, SAUDI ARABIA

DEANSHIP OF GRADUATE STUDIES

This thesis, written by Zahid Hafeez Khokhar under the direction of his thesis advisor and approved by his thesis committee, has been presented to and accepted by the Dean of Graduate Studies, in partial fulfillment of the requirements for the degree of MASTER OF SCIENCE IN CHEMICAL ENGINEERING

Thesis Committee

Dr. Habib D. Zughbi
(Thesis Advisor)

Prof. Rajendra N. Sharma
(Member)

Dr. Kevin F. Loughlin
(Member)

Prof. Mohamed B. Amin
(Department Chairman)

Prof. Osama Ahmed Jannadi
(Dean of Graduate Studies)

Date: 21/5/2003

Dedicated to

The top most learned,

The gateway to The City of knowledge,

Imam Aali muqam, Amir-ul Momeneen,

Abu ul Hasan Ali bin Abi Talib,

Al Murtaza, karam ALLAH wajhu.

Acknowledgments

In the name of ALLAH, the Most Beneficent, the Most Merciful.

And it is HE Who has let free the two seas (kind of water), one palatable and sweet, and the other salt and bitter, and HE has set a barrier and a complete partition between them. And it is HE Who has created man from water, and has appointed for him kindred by blood, and kindred by marriage. And your Lord is Ever All-Powerful to do what He will. (The Quran, Al-Furqan, 53-54). HE has let loosed the two seas (the salt water and the sweet), meeting together. Between them is a barrier which none of them can transgress. Then which of the Blessing of your Lord will you both (jinns and men) deny? (The Quran, Ar-Rahman, 19-21).

And God said, "Let there be an expanse between the waters to separate water from water" (The Bible (NIV), Genesis 1:6).

One attains peace, within whose mind all desires dissipate without creating any mental disturbance, as river waters enter the full ocean without creating any disturbance. One who desires material objects is never peaceful.

(Gita (IGS), Transcendental knowledge 2.70)

The support and the very good opportunity provided by King Fahd University of Petroleum & Minerals to enrich my knowledge in my chosen field are highly acknowledged.

With deep sense of gratefulness, I would like to express my heartfelt thanks to my advisor Dr. Habib D. Zughbi for his inspirational guidance, and help and unique supervision of the thesis work. Working with him was indeed a wonderful and learning experience, which I thoroughly enjoyed.

I am also very indebted to Dr. Rajendra N. Sharma for his grand help, continuous encouragement and numerous discussions especially those experimentally oriented.

I owe special thanks to Dr. Kevin F. Loughlin, Graduate Advisor and a member of my thesis committee for his comments and critical review of the thesis.

I would like to thank the laboratory staff and technicians especially Mr. Yunus, Mr. Romeo, Mr. Ibrahim and Mr. Mehdi for their services during the experimental setup fabrication and installation.

I would also like to thank brother Shehzada, Asad, Abdul Hameed, Zahid Qamar, Shafiq, Khalid, Zeshaan, Noman, Khurshaid and Shafayat for their continuous encouragement. I am thankful to Ifadat bhai, Rakib, Saif for their guidance. I am also thankful to all my fellows including, Sarfraz, Zaman, Rehan, Afzal, Arshad, Amjad, Tariq, Mamdouh, Giri, Nabeel, Muftah, Tayyab, Mubarak, Aminuddin, Waziri, especially CFD colleagues Iqtedar, Abdur Razaq and Shad. I am also thankful to NC-Mataam-113 members, Qazi, Sabeer, Owais, Faisal, Abid, Munir, Ahmed, Naveed, Khuramm and all NC, 903 building residents including NC-188-127, 31-flat mates Wasif, Ahmer, Saad, Asif, Arshad, Hamid, Abdy, Suhail, Ghayaas, and Rizwan. I am also thankful to brothers and friends, Rehan, Nasir, Abid, Imran, Yousuf, Yousaf, Rashid, Abid, Danish, and Moazzam, Suhail, Kamran, Alvi and Muneeb who provided a wonderful company.

I am thankful to the chairman of the Chemical Engineering Department, Dr. Mohammed B. Amin for his help and cooperation. I am also thankful to all Faculty and Staff members for their cooperation.

Finally, I offer my sincere thanks to my father, mother, and wife, sisters, brothers (Aabid and Shahid), in-laws and cousins (Hamza, Zaheer, Anwar, Qasim, Faisal, Aamir, Bilal, Jawaad and all), AbdurRehman Sudais and Shahzaib for their love and affection and for enduring the geographical distance from me during my studies.

At last, but not least, I praise ALLAH, The Cherisher and Sustainer of the worlds, WHO gave me courage and patience to carry out this work. May HE make these efforts beneficial to the writer and all human kind. HE has the power over all things and all hopes are towards HIM. May the peace and blessing of ALLAH be upon, master and seal of all prophets, Muhammad and his family, and his all companions and upon whom follow them with *Ehsan* and preach their preaching till the Doomsday.

> "Glorified be your Lord, the Lord of Honour and Power! (He is free) from what they attribute unto HIM! And peace be on the Messengers! And all the praise and thanks be to ALLAH, Lord of the '*Alamin* (mankind, jinns and all that exists)."

[zahid]

TABLE OF CONTENTS

LIST OF TABLES

LIST OF FIGURES

ABSTRACT

Name:	ZAHID HAFEEZ KHOKHAR
Title:	INVESTIGATIONS OF MIXING IN PIPELINES WITH SIDE-, OPPOSED- AND MULTIPLE-TEES
Degree:	MASTER OF SCIENCE
Major Field:	CHEMICAL ENGINEERING
Date:	November 2002

Mixing is one of the most common operations carried out in the chemical, petrochemical, oil and metallurgical industries. Mixing can be achieved either mechanically as in stirred tanks, or by fluid jet side stream agitation. Jet mixing principles can be described as a fast moving stream of fluid, the jet or side fluid, being injected into a slow moving or stationary fluid- the main fluid.

In this present work, numerical and experimental investigations of mixing in pipelines with side-, opposed- and multiple tees are carried out. Cold water flowing in a main pipe is mixed with warmer water flowing through a tee. Temperature is measured experimentally to quantify the degree of mixing. The velocity and temperature fields are solved numerically. The effects of mesh size, mesh localized refinement, the dependence of the fluid physical properties on temperature, and the turbulence models on numerical results are examined. Experimental results show good agreement with corresponding predictions of the numerical model over a relatively wide range of Reynolds number; however, close agreement is harder to obtain in the vicinity of the incoming jet through the tee. The pipe length required to achieve 95% mixing is found to be a function of U_j/U_m.

The angle at which the side jet is injected is found to determine whether or not the jet impinges on the opposite wall and also affects the pipe length required to achieve 95% mixing. For opposing jets, numerical convergence was harder to obtain due to the jet-jet interaction at high Reynolds numbers. Some modifications including the staggering of the two jets made it easier for the solution to converge. Multiple tees also reduced the mixing length. This can be used for mixing a large quantity of fluid where lower side velocities are needed. The results of this investigation assist in deciding where it is possible to use pipelines as mixers in place of holding/mixing vessels and which type of tees will be suitable.

Master of Science Degree
King Fahd University of Petroleum & Minerals
Dhahran, Saudi Arabia
November 2002

ARABIC ABSTRACT

خلاصة البحث

الاســـــم : زاهد حفيظ كهوكهر
العنــوان : بحوث في الخلط في أنابيب مزودة بأنابيب جانبية وعكسية ومتعددة التفرع
الدرجـــة : الماجستير
التخصص : هندسة كيميائية
التاريـــخ : رمضان ١٤٢٣هـ

الخلط هو إحدى أهم العمليات في الصناعات الكيميائية والبتروكيميائية والزيوت والمعادن، ويمكن أنجازة في الخزانات أو خطوط الأنابيب.

في هذا البحث تم إجراء بحوث عددية ومعملية لدراسة الخلط في أنابيب مزودة بأنابيب جانبية وعكسية ومتعددة التفرع. لقد تم خلط ماء بارد جار في أنبوب رئيسي مع ماء دافئ جار في أنبوب جانبي التفرع، وقيست الحرارة معملياً لتحديد درجة الخلط. وتم حل الضغط والسرعة والحرارة عددياً. كما تم أختبار تأثير حجم الشبكة، وتحسين موضعي للشبكة، واعتماد الخواص الفيزيائية للسائل على درجة الحرارة والنموذج الأحتطراب الدوامي على النتائج العددية.

وقد أظهرت النتائج المعملية تطابقاً جيداً مع النتائج العددية على مدى واسع من أرقام رينولدز. وكان من الصعب الحصول على مطابقة كاملة بجوار نفاث السائل عبر أنبوب التفرع إلا بعد إدخال بعض التحسينات ووجد أن طول الأنبوب اللازم لتحقيق ٩٥% من الخلط يعتمد على نسبة سرعة السائل في الانبوب الجانبي والأنبوب الرئيسي. كما لا بد من إيجاد الزاوية التي يحقن النفاث الجانبي والتي قد تؤدي إلى ارتطام النفاث على الجدار المقابل ام لا، وذلك نظراً لتأثيرها البالغ على طول الأنبوب اللازم للحصول على ٩٥% من الخلط. أما بالنسبة للنفاثات المتعاكسة، فمن الصعب الحصول على حلول عددية لتأثير نفاثي متبادل على درجات رينولدز العالية. وأجريت بعض التعديلات بما فيها تدريج خلافي لأثنين من النفاثات لتسهيل تقارب الحلول. وقد أدى استعمال أنابيب متعددة ثلاثية التفرع للتقليل من طول الانبوب اللازم لتخفيف ٩٥% من الخلط.

درجة الماجستير في العلوم
جامعة الملك فهد للبترول والمعادن
رمضان ١٤٢٣هـ

CHAPTER ONE

INTRODUCTION

1.1 Introduction

Mixing is one of the most common operations playing an important, and sometimes controlling, role in industrial processes including chemical, petrochemical, oil and metallurgical industries. Mixing is used in diverse process situations such as blending, dispersing, emulsifying, suspending and enhancing heat and mass transfer. Consequently, a very wide range of mixers and/or mixing equipment is available to suit various applications.

Mixing problems, such as the design and scale-up of a mixer and quantification of mixing, have been traditionally tackled by developing empirical design equations mainly due to the complexity of the fluid dynamics of mixing. For example, for a given unit, the degree of mixing is deduced by analyzing the residence-time distributions of a tracer. Although this approach has proven to be satisfactory for many applications, it is rather limited because it neglects the complexity of flow in most mixing applications. Moreover, the empirical equations are usually highly specific and seldom contribute to the development of theory.

In the last twenty years computational fluid dynamics (CFD) and advanced experimental techniques such as laser-Doppler velocimetry (LDV) were increasingly used to obtain better understanding of the mixing process, including detailed knowledge of the flow characteristics. Such a detailed understanding of the process is essential for equipment design and selection. These improvements become more effective if coupled with the significant advances made in the theoretical understanding of fundamental processes governing mixing. Recently Photoactivable fluorescence techniques (PIV, PLIF) were used [Pan and Meng, 2001].

Computer simulation of turbulent flow phenomena has been successfully applied to many industrial applications. Patterson [1975] described the principles of applying mathematical models to various mixing operations. More recently, the advances in CFD software and computer power raised the possibility of determining the performance of pipeline mixing with tees by simulation rather than by experiments. A survey of the literature shows that simulation using CFD of pipeline mixing with tees has been carried out by Cozewith *et al.* [1991] and Forney and Monclova [1994]. Now CFD is extensively being used in application investigations of mixing. Morchain *et al.* [2000] studied CFD modeling of a two phase jet aerator under the influence of a cross flow.

Advances towards better understanding of mixing have not been only numerical and experimental but also theoretical. Ottino [1990] proposed a kinematic theory of mixing rate. Other publications, which dealt with mixing, include Oldshue [1983], and Middleman [1977]. Yao *et al.* [1998] presented a theoretical tool for optimum design of a mixer and visualization and quantification of mixing performance based on Ottino theory and using CFD results.

In this study, the main focus is on mixing in pipelines with side-, opposed- and multiple-tees. The literature has been surveyed for numerical and experimental studies of pipeline mixing. The literature survey sheds light on the problem of mixing and shows clearly the applicability and usefulness of the methods proposed for the tee mixers.

1.2 Mixing

The term “mixing” is applied to processes used to reduce the degree of non-uniformity or system gradient property such as temperature, concentration, and viscosity. Mixing occurs when a material is moved from one region to another region. In the past it may have been of interest to achieve a required degree of homogeneity but now it is also being used to enhance heat and mass transfer, often with a system undergoing chemical reaction.

In order to produce a uniform mixture by mixing, two things need to occur. First, there must be a bulk or convective flow so as to avoid any dead/stagnant zones. Secondly, there must be an intensive or high-shear mixing zone, in which the homogeneities are broken down. Laminar and turbulent flow type occur simultaneously in the different part of the mixer with a substantial transitional zone in between them depending upon the fluid properties, primarily viscosity.

1.2.1 Quantification of Mixing

Various criteria are available to quantify mixing and the most common criterion is 95% mixing. This is defined when the value of the measured variable (conductivity or

temperature) at any point satisfies: $\left|\frac{C-\overline{C}}{\overline{C}}\right| < 0.05$, where C is the concentration of the tracer any where in the mixing vessel and $\overline{C}$ is the equilibrium concentration. This relationship implies that the initial value of C before the addition of electrolyte is zero. If the measured variable is temperature, the main flow is set initially at a certain temperature, while the flow through the side-tee is set also at a known temperature higher or lower than main flow temperature. Thus, the equilibrium temperature $\overline{T}$ can be calculated. The 95% mixing is reached when the temperature anywhere across a plane inside the pipe is within the range of $(\overline{T} \pm (\overline{T} - T_{im}) * 0.05)$ where T_{im} is the initial temperature of the fluid in the main pipe, i.e. before the inlet of the side-tee. The length required for the injected fluid to mix is then measured according to this criterion, that means the maximum temperature difference between any two points across a cross sectional area of the pipe should not exceed a certain value which is a function of the initial temperatures and the flow rates of the fluids in the main and side pipes.

1.2.2 Turbulent Mixing

Most important chemical reactions, heat transfer operations, combustion processes and mixing are promoted with turbulence. Effective use of turbulence creates small contagious masses of reactant species or eddies which reduce the necessary time for molecular mixing and reaction, increasing reactant contact on the scale of eddy size, which can significantly reduce the cost of producing many chemicals.

Turbulent flows are characterized by fluctuating velocity fields. These fluctuations mix transported quantities such as momentum, energy, and species

concentration, and cause the transported quantities to fluctuate as well. Since these fluctuations can be of small scale and high frequency, they are too computationally expensive to simulate directly in practical engineering calculations. Instead, the instantaneous (exact) governing equations can be time-averaged, ensemble-averaged, or otherwise manipulated to remove the small scales, resulting in a modified set of equations that are computationally less expensive to solve. However, the modified equations contain additional unknown variables, and turbulence models are needed to determine these variables in terms of known quantities.

1.2.3 Pipe Mixing

Mixing in pipe flow has applications in numerous industries including chemical manufacturing, waste processing and combustion related industries but the specific mechanisms governing mixing in pipe flow are not fully understood. The design of the most efficient mixing process is of interest. In waste processing, for example, a hazardous substance requires neutralization. The level of mixing efficiency directly impacts the amount of harmful pollutant emitted in this case. Mixing in a pipe approximates a one-dimensional domain because the length over which scalar fluctuations can exist is potentially much larger than the pipe diameter.

Most methods of bringing two fluid components together to mix them in a pipe involve injection at right angles to the mixing pipe axis. However, parallel and tangential injection of feeds can be used. In this study side-, opposed- and multiple-tees are considered. These different geometries are basically a side injection geometry. There are three considerations for each configuration of geometry, 1) a main fluid pipe, 2) a side

fluid pipe, which is combining with the first one and 3) a downstream pipe, where mixing takes place starting at the point of combination of first two parts or even earlier depending uon the arrangement of the flow.

1.2.4 Tee Mixing

If the Reynolds number, Re, is greater than 2000, the flow in a pipe is turbulent and mixing results from turbulent diffusion. For good mixing to obtain profitable yields or to eliminate excessive corrosion in reactor or combustion chambers it is common in many existing chemical process units to continuously mix two fluids in a pipeline with subsequent transport to other location. Although the continuous mixing of two fluid streams can be achieved using a number of mixer geometries, many procedures such as the use of baffles or complex geometries will introduce excessive pressure drop and significantly increase the cost of the mixing device.

A pipe tee provides an effective and simple method of bringing together two fluid streams for mixing. One stream may pass straight through the tee while the other enters vertically at one side such that jet contact with pipeline walls is minimized and mixing occurs within the turbulent core of the flow in the pipe. For fast reaction applications that require short residence times, a tee-mixer is an attractive alternative to stirred tanks.

A tee mixer is easier to scale up and represents a more economical, reproducible and efficient design for rapid mixing. Examples of specific applications of tee mixing are such as dilution of concentrated acids or bases, wastewater treatment, or blending petrochemical products. Mixing performance data for side tee mixers and opposed tee mixers are presented in Gray [1986].

1.2.5 Angle Injection

In chemical engineering, it is sometimes said that it is desirable to have the side-issued jet contact the opposite wall in order to enhance rapid mixing and it is assumed that at that time optimal mixing and reaction take place (Forney *et al.* 1997). In some industries like paper industry, in order to minimize the pressure pulsation and flow disturbance in the approach flow system, it is desirable to avoid having the jet impact on the wall and the jet is often issued at an angle 45^{o} to 60^{o} (Feng *et al.* 1999). Contrary to the above statement, this study will show that, for efficient and rapid mixing the side-jet should not impinge on the opposite wall.

1.3 Computational Fluid Dynamics

In most industrial operations high pressure, high temperature and processes with hazardous materials are often involved. With limited access during operations and, except for a few temperature or pressure measurements, there is often little data available on the structure of the flow within the vessel. The performance of any process unit is only measured in terms of the output of that unit or even some other unit farther downstream. To measure the details of operation of the unit is normally not practical. Consequently, the effects of any malfunctioning and its cause may only be observed at shut down.

Computational Fluid Dynamics (CFD), previously regarded as a methodology only for applications in 'high-tech' industries by highly trained specialists has undergone a significant change during the period from the mid 1980's until now. It has been adopted by a whole range of industries, including chemical, petrochemical, oil, automotive, built-

environment (architecture, industrial design, building construction management, town planning), food processing and many others enabling the process engineer to begin to understand in greater detail the internal operation of individual units by relating an analysis of the flow field and other transfer processes with observed phenomena and thereby identify the cause of a problem and evaluate solutions. Moreover, it has steadily spread from research groups into the design and development departments. In short, CFD is being used as an engineering tool to aid in the understanding and design of process operations.

Gosman [1998] reviewed the developments in industrial computational fluid dynamics over the last decade. The key area of development has been geometry handling, which has been greatly improved with techniques such as unstructured mesh methodology combined with the ability to insert or remove selected regions. With this and other development in numerical solvers and physical modeling, CFD can be applied to virtually all types of industrial equipment.

1.3.1 Computational Code

Different computational codes are available for modeling fluid flow and heat transfer in complex geometries. In this study, FLUENT 6.0.12 is used. It solves flow problems with unstructured meshes that can be generated about complex geometries with relative ease structures are also available. Supported mesh types include 2D triangular/quadrilateral, 3D tetrahedral / hexahedral/ pyramid/ wedge, and mixed (hybrid) meshes. FLUENT also allows refining or coarsening grid based on the flow solution.

This solution-adaptive grid capability is particularly useful for accurately predicting flow fields in regions with large gradients, such as jet boundaries, free shear layers and boundary layers. In comparison to solutions on structured or block-structured grids, this feature significantly reduces the time required to generate a “good” grid. Solution-adaptive refinement makes it easier to perform grid refinement studies and reduces the computational effort required to achieve a desired level of accuracy, since mesh refinement is limited to those regions where greater mesh resolution is needed.

FLUENT is written in the ‘C’ computer language. It uses a client/ server architecture, which allows it to run as separate simultaneous processes on client desktop workstations and powerful computer servers, for efficient execution, interactive control, and complete flexibility of machine or operating system type.

All functions required to compute a solution and display the results are accessible in FLUENT through an interactive, menu-driven interface. These capabilities allow FLUENT to be used for a wide variety of applications. FLUENT is suited for incompressible and compressible fluid flow simulations in complex geometries.

CHAPTER TWO

LITERATURE SURVEY

2.1 Pipeline Mixing with Tees

A pipe tee is a simple device for mixing two fluid streams. A tee is formed by two pipe sections joined traditionally at a right angle to each other. In this study, the benefits of angles other than 90^o are highlighted. One stream passes straight through the tee while the other enters perpendicularly at one side as shown in Figure 2.1. This flow arrangement is known as a side-tee. However, other flow arrangements may be used, such as having the two opposing streams entering co-axially and leaving through a pipe, which is perpendicular to the entering direction (Figure 2.2). This is known as an opposed-tee. A third configuration is a coaxial one, when the (feed) stream (the one to be mixed) enters co-axially with the main stream (Figure 2.3). A review of various flow arrangements is presented by Gray [1986].

The main interest in this study concentrates around the side-, opposed- and the multiple-tee mixers such as the one shown in Figure 2-3. For all designs of pipe tees, mixing takes place in shorter distances compared with distances required for mixing in a pipe with undisturbed turbulent flow [Gray 1986].

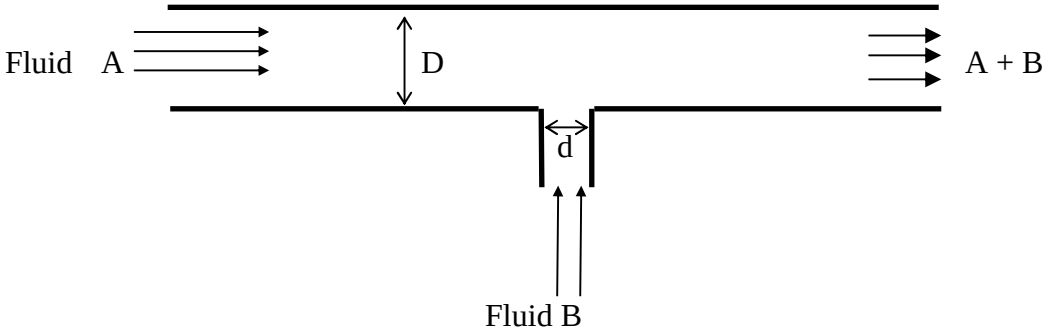

Figure 2.1: Schematic diagram of a pipeline with a side-tee

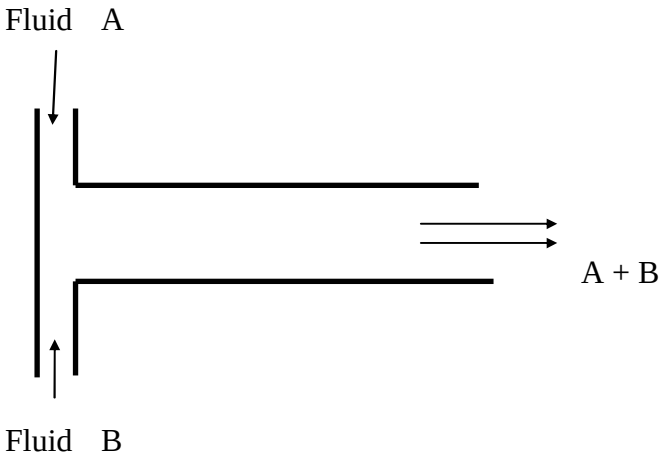

Figure 2.2: Schematic diagram of an opposed-tee mixer

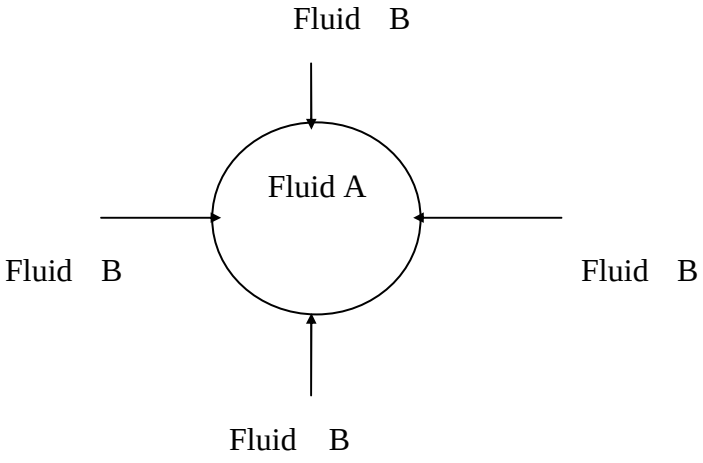

Figure 2.3: Schematic diagram of a multiple-tee mixer

Applications where pipeline mixing with tees is used include low viscosity mixing such as the dilution of concentrated acids or bases, waste water treatment and blending of some oils (injection of additives) and petrochemical products. Other applications include blending of fuel gas, mixing of feed streams for catalytic reactors and mixing of hot flue gases with ambient air. A number of local companies use many of the above mentioned processes.

A review of pipeline mixing with tees has been presented by Simpson [1974], Gray [1986] and Forney [1986].

In the absence of substantial re-circulating flows, all pipeline mixers, such as simple pipes, baffled pipes, tees and in-line motionless mixers are continuous radial mixers. In contrast to mixing in stirred tanks, no significant back mixing is present in pipeline mixing.

2.2 Experimental Measurements of Mixing in Pipeline with tees

A number of researchers have experimentally investigated mixing in pipelines with tees. The first systematic study of pipeline mixing by side injection was conducted by Chilton and Genereaux [1930], who used smoke visualization technique to determine optimum mixing conditions at a glass tee. They concluded that right-angle configurations were effective for good mixing. Chilton and Genereaux also found that when the ratio of the velocity of side-to-main flow was in the range of 2 to 3, satisfactory mixing was obtained in 2 to 3 pipeline diameters. Reed and Narayan [1979] used quantitative methods to measure the degree of mixing of air-carbon dioxide feed streams in three pipeline mixers. Reed and Narayan, like Chilton and Genereaux, found it was possible to achieve quality

mixing in a few diameters with perpendicular jet/side injection devices but that parallel flow geometries required up to 250 pipeline diameters. A general review of turbulent mixing in chemically reactive flow is provided by Brodkey [1975]. A common method of mixing fluids for the purpose of promoting chemical reactions is to use turbulent jets. Fluid jets play an important role in pipe mixing, combustion, jet mixing in tanks or reactors and the dilution of toxic by-products from power plants and other industrial operations. Reviews of the mechanics of jet behavior of many kinds are given by Rajaratnam [1976] and Fischer *et al.* [1979]. Investigations of chemically reactive flows within turbulent jets have been largely confined to studies of fully developed turbulent jets in a stagnant or coaxial flowing ambient fluid. Gouldin [1974], Lin and O'Brien [1974], McKelvey *et al.* [1975], and Singh *et al.* [1974] studied this problem. The turbulent properties of simple asymmetric jets in a stagnant environment are well established. The flow fields are self-similar and several theoretical approaches such as dimensional considerations, similarity analyses, Prandtl mixing length arguments and several entrainment hypotheses can be used to correlate empirical results [Rajaratnam, 1976]. It is common, however, to employ turbulent jets in an ambient cross flow. Deflected jet of this nature diluting more rapidly than jets without cross flows, are not axisymmetric or uniformly self similar. Deflected jets are further complicated if they are buoyant relative to the ambient cross flow. In this case, the trajectories of the jet and dilution rate are dominated by momentum in the near field, buoyancy in the far-field and intermediate transition regions. The physical extent of each of these regimes may be difficult to predict [Fischer *et al.*, 1979]. Forney *et al.* [1979, 1982, 1985], Winter [1977],

and Marauyama *et al.* [1981, 1982, and 1983] studied the jet injection of fluid into a pipeline over the first twelve pipe diameters from the injection point.

Ger and Holley [1976] and Fitzgerald and Holley [1981] compared standard deviations of measured tracer concentrations far downstream (7-120 pipe diameters) from the side tee. Although the objective of the above mentioned research, in both the near and the far field, was to establish optimum conditions for pipeline mixing, the experimental data were limited and the results were inconclusive. Typically, the standard deviation or second moment of the tracer concentration was observed to decrease with increasing jet momentum at a fixed measurement point downstream. However, it was difficult to establish a distinct minimum in the second moment of the tracer concentration distribution with increasing jet momentum, particularly within the first twenty pipe diameters from the injection point. For example, Maruyama *et al.* [1981] suggested that impaction of the jet against the opposite wall was necessary to optimize mixing over short distances downstream from the injection point. Fitzgerald and Holley [1981] failed to demonstrate a distinct minimum in the recorded second moment of the tracer concentration having limited range of operating conditions.

Bourne *et al.* [1982] developed a new method to monitor mixing along a tubular reactor. HCl solution and NaOH solutions with a color indicator were introduced co-axially, one of them as an annular jet. Continuous change of color along the axial distance was related to local degree of mixing through a calibration curve generated by a photocell transmittance.

The mixing criteria in many of the experiments assumed that optimum mixing in a pipeline was achieved if the side jet was centered along the pipeline axis after entering

the main flow. The above assumption of a geometrically centered jet appeared to be useful if the measurement point was at distances far from the injection point or $15 < x/D < 120$ [Forney *et al.*, 1979, 1982, and 1986]. Sroka and Forney [1989] provided a mathematical basis for the prediction of concentration second moments for the first 15 pipe diameters downstream from the injection point. The latter results indicate that the second moment of the tracer concentration decreases with the increasing jet momentum and distance from the injection point. The simple scaling law developed by Sroka and Forney appeared to correlate the data of Ger and Holley. [1976], and Fitzgerald *et al.* [1981] and Murayama *et al.* [1981, 1983].

Although these conclusions are correct for certain values of jet-to-pipe diameter ratio or distance to mix, clearly additional experimental data would be useful to characterize the quality of mixing downstream from a pipeline tee.

It may be desirable, however, to promote rapid mixing of two fluids with a tee mixer in a short distance downstream from the injection point at $x/D < 3$. In particular, the suitability of pipeline mixing tees for reactor applications, where the reaction times are small, depends on achieving homogeneity of the reactant concentrations in short times. Tosun [1987] studied the product yield of tee mixer with competitive consecutive reactions. The experimental data of Tosun demonstrated a distinct minimum in the undesirable product yield for certain tee mixer geometries. Cozewith and Busko [1989] measured the distance downstream from the tee inlet required for the neutralisation of a base indicator. Cozewith and Busko found a minimum distance to mix for certain tee mixer geometries.

The experimental work of Cozewith and Busko [1989] demonstrated that it is necessary to increase the momentum of the side tee such that the secondary/side tee fluid impinges on the opposite wall of the pipe near the tee inlet. Cozewith *et al.* [1991] also attempted to show for a polymerization reaction that the narrowest copolymer composition at one diameter ratio occurred at the same condition that optimized mixing in the absence of reaction.

Some of the data of Maruyama *et al.* [1983] and Gosman and Simitovic [1986] also indicated that mixing of an inert tracer could be improved by the impingement of secondary/side tee fluid against the opposite wall of the pipe near the tee inlet.

Guilkey *et al.* [1997] carried out a set of experiments specifically designed to match the idealized conditions utilized in the work of Kresta and Wood [1991]. In particular, a distinctive inlet condition was achieved in which the scalar field was introduced in cylindrical blocks with a length equal to the pipe diameter in a fully developed pipe flow. The initial flow-field therefore contained scalar and velocity length scales of equal magnitude. This idealized inlet condition was accomplished using “caged” fluorescent dyes, as described by Guilkey *et al.* [1996].

Chyu *et al.* [1999], using a mass transfer analogy, carried out an experimental study, to investigate the effect of three different perpendicular flow entries on the heat transfer performance of a pin-fin array.

Liou *et al*. [1999] experimentally investigated side-jet injection near a rectangular duct entry with various angles. They obtained reasonable agreement between laser-doppler velocimetry measurements and numerical computations with the numerical

model under-predicting. Other experimental studies of a jet issuing in an open rectangular channel have been done by Lam and Xia [2001], and Weber *et al.* [2001].

Hansen *et al.* [2000] studied the effects of inlet condition on downstream mixing in turbulent pipe flow with the use of photoactivable fluorescence techniques. The different inlet conditions included both geometry changes and changes in the manner in which the constituents were introduced into the flow. Results indicate that small changes in inlet geometry can affect the downstream mixing more than the manner in which constituents were introduced into the flow. They also did experiments including static mixer.

Shiau and Lu [2001] presented a model to investigate the interactive effects of the segregation and mixing of crystals assuming that the liquid phase moves upward through the fluidized bed crytallizer operated in a batch mode in plug flow and the solid phase is represented by a series of equal sized ideal mixed bed of crystals. Epstein and Burelbach [2001] studied vertical mixing using the theory of vertical diffusion (or dispersion) coefficient injecting fresh water (lighter fluid) upward at very low velocity through a circular porous plate into a tank containing heavier brine.

Seo *et al.* [2001] investigated the characterization of the near field dilution and plume trajectories for tee diffusers over wide range of momentum reactors. Extensive experimental work was carried out in order to collect mixing and dilution data for tee diffuser.

Pan and Meng [2001] presented an experimental investigation of turbulent mixing in a round tee mixer. They carried out a relatively detailed experimental study of turbulent scalar mixing in the near field region of a tee mixer using full-field, laser-based

non intrusive experimental techniques for this complex geometry. They focused on the near field region of the tee mixer not only because it is critical for rapid chemical reaction, but also because the turbulent flow in this region deviates greatly from the homogeneous and isotropic flow assumptions employed by common turbulence models in CFD.

A summary of most of the previous experimental work on side-tee mixers is shown in Table 2.1.

Mixing in a pipeline with an opposed-tee is another option. A side-tee with same diameter for entering and leaving streams mixes in a shorter distance than opposed-flow streams with the same diameter and flow rate, however, opposed-tees could have some advantages under certain conditions as specified by Gray [1986].

A review of literature has been presented by Gray [1986]. The techniques, measured variables (thermal conductivity, electrical conductivity, species concentration or temperature) and mixing criterion (standard deviation or equal tracer concentration) are somewhat similar to those shown in Table 2.1 for side-tees.

It is observed that less work has been done on opposed-tee compared with side-tee. It is also noted that, to the best of our knowledge, no numerical simulation of the opposed-tee has been reported in literature.

Table 2.1[a]: Previous Work on Side-Injection Tee Mixers

Jet (Side feed) fluid	Pipe (Straight through feed) fluid	Jet dia. (cm)	Pipe dia. (cm)	Velocity ratio U_{jet}/U_{pipe}	Mixing tube Re, Re_m	Measurement point in diameters	Measured Variable	Mixing criterion	Reference
Air/ $TiCl_4$ Vapor	Air	0.64 - 3.8	4.45	1 to 6	4000 to 18000	2-3	$TiCl_4$ smoke (by eye)	Visual smoke uniformity	Chilton and Genereaux, 1930
0.5 N HNO_3	0.5 N NaOH	0.635 0.635 0.635	0.635 0.635 0.635	1 1 10	10^4 2.1×10^4 4×10^4	7 6.4 6	Temperature	periphery 97% of final temp. rise	Gray 1986
3-6 °C water	50-70 °C water	0.48, 1.0	12.5		2.5×10^5	4-5	Temperature	$(T_m-T_p)/(T_m-T_s)_I$	Gray 1986
Air & $TiCl_4$	Air	0.42-1.5	5.0	1.5-3.3	4×10^3 - 2×10^4	2-3	Visual smoke conc.	Visual smoke uniformity	Winter 1975
Aq. NaCl	Water	0.32 0.158 0.079	15.24	6 12 24	6×10^4	105 105 105	Electrical Conductivity	$\sigma_o/\bar{c}$ = 0.01	Ger and Holley 1976
19% CO_2, 81% air,	Air	1.58	5.25	2.7	4.6×10^4	10	CO_2 conc. Calc. from specific gravity	Approx. equal CO_2 conc. at pipe axis and periphery	Reed and Narayan, 1979
Air at 25 C	Air at 35	0.5-1.3	5.1	3-4	1.6×10^4 - 6.3×10^4	2-10	Temp.	Temp. std deviation	Maruyama Suzuki and Mizushina 1981
Air & 0.3% CH_4	Air	0.1-1.27	11.43	2.9-28.3	1.3×10^4 - 3.2×10^4	2-10	CH_4 conc.	Max. conc. Centered on pipe axis	Forney & Lee 1982
HCl Solution	NaOH solution	0.119 -1.27	2.54-5.08	2.0-7.5	5.0×10^3 - 6.0×10^4	$L/D\alpha((d/D)/U)^2$	Indicator color, pH	Reaction Completeness, pH	Cozewith and Busko 1989
99.7% Air 0.3% CH_4	Air	0.07-0.95	10.1		4.0×10^4 - 1.2×10^5	2, 5 & 10	CH_4 conc.		Sroka and Forney 1989
Fluorescein dye	Water	2.5	2.5		7500		Dye conc./ Photoactivable fluorescence techniques, (Fluorescence intensity)	Scalar (Fluorescence dye) Variance	Hansen. [1997]
Dilute dye	Water	2.5	2.5	U = $3ms^{-1}$	7500	L/D = 390	Photoactivated fluorophores, Light/ Dye conc.	Scalar (Fluorescence dye) Variance	Hansen, Guilkey, McMurtry and Klewicki 2000
Water	Water	1.27	7.62	3.06, 5.04	4.1×10^4		PIV, PLIF (dye Conc)	Scalar PDF	Pan and Meng 2001

[a] Partly adapted from Gray [1986]

2.3 Numerical Simulation of Pipeline Mixing with Tees

The flows generated by a tee mixer have been studied by Moussa *et al.* [1977] Crabb *et al*. [1981] and Andreopoulos [1983]. Simulation studies appeared somewhat later. Cozewith *et al*. [1991] simulated tee mixing characteristics in both the absence and presence of a reaction for a tee with d/D = 0.188 over a range of side stream/main stream velocity ratios from 1.2 to 6.5. The flow and pressure fields for a tee mixer were solved using the TEACH-T flow code of Imperial College, London. TEACH uses the SIMPLE algorithm of Patankar and Spalding [1972]. A three-dimensional model was constructed and the k-ε model was used to model turbulence.

Sharma and Patankar [1982] while evaluating four models of turbulence through comparisons of their extensive turbulent conical wall-jet data observed that k-ε model successfully predicted most of their flows. Earlier literature also recommends and uses the k-ε model especially for non-circulating flows, although with the increased availability of high powered computers, more advanced turbulence models are being used including Reynolds averaged Navier-Stokes (RANS) model or Large eddy simulation (LES) or the direct numerical simulation (DNS).

Cozewith *et al.* [1991] compared their numerical results with the experimental results of Cozewith and Busko [1989] and got reasonable agreement for concentration trajectory for x/D > 0.7. Concentration trajectory is defined as the locus of maximum concentration. Other comparisons also showed qualitative agreement between experimental and numerical results.

Cozewith *et al.* [1991] also simulated the case of reactive flows. A copolymerization reaction mechanism was used to investigate the effects of mixing on the reaction rate. It was found that the copolymer composition distribution is considerably broader than for the instantaneous mixing case due to inhomogeneity in concentration.

Forney and Monclova [1994] simulated pipeline side-tee mixing quality with the commercially available fluid flow package PHOENICS. The $k-\varepsilon$ model was used to model turbulence. They compared numerical results with the experimental results of Sroka and Forney [1989] and obtained reasonable agreement.

Both of the above numerical models solved the conservation equations for mass and momentum in primitive variables for steady turbulent flow of a single-phase fluid with an inert tracer introduced at the injection point. Both models also used a mixing criteria based on the standard deviation of the component mixed and the mean value of the tracer over the pipe cross sectional area $\overline{C}$.

The use of CFD, despite the two above-mentioned papers, has still a lot to offer in analysing and understanding mixing at pipeline tees. Simulation of variations of tees mixers, opposed flow tee, multiple side stream mixers and the orifice and annulus baffles have not been reported in literature.

Simulation can help, for example, explain and understand the findings of Guilkey *et al.* [1997], and Hansen and Klewicki [1997]. Based on experimental work, they stated that changes in the geometry of the inlet at which the scalar is introduced can lead to substantial differences in the rate of scalar variance decay downstream. Hansen and Klewicki investigated the effects of two different initial conditions on mixing in turbulent

pipe flow in addition to the open pipe, partitioned pipe and T-junction conditions tested by Guilkey *et al.* These experiments demonstrated that the method used to introduce two constituents to be mixed in pipe flow can profoundly affect the downstream mixing rate.

Souvaliotis *et al.* [1995] presented an analysis of errors in numerical simulations of mixing. They identified and examined three types of errors: discretization, time integration and round off. They reported that accurate quantitative information including the location of periodic points and the length of a deformed line can be obtained from numerical simulations. A degree of mesh refinement is desirable but it is limited by the increase in computational costs.

Baldyga, *et al*. [1995] worked at jet reactor scale-up for mixing-controlled reactions. Product distributions of fast reactions were measured at small scale in turbulent viscous and aqueous solutions as well as using two larger nozzles (0.012 m and 0.031 m) and two larger semi-batch reactors (0.10 m^3 and 0.25 m^3).

Yuan *et al*. [1999] reported a series of large-eddy simulations of a round jet issuing normally into a cross flow. Simulations were performed at two jet-to-cross flow velocity ratios, 2.0 and 3.3, and two Reynolds numbers, 1050 and 2100, based on cross flow velocity and jet diameter. Mean and turbulent statistics computed from the simulations match experimental measurements reasonably well.

Feng *et al*. [1999] stated that impingement might be desirable in some cases in order to enhance rapid mixing. However in the paper industry, the tracer is often injected at an angle $\theta°(45 \leq \theta° \leq 60)$ to avoid impingement and to minimize pressure pulsation. Morchain *et al.* [2000] studied CFD modeling of a two phase jet aerator under influence of a cross flow.

Johnson and Wood [2000] studied self-sustained oscillations in opposed impinging jets in an enclosure. They examined the flow field of opposed axisymmetric jets in a confined cavity for instabilities due to various geometrical and fluid parameters using flow visualization, laser Doppler anemometry, and numerical simulations. Baldyga *et al*. [2001] did an experimental study and CFD modelling of barium sulphate precipitation in a pipe. A closure previously proposed by Baldyga *et al*. [1997] employed the presumed beta PDF of the inert type composition variables formed with the local values of Ba^{2+} and SO_4^{2-} concentrations and the turbulent mixer model. They computed flow field using the k-ε model. Azzopardi *et al*. [2002] studied plant application of a tee-junction as a partial phase separator. They used the tee as separation of fluid phases instead of mixing fluids presenting an alternative, more economical approach to tackle the task of phase separation which is normally effected in a cylindrical vessel.

Devahastin *et al.* [2002] numerically simulated laminar-confined impinging streams to study the flow and mixing characteristics. They found that both the geometry of the system and inlet jet Reynolds number have strong effects on mixing in impinging streams.

It is clear from surveying the literature that mixing in pipelines with tees has been investigated experimentally and to a lesser degree numerically. There is a need for further investigations as there are many differences in opinion regarding the need for the side jet to impinge or not to impinge on the opposite surface. It is also clear that the angle of injection has not been fully investigated. Moreover, previous numerical simulation of mixing in pipeline with tees is very limited and it has still a lot to offer towards better understanding of pipeline mixing.

CHAPTER THREE

MATHEMATICAL MODEL

3.1 Preliminary Model Equations

The flow of fluids in a pipe is governed by the equations of continuity and motion.

The equation of continuity in three-dimensional cylindrical coordinates is:

$$\frac{\partial \rho}{\partial t}+\frac{1}{r}\frac{\partial}{\partial r}\left(\rho r u_r\right)+\frac{1}{r}\frac{\partial}{\partial \theta}\left(\rho u_\theta\right)+\frac{\partial}{\partial z}\left(\rho u_z\right)=0 \tag{3.1}$$

The equations of motion are as follows:

The r - component,

$$\left[\frac{\partial u_r}{\partial t}+u_r\frac{\partial u_r}{\partial r}+\frac{u_\theta}{r}\frac{\partial u_r}{\partial \theta}-\frac{u_\theta^2}{r}-u_z\frac{\partial u_r}{\partial z}\right]=$$

$$-\frac{1}{\rho}\frac{\partial p}{\partial r}+\nu\left[\frac{\partial}{\partial r}\left(\frac{1}{r}\frac{\partial}{\partial r}\left(ru_r\right)\right)+\frac{1}{r^2}\frac{\partial^2 u_r}{\partial \theta^2}-\frac{2}{r^2}\frac{\partial u_\theta}{\partial \theta}+\frac{\partial^2 u_r}{\partial z^2}\right]+g_r \tag{3.2}$$

The $\theta-$component,

$$\left[\frac{\partial u_\theta}{\partial t}+u_r\frac{\partial u_\theta}{\partial r}+\frac{u_\theta}{r}\frac{\partial u_\theta}{\partial \theta}-\frac{u_r u_\theta}{r}-u_z\frac{\partial u_\theta}{\partial z}\right]=$$

$$-\frac{1}{r}\frac{1}{\rho}\frac{\partial p}{\partial \theta}+\nu\left[\frac{\partial}{\partial r}\left(\frac{1}{r}\frac{\partial}{\partial r}\left(ru_\theta\right)\right)+\frac{1}{r^2}\frac{\partial^2 u_\theta}{\partial \theta^2}-\frac{2}{r^2}\frac{\partial u_r}{\partial \theta}+\frac{\partial^2 u_\theta}{\partial z^2}\right]+g_\theta \tag{3.3}$$

and the $z-$component,

$$\left[\frac{\partial u_z}{\partial t}+u_r\frac{\partial u_z}{\partial r}+\frac{u_\theta}{r}\frac{\partial u_z}{\partial \theta}+u_z\frac{\partial u_z}{\partial z}\right]=$$
$$-\frac{1}{\rho}\frac{\partial p}{\partial z}+\nu\left[\frac{\partial}{\partial r}\left(r\frac{\partial u_z}{\partial r}\right)+\frac{1}{r^2}\frac{\partial^2 u_z}{\partial \theta^2}+\frac{\partial^2 u_z}{\partial z^2}\right]+g_z \qquad (3.4)$$

The temperature field of the fluid flowing in pipes can be resolved by solving the energy equation.

$$\rho\hat{C}p\left(\frac{\partial T}{\partial t}+u_r\frac{\partial T}{\partial r}+\frac{u_\theta}{r}\frac{\partial T}{\partial \theta}+u_z\frac{\partial T}{\partial z}\right)=$$
$$k\left[\frac{1}{r}\frac{\partial}{\partial r}\left(r\frac{\partial T}{\partial r}\right)+\frac{1}{r^2}\frac{\partial^2 T}{\partial \theta^2}+\frac{\partial^2 T}{\partial z^2}\right]+2\mu\left\{\left(\frac{\partial u_r}{\partial r}\right)^2+\left[\frac{1}{r}\left(\frac{\partial u_\theta}{\partial \theta}+u_r\right)\right]^2+\left(\frac{\partial u_z}{\partial r}\right)\right\}$$
$$+\mu\left\{\left(\frac{\partial u_\theta}{\partial z}+\frac{1}{r}\frac{\partial u_z}{\partial \theta}\right)^2+\left(\frac{\partial u_z}{\partial r}+\frac{\partial u_r}{\partial z}\right)^2+\left[\frac{1}{r}\frac{\partial u_r}{\partial \theta}+r\frac{\partial}{\partial r}\left(\frac{u_\theta}{r}\right)\right]^2\right\} \qquad (3.5)$$

These differential equations representing the conservation equations (mass, momentum and energy) may be written in a general form as*:*

$$\frac{\delta\left(R_i\rho_i\phi_i\right)}{\delta t}+div\left(R_i\rho_i U_i\phi_i-R_i\Gamma_{\phi_i}\,grad\,\phi_i\right)=R_i S_i \qquad (3.6)$$

[Transient Term] [Convection Term] [Diffusion Term] [Source Term]

where,

Γ_{ϕ_i} Exchange coefficient of ϕ in phase *i*

R_i Volume fraction of phase *i*

S_ϕ Source rate of ϕ_i

ϕ_i Any conserved property of phase *i*

U_i Velocity vector of phase *i*

Thus, the continuity equation for phase *i* become:

$$div\left(R_i \rho_i U_i\right) + \frac{\partial(R_i \rho_i)}{\partial t} = m_i \qquad (3.7)$$

where,

m_i Mass per unit volume entering phase i from all sources

ρ_i Density of phase *i*

D_i Diffusivity of phase *i*,

and the conservation of momentum for variable ϕ_i becomes:

$$div\left(R_i \rho_i U_i \phi_i - R_i \mu_{eff} \, grad \, \phi_i\right) = R_i S_{\phi_i} \qquad (3.8)$$

where,

μ_{eff} Effective viscosity

$S_{\phi i}$ Source of ϕ_i per unit volume

The boundary conditions used in this study are (*i*) at all walls, no-slip condition is applied (velocity = 0), (*ii*) values of velocities are specified at the entrance of the main pipe and entrance of the side-tee.

Temperatures are specified for the main fluid and the side fluid. No initial conditions are required as all the runs in this study were done under steady state conditions.

3.2 Solution Algorithm

The equations of motion and continuity have been solved using an algorithm based on the Pressure-Implicit with Splitting of Operators (PISO), which is a pressure-velocity coupling scheme, part of the SIMPLE family of algorithms. To solve the Navier-Stokes equations, a linkage between velocity and pressure is required. The difficulty in calculating the velocity field lies in the unknown pressure field. For a momentum equation source term is contributed a part by the pressure gradient. Yet there is no obvious equation for obtaining pressure. It is true that for a given pressure field, there is no particular difficulty in solving the momentum equations. However, the way to determine the pressure field seems rather obscure. The choice of algorithms is a critical issue for solving the system of transport equations involving several dependent variables.

Pressure-velocity coupling is achieved by discretization of the continuity equation to derive an equation for pressure from the discrete continuity equation. FLUENT provides the option to choose among three pressure-velocity coupling algorithms: SIMPLE, SIMPLEC (SIMPLE-Consistent), and PISO

In FLUENT, SIMPLE is the default, but many problems will benefit from the use of SIMPLEC, particularly because of the increased under-relaxation that can be applied.

For relatively uncomplicated problems (laminar flows with no additional models activated) in which convergence is limited by the pressure-velocity coupling, a converged solution can often be obtained more quickly using SIMPLEC. With SIMPLEC, the pressure-correction under-relaxation factor is generally set to 1.0, which aids in convergence speed-up. In some problems, however, increasing the pressure-correction under-relaxation to 1.0 can lead to instability. For such cases, a more conservative under-

relaxation value or the SIMPLE algorithm is needed. For complicated flows involving turbulence and/or additional physical models, SIMPLEC will improve convergence only if it is being limited by the pressure-velocity coupling. Often it will be one of the additional modeling parameters that limit convergence; in this case, SIMPLE and SIMPLEC will give similar convergence rates.

3.2.1 Pressure-Implicit with Splitting of Operators

The Pressure-Implicit with Splitting of Operators (PISO) [Fluent 5 manuals, 1998] pressure-velocity coupling scheme, part of the SIMPLE family of algorithms, is based on the higher degree of the approximate relation between the corrections for pressure and velocity. One of the limitations of the SIMPLE and SIMPLEC algorithms is that new velocities and corresponding fluxes do not satisfy the momentum balance after the pressure-correction equation is solved. As a result, the calculation must be repeated until the balance is satisfied. To improve the efficiency of this calculation, the PISO algorithm performs two additional corrections: neighbor correction and skewness correction.

The main idea of the PISO algorithm is to move the repeated calculations required by SIMPLE and SIMPLEC inside the solution stage of the pressure-correction equation. After one or more additional PISO loops, the corrected velocities satisfy the continuity and momentum equations more closely. This iterative process is called a momentum correction or “neighbor correction”. The PISO algorithm takes a little more CPU time per solver iteration, but it can dramatically decrease the number of iterations required for convergence, especially for transient problems.

For meshes with some degree of skewness, the approximate relationship between the correction of mass flux at the cell face and the difference of the pressure corrections at the adjacent cells is very rough. Since the components of the pressure-correction gradient along the cell faces are not known in advance, an iterative process similar to the PISO neighbor correction described above is desirable. After the initial solution of the pressure-correction equation, the pressure-correction gradient is recalculated and used to update the mass flux corrections. This process, which is referred to as “skewness correction”, significantly reduces convergence difficulties associated with highly distorted meshes. The PISO skewness correction allows FLUENT to obtain a solution on a highly skewed mesh in approximately the same number of iterations as required for a more orthogonal mesh.

The PISO algorithm with neighbor correction is highly recommended for all transient flow calculations. It allows you to use a larger time step, and possibly an under-relaxation factor of 1.0 for both momentum and pressure. For steady-state problems, PISO with neighbor correction does not provide any noticeable advantage over SIMPLE or SIMPLEC with optimal under-relaxation factors. In this study, the PISO algorithm is used.

3.3 Turbulence Model

No single turbulence model is universally accepted as being superior for all classes of problems. The choice of a turbulence model will depend on considerations such as the physics encompassed in the flow, the established practice for a specific class of problem, the level of accuracy required, the available computational resources, and the amount of

time available for the simulation. To make the most appropriate choice of model for a certain application, one needs to understand the capabilities and limitations of the various options.

Turbulence models are commonly labeled as zero-equation, one-equation or two-equation showing the number of differential equations, which must be solved to compute the eddy viscosity for momentum, μ_t.

3.3.1 Classification of Turbulence Model

Zero equation models

These are simple models and do not involve the transport equations for turbulence quantities. These employ eddy viscosity concept specifying either from experiments through empirical formulae or by relating it to the mean velocity distribution. e. g.,

1) Constant eddy viscosity/ diffusivity
2) Mixing length model

One-equation models

These involve solving the *k*-equation, where *k* is the kinetic energy of the turbulent motion (per unit mass).

Two equation models

The *k*-ε model has much in common with the one-equation models. Its main additional feature is a differential equation for ε.

3.4 The Standard k-ε Model

In addition to the above models, there are more sophisticated turbulence models available. There include the Reynolds average Navier-Stokes (RANS) model also known as the Reynolds Stresses model (RSM), Large eddy simulation (LES) and the direct numerical simulation (DNS). The simplest "complete models" of turbulence are two-equation models in which the solution of two separate transport equations allows the turbulent velocity and length scales to be independently determined. The standard k-ε model in FLUENT falls within this class of turbulence model and has become widely used in practical engineering flow calculations. Robustness, economy, and reasonable accuracy for a wide range of turbulent flows explain its popularity in industrial flow and heat transfer simulations. The standard k-ε model is a semi-empirical model based on model transport equations for the turbulent kinetic energy (k) and its dissipation rate (ε). The model transport equation for k is derived from the exact equation, while the model transport equation for ε was obtained using physical reasoning and bears little resemblance to its mathematically exact counterpart. In the derivation of the k-ε model, it was assumed that the flow is fully turbulent, and the effects of molecular viscosity are negligible. The standard k-ε model is therefore valid only for fully turbulent flows.

3.4.1 Transport Equations for the Standard k- ε Model

The turbulent kinetic energy, k, and its rate of dissipation, ε, are obtained from the following transport equations:

$$\rho \frac{Dk}{Dt} = \frac{\partial}{\partial x_i}\left[\left(\mu + \frac{\mu_t}{\sigma_k}\right)\frac{\partial k}{\partial x_i}\right] + G_k + G_b - \rho\varepsilon - Y_M \qquad (3.9)$$

and

$$\rho \frac{D\varepsilon}{Dt} = \frac{\partial}{\partial x_i}\left[\left(\mu + \frac{\mu_t}{\sigma_k}\right)\frac{\partial \varepsilon}{\partial x_i}\right] + C_{1\varepsilon}\frac{\varepsilon}{k}\left(G_k + C_{3\varepsilon}G_b\right) - C_{2\varepsilon}\rho\frac{\varepsilon^2}{k} \qquad (3.10)$$

where, G_k represents the generation of turbulent kinetic energy due to the mean velocity gradients, G_b is the generation of turbulent kinetic energy due to buoyancy, Y_M represents the contribution of the fluctuating dilatation in compressible turbulence to the overall dissipation rate, $C_{1\varepsilon}$, $C_{2\varepsilon}$, and $C_{3\varepsilon}$ are constants, σ_k and σ_ε are the turbulent Prandtl numbers for k and ε, respectively. The turbulent or eddy viscosity, μ_t, is computed by combining k and ε as follows

$$\mu_t = \rho C_\mu \frac{k^2}{\varepsilon} \qquad (3.11)$$

where $C_\mu = 0.9$.

The model constants $C_{2\varepsilon}$, σ_k, and σ_ε have been established to ensure that the model performs well for certain canonical flow. The model constants are $C_{1\varepsilon} = 1.44$, $\sigma_k = 1.0$, $C_{2\varepsilon} = 1.9$, $\sigma_\varepsilon = 1.3$, and $C_\mu = 0.9$. As the strengths and weaknesses of the standard k–ε model have become known, improvements have been made to the model to improve its performance. Two of these variants are available in FLUENT: the RNG k–ε model (derived using a rigorous statistical technique called renormalization group theory) and the realizable k-ε model. For the earlier simulations, in this study the standard k–ε model is used. In later simulations the RSM model is used and results from both models were compared.

CHAPTER FOUR

NUMERICAL SCHEMES

4.1 Grid System

FLUENT uses a control-volume-based technique to convert the governing equations to algebraic equations that can be solved numerically. This control volume technique consists of integrating the governing equations about each control volume, yielding discrete equations that conserve each quantity on a control-volume basis.

FLUENT can use grids comprised of triangular or quadrilateral cells (or a combination of the two) in 2D, and tetrahedral, hexahedral, pyramid, or wedge cells (or a combination of these) in 3D. The choice of which mesh type to use depends on application. When choosing mesh type, one should consider set-up time, computational expense, and numerical diffusion.

4.2 Types of Solver

There are two choices of numerical methods provided by fluent segregated solver ("FLUENT/UNS") and coupled solver ("RAMPANT"). Using either method, FLUENT will solve the governing integral equations for the conservation of mass and momentum, and (when appropriate) for energy and other scalars such as turbulence and chemical

species. In both cases a control-volume-based technique is used that consists of division of the domain into discrete control volumes using a computational grid, integration of the governing equations on the individual control volumes to construct algebraic equations for the discrete dependent variables ("unknowns") such as velocities, pressure, temperature, and conserved scalars, and linearization of the discretized equations and solution of the resultant linear equation system to yield updated values of the dependent variables.

The two numerical methods employ a similar discretization process (finite-volume), but the approach used to linearize and solve the discretized equations is different. In this study the segregated solution method is used and more details are given in the next section.

4.2.1 Segregated Solution Method

Using this approach, the governing equations are solved sequentially (i.e., segregated from one another). Because the governing equations are non-linear (and coupled), several iterations of the solution loop must be performed before a converged solution is obtained. Each iteration consists of the steps illustrated in Figure 4-1 and outlined below:

1. Fluid properties are updated, based on the current solution. (If the calculation has just begun, the fluid properties will be updated based on the initialized solution.)

2. The three momentum equations are each solved in turn using current values for pressure and face mass fluxes, in order to update the velocity field.

3. Since the velocities obtained in step 1 may not satisfy the continuity equation locally, a “Poisson-type” equation for the pressure correction is derived from the continuity equation and the linearized momentum equations. This pressure correction equation is then solved to obtain the necessary corrections to the pressure and velocity fields and the face mass fluxes such that continuity is satisfied.

4. Where appropriate, equations for scalars such as turbulence, energy, species, and radiation are solved using the previously updated values of the other variables.

5. When interphase coupling is to be included, the source terms in the appropriate continuous phase equations may be updated with a discrete phase trajectory calculation.

6. A check for convergence of the equation set is made.

These steps are continued until the convergence criteria are met.

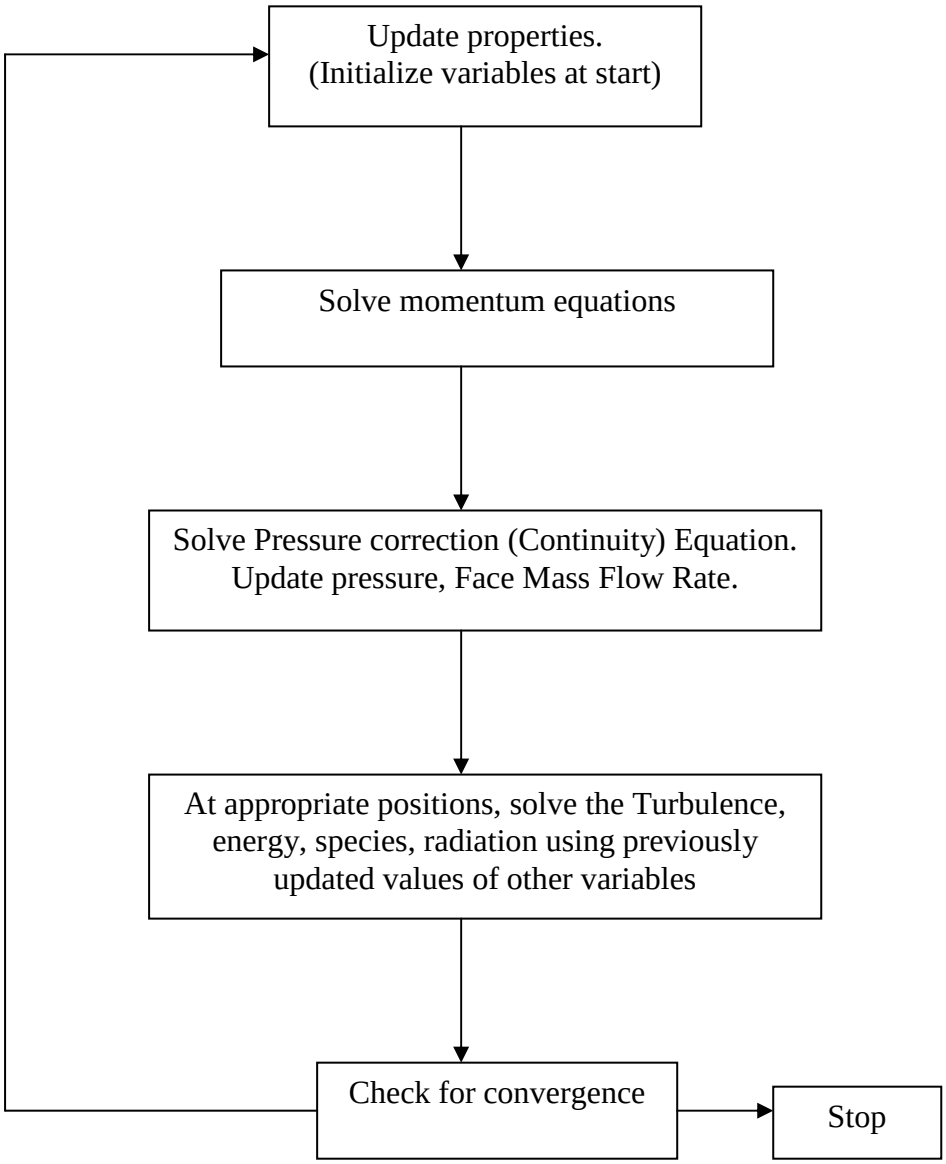

Figure 4.1: Overview of the Segregated Solution Method

4.3 Discretization of the Governing Equations

A control-volume finite-element method to solve the momentum and continuity equations is used by Fluent. This control volume technique consists of integrating the governing equations about each control volume, yielding discrete equations that conserve each quantity on a control-volume basis.

Discretization of the governing equations can be illustrated most easily by considering the steady-state conservation equation for transport of a scalar quantity ϕ. This is demonstrated by the following equation written in integral form for an arbitrary control volume V as follows:

$$\oint \rho \phi_i v \, dA = \oint \Gamma_\phi \nabla \phi_i \, dA + \int_v S_\phi dV \qquad (4.1)$$

where Γ_ϕ is diffusion coefficient of ϕ in phase i, ϕ_i is any conserved property of phase i, and V is an arbitrary control volume.

Equation 4-1 is applied to each control volume, or cell, in the computational domain. Discretization of Equation 1 on a given cell yields

$$\sum_f^{N_{faces}} f \phi_f v A_f = \sum_f^{N_{faces}} \Gamma_\phi (\nabla \phi)_n A_f + S_\phi V \qquad (4.2)$$

The continuity equation can be written as:

$$\oint \rho v \, dA = 0 \quad ,$$

while on discretization gives:

$$\sum_f^{N_{faces}} J_f = 0 \, ,$$

Thus

$$\sum_{f}^{N_{faces}} \rho v_n A_f = 0. \tag{4.3}$$

The steady state momentum equation in integral form is given as:

$$\oint \rho v v dA = -\oint pI\, dA + \oint \tau dA + \int_v F dV \tag{4.4}$$

where I is the identity matrix, τ is the stress tensor, and F is the force vector.

On discretization equation 4.1 formed by setting $\phi_t = u$:

$$a_p u = \sum a_{nb} u_{nb} + \sum p_f \hat{i} A + S \tag{4.5}$$

The equations solved by FLUENT take the same general form as the one given above and apply readily to multi-dimensional, unstructured meshes composed of arbitrary polyhedra. FLUENT stores discrete values of the scalar f at the cell centers (C_o and C_1 in Figure 4.2). However, face values ϕ_f are required for the convection terms in Equation 4.3 and must be interpolated from the cell center values. This is accomplished using an upwind scheme. Upwinding means that the face value ϕ_f is derived from quantities in the cell upstream, or upwind, relative to the direction of the normal velocity v_n in Equation 4-3. FLUENT allows choosing from several upwind schemes, which are first-order upwind, second-order upwind, power law, and QUICK.

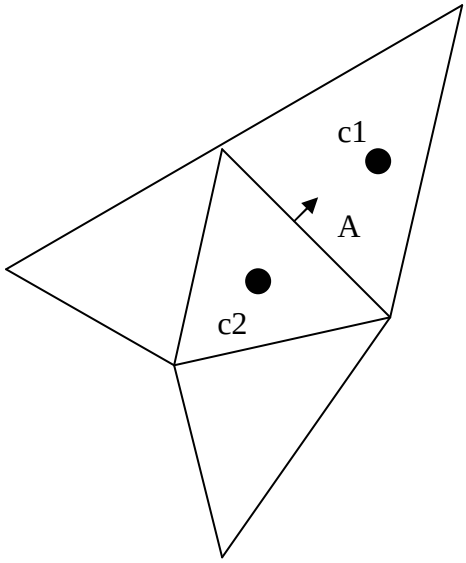

Figure 4.2: Control Volume Used to Illustrate Discretization of a Scalar Transport Equation

4.4 Problem Solving Procedure

After determining the important features of the problem, the following procedure is followed to solve the problem.

1. Create the model geometry and grid using GAMBIT or other FLUENT supported software.
2. Start the appropriate solver (FLUENT 6.0.12) for 2D or 3D modelling.
3. Import the grid created.
4. Check the grid and scale (if required).
5. Check the skewness/ smoothness.
6. Select the solver formulation.
7. Choose the basic equations to be solved: laminar or turbulent (or inviscid), chemical species or reaction, heat transfer model, etc.
8. Specify material properties (fluid or solid etc.).
9. Specify the boundary conditions.
10. Adjust the solution control parameters.

For first run standard pressure with PISO, pressure-velocity coupling, and first order upwind momentum and turbulent kinetic energy were adjusted under relaxation factors: pressure, momentum, turbulent kinetic energy, and turbulent dissipation rate equal to 0.3, 0.7, 0.8, and 0.8 respectively with unit viscosity, unit density and unit body force.

11. Initialize the flow field.

12. Calculate a solution (Iteration is to be done till convergence).

13. Examine the results.

14. Save the results (case and data files to be made).

15. If necessary, refine the grid or consider revisions to be numerical or physical model.

Results will indicate plots of the total temperature, and velocity fields that show clearly the effects of parameters, under investigation including geometry, boundary conditions, physical properties and flow rates.

The models developed are validated using experimental results derived in our laboratories.

CHAPTER FIVE

EXPERIMENTAL FACILITIES

Validation of the numerical models is of paramount importance. An experimental apparatus was built where results for certain design and modifications were collected and used for comparison with the numerical results.

5.1 Experimental Set up

The experimental apparatus is shown schematically in Figure 5.1. An assembly consisting of a main horizontal PVC pipe 3 m long is employed as the main part of the rig. The rig has a replaceable facility (unions at both ends of a replaceable horizontal pipe) so that different diameters of main pipe may be used. Runs reported in this thesis were carried out using 1” diameter main pipe and side-tee of 1/4” and 1/8”.

Experiments with different velocities were also carried out. Tests were done in Reynolds number range of 5000-50000. Suitable pumps are chosen to supply main fluid and tee side fluid respectively. Thermocouples are available and a PC having data logging software OMEGA with suitable hardware to connect thermocouples (at most sixteen) to PC. Output data from thermocouples is fed to PC for data logging and storage. Figure 5.2 shows the thermocouple arrangement on main and side pipes.

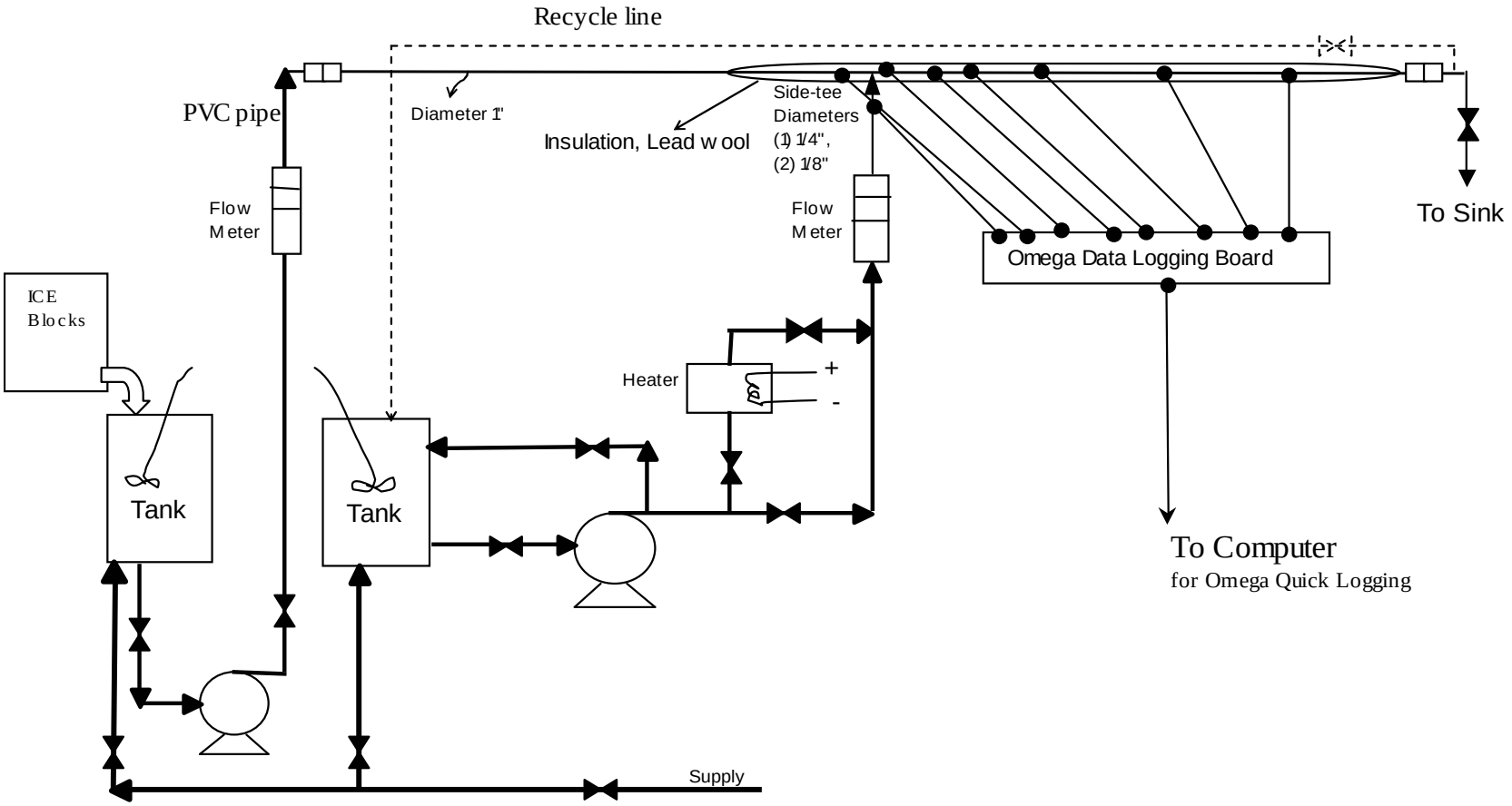

Figure 5.1: Schematic diagram of experimental setup

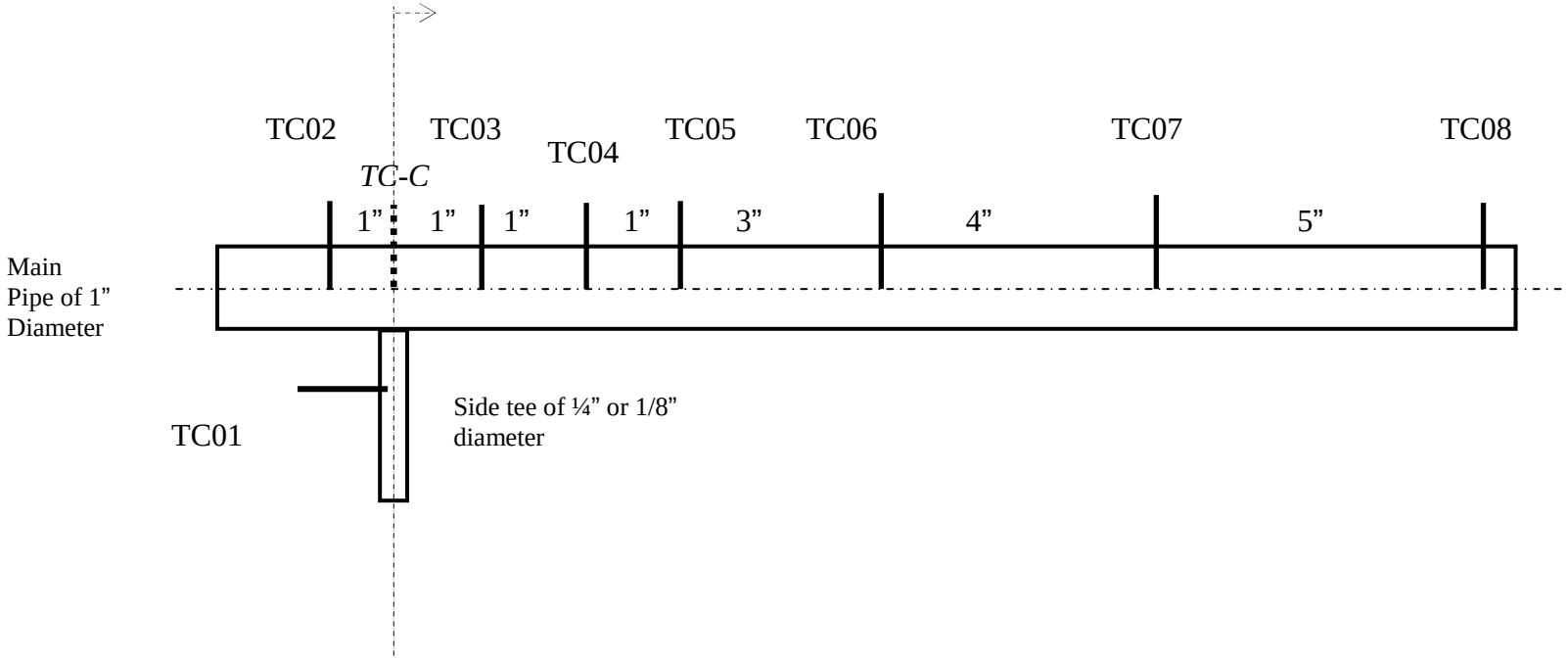

Figure 5.2: Thermocouple (TC) arrangement of experimental set-up, *TC-C* for center.

5.2 Commissioning

The commissioning of the experimental set up was done prior to the first experimental run. Some leakages found were sealed and other faults were rectified. A major electrical faulty connection to pump was found and corrected. Flow meters were calibrated and thermocouple reading for cold water supply (main) pump and hot water supply (side) pump was logged. Results showed that thermocouples were working correctly and data logging software OMEGA was also running correctly. To try to reduce heat losses from main pipe, mainly the part where the two streams (main and side) were being mixed, insulation was done with lead wool. Less storage tank capacity of main supply slows down the main flow rate as the level of fluid in the tank comes down during operation. This cause was overcome by doubling the main supply fluid storage capacity. Figure 5.3 also shows the experimental setup.

5.3 Experimental Procedure

The experimental procedure is:

1. Check the data logging program OMEGA Quick Log is working and enabled
2. Check and adjust the inlet and outlet valves of the both main and side pumps to required flow rates.
3. Start the heater
4. Start the main pump, check the flow rate until it is constant and also note down the main fluid temperature

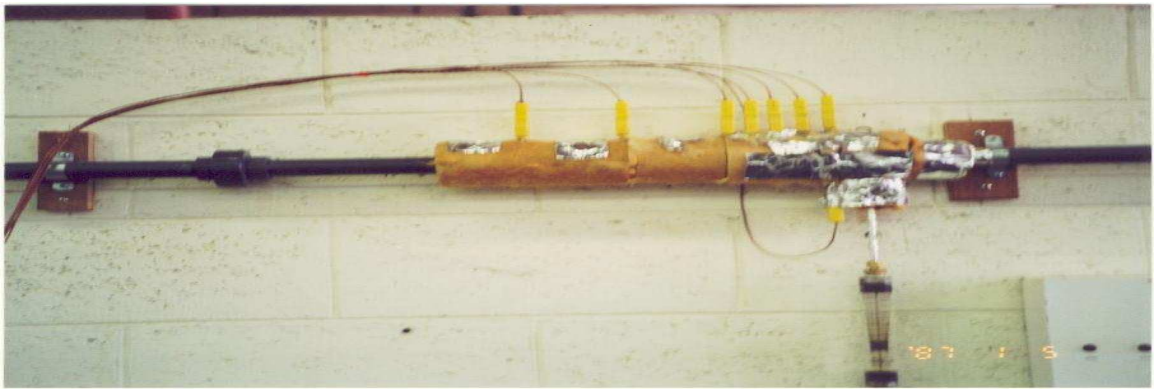

a) Tee-junction view (insulated pipe parallel to ground with 90^{o} side-tee)

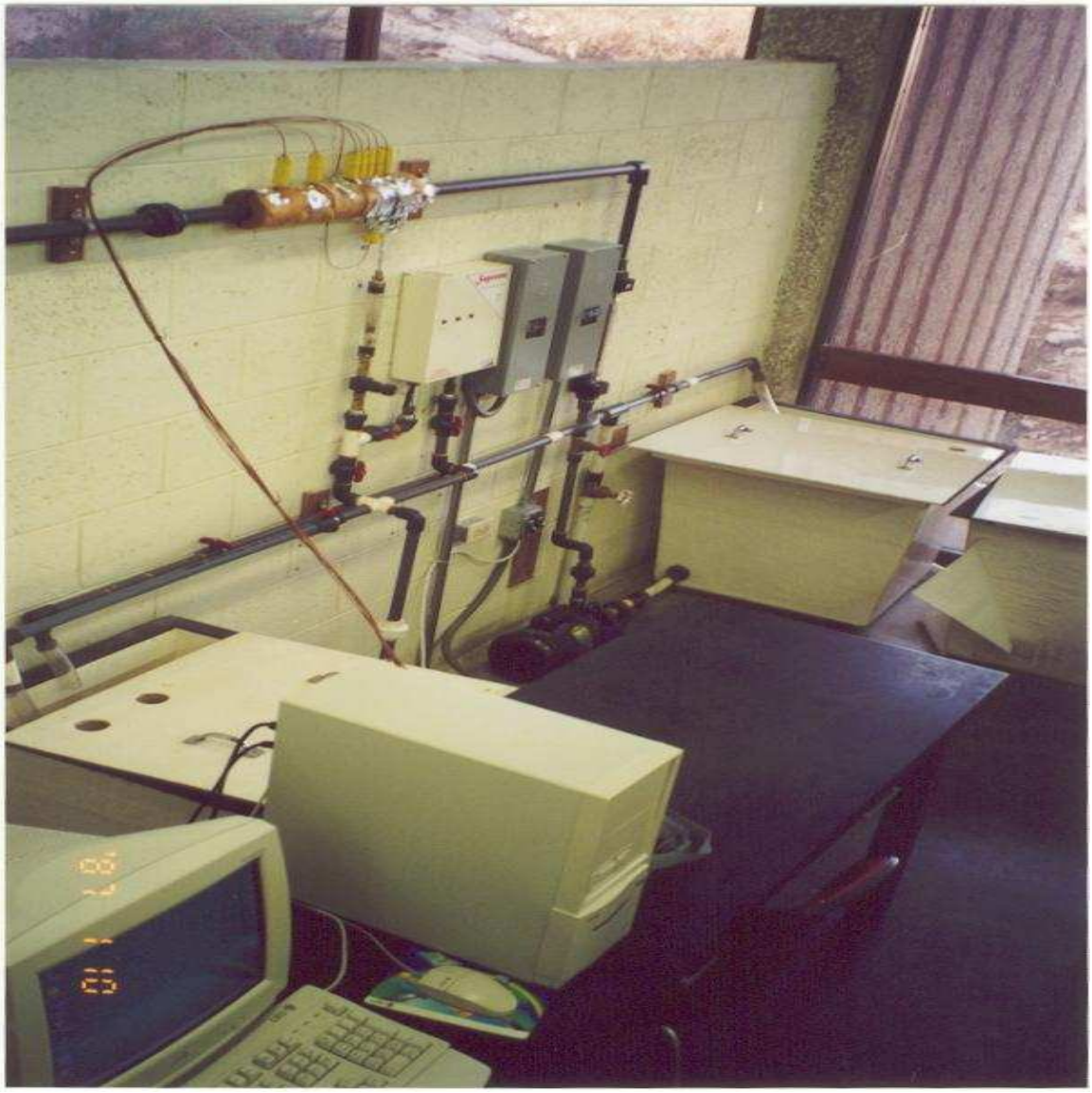

b) Full view, main flow direction from right to left.

Figure 5.3: Experimental setup

5. Then start the side pump. Check until both flow rates become constant.

6. Write down the flow rates and continue checking the flow rates to ensure they remain constant and add more fluid to feed storage supply tanks if needed to maintain flow rate constant.

7. After sufficient time, stop the main pump.

8. Check the side fluid temperature and stop the side pump.

9. Stop the heater.

10. Save the data logged and exit OMEGA Quick Log.

CHAPTER SIX

MODEL VALIDATION

6.1 Numerical model

Flow in pipeline is simulated by solving the mass and momentum conservation equations. The degree of mixing is investigated by solving the energy equation and by monitoring the temperature at various positions along the flow. The flow computations employ the 6.0.12 version of the Computational Fluid Dynamics package FLUENT on Pentium-III, and Pentium-IV processor having system of Microsoft Windows 2000. This code uses the Finite Volume Method for the discretization of the Navier-Stokes equations. Gravity was taken in negative y-direction i.e., $-9.8 m/s^2$. Operating conditions were considered as 101.325 kPa atmospheric pressure with ambient temperature 288.16K. This allows the investigation of a range of conditions and geometries quite efficiently once a general model has been established and validated against experimental results.

A segregated solver was used to solve the Reynolds Averaged Navier-Stokes equations along with the energy equation. With this numerical method, computational work is reduced by comparison to fully coupled solvers but higher convergence criteria have to be chosen. Typically, the default set of FLUENT 6.0.12 that is 10^{-3} for x, y, z-velocity, k and ε and 10^{-6} for energy. The Standard k-ε model and Reynolds Stress model were used to model turbulence.

A three-dimensional geometry representing a main pipe with a side-tee was created and meshed. A part of the grid is shown in Figure 6.1. An unstructured tetrahedral grid was chosen. A base case is used to test the dependence of the numerical solution on the grid size and to test the effects of various turbulence models.

In this study, the pipe length required to achieve 95% mixing is determined. This is the length from the jet inlet to the location along the pipe where the value of the measured quantity anywhere in the pipe is less than 5% of the mean value. The step input is defined as the difference between the initial value and the final mean value.

In terms of a concentration tracer, *m* can be defined as:

$$m = \left| \frac{C - \overline{C}}{\overline{C}} \right| < 0.05 \qquad (6.1)$$

where $\overline{C}$ is the equilibrium concentration and C is the concentration at any monitoring point at any time. When the above condition is met at all points in a cross sectional plane of the main pipe, it can then be said that concentration at any point of the pipe after that length has reached 95% or more of the equilibrium concentration.

In the present study, the flow in the main pipe before the jet inlet is set initially at a certain temperature. The flow through the side-tee is set at a higher but known temperature. Since the flow rate and temperature of the main and side streams are, known the equilibrium temperature of the combined stream $\overline{T}$ can be calculated. The 95% mixing is reached when the temperature anywhere across a plane inside the pipe is within the range of $((\overline{T} \pm (\overline{T} - T_{im}) * 0.05)$ where T_{im} is the initial temperature of the fluid in the main pipe, i.e. before the inlet of the side-tee.

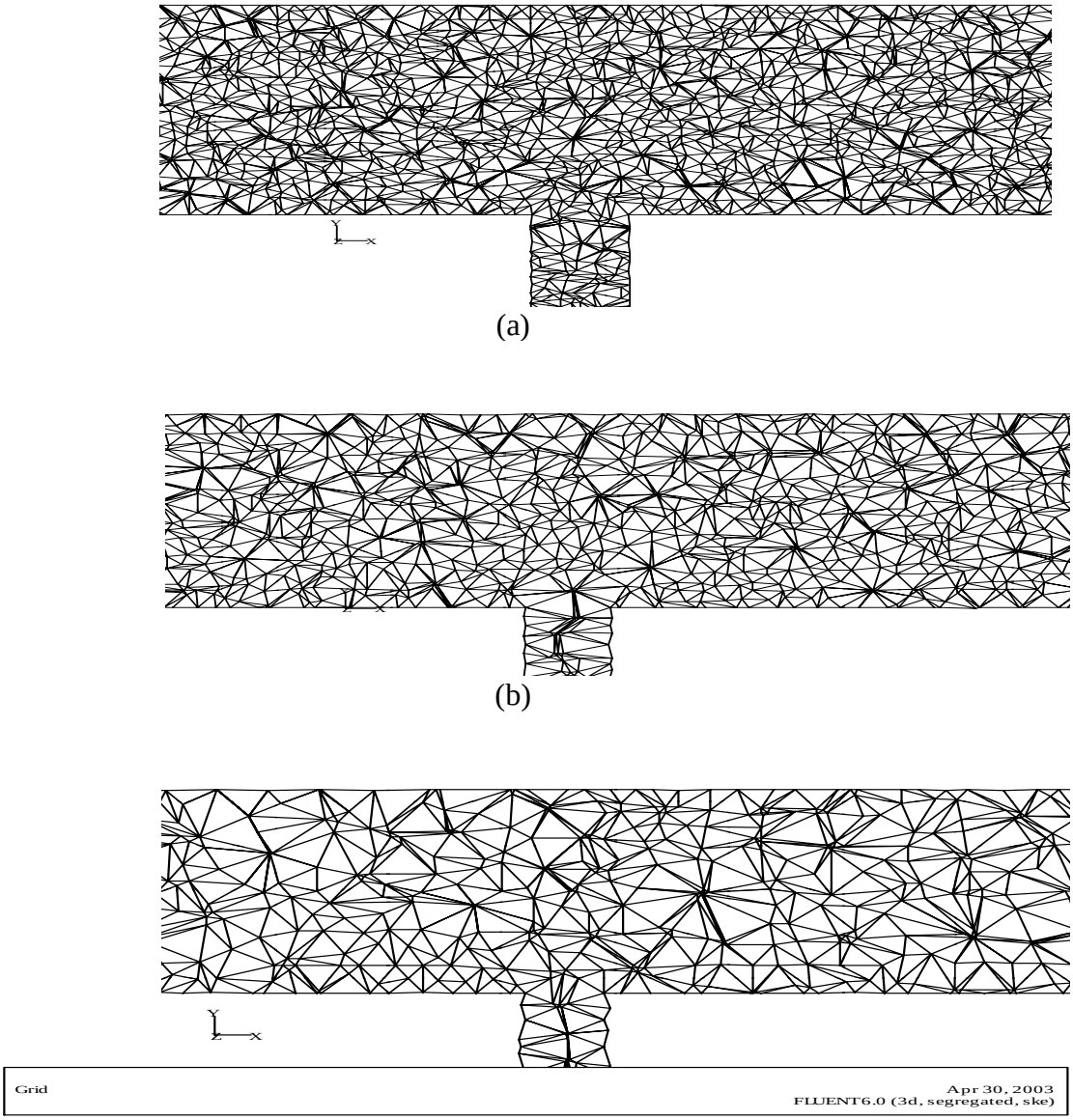

(a)

(b)

(c)

Figure 6.1: Mesh sizes (a) 2 mm, (b) 3 mm, and (c) 4 mm

6.2 Length measurement based on cross-section

The length required for the hot fluid to mix is then measured according to this criterion that means that the maximum temperature difference between any two points across a cross sectional area of the pipe should not exceed a certain value which is a function of the initial temperatures and the flow rates of the fluids in the main and side pipes.

Other researchers (Forney *et al*. 1986, Cozewith *et al.* 1991) used the second order moment of inertia as a criterion to determine the degree of mixing, however, the coefficient of variance is used in this study and it is the preferred criterion in the industry. It should also be mentioned that industry uses a more stringent criterion than 95%.

The preferred criterion industrially is 99% mixing time or length required for mixing; which has a similar definition to the 95% mixing criterion. The numerical results are compared with the experimentally measured temperatures. Due to the limited number of thermocouples used, it was not always possible to establish experimentally the length required for 95% or 99% mixing.

However, in this study, the numerically predicted temperatures are validated against the experimentally measured ones and once good matching is established, the position for the desired mixing is established numerically.

To determine experimentally the location along the pipe where the desired mixing is achieved requires a very large number of thermocouples to be inserted along the pipe and across various planes. This is not easy to implement as it is faced by physical limitation.

6.3 Effect of mesh size

The mesh size often has an impact on the accuracy of the solution. The size has to be of a size small enough in order to resolve properly the fields that are solved. In this case meshes of size 4, 3, and 2 mm have been attempted. The number of computational mesh cells for mesh size 2, 3, and 4 mm are 162367, 56463, 18610 respectively Reducing the mesh size from 4 mm to 2 mm increased the number of cells by a factor of about 9.

A mesh of size 2, 3, and 4 mm is already shown in Figure 6.1. Main pipe is in x-direction whereas side tee is in negative y direction. Views are shown in a constant z-plane. The increase in the number of cells can be clearly seen. The values of temperature along an axis of the main pipe versus position along this axis are shown in Figure 6.2. These results show a significant change when the mesh size is reduced from 4 to 3 mm. The solution also changes when the mesh size is further reduced from 3 to 2 mm, but the difference between solutions of mesh size of 3 and 2 mm is not very significant. The number of cells for a mesh size of 2 mm is relatively very high, however, since the solution still shows some change, a mesh size of 1 was attempted. This exercise could not be completed, because the time required to perform the meshing of the computational domain is prohibitively excessive. Therefore, a mesh size of 2 was used for all the main runs in this study. In order to improve the accuracy of the solution grid refinement is used as explained in the next subsection. Figure 6.3 shows a comparison of the numerical results using the Reynold stress model (RSM) of turbulence for mesh sizes 2 and 3 mm. A small difference is observed especially around the jet zone. Grid refinement is also done for this case and good agreement is found which will be discussed in the next subsections.

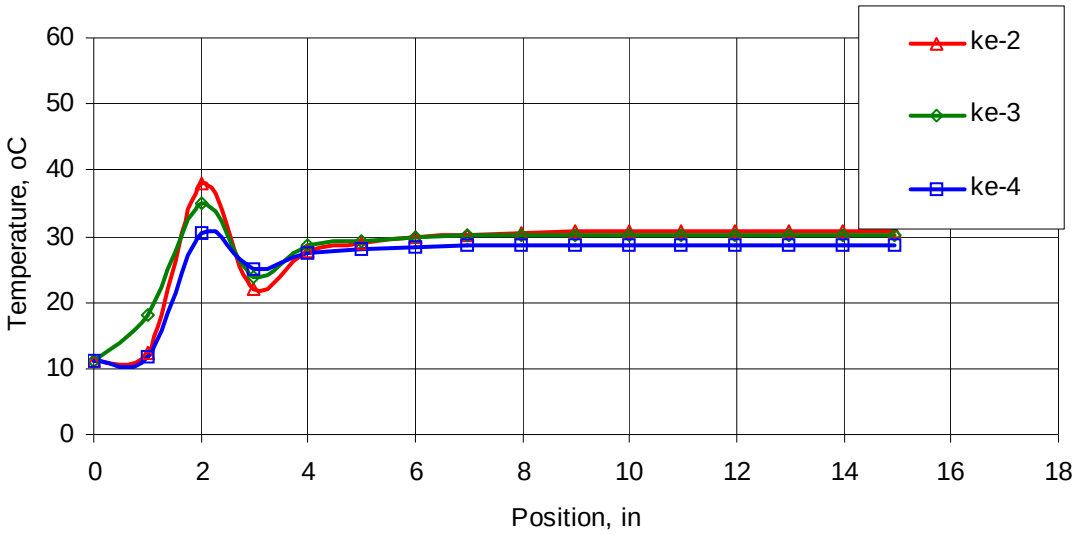

Figure 6.2: Comparison of axial temperatures for case U_j/U_m = 17.1 for mesh size 2, 3, and 4 mm for main diameter of 1" with 1/4" side-tee

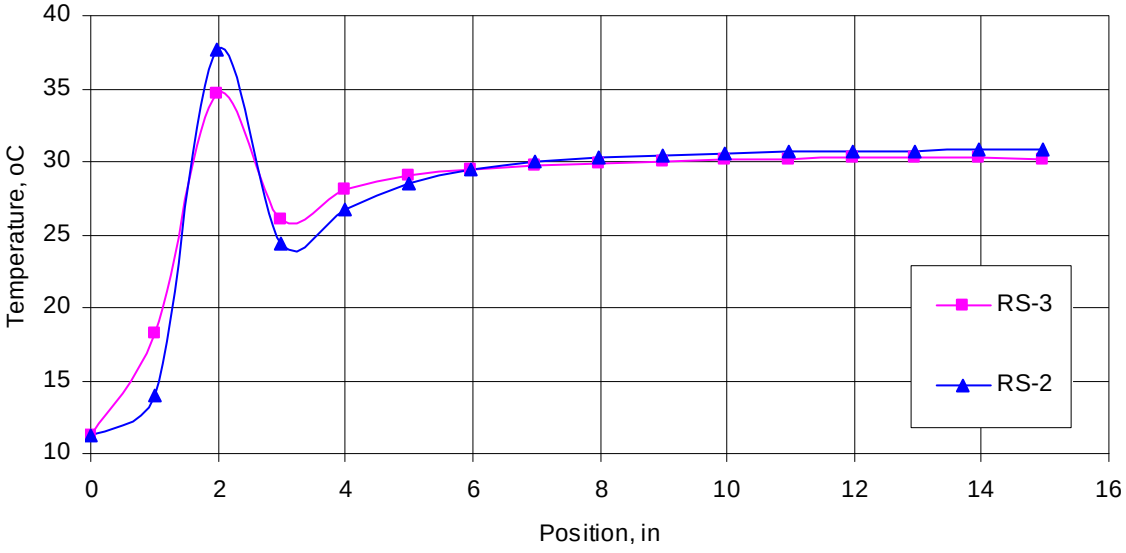

Figure 6.3: Comparison of axial temperatures for case U_j/U_m = 17.1 for mesh size 2, and 3 mm, using RSM model for main diameter of 1" with 1/4" side-tee

6.4 Grid Refinement

The grid is refined especially in the area where the gradient of temperature or velocity is high. A temperature gradient of 0.001 K/m is used as the basis for mesh refinement. This refinement has increased the number of cell from 162367 to 183161. A further refinement is introduced and the number of cells becomes around 215893 cells when a gradient of 0.0005 K/m is used. This local refinement is called grid adaption.

An adapted grid is shown in Figure 6.4. More cells can be seen along the boundaries of the jet, where the temperature gradient is greatest. Temperature profiles along a centerline of the main pipe are shown for all three cases in Figure 6.5. This Figure shows that the temperature profile along the center of the pipe away from the jet is almost identical for all three cases, however for the jet zone the temperature profile shows certain differences and the use of the finest adaption is recommended if the interest includes the jet zone. It is also noted that increasing the number of cells by 41% results in a large increase in the CPU time required for convergence varying for machine to machine.

The gradient refinement of 0.0005 K/m gave the best approximation for the highest temperature at side fluid entrance than others but it took such a long computational time that it was not feasible to use this for all cases. An excellent agreement between the experimental results and numerical predictions was observed when the grid was adapted using a gradient of 0.0005 K/m as shown in Figure 6.6.

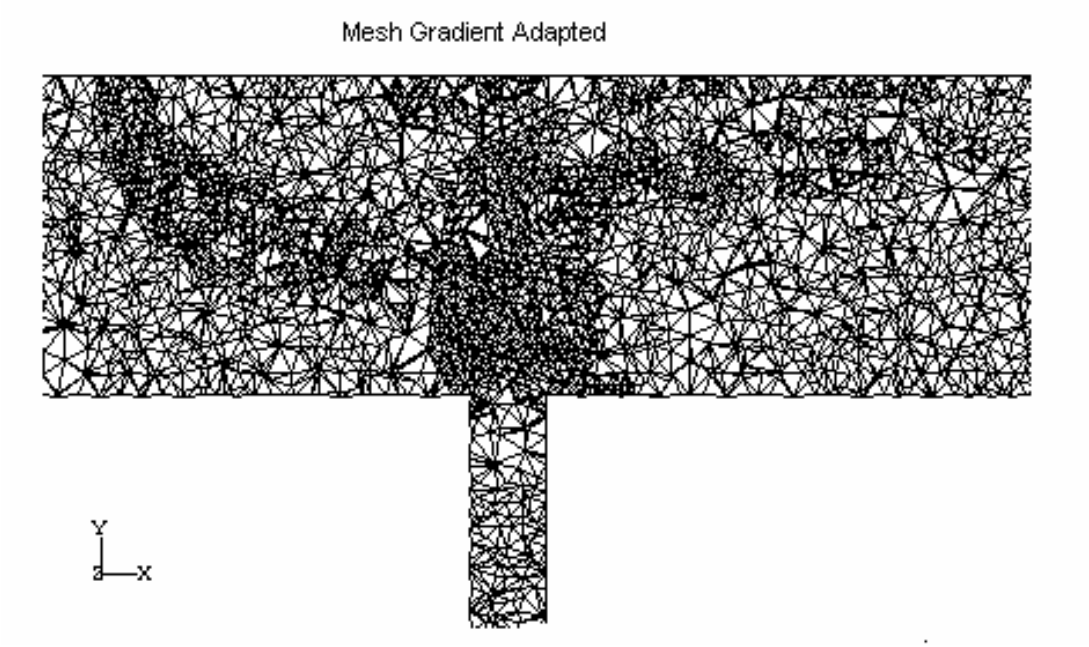

Figure 6.4: Local grid refinement based on a temperature gradient of 0.001 K/m

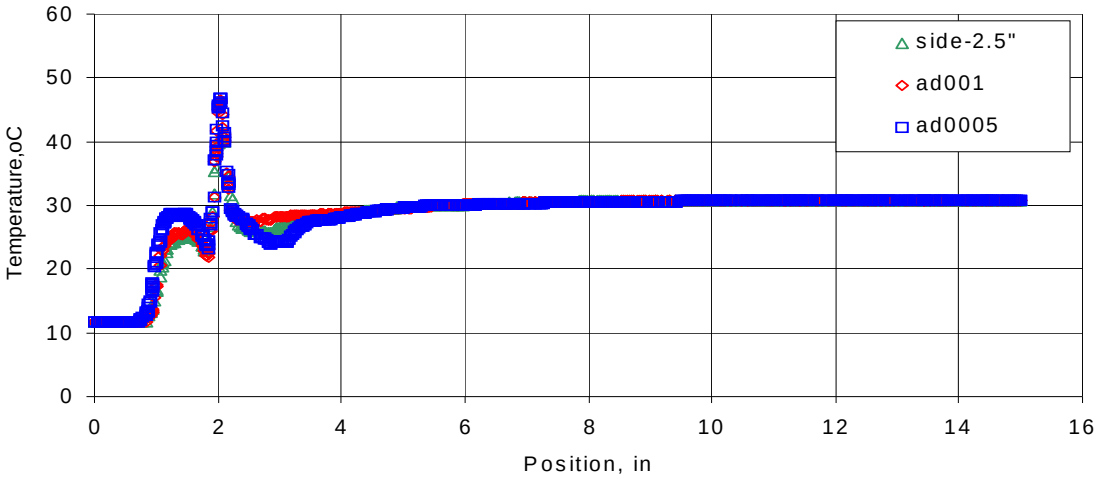

Figure 6.5: Comparison of temperatures along a centerline for the unadapted grid and adapted grid using 0.001 K/m and 0.0005 K/m gradients respectively

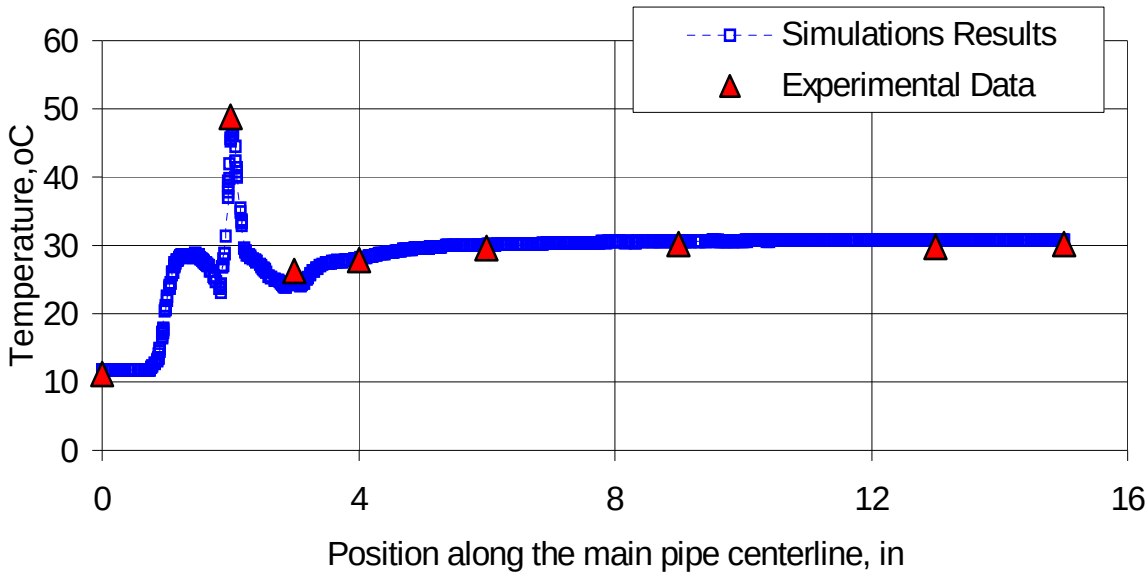

Figure 6.6: Comparison of numerical results using an adaption (gradient) of frequency 0.0005 K/m with experimental for case U_j/U_m = 17.1.

6.5 Fully Developed versus Developing Flows

The lengths of the main and side pipes upstream of tee location required to ensure that the flow in the main and in the side pipes is fully developed are tested in this subsection to find out their effects on the pipe length required for mixing. First a main pipe section of 15” is used with the inlet located 2” away (up) from the tee. The tee length is also taken to be 2”.

The length of the main pipe section was changed to 15, 18, and 21”, i.e. 3D, 6D and 9D up from the side-tee entrance respectively. Results are shown in Figure 6.7. Results show that the temperature profile along a centerline of the main pipe is different for 15 and 18” in the vicinity of the jet. However, the results are the same for 18 and 21”. Hence, 18” is adopted which means 6 diameters away (up) from the jet entry point. Similar tests were done on the side pipe section of 2½”, and 4” (10 and 16 diameters). Results with the 2½” and 4” were identical as shown in Figure 6.8. As mentioned earlier, in order for a numerical model to predict the length of the pipe needed to achieve 95% mixing, it is preferable to have many refinements. However, these refinements become necessary if good agreement is required between numerical and experimental results near the jet zone. Hence, the computational domain is chosen to be 18” main pipe and a 2½” long side pipe.

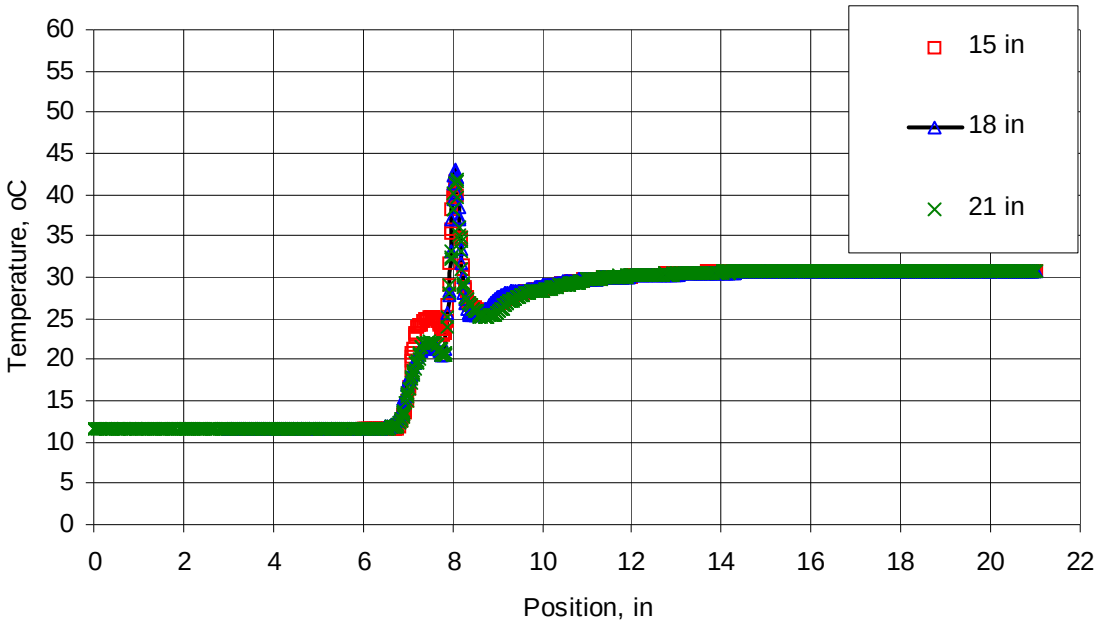

Figure 6.7: Comparison of temperatures along a centerline for 15”, 18”, and 21” geometries

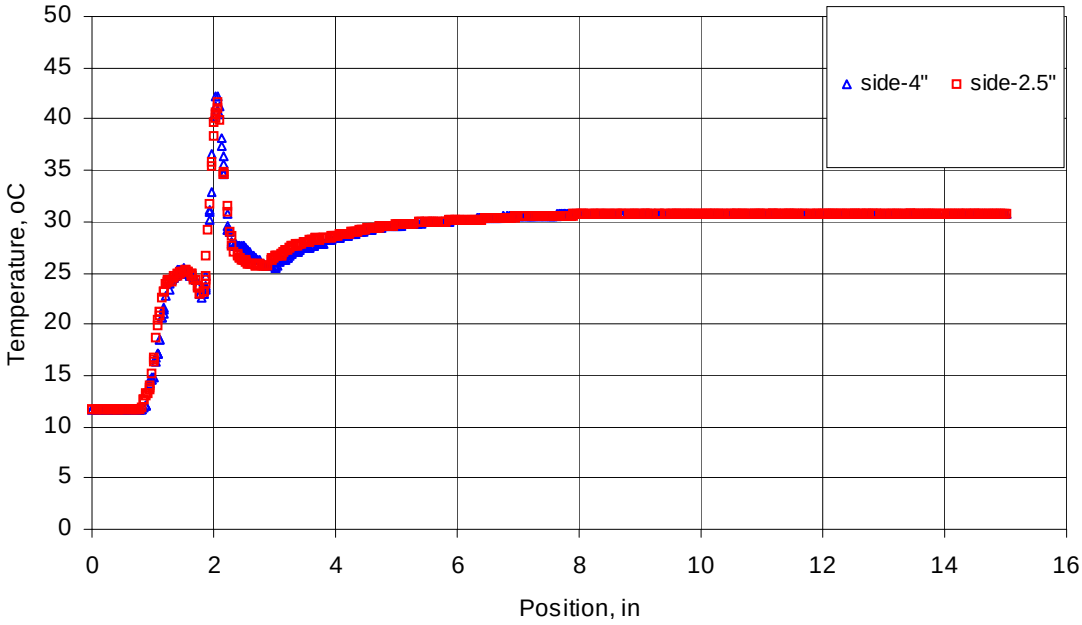

Figure 6.8: Comparison of temperatures along a centerline for side-tee lengths of 4” and 2.5” respectively.

6.6 Turbulence Modeling

Many researchers have recommended and used the k-ε model to model turbulence in mixing studies. Cozewith *et al.* [1991] and Forney and Monclova [1994] used this model for their mixing in pipelines studies, Jayanti [2001], Zughbi and Rakib [2002] and Patwardhan [2002] have used the k-ε model in investigations of mixing in fluid jet agitated vessels. In general, the k-ε model proved to be satisfactory especially when used for non-circulating flows. In the present study, simulations are carried out using the k-ε model or the Reynolds Stress model (RSM).

Figure 6.9 shows comparison of numerical results for a base case with these two models of turbulence. It shows that both RSM and k-ε model predicted the same value of the pipe length required to achieve 95% mixing. However, for the results in the vicinity of the incoming jet, a somewhat significant difference in the results is observed. The RSM gives better estimate of the temperature profile in the vicinity of the jet as shown in Figure 6.6.

The computational time required when using RSM is about 3 times that when using k-ε model. However, since this study attempts to analyze results near the jet as well as calculating the pipe length required for 95% mixing, the RSM and the k-ε model are used. Another option would have been to change the constants in the k-ε model to get a better fit. However, Patwardhan [2002] used this option and reported a limited improvement.

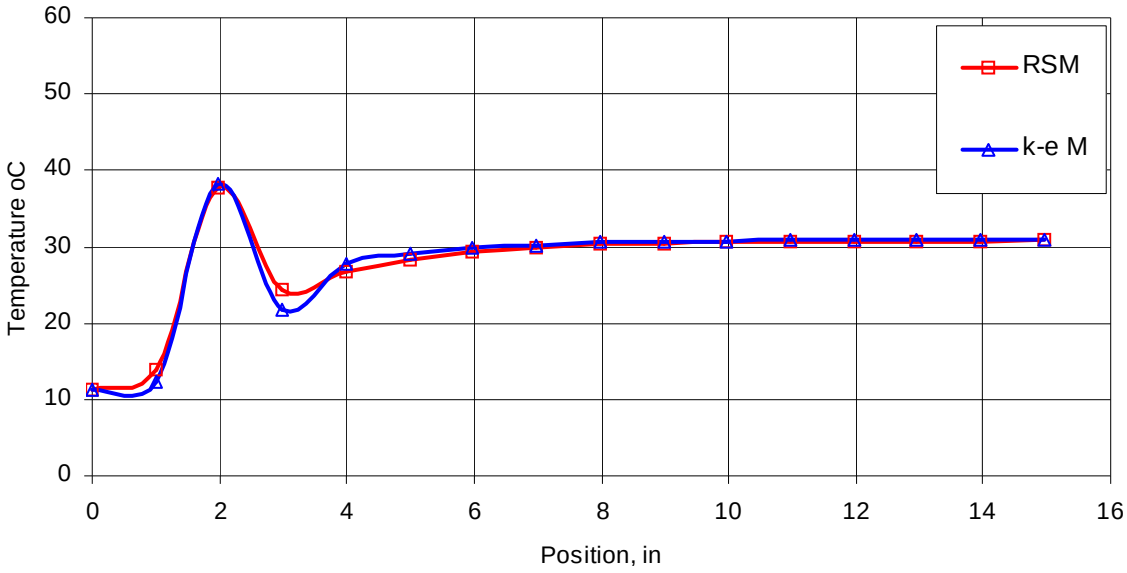

Figure 6.9: Comparison of temperatures along a centerline for case with *k-ε* model and RSM model

6.7 Effect of the Dependence of Physical Properties of Liquid-water on Temperature

Numerical results so far are obtained using constant values of density, viscosity and heat capacity of water. Each of these three properties is a function of temperature. Another numerical run was carried out with the dependence of these physical properties on temperature taken into consideration. Results are shown in Figure 6.10.

Results show that the temperature profile along a centerline of the main pipe does not show any significant difference. The only difference observed is a very little increase in the final equilibrium temperature. This is expected as values of the heat capacity increase with an increase in temperature. The effects of variations in the values of density and viscosity due to a change in temperature do not seem to be significant.

However, for this study, the dependence of viscosity, density and heat capacity on temperature is only taken into consideration when very fine comparison is needed. Results with and without the dependence of physical properties on temperature and using RSM turbulence model are shown in Figure. 6.11. The dependence of physical properties on the temperature showed an effect on the temperature profile in the vicinity of the incoming jet.

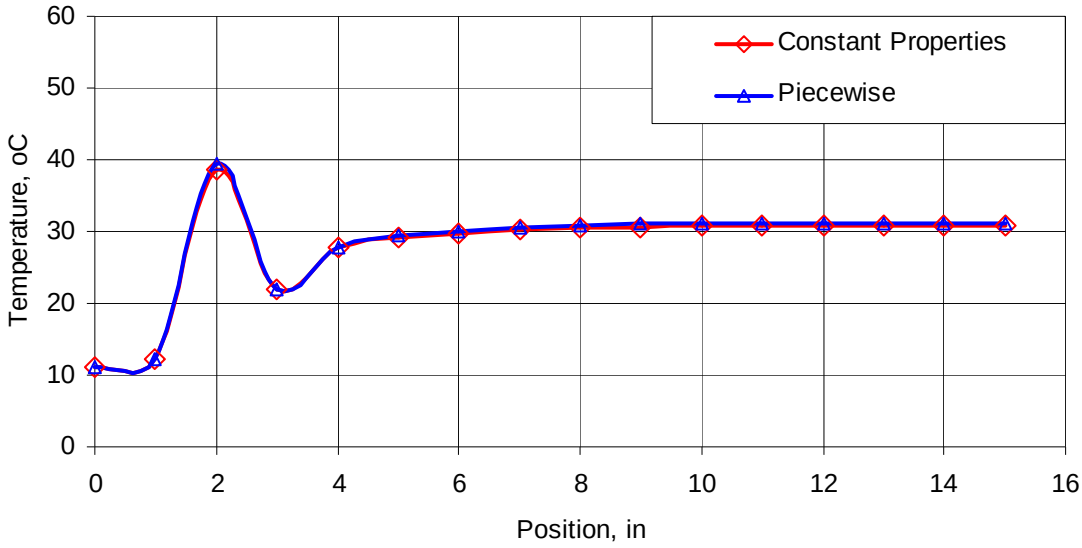

Figure 6.10: Effects of the dependence of physical properties on temperature on the values of temperature along centerline using k-ε model

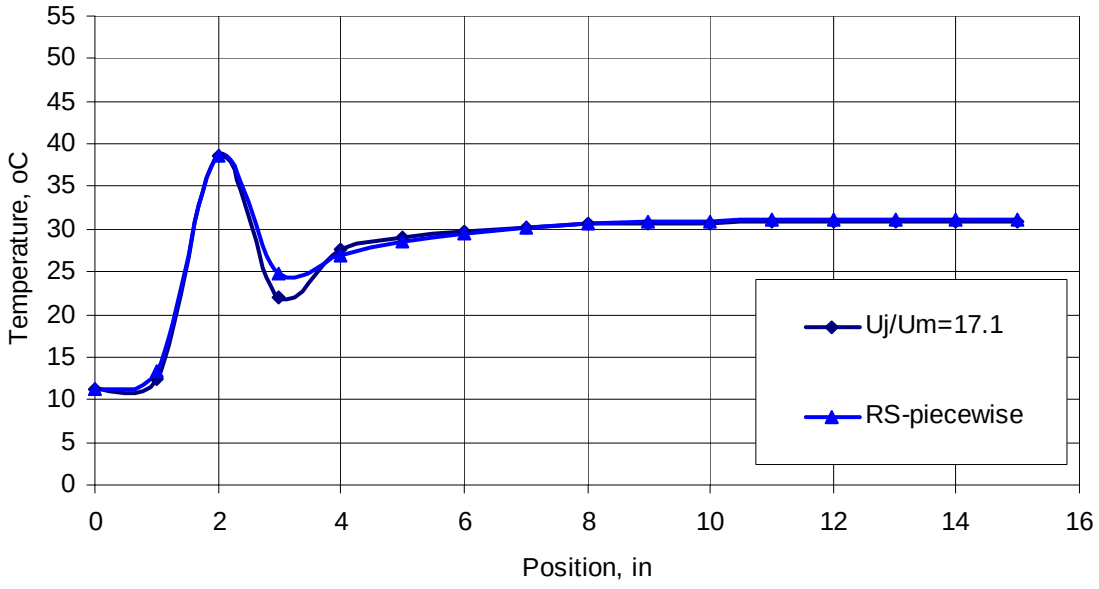

Figure 6.11: Comparison of the temperatures along a centerline using *RSM* model with and without dependence of physical properties on temperature. U_j/U_m = 17.1, U_j = 3.94 m/s.

6.8 Validation of numerical model

Following the previous tests, a model simulating an 18” piece of 1” diameter pipe and a side tee formed by a 2½” piece of 1/4” diameter pipe connected at 5” from the inlet of the main pipe is constructed. A mesh size of 2 with grid refinement based on a temperature gradient of 0.001 is used.

A tetrahedral unstructured mesh is used. 210,000 cells are needed to mesh this geometry. The part of this mesh is already shown in Figure 6.4. That Figure shows that many more cells are used in the zone of high temperature gradient. The experimental results showed almost perfect agreement with numerical prediction as has been shown in Figure 6.6.

6.9 Effects of Adding Thermocouples to the Computational Geometry

In the actual experimental set-up, thermocouples are installed inside the main pipe as was shown in Figure 5.2. Thermocouples recorded temperature values at the centerline of the main pipe along main pipe flow. The diameter of thermocouples was 1/8”.

A geometry is also created having thermocouples placed as a solid object inside the main pipe for simulation. A part of it is shown in Figure 6.12. A case of Uj/Um = 17.1 for this geometry was also run and no significant effect was observed on the length required for mixing as shown in Figure 6.13. Therefore, a relatively simple geometry i.e., without presence of thermocouples was used to simulate all other runs.

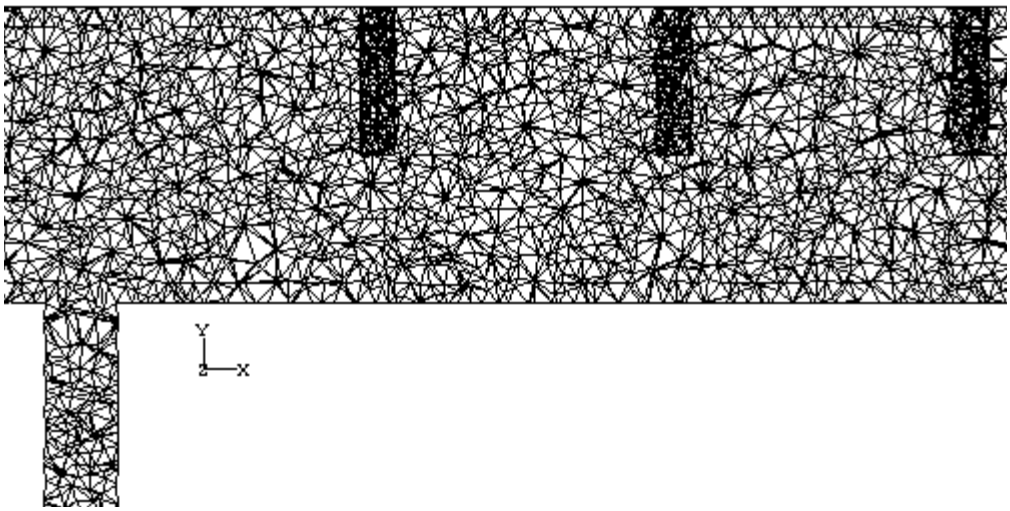

Figure 6.12: Computational geometry with thermocouples

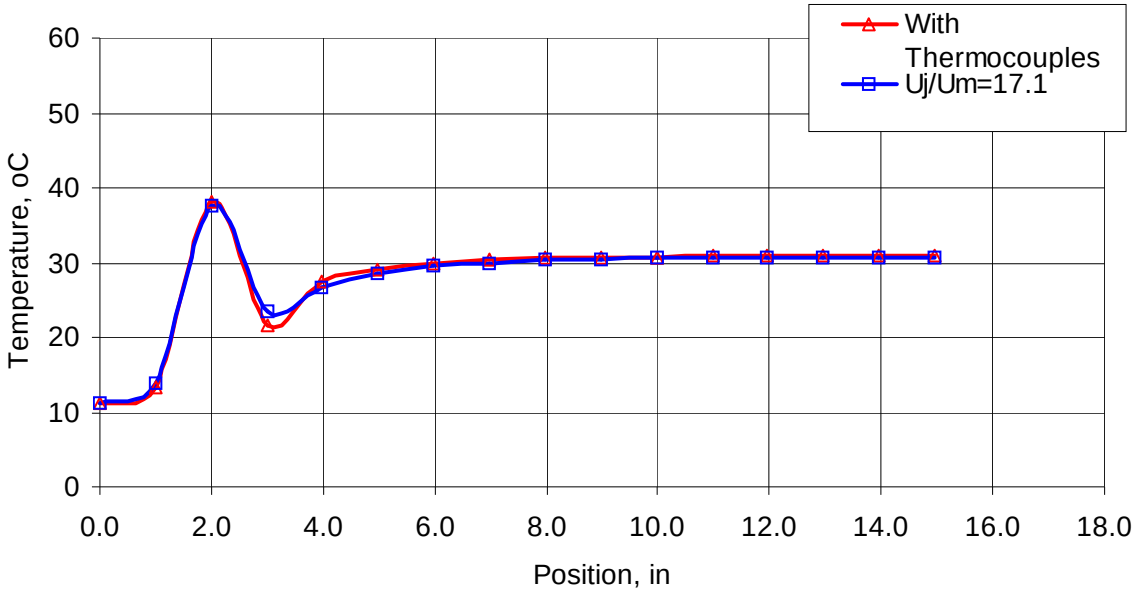

Figure 6.13: Comparison of results for geometry created with and without inserted thermocouples

6.10 Numerical Schemes

Three velocity coupling schemes (SIMPLE, SIMPLEC, and PISO) were also used to simulate cases with constant velocities and constant flowrates. PISO was also simulated with a constant flow rate to test the scale up validation. Temperatures along the centerline of main pipe are plotted against the position along the main pipe.

The Comparison of results is shown in Figure 6.14. A very good agreement is found from the point of jet injection to down stream. A little deviation in results is observed in the back-mixing region and this may be due to k-ε. turbulence model. The difference observed was only an increase in computational time when SIMPLE was changed to SIMPLEC and then to PISO. PISO consumed more computational time.

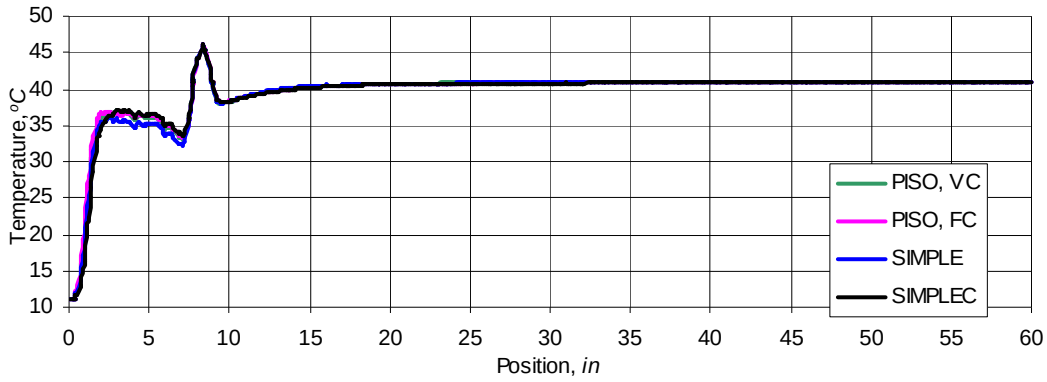

Figure 6.14 Temperature versus position along main pipe centerline for different numerical schemes

CHAPTER SEVEN

RESULTS AND DISCUSSION

7.1 Introduction

In this chapter, experimental results are presented for mixing in a pipe with 1/4” and 1/8” side-tee diameters with a 1” main pipe. Experimental results are compared with numerical results generated for the same geometries. The model validation was done as discussed earlier in chapter six, and this model is used for all subsequent simulation runs.

Experimental work is detailed in section 7.2. In section 7.3 numerical results are presented for side-tee sizes of 1/4” and 1/8”. The sensitivity of temperature to radial position is discussed in section 7.4. Section 7.5 details the variation of length required for 95% mixing for 1/4”-1” and 1/8”-1” arrangements.

Enhancement in mixing length due to change in the angle of the tee is discussed in section 7.6. A comparison of the pipe length required to achieve 95% mixing is done for 30^o, 45^o, 60^o and 90^o injection angles. Velocity fields are also shown to view the flow of fluid from different angles. Temperature contours are also shown to observe further details of mixing inside the pipe. Section 7.7 considers mixing in pipes using opposed-tee. Different cases of opposed-tee are discussed therein. Scaling up of the model of 1” main pipe with 1/4” side-tee is also performed and results are shown in section 7.8. The side stream entering into the main fluid behaves as a jet in cross flow. The side jet

temperature along the main pipe after injection into main fluid stream is plotted in section 7.9. Section 7.10 discusses the multiple-tee.

7.2 Experimental Work

Experiments were performed for two geometries, a side-tee of 1/4" and 1/8", as shown in Figure 7.1. Data were collected at different flow rates. Three main velocities of 0.63, 0.40, and 0.23 m/s and three side velocities of 14.73, 10.52, and 6.31 m/s were used. This makes a total of nine different ratios of jet to main velocity U_j/U_m.

The liquid used was liquid-water for all experiments. For all the above-mentioned nine cases, cold water was placed in the main pipe and hot water was placed on the tee side. In addition, some experiments were done by reversing the order, i.e., hot fluid in the main pipe and cold fluid in the side-tee for 1/8" side tee geometry.

Experiments were repeated more than five times giving the same results and proving that these experiments are reproducible. A typical set of data was chosen for presentation and analysis.

The experimental results (thermocouple temperature readings) are plotted versus their corresponding position along the axis of the main pipe.

The three side velocities with three main velocities give nine side- to main-velocity ratios, i.e. three velocity ratios for each side- or main-velocity as shown in Table 7.1.

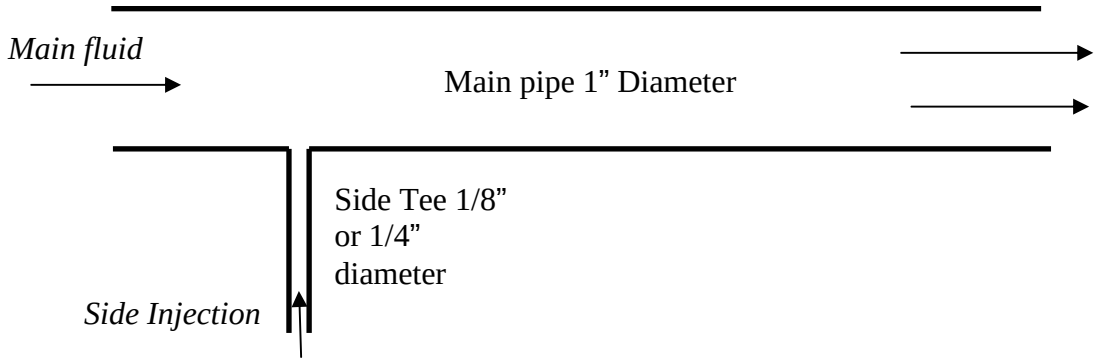

Figure 7.1: Geometry of 1/8", and 1/4" side-tee with 1" main pipe.

Table 7.1: Velocity ratios of side stream velocity (U_j, m/s) to mainstream velocity (U_m, m/s) for each geometry of 1/8" and 1/4" side-tee with 1" main pipe.

Case	U_m, main velocity, m/s	U_j, Side velocity, m/s		U_j/U_m	
		For side 1/8”	For side 1/4”	For side 1/8”	For side 1/4”
1	0.63	14.73	3.94	23.21	6.25
2	0.40	14.73	3.94	36.48	9.85
3	0.23	14.73	3.94	63.84	17.13
4	0.63	10.52	2.63	16.58	4.17
5	0.40	10.52	2.63	26.06	6.57
6	0.23	10.52	2.63	45.60	11.43
7	0.63	6.31	1.57	9.95	2.49
8	0.40	6.31	1.57	15.63	3.92
9	0.23	6.31	1.57	27.4	6.83

For each side- and main-velocity ratio, the temperature is plotted versus the position along the axis of the main pipe and results are shown in Figures 7.2-7.4. Cold liquid-water at around 10^{o}C flows in the main pipe and hot liquid-water at around 50^{o}C flows in the side-pipe. Experimental readings are taken at the points along the centerline of the main pipe. The distance from the side-tee to the point at which the equilibrium temperature becomes constant at the centerline of the main pipe is an indication that mixing along that line has been achieved.

The hot and cold fluids may, however, be still unmixed at an off-center position. To establish that complete or 95% mixing has been achieved, one has to examine the numerical results. Experimental results are plotted and comparison of the length of the pipe needed for the centerline temperature to reach a constant value is made. Figures 7.2-7.4 show the plots of temperature versus position along the centerline of pipe. These Figures show that the temperature reaches a constant value close to the equilibrium value at a shorter distance as U_j/U_m increases. Figure 7.2 shows the line plots for the side to main velocity ratio U_j/U_m = 23.21, 36.48, and 63.84, for a constant jet velocity (U_j) of 14.73 m/s with a varying main fluid velocity (U_m) of 0.63, 0.40, and 0.23 m/s respectively. Figure 7.3 shows the plots of temperature along centerline position for constant U_j = 10.52 m/s with varying main fluid velocity (U_m) of 0.63, 0.40, and 0.23 m/s respectively. Figure 7.4 shows the plots of temperature along centerline position for constant U_j = 6.31 m/s with the same above-mentioned mainstream velocities. It can be seen that as U_j/U_m increases, the temperature reaches a constant value along the centerline in a shorter pipe length.

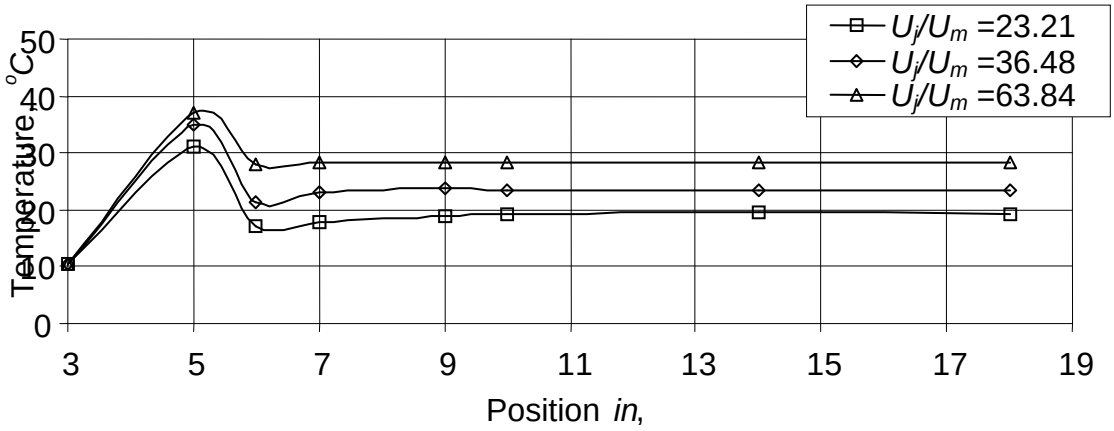

Figure 7.2: Experimental plots of temperature versus position for U_j = 14.7 m/s for U_j/U_m = 23.21, 36.48, and 63.84 for 1/8" side-tee. The distance from 0 to 3" of the main pipe did not have any thermocouple in it.

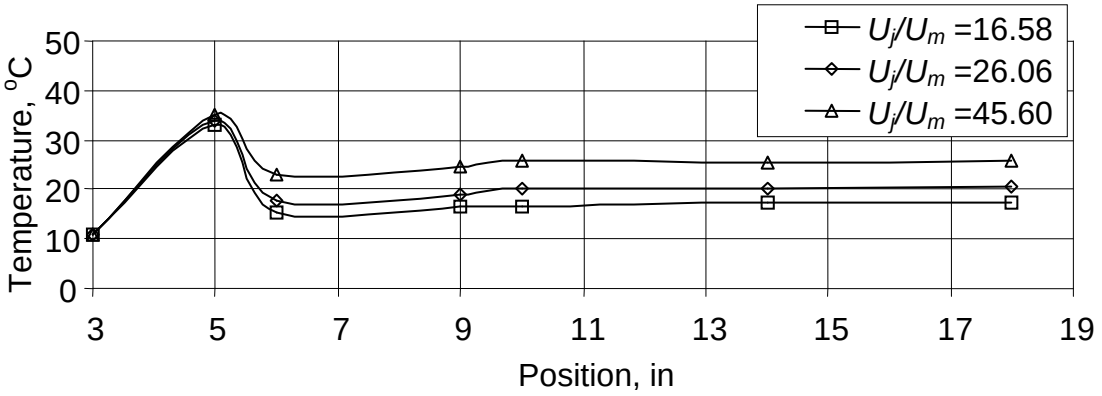

Figure 7.3: Experimental plots of temperature versus position for U_j = 10.52 m/s for U_j/U_m = 16.58, 26.06, and 45.60.

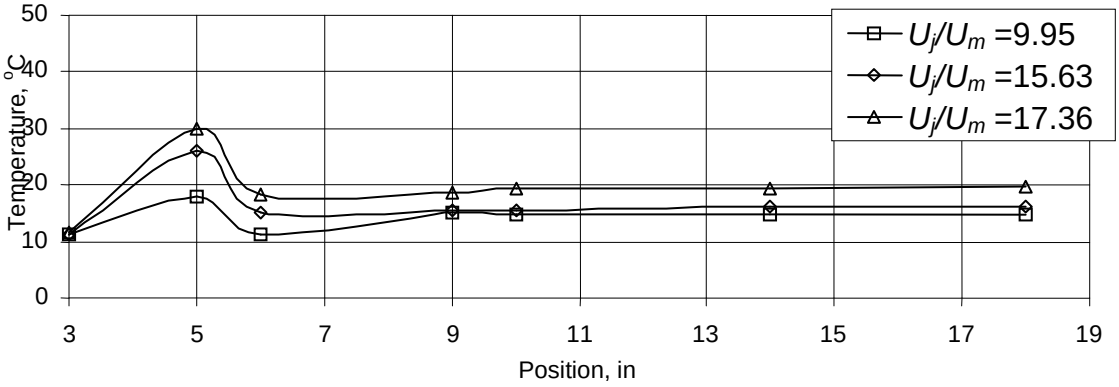

Figure 7.4: Experimental plots of temperature versus position along centerline for U_j = 6.31 m/s for U_j/U_m = 9.95, 15.63, and 17.36

The decrease in the pipe length required for the temperature along the centerline to become constant as the velocity ratio is increased can be seen clearly from Figure 7.2 and to a lesser degree from Figure 7.3 and 7.4. The temperature of the 1” main- and side-streams after they become well mixed is referred to as the equilibrium temperature.

This equilibrium temperature is, as expected, higher for higher velocities ratios (U_j/U_m). In these cases the initial temperature of both streams and the diameters of the main and side pipes are kept constant. Higher velocity ratio means that a higher flow rate of the hot stream is mixed with the same flow rate of the cold stream and consequently higher equilibrium temperature. This equilibrium temperature can be calculated from a simple energy balance. Details are given in Section 7.5 where the length required for 95% mixing is calculated.

The previous plots are for 1” main pipe and 1/8” side-tee. Now for the same main fluid velocities of 0.63, 0.40, and 0.23 m/s, the three side velocities 3.94, 2.63, and 1.57 m/s are used for 1/4" side tee and the results of temperature versus position in sets of three (one set for each side velocity) are plotted in Figure 7.5-7.7.

These Figures show that at centerline of main pipe, 95% mixing is achieved at a shorter pipe length for higher U_j/U_m. As the U_j/U_m is decreased while keeping U_j, constant (i.e., increasing U_m, increasing the mass flow rate of cold water) the length required for 95% mixing is increased and the final equilibrium temperature of mixed stream is decreased. When the temperature becomes constant at the center of main pipe, 95% mixing is considered achieved at the center of main pipe. Mixing in a cross section of the pipe is discussed in a later section after comparing experimental results with simulated results.

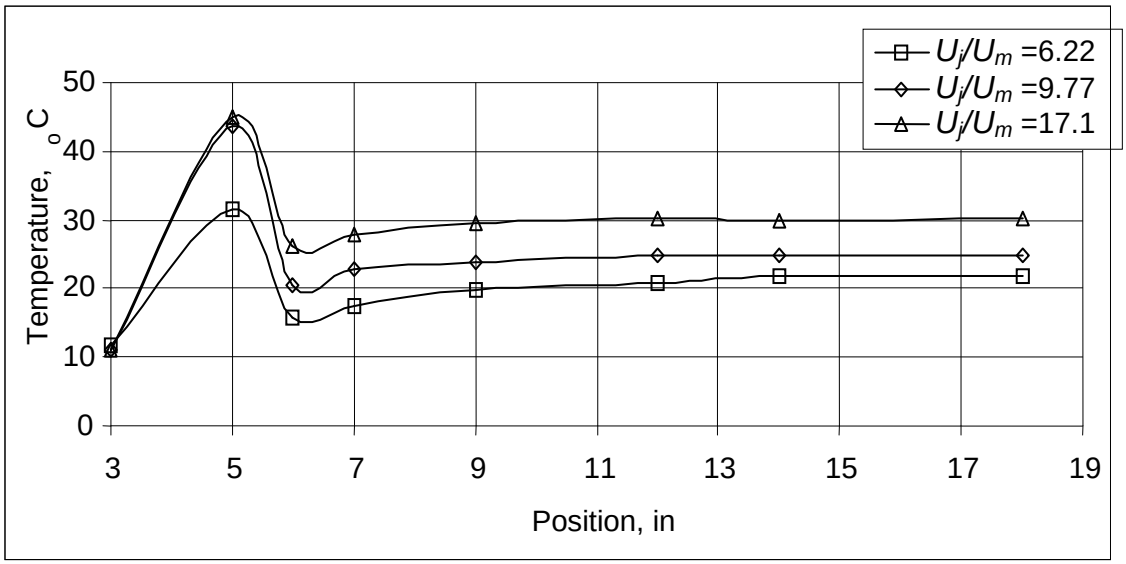

Figure 7.5: Experimental plots of temperature versus position along centerline for U_j = 3.94 m/s for U_j/U_m = 6.22, 9.77, and 17.1 for 1/4" side-tee.

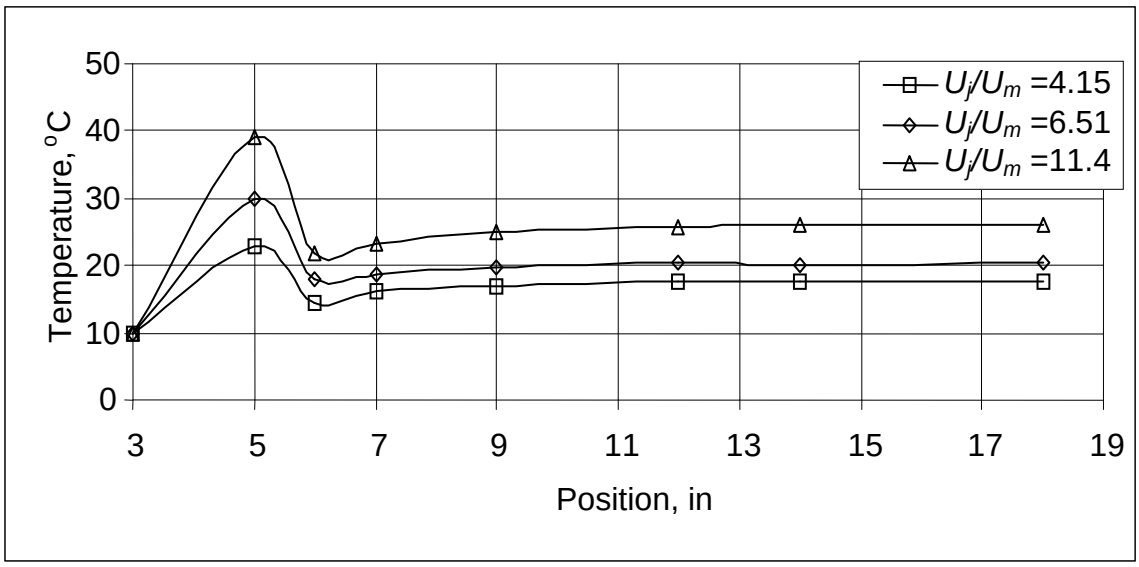

Figure 7.6: Experimental plots of temperature versus position along centerline for U_j = 2.63 m/s for U_j/U_m = 4.15, 6.51, and 11.4 for 1/4" side-tee.

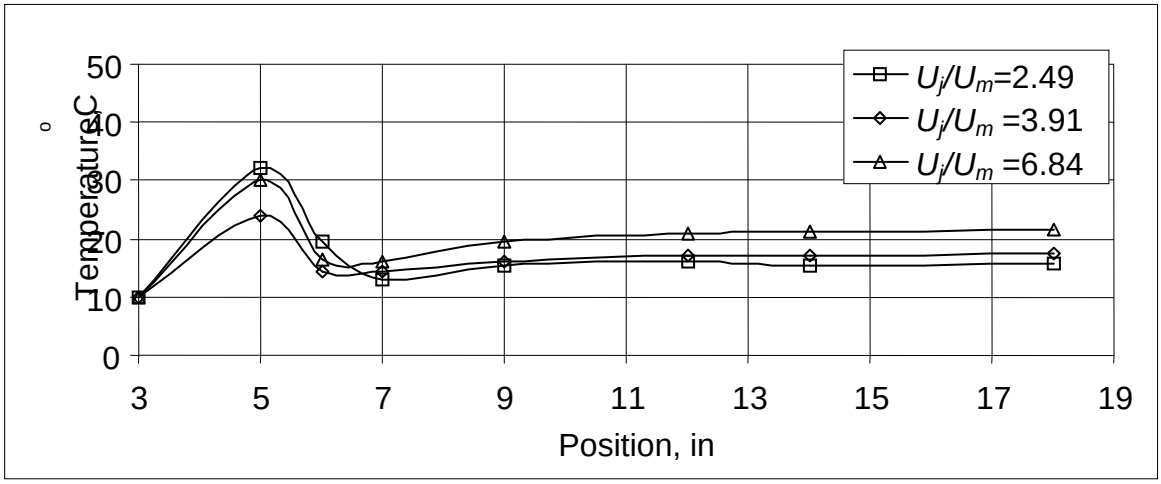

Figure 7.7: Experimental plots of temperature versus position along centerline for U_j = 1.57 m/s for U_j/U_m = 2.49, 3.91, and 6.84 for a 1/4" side-tee.

Figure 7.5 shows plots, similar to those in the previous two figures, of temperature versus position along the centerline of the main pipe for a constant U_j of 3.94 m/s and U_m of 0.60, 0.40, and 0.23m/s. The temperature of the incoming side- and main- streams were kept at 10 and 50^{o}C respectively.

Higher side-tee velocities results in higher velocity ratios and higher equilibrium temperature. The pipe length required to achieve a constant centerline temperature decreases as the ratio U_j/U_m increases. Figures 7.6 and 7.7 show similar plots for the same main velocities of 0.60, 0.40, and 0.23 m/s and for a side-tee velocity of 2.63 and 1.57 m/s respectively. These two Figures show similar trends as those of Figure 7.5.

It is also seen from the plots that after the entrance of side stream the bending of the side jet towards the center of the main pipe depends upon the U_j/U_m for side-tee at 90^o with *d/D* equal to 0.125. A temperature higher than the equilibrium temperature of mixed-stream at the centerline of main pipe after entrance of side-jet shows that the hotter side-stream is bending towards center of the main pipe. This phenomenon can be seen more clearly for the cases where *d/D* is 0.25. This phenomenon will be more apparent from the Temperature contours. As seen from the dip of temperature in the above Figures 7.2-7.7, for lower velocity ratio the dip is high showing that jet side-stream is bent towards the center of main pipe away from the opposite wall as U_m increases for constant U_j. When U_m increases, decreasing U_j/U_m, makes temperature dip lower and 95% mixing accomplishment position increases at the center of pipe. When U_m is constant as shown in Figure 7.8 and U_j is changed, the same trend is observed. An increase in U_j that is an increase in U_j/U_m, makes the jet-stream bend further away from the opposite wall resulting in a smaller temperature dip and in early mixing.

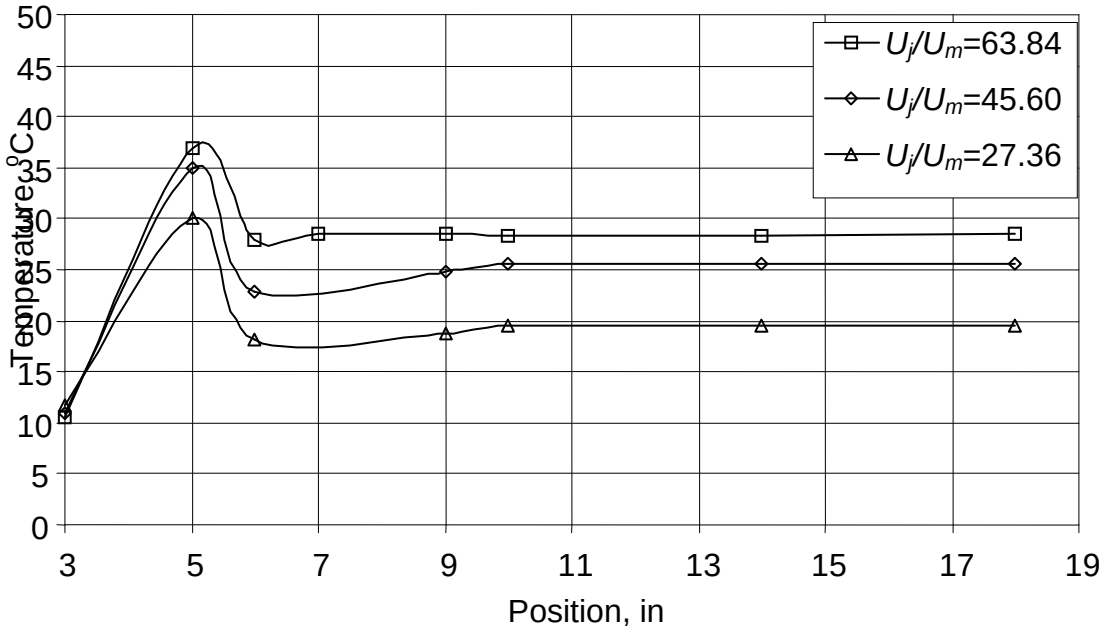

Figure 7.8: Experimental plots of temperature versus position along centerline for U_m = 0.23 m/s for U_j/U_m = 63.84, 45.60, and 27.36 for 1/8" side-tee.

These experimental plots do not show impingement and back mixing of the jet side-stream. To observe the impingement and back flow accurately within the entrance of jet side-stream and within one diameter downstream and upstream from entrance very close temperature readings are required. Therefore, more thermocouples would be required to read the temperature at those points but installation of thermocouples so near to each other is difficult due to the dimensions of thermocouple holders. It may be possible that a source of turbulence is introduced due to these thermocouples. The impingement and back mixing will be clear from the simulated contour plots of the same experimental cases discussed in next the sections.

7.3 Numerical Results

A main interest of this study is achieving 95 % mixing efficiently, so all the discussed results are mixing length oriented. First, the experiments are simulated for 1" diameter main pipe with 1/8" and 1/4" diameter side-tee. The boundary conditions applied are shown in Figure 7.9 namely a main velocity inlet, U_m, and a side velocity inlet, U_j, and an outflow boundary condition.

The pipe has a total length of 18". It has three parts, one upstream pipe of length 5" having 1" diameter. Second, a 90^o tee of length 3" of 1/8" or 1/4" diameters. After entrance of the side-stream at 5" of main-pipe, the third part of the 1" diameter pipe is 13" long, which makes the total length of the main pipe 18". U_j/U_m values for all nine cases are also tabulated in Table 7.2 with number of iterations required for convergence. In chapter six, the model validation was done and that model with different boundary condition for different cases tabulated in Table 7.1 now is used here.

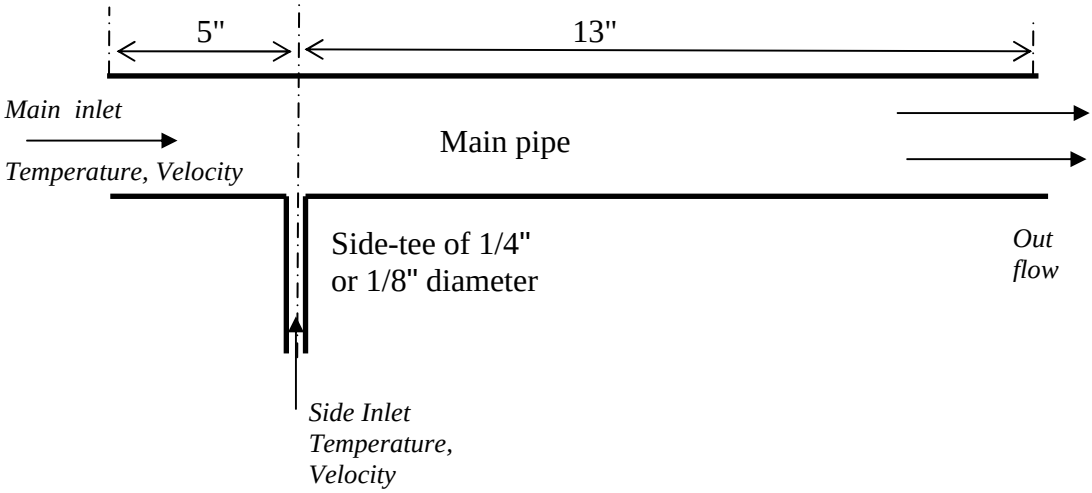

Figure 7.9: Boundary conditions applied on geometry for computations.

Table 7.2: Iteration data and swapping of cells for 1/8” side tee with 1” main pipe

Case	U_j/U_m	Cell Swapped	Cell Visited	Cell Visited with zero swapped	Number of iterations till convergence	Total number of iterations after adaption
1	16.58	10	1845	1830	292	350
2	26.06	10	1845	1830	316	374
3	45.60	10	1845	1830	330	352
4	23.21	10	1845	1830	254	317
5	36.48	10	1845	1830	273	332
6	63.84	10	1845	1830	283	329
7	9.95	10	1845	1830	320	379
8	15.63	10	1845	1830	389	443
9	27.36	10	1845	1830	393	445

The set of nine cases is simulated with a geometry 18” (0.4572m) long, 1” (0.0254m) diameter main pipe and 3” (0.0762m) long, 1/8” (0.003175m) diameter side-tee for each case. A mesh size of 2 mm was used resulting in 197,580 cells, 38,817 nodes, and 406,413 faces. A region bounded by the x-axis from +0.12065 m to +0.13335 m and the y-axis from –0.0762 m to +0.0127 m, and the z-axis from –0.0127 m to +0.0127 m is marked, and adapted. 6,169 cells is adapted and changed to 43183 cells, 8552 nodes, and 88,952 faces in this region, refining that region resulted in final figures of 240,763 cells, 47,369 nodes, and 495,365 faces.

7.3.1 Hanging node mode

Hanging node mode was observed during refinement by region adaption. Since the problem deals with 3D, the hanging node mode did not hinder refinement. Grids produced by the hanging node adaption procedure are characterized by nodes on edges and faces that are not vertices of all the cells sharing those edges or faces, as shown in Figure 7.10. Hanging node grid adaption provides the ability to operate on grids with a variety of cell shapes, including hybrid grids. However, although the hanging node scheme provides significant grid flexibility, it does require additional memory.

Standard pressure with pressure-velocity coupling scheme PISO and with first order upwind scheme for momentum and turbulence kinetic energy was used for all cases. The constants for the k-ε model were C_{μ} = 0.09, $C_{1\varepsilon}$ = 1.44, and $C_{2\varepsilon}$ = 1.92. The number of swapped cell, the number of iterations needed to attain convergence criteria before and after region adaption which may vary for machine-to-machine are tabulated in Table 7.2 with minimum skewness of 0.8 using the method of skewness for smoothing.

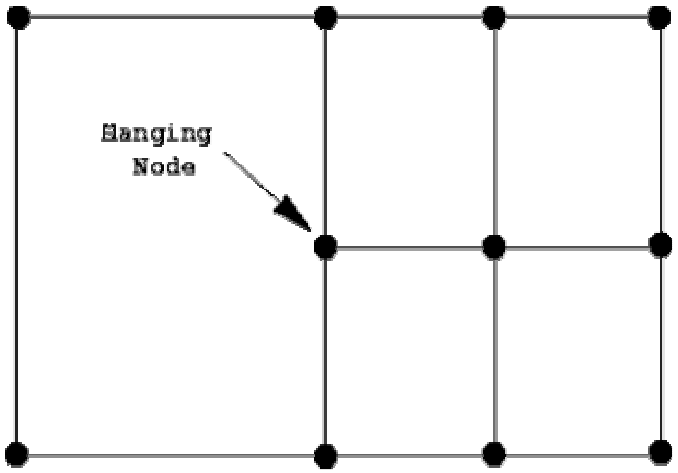

Figure 7.10: A hanging node example

7.3.2 Temperature and Velocity (m/s) contours for 1/8", Right-angle, Side-Tee

Temperature and Velocity contours are shown in Figures 7.11-7.16 for nine cases for an 1/8" side-tee. It can be seen from the contours that for all nine cases the side stream is impinging on the opposite side of the pipe. Figures 7.11 and 7.12 show the temperature and Velocity contours for (a) U_j/U_m = 16.58, (b) U_j/U_m = 26.06, and (c) U_j/U_m = 45.60 for 1/8" side-tee respectively. The main flow is along the x-axis whereas the side flow is along the positive y-axis opposing gravity. A temperature color scale in Kelvin is shown on the right hand side of the Figures ranging from blue representing the cold main fluid to red representing the hot side-fluid. The Figures clearly show that as the velocity ratio increases, impingement and back mixing increases because of higher side-stream velocity. A lower temperature zone can be seen after entrance of side-jet due to impingement on the opposite wall and passage of the hot fluid along the wall. This zone decreases as the impingement increases. This shows that if a main pipe centered-jet is disturbed from the center towards the upper wall this zone increases and as the jet impinges the opposite wall it starts to decrease due to circulation and back flow of hotter side-fluid. From Figure 7.12, it can be seen that the low velocity zone near the tee-sidewall after entrance of the jet increases for higher velocity ratios where the impingement is stronger. Figures 7.13 and 7.14 show temperature (K) and velocity (m/s) contours of (a) U_j/U_m = 23.21 (b) U_j/U_m = 36.48, and (c) U_j/U_m = 63.84 for the same geometry. These Figures show the same behavior i.e. as the velocity ratio increases the impingement and back mixing in the vicinity of side stream entrance increase.

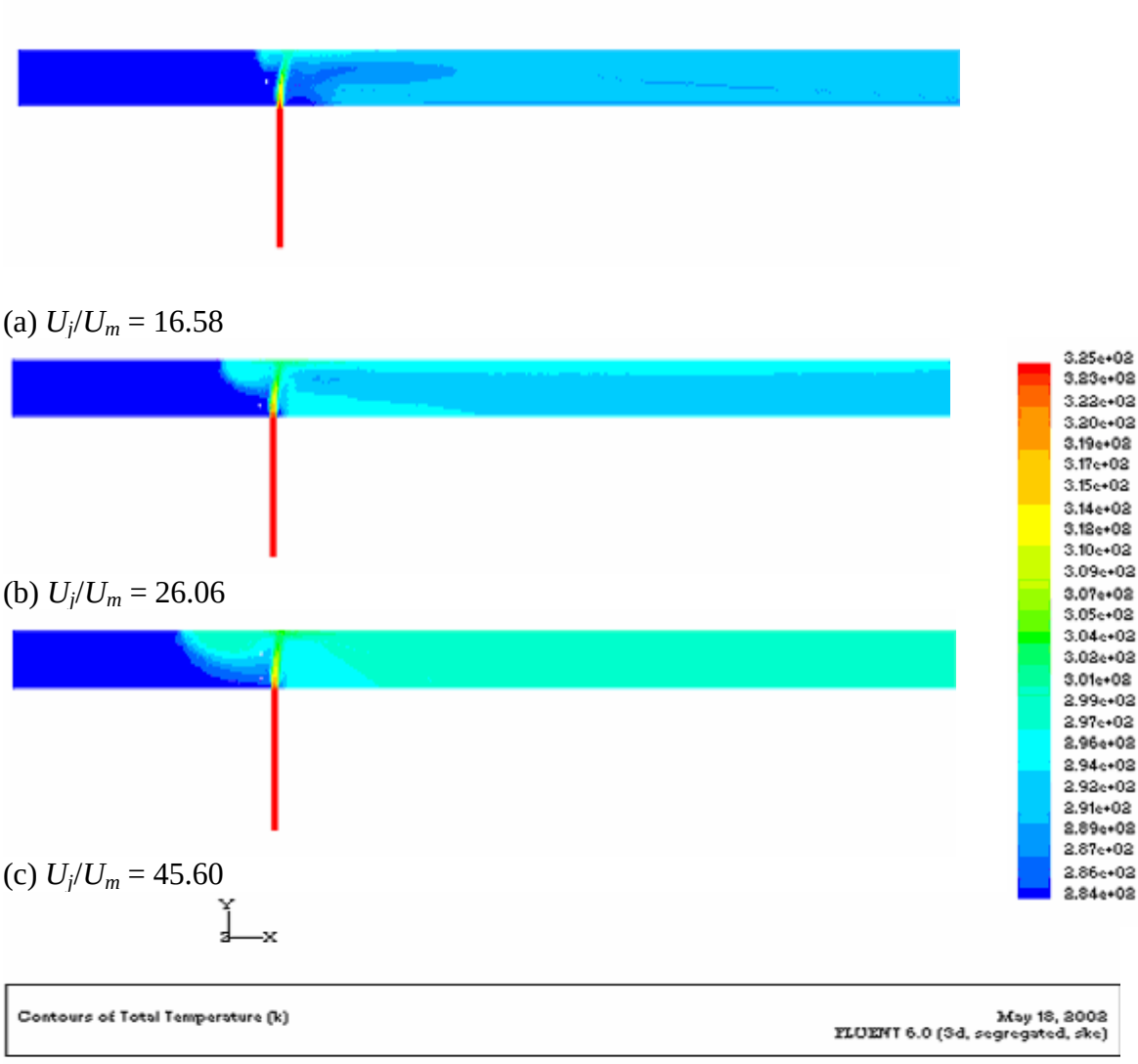

(a) U_j/U_m = 16.58

(b) U_j/U_m = 26.06

(c) U_j/U_m = 45.60

Figure 7.11: Temperature (K) contours of (a) U_j/U_m = 16.58 (b) U_j/U_m = 26.06 (c) U_j/U_m = 45.60 for 1/8" side-tee.

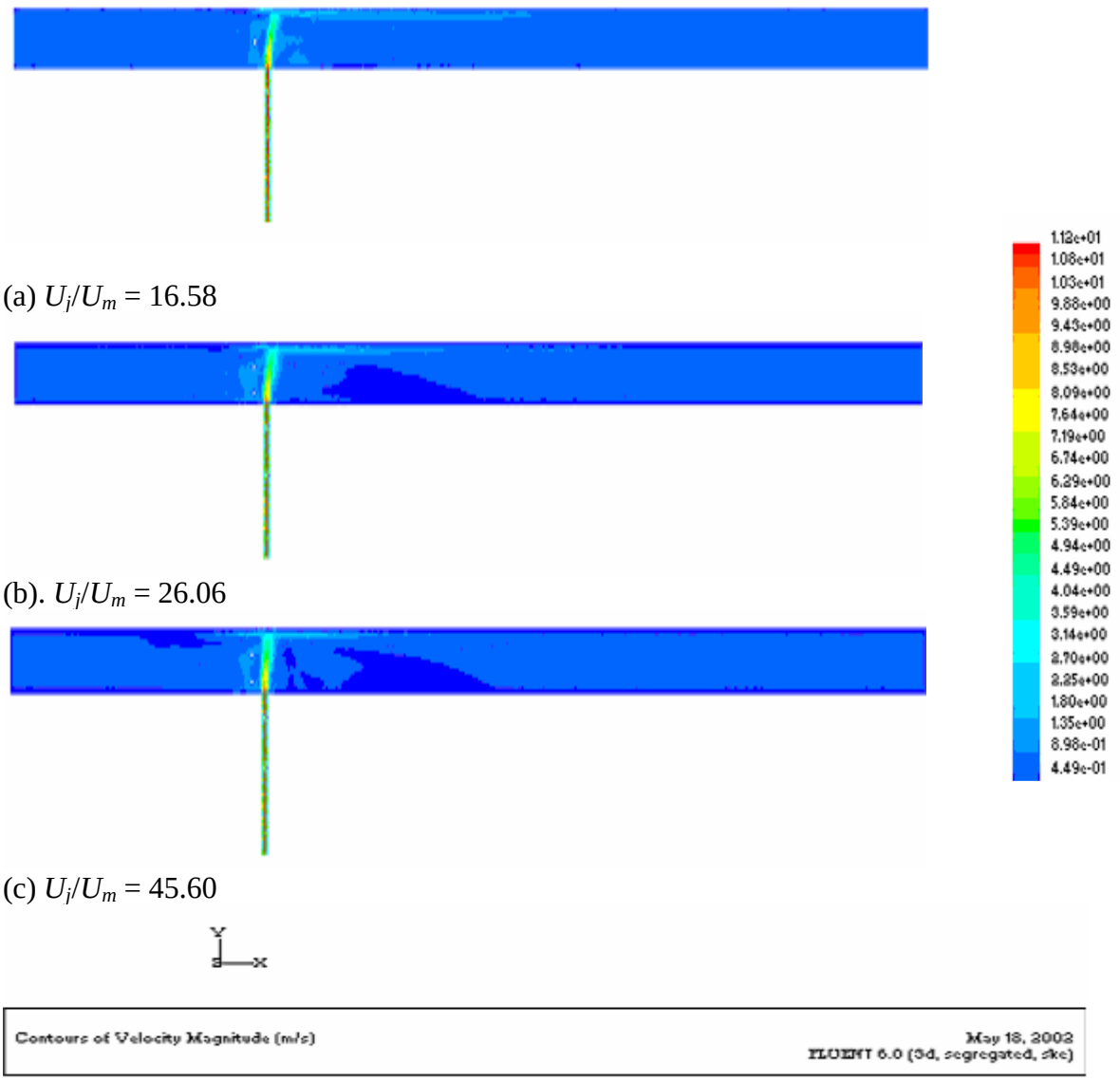

(a) U_j/U_m = 16.58

(b). U_j/U_m = 26.06

(c) U_j/U_m = 45.60

Figure 7.12: Velocity (m/s) contours of (a) U_j/U_m = 16.58 (b) U_j/U_m = 26.06 (c) U_j/U_m = 45.60 for 1/8" side-tee.

.

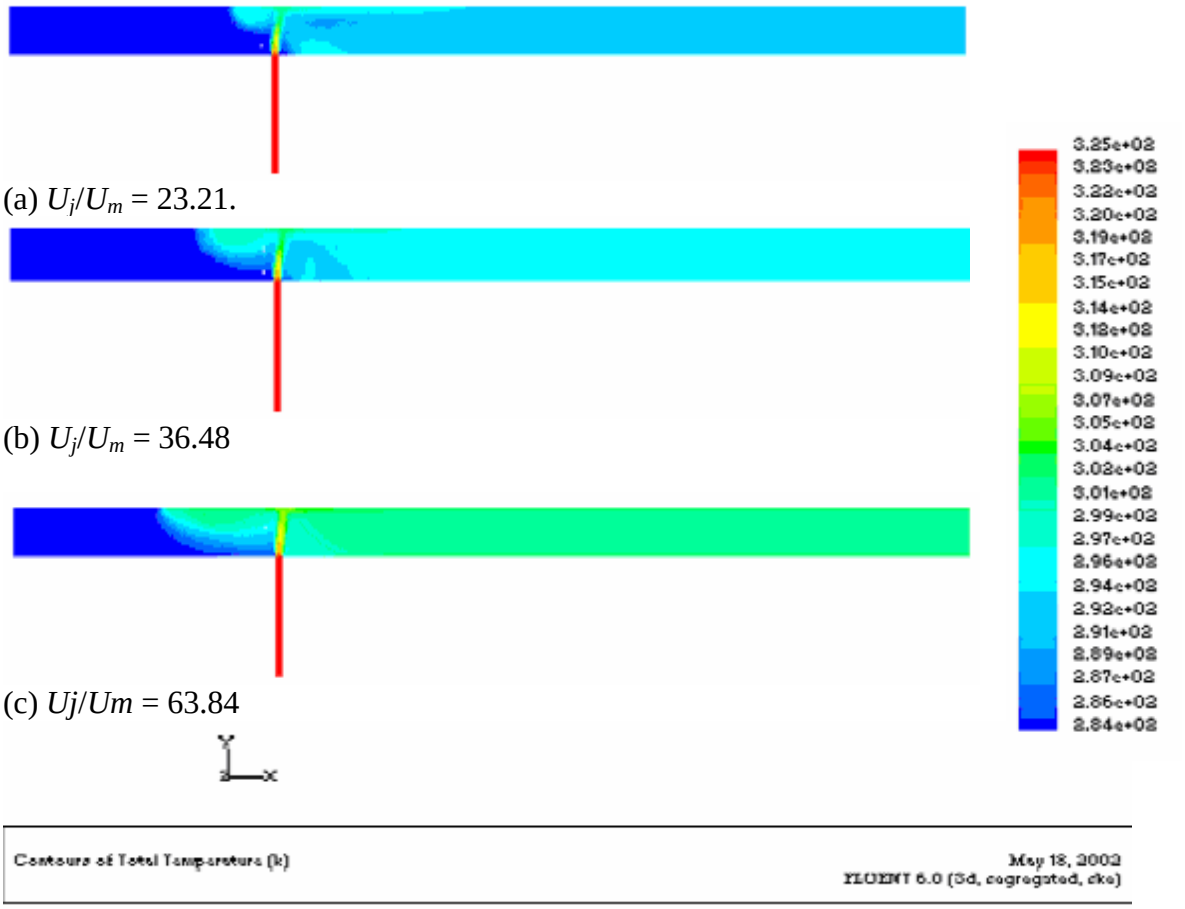

(a) U_j/U_m = 23.21.

(b) U_j/U_m = 36.48

(c) Uj/Um = 63.84

Figure 7.13: Temperature (K) contours of (a) U_j/U_m = 23.21 (b) U_j/U_m = 36.48 (c) U_j/U_m = 63.84 for 1/8" side-tee.

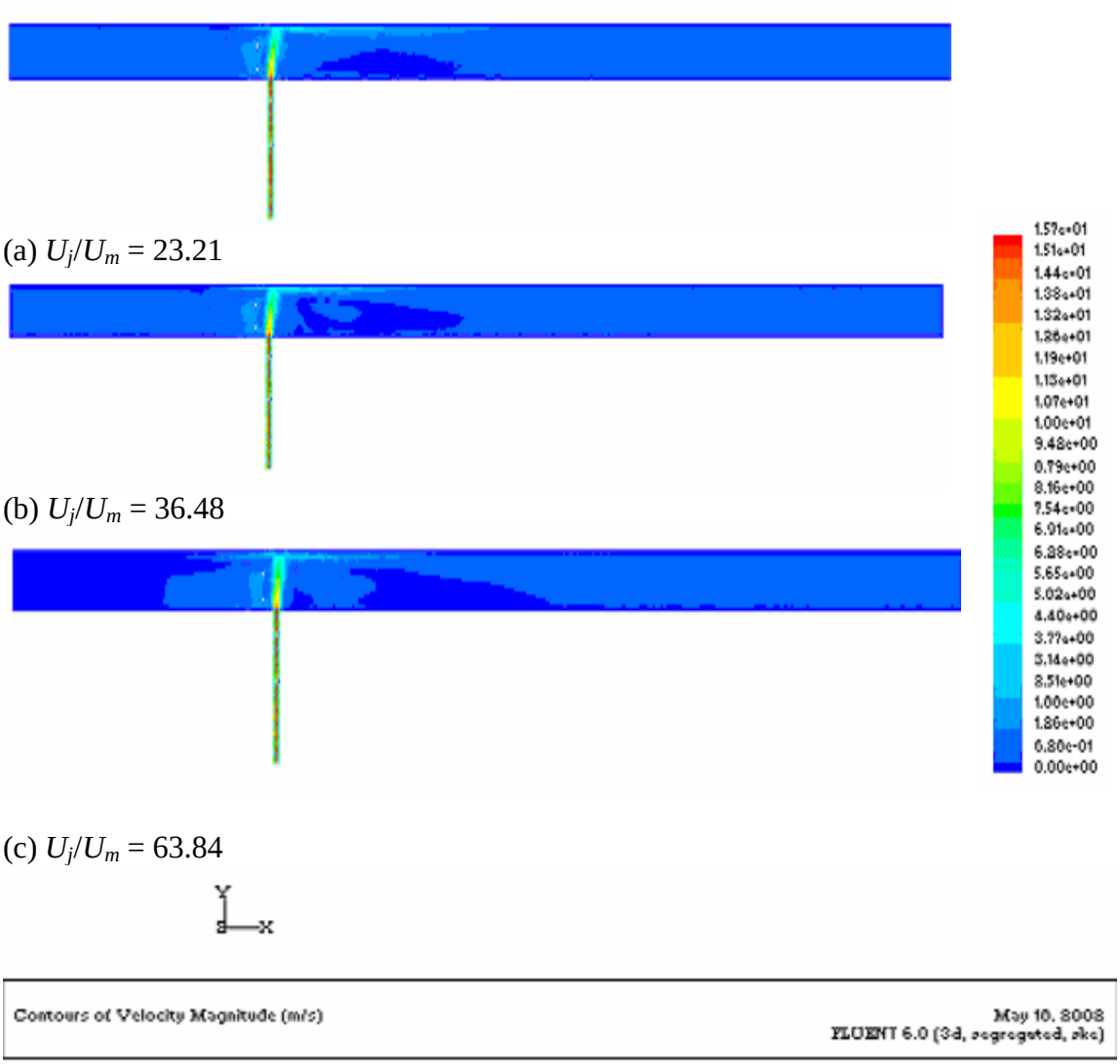

Figure 7.14: Velocity (m/s) contours of (a) U_j/U_m = 23.21, (b) U_j/U_m = 36.48, (c) U_j/U_m = 63.84 for 1/8" side-tee.

For the case of U_j/U_m = 63.84, which is the highest velocity ratio among all the cases attempted, almost two pipe diameter back mixing is observed which shows that this back mixing length should also be of interest for design purposes to calculate the total length of main pipe required for mixing.

Unlike the trend for the low velocity zone, the low temperature zone virtually became non-existent for a velocity ratio of 63.84. Larger low temperature zone is observed for lower velocity ratios of 23.21 and 36.48. Low temperature zone near the entrance of side stream is significant for lower velocity ratios.

Figure 7.14 shows velocity (m/s) contours for velocity ratios of 23.21, 36.48, and 63.84 respectively. The low velocity zone is more prominent for higher velocity ratio after the injection of side-fluid. Higher side-velocities result in more back flow. The jet is at almost a right-angle with the main pipe for a velocity ratio of 63.84. For lower velocity ratios, more bending towards the main pipe axis can be observed.

Figures 7.15 and 7.16 show temperature (K) and Velocity (m/s) contours for (a) U_j/U_m = 9.95, (b) U_j/U_m = 15.63, and (c) U_j/U_m = 27.36 respectively producing the same trend of results. For a velocity ratio U_j/U_m = 9.95, which is the minimum among the set of nine cases simulated, there is no back flow mixing at the jet impingement point. For all the remaining eight velocity ratios, back flow mixing is observed and it increases as the velocity ratio increases.

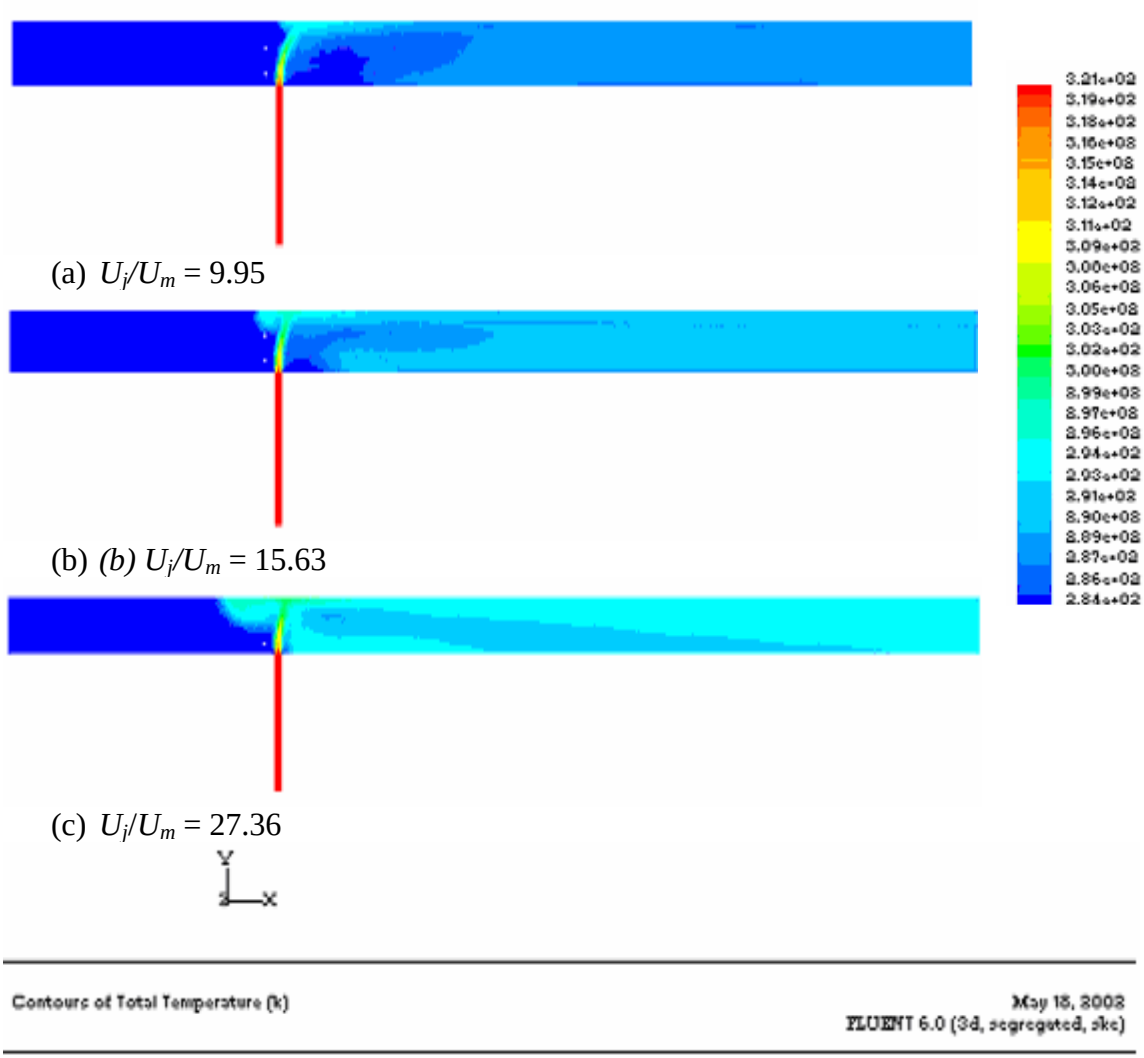

Figure 7.15: Temperature (K) contours of (a) U_j/U_m = 9.95, (b) U_j/U_m = 15.63, (c) U_j/U_m = 27.36 for 1/8" side-tee.

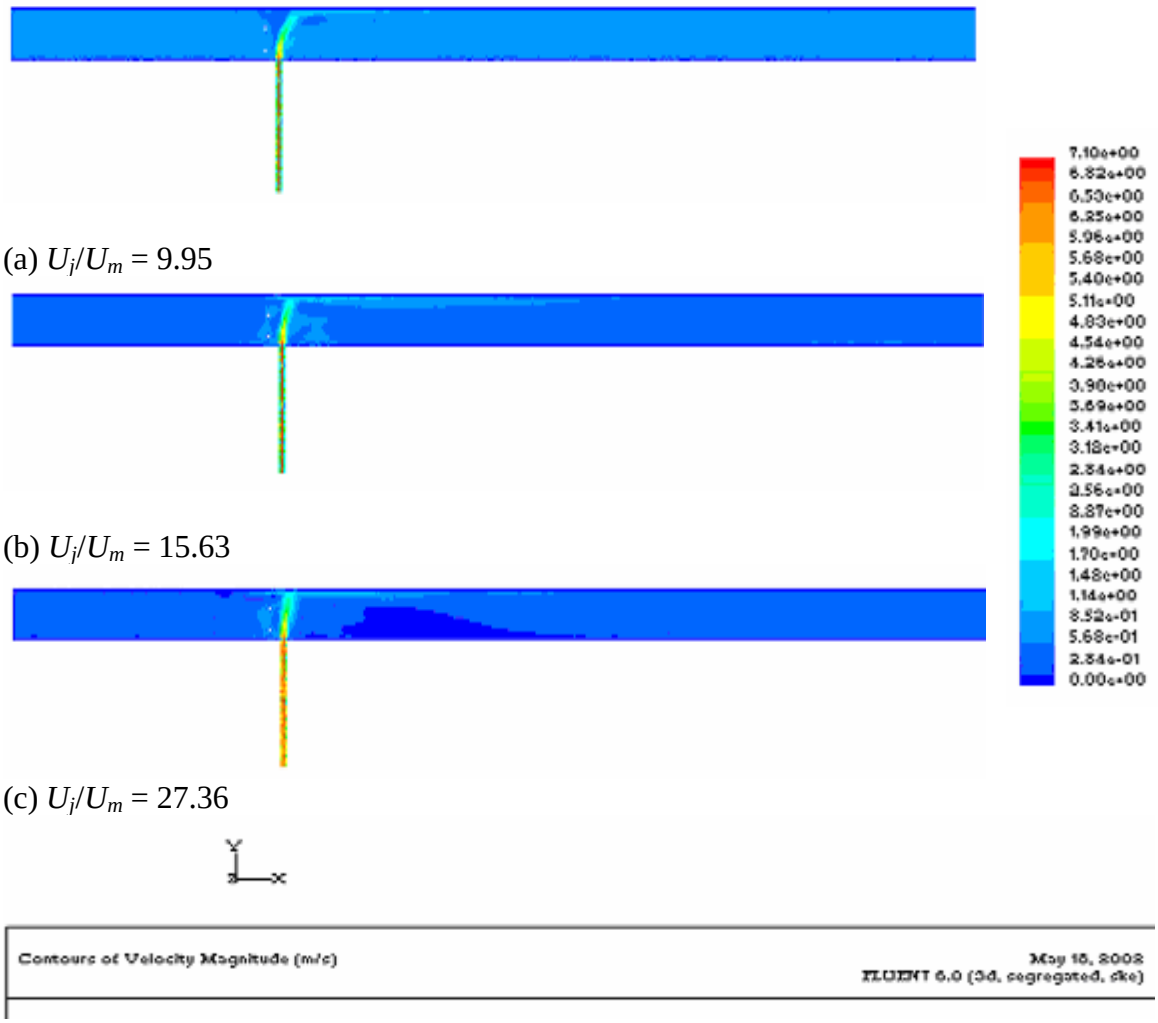

(a) U_j/U_m = 9.95

(b) U_j/U_m = 15.63

(c) U_j/U_m = 27.36

Figure 7.16: Velocity (m/s) contours of (a) U_j/U_m = 9.95, (b) U_j/U_m = 15.63, (c) U_j/U_m = 27.36 for 1/8" side-tee.

For higher velocity ratios, the side-jet impinges on the opposite wall of the pipe and this creates a region of back flow. It is clear that mixing is accomplished for higher velocity ratios due to impingement. This is not included in the length required for accomplishing 95% mixing.

From the velocity (m/s) contours, back mixing is not so significant but observing temperature (K) contours, the temperature effects significantly show the back mixing length. It was shown in the last chapter that an upstream length from the side-stream entrance equal to five diameters of main pipe is sufficient for flow to be fully developed. Therefore, this back mixing length is included in that upstream length already and no further modification is required.

The region of back mixing could be significant and it can be observed that there is a low temperature and velocity zone next to the entrance of the side-stream in the lower half of the main pipe. This low temperature zone is shown in centerline plots as the dip after the entrance of the side-stream. It could explain some problems faced by some process industries.

These problems are corrosion related and could be due to this zone of low velocity. In the literature, many researchers mentioned that in chemical engineering, except in the paper industry, it is desirable to have the side-issued jet contact the opposite wall in order to enhance rapid mixing (Cozewith [1989], Moruyama [1983]).
However, as this study shows, this impingement could cause a zone of low velocity and consequently corrosion related problems. In the sections below an attempt is made to find a jet arrangement that is better for mixing and does not constitute a source for corrosion problems. This approach will mainly deal with changing the angle of the jet.

7.3.3 Analysis and Comparison

In order to analyze the results quantitatively, values of temperature versus location along the pipe axis are plotted. These numerical values are compared with experimental values measured at exactly the same locations.

Experimental results are compared with simulated cases for 1/8" side-tee in Figures 7.17-7.19 using k-ε turbulence model. For all cases, the side-fluid is injected at 5" from the main-pipe entry and with different velocities. Velocity of the main-fluid is also varied. The temperature readings are along the centerline of the main pipe.

The discrete points are the experimental values whereas the lines show the simulated results. Differences between experimental and numerical results are observed in the vicinity of the incoming jet due to the complexity of flow in that region. The temperature peak coincides with the hot side-fluid injection into the cold mainstream. Following the injection and due to the mixing of hot and cold fluid, the temperature approaches the thermal equilibrium temperature as shown in Figure 7.17-7.19.

The discrepancy between experimental and numerical results could be minimized by using the enhancements discussed in chapter 6, namely grid adaption and the RSM model for turbulence. Any further discrepancy could be due to the fact that the thermocouples may not be recording the temperature of the hottest point of the incoming jet. This may be the case because the thermocouple is fixed while the jet behaviour (degree of bending and penetration) depends on the velocity ratio. From Figure 7.23 and chapter 6, it is observed that the k-ε model underestimates the size of peaks in the vicinity of the side-jet.

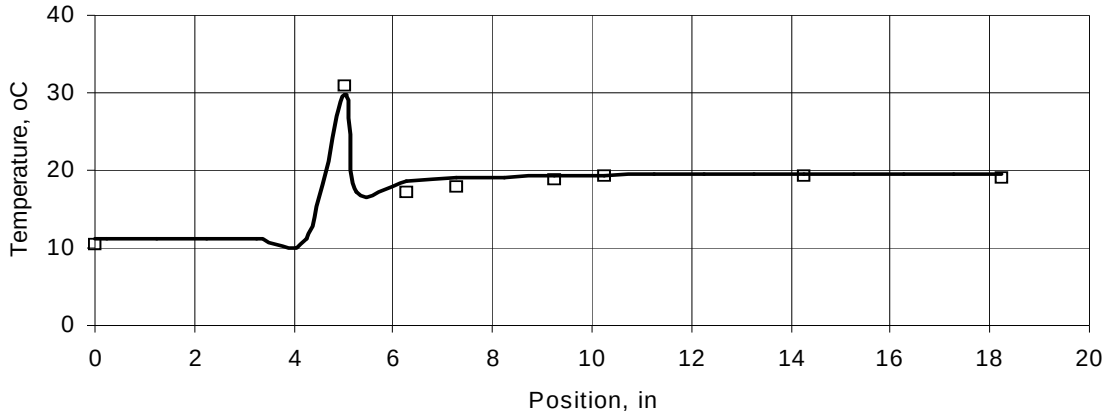

(a) U_j/U_m = 23.21 for U_m = 0.63 m/s, □ Experimental, ▬ Simulation

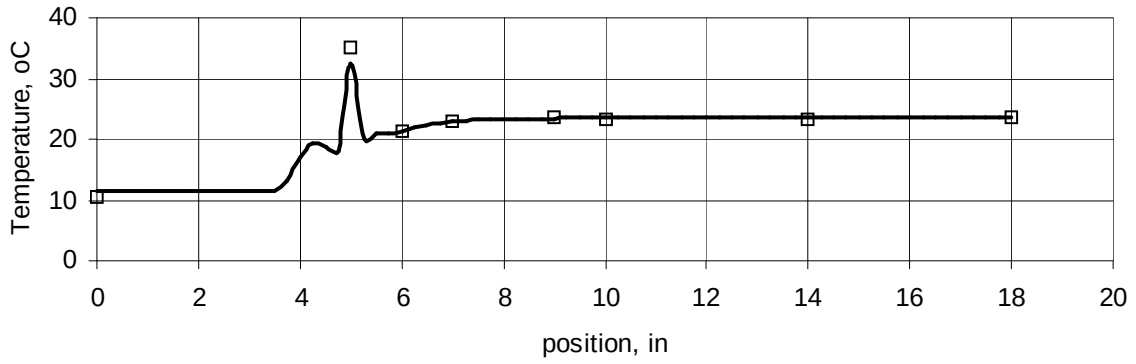

(b) U_j/U_m = 36.48 for U_m = 0.40 m/s, □ Experimental, ▬ Simulation

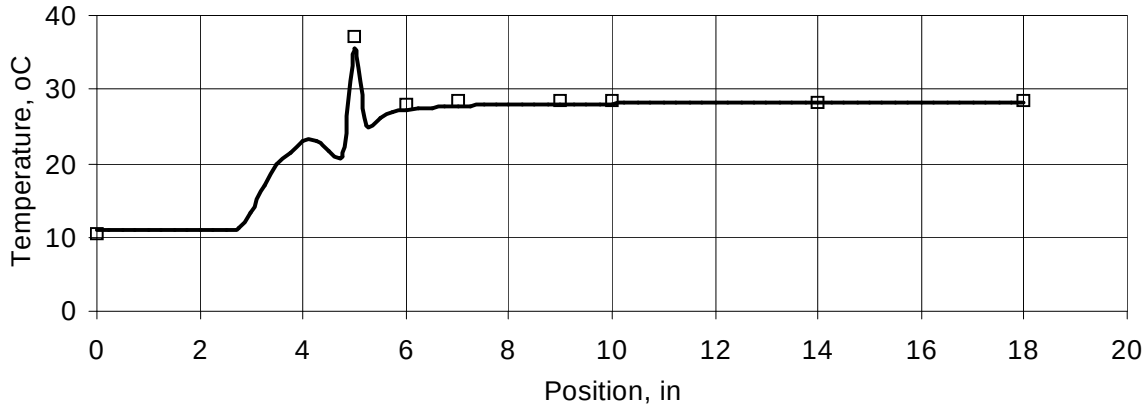

(c) U_j/U_m = 63.84 for U_m = 0.23 m/s, □ Experimental, ▬ Simulation

Figure 7.17: Comparison of experimental and simulation results for a side-tee of 1/8" and U_j = 14.73 m/s for (a) U_j/U_m = 23.21, (b) U_j/U_m = 36.48, and (c) U_j/U_m = 63.84

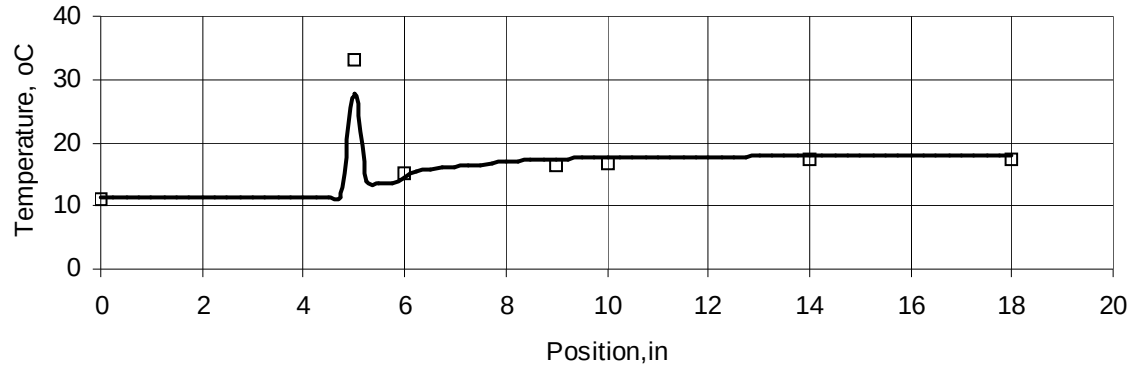

(a) U_j/U_m= 16.58 for U_m = 0.63 m/s, □ Experimental, ▬ Simulation

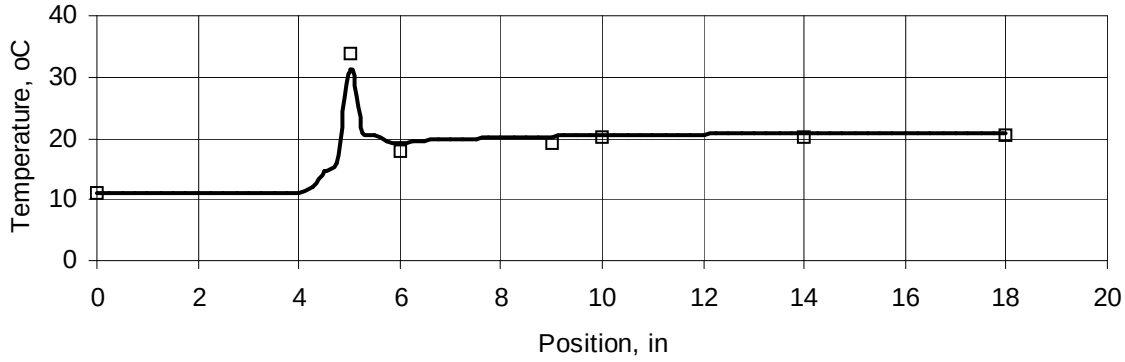

(b) U_j/U_m = 26.06 for U_m = 0.40 m/s, □ Experimental, ▬ Simulation

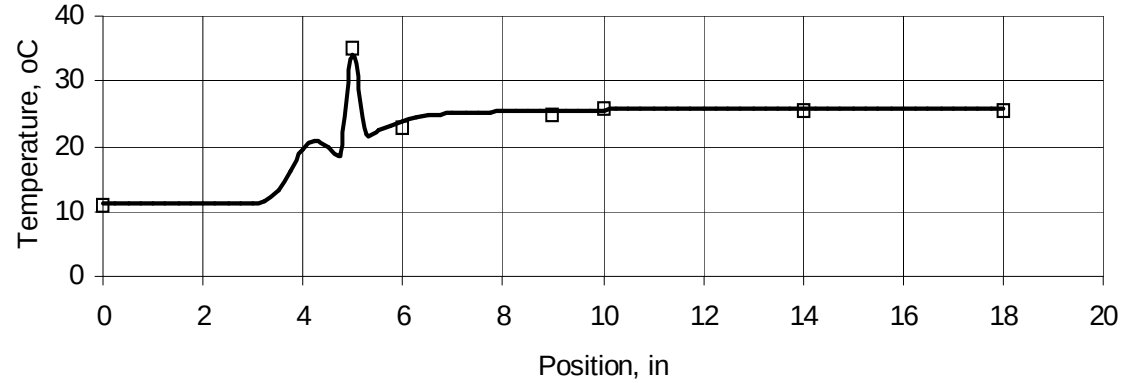

(c) U_j/U_m = 45.60 for U_m = 0.23 m/s, □ Experimental, ▬ Simulation

Figure 7.18: Comparison of experimental and simulation results for a side-tee of 1/8", where U_j = 10.52 m/s (a) U_j/U_m = 16.58 (b) U_j/U_m = 26.06, and (c) U_j/U_m = 45.60

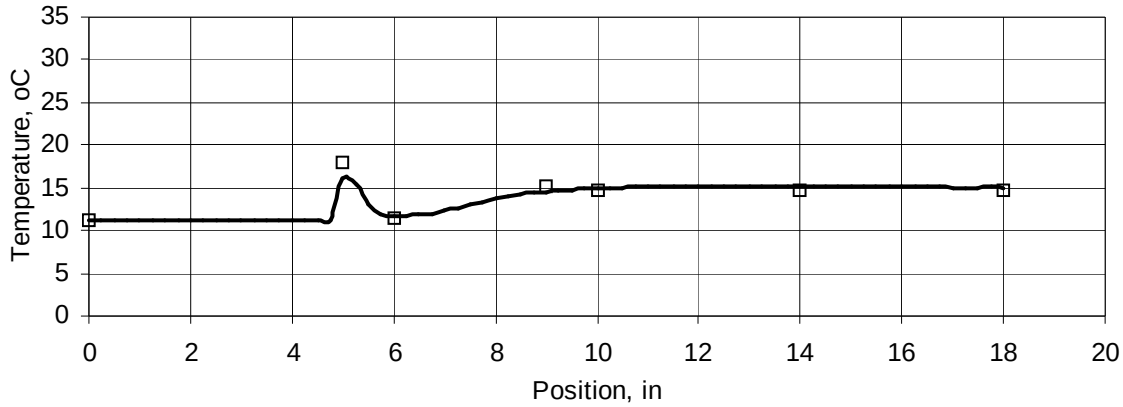

(a) U_j/U_m = 9.95 for U_m = 0.63 m/s, □ Experimental, ▬ Simulation

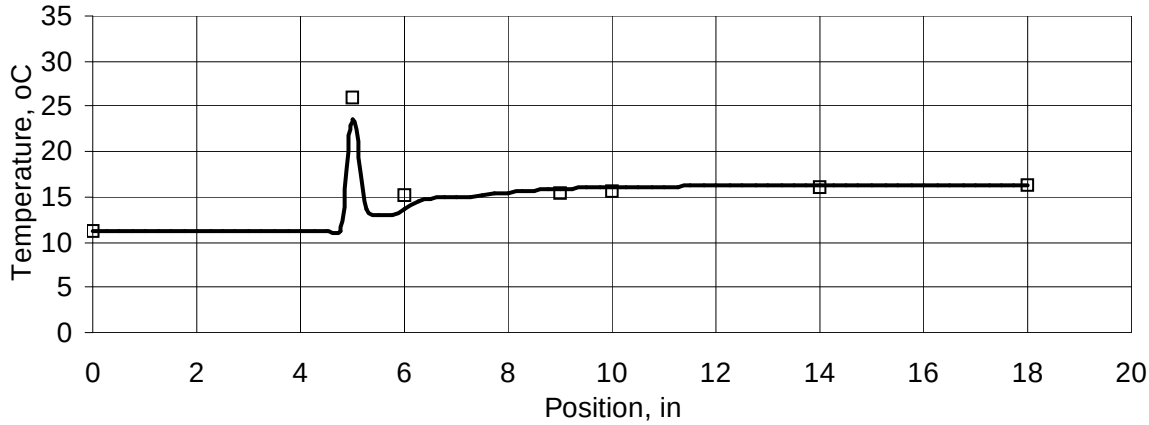

(b) U_j/U_m = 15.63 for U_m = 0.40 m/s, □ Experimental, ▬ Simulation

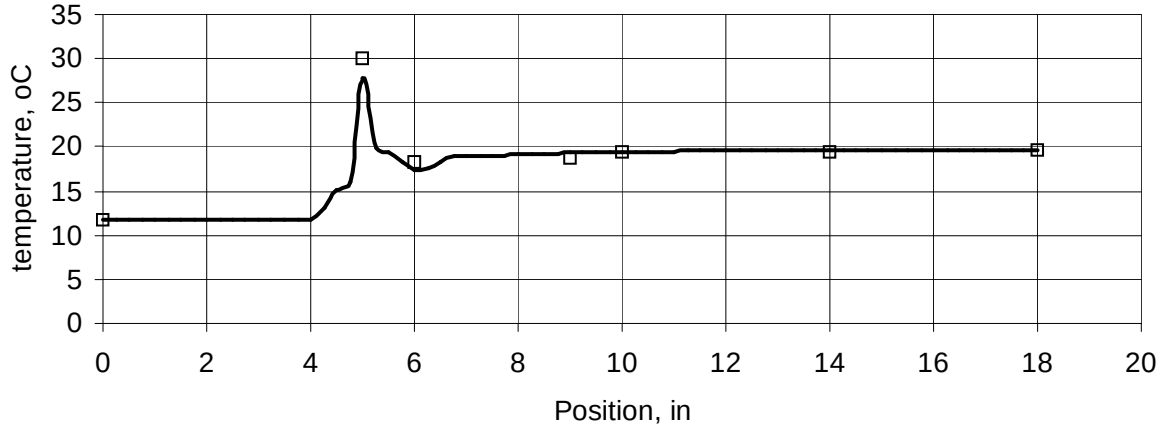

(c) U_j/U_m = 27.36 for U_m = 0.23 m/s, □ Experimental, ▬ Simulation

Figure 7.19: Comparison of experimental and simulation results for a side-tee of 1/8", and U_j = 6.31m/s (a) U_j/U_m = 9.95 (b) U_j/U_m = 15.63, and (c) U_j/U_m = 27.36.

For higher velocity ratios, another temperature peak is observed along the centerline just before the injection point. This shows that back mixing of hot fluid is occurring. For all cases, it can be seen that past the injection point, there is a temperature dip, which is due to the fact that hot fluid-jet is not along the centerline of main pipe, but it is away from the center towards the opposite wall. The value of the temperature at the dip is higher than the cold fluid temperature showing that some mixing of hot fluid with cold fluid has taken place in that region. For higher velocity ratios of 63.84 and 45.60, another temperature dip between two peaks of temperature is observed which shows that back mixing is very large and some parts of this back-mixed zone approaches the center of the main pipe.

Figure 7.19 shows that for lower velocity ratios there is much less back mixing. For velocity ratio of 9.95 (Figure 7.19-a), the side-fluid is neither impinging nor is bending along the center of main pipe because the dip temperature following the injection of hot side-fluid is closer to the upstream main-fluid temperature. For a velocity ratio of 26.06 (Figure 7.18-b) there is no significant temperature dip after the side-fluid entrance.

Since the side-jet for this case does not immediately follow the centerline of the main pipe (Figure 7.12), it can be deduced that mixing is taking place due to the turbulence of the jet and the flow in the main pipe.

Figure 7.20 shows a plot of temperature along the centerline of the main pipe. The change in temperature plots is observed as the number of reading points is increased along the centerline of main pipe. For U_j/U_m = 17.1 different racks of 16, 61, and 100 points are considered along the centerline of main pipe. For these racks, the temperature is plotted against the points in Figure 7.20. These plots show that some temperature peaks

could be easily missed if the number of points (readings) is not enough. These peaks in the vicinity of the side-jet are very sensitive to the number of points and their proximity to each other. The plot shows that a few millimeter change of thermocouple position changes the temperature reading significantly, which may effect the results final appearance. The installation of thermocouples very close to each other was also physically difficult.

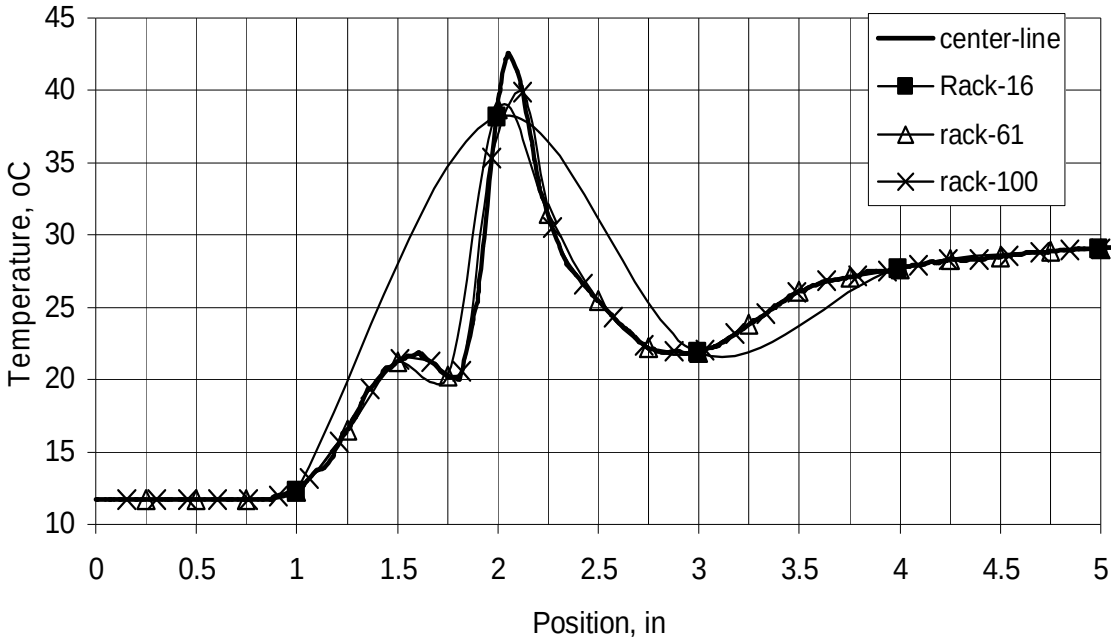

Figure 7.20: For a side-tee of 1/4", U_j/U_m = 17.1 for U_j = 3.94 m/s using RSM model. Jet entrance is at 2". A part of 5" of total pipe length along x-axis is taken.

7.3.4 Results for 1/4", 90^{o} Side-Tee

For a 1/4” right-angle side-tee with 1” main pipe, experiments are also done for a set taking U_j = 3.94, 2.63, and 1.57 m/s with U_m = 0.63, 0.40, 0.23 m/s. Temperatures averaged over a few seconds are used for the main- and side-fluids. Flow rates are measured using calibrated rotameters for velocity calculations. Temperature of fluid along the centerline of the main pipe is plotted versus position.

All the experimental cases are simulated. Experimental and numerical results show good agreement as shown in Figures 7.21-7.23. Line plots show the simulation results of temperature at centerline of main pipe whereas, square points show experimental results as read by thermocouples. A higher temperature peak shows the side hot-fluid entrance. The temperature then decreases as the cold fluid of the main pipe is mixed with the hot fluid of side-tee. The k-ε model is used to model turbulence and as mentioned earlier, it tends to underestimate the temperature peaks. At around 5 inch, in the vicinity of side stream entrance some discrepancies exist for some velocity ratios. These are due to complex flow geometry and thermocouple reading sensitivity already discussed in the previous section and in section 7.1.

These discrepancies were reduced by using grid adaption and the RSM model. When RSM model is used instead of the k-ε model, with grid adaption, better agreement is obtained for the temperature in the vicinity of the jet entrance. Figure 7.23a show temperature plots along main pipe centerline using RSM with adaption for velocity ratios of 17.1, 6.22, 9.77, and 11.4. These plots show much better agreement with experiments.

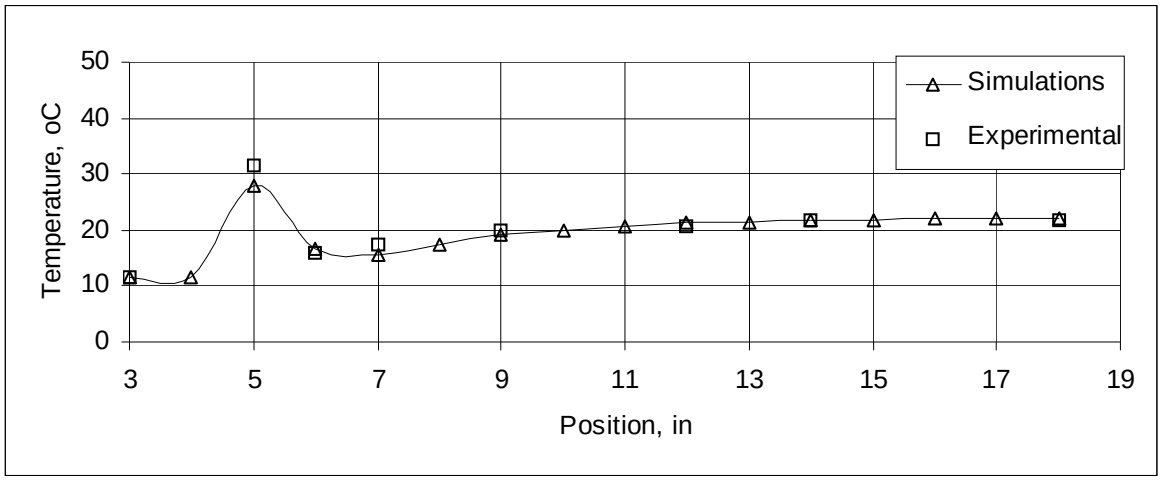

(a) U_j/U_m = 6.22, U_m = 0.63 m/s

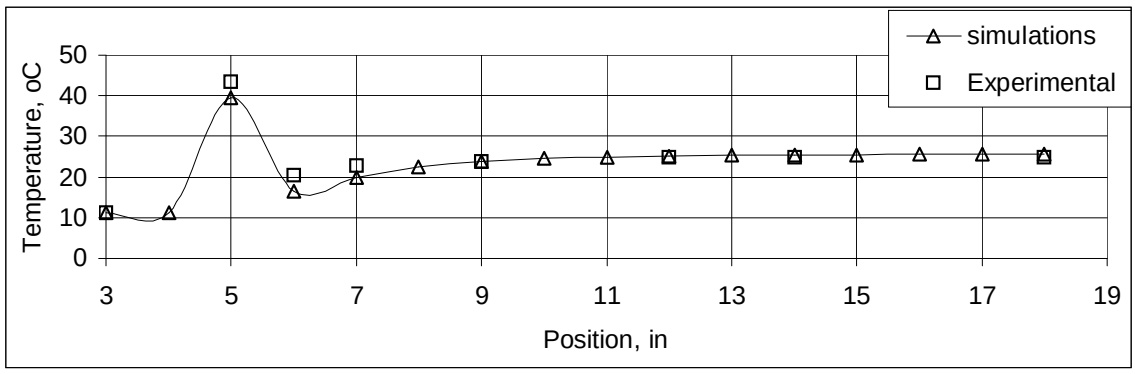

(b) U_j/U_m = 9.77, U_m = 0.40 m/s

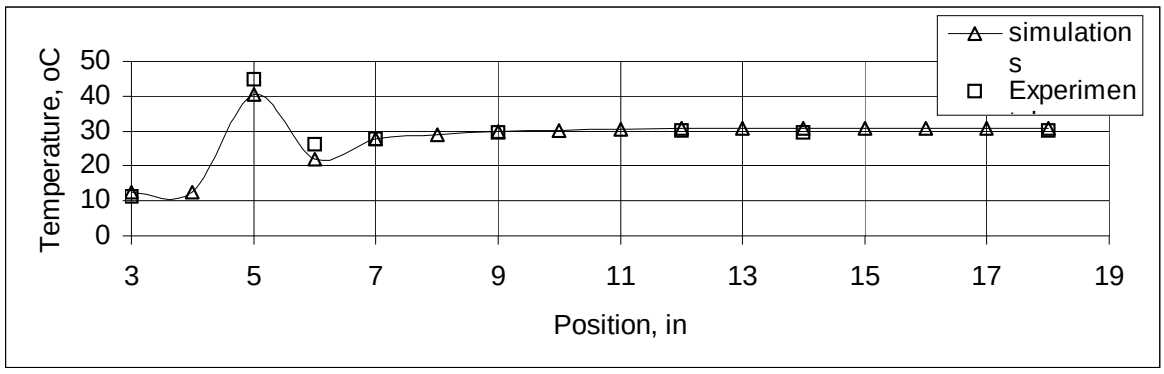

(c)U_j/U_m = 17.10, U_m = 0.23 m/s

Figure 7.21: Comparison of experimental and simulation results for 1/4" side-tee, U_j = 3.94 m/s (a) U_j/U_m = 6.22, (b) U_j/U_m = 9.77, and (c) U_j/U_m = 17.1, (k-ε)

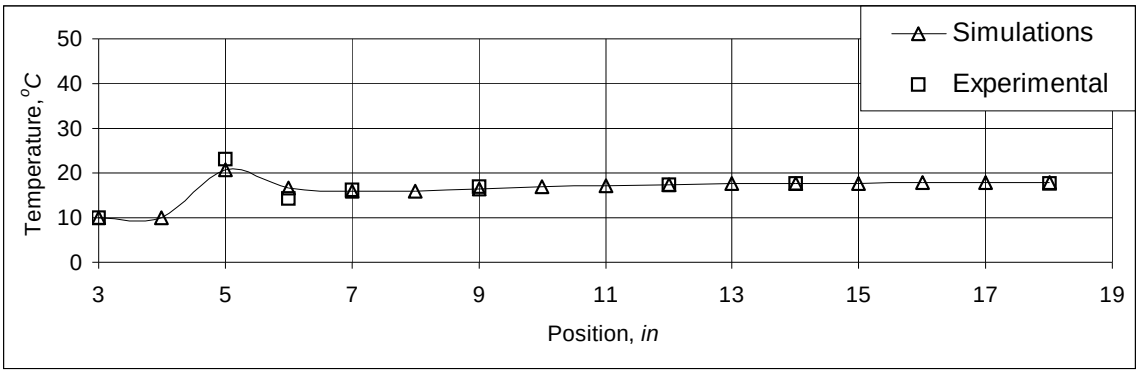

(a) U_j/U_m = 4.15, U_m = 0.63 m/s

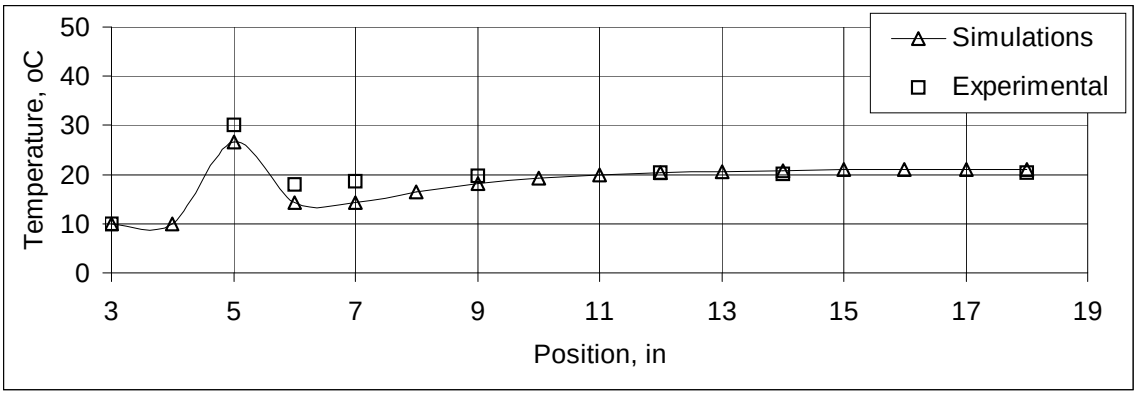

(b) U_j/U_m = 6.51, U_m = 0.23 m/s

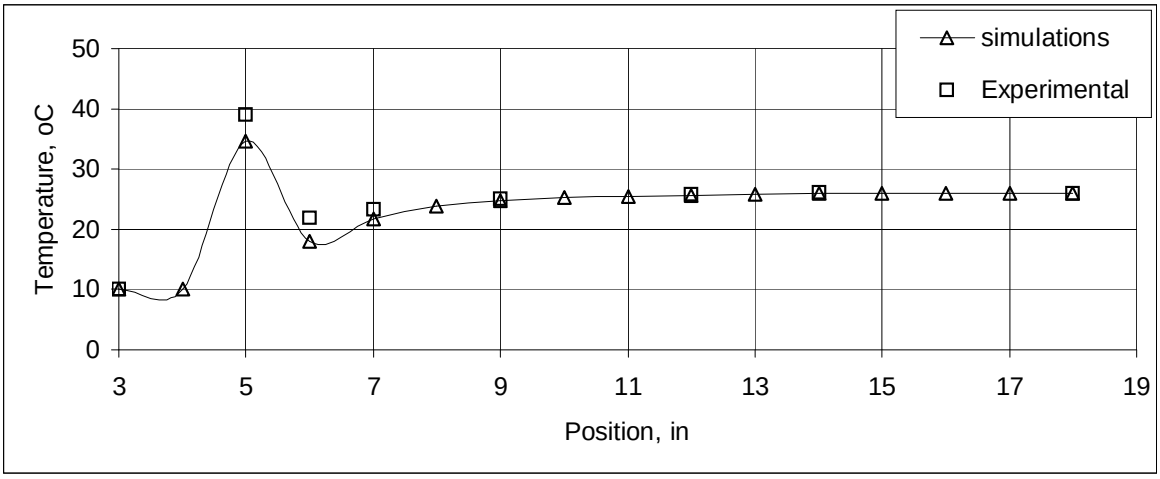

(c)U_j/U_m = 11.4, U_m = 0.23 m/s

Figure 7.22: Comparison of experimental and simulation results for 1/4" side-tee, U_j = 2.63 m/s (a) U_j/U_m = 4.15, (b) U_j/U_m = 6.51, and (c) U_j/U_m = 11.4, (k-ε)

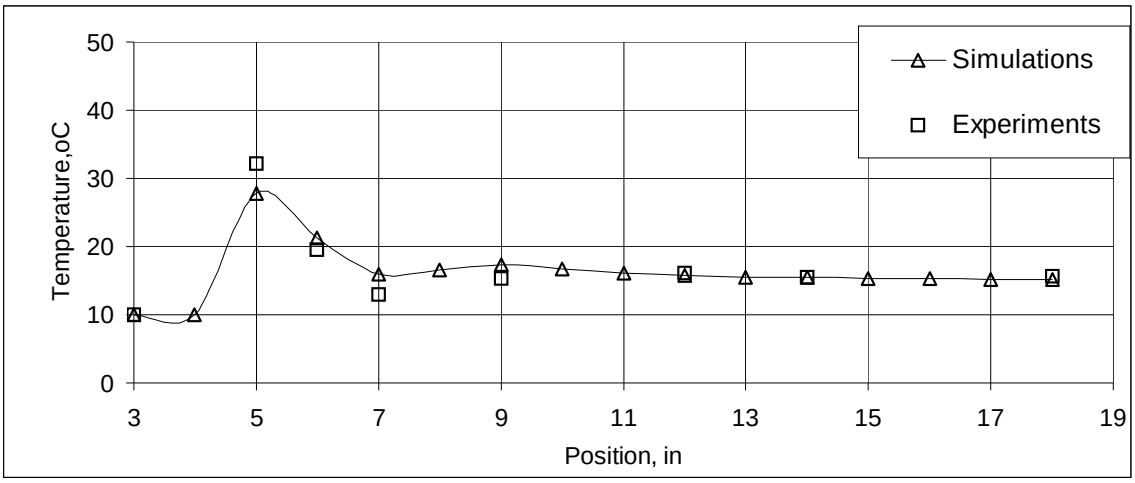

(a) U_j/U_m = 2.49, U_m = 0.63 m/s

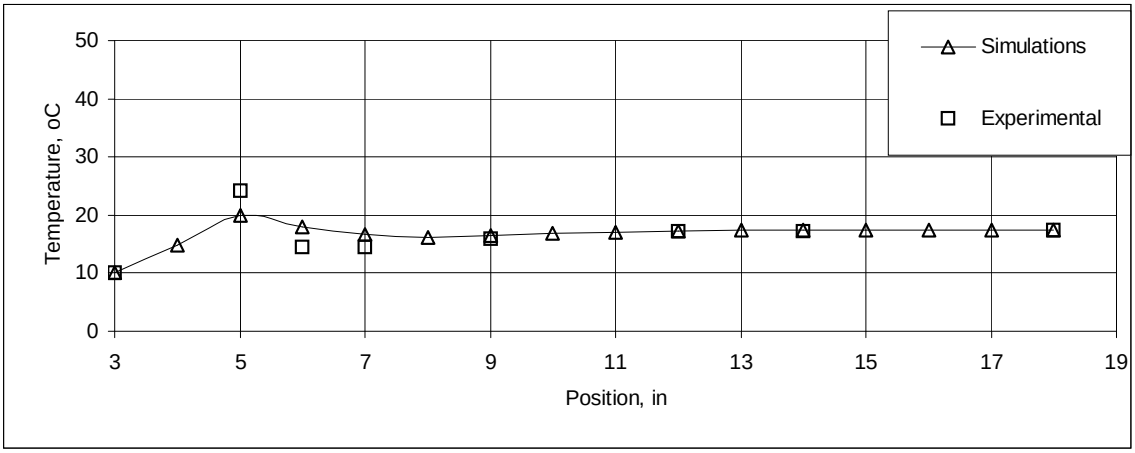

(b) U_j/U_m = 3.91, U_m = 0.40 m/s

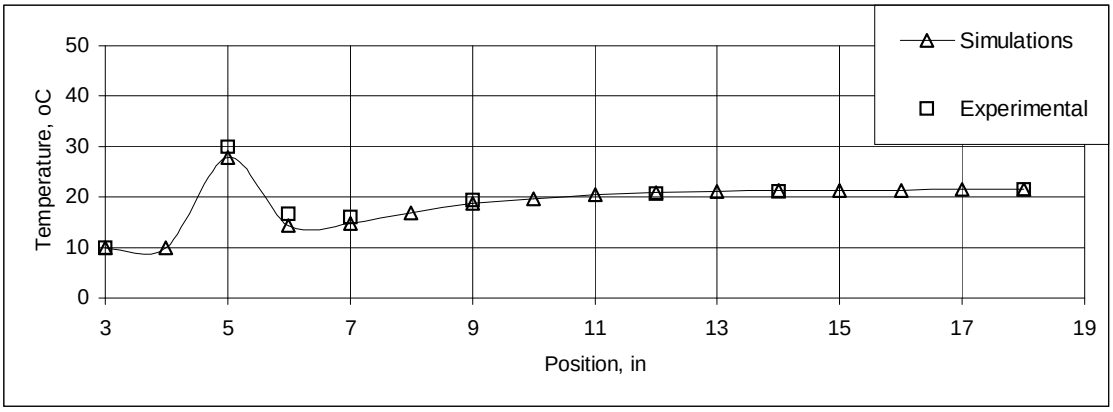

(c) U_j/U_m = 6.84, U_m = 0.23m/s

Figure 7.23: Comparison of experimental and simulation results for 1/4" side-tee, U_j = 1.57 m/s (a) U_j/U_m = 2.49, (b) U_j/U_m = 3.91, and (c) U_j/U_m = 6.84, (k-ε)

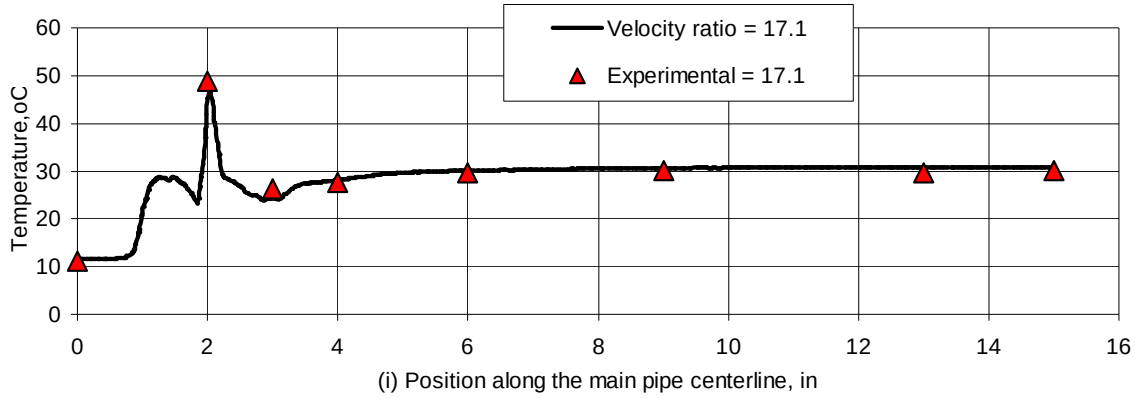

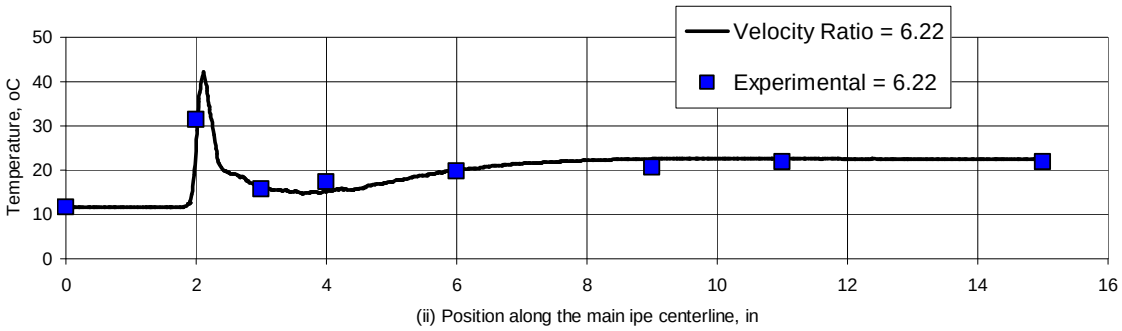

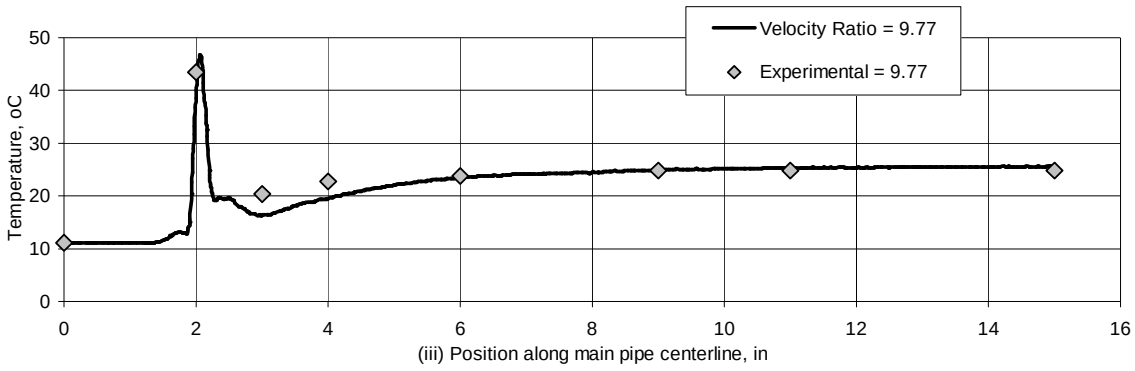

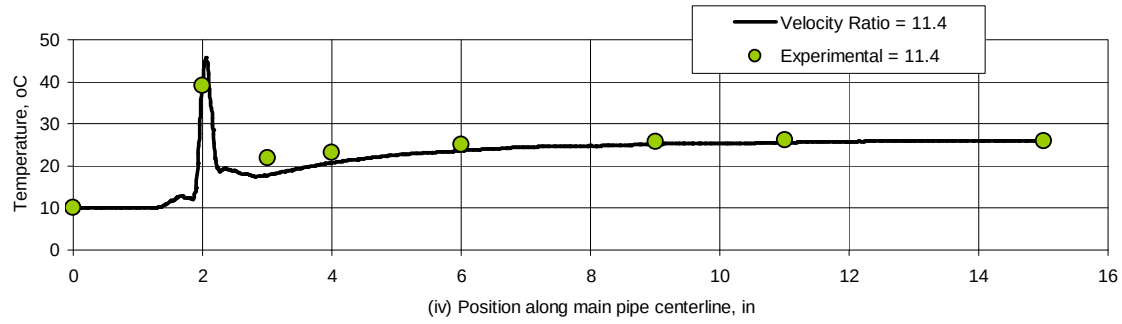

Figure 7.23a: Comparison of experimental and simulation results for 1/4" side-tee, for U_j/U_m = 17.10 (U_j = 3.94 m/s, U_m = 0.23 m/s), U_j/U_m = 6.22 (U_j = 3.94 m/s, U_m = 0.63 m/s), U_j/U_m = 9.77 (U_j = 3.94 m/s, U_m = 0.40 m/s), and U_j/U_m = 11.4 ((U_j = 2.63 m/s, U_m = 0.23 m/s), (RSM)

7.3.5 Temperature (K) and Velocity (m/s) contours for 1/4", 90^o Side-Tee

The line plots presented in the Figures of the previous section illustrated how the temperature varies along the main pipe centerline for various U_j/U_m ratios. They also showed that experimental results agree well with numerical predictions. However, it was difficult to predict the degree of back mixing and impingement from the line plots. It was also not clear from those plots whether side-stream is bending towards the center of the main pipe or away from it. This information can be easily obtained from plots of temperature (K) and/or velocity (m/s) contours. Figures 7.24-7.26 show the temperature (K) and the velocity (m/s) contours for geometry of 1" main pipe and 1/4" side-tee and for velocity ratio U_j/U_m of 17.10, 9.77, and 6.22 respectively. The jet-velocity for these three cases is kept constant at 3.94 m/s. These plots show clearly the degree of back mixing for various velocity ratios. It is clear that the degree of impingement and consequently back mixing decreases as the velocity ratio decreases. Figures 7.24-7.25 show clear impingement of the incoming side-jet on the opposite wall. Figure 7.26 shows a weak or no impingement on the wall for a velocity ratio of 6.22.

A close inspection of these plots show that the pipe length required to achieve mixing decreases as the velocity ratio and consequently the impingement increases. These results agree with the finding of Maruyama *et al.* [1983], Cozewith and Busko [1989] and Forney and Monclova [1994]. However, this study shows in section 7.6 that better mixing is achieved by adjusting the angle of the side-jet injection.

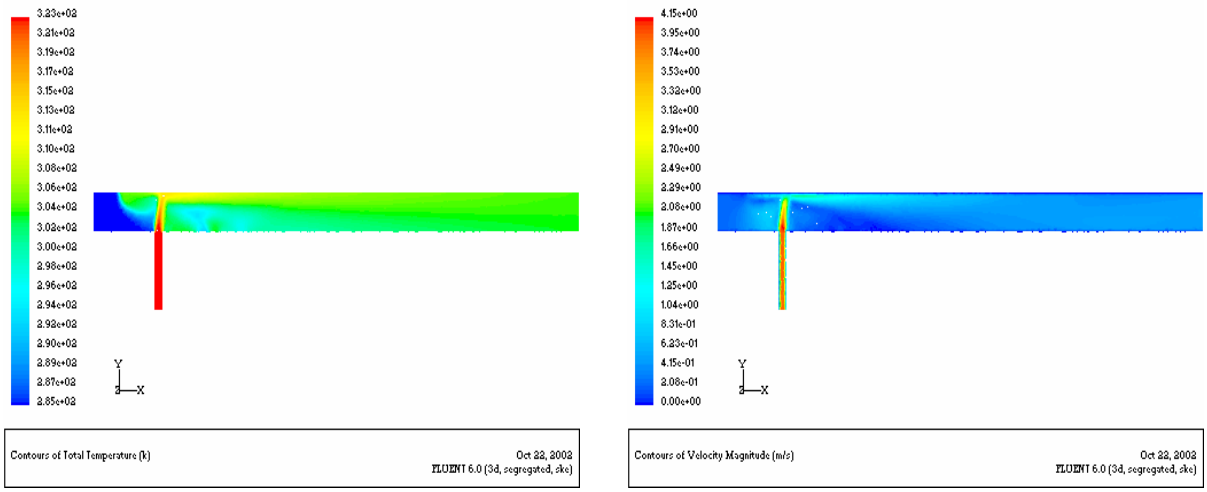

(a) (b)

Figure 7.24: (a) Temperature (K) and (b) Velocity (m/s) contours of case, U_j/U_m = 17.10, for U_j = 3.94 m/s in 1/4" side-tee velocity.

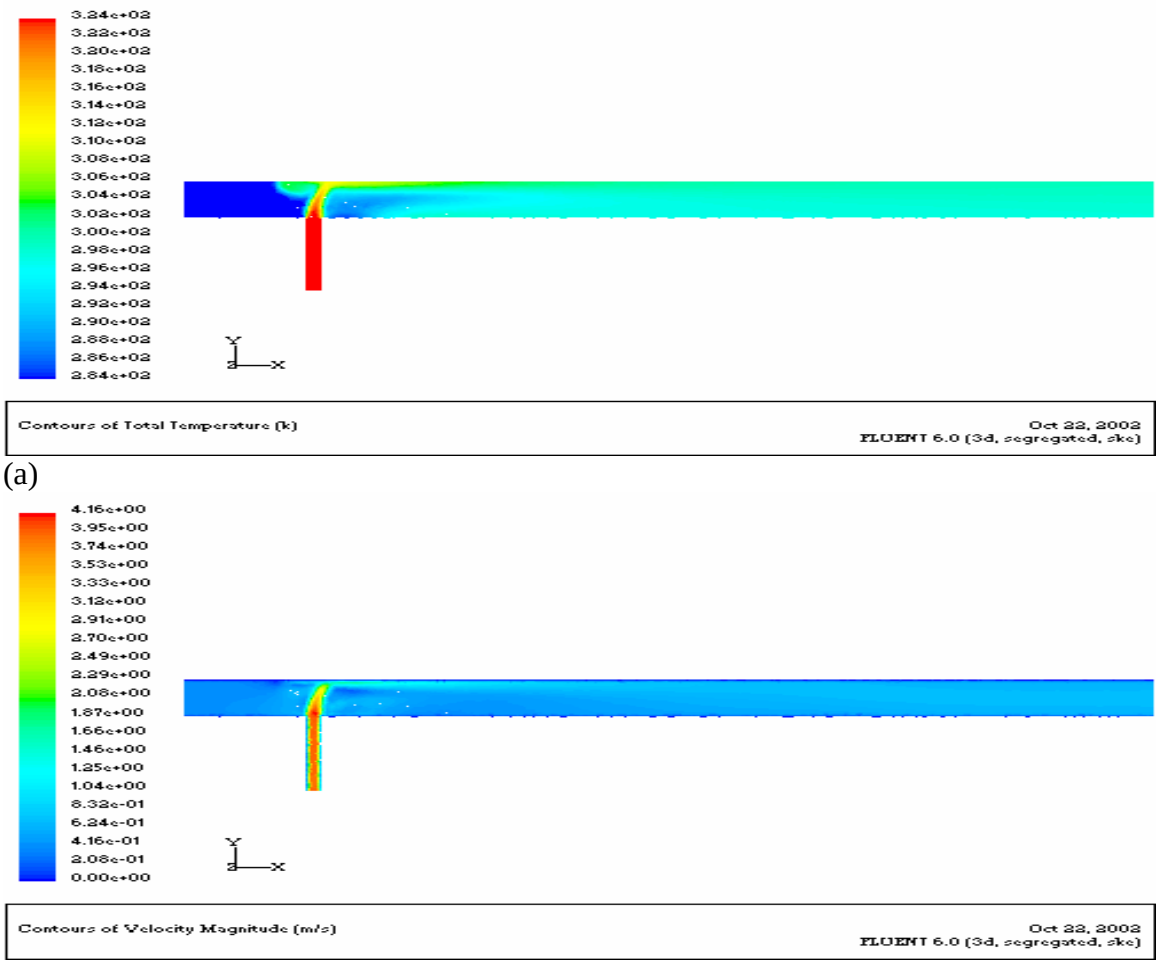

(a)

(b)

Figure 7.25: (a) Temperature (K) and (b) Velocity (m/s) contours for U_j/U_m = 9.7, for U_j = 3.94 m/s in 1/4" side-tee velocity.

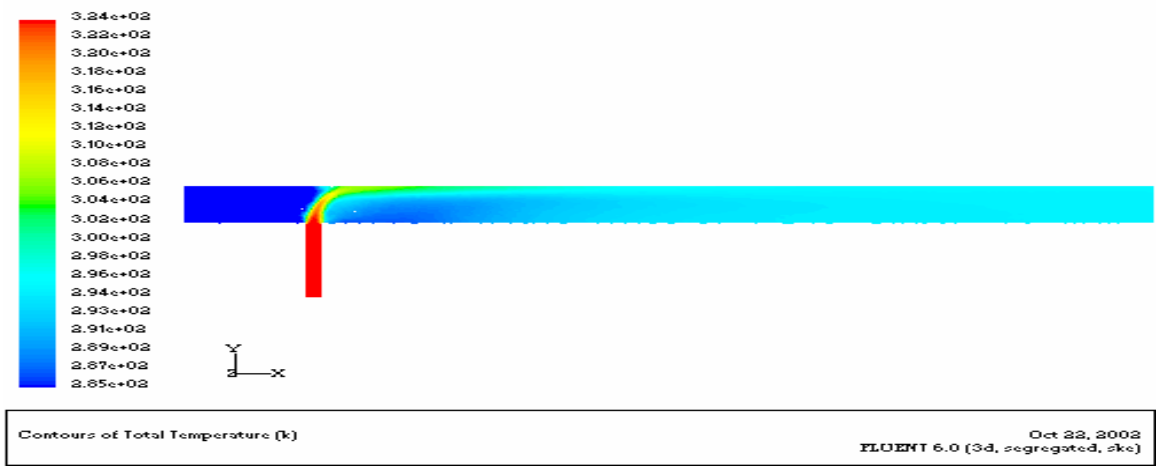

(a)

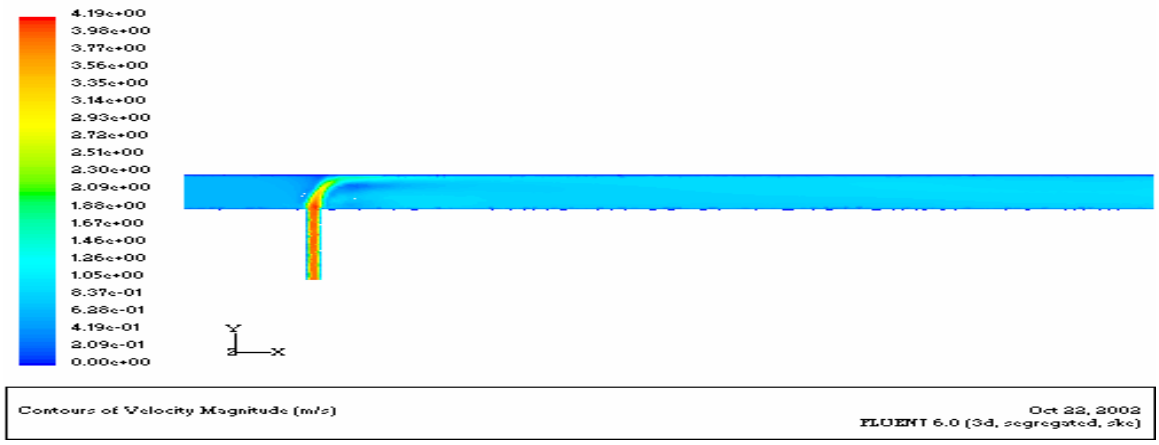

(b)

Figure 7.26: (a) Temperature (K) and (b) Velocity (m/s) contours, U_j/U_m = 6.22, for U_j = 3.94 m/s in 1/4" side-tee velocity.

More velocity ratios are considered by changing the jet velocity to 2.63 m/s and using the same velocities in the main pipe. Three velocity ratios of 11.4, 6.5 and 4.1 are obtained. Figures 7.27-7.29 show temperature (K) and velocity (m/s) contours for the above three cases. Since the jet-velocity in these cases is lower than that in Figures 7.24-7.26, the jet shows less impingement. In fact, limited back mixing and impingement are observed only for higher velocity ratio of 11.4 in Figure 7.27. The side-jet shows earlier bending towards the pipe center as the velocity ratio decreases. However, the jet penetrates most of the main fluid and reaches the opposite wall of pipe in all three cases. It can be seen that as velocity ratio decreases, the jet tends to bend faster towards the center of the main pipe. For higher velocity ratios, there is a smaller temperature zone after injection, which increases as the velocity ratios decreases. This zone is almost negligible for a velocity ratio of 2.49 where the jet side-injection from tee is bent towards center. As the side-velocity is increased, side to main velocity ratio is increased and 95% mixing is accomplished earlier.

Figures 7.30-7.32 show the temperature (K) and velocity (m/s) contours for velocity ratios of 6.8, 3.9, and 2.5. For a jet to main velocity ratio 2.5, Figure 7.32 shows that the jet is bending towards the center. There is no significant impingement except a little for the velocity ratio of 6.8 and no back mixing for any of the three cases. The pipe length required for 95% mixing is more than 13 diameters of the main pipe for velocity ratios of 4.1, 3.9, and 2.5. For these cases, the side-stream is bending towards center and cold fluid is flowing around it. Less turbulence increases the length required for fluid mixing.

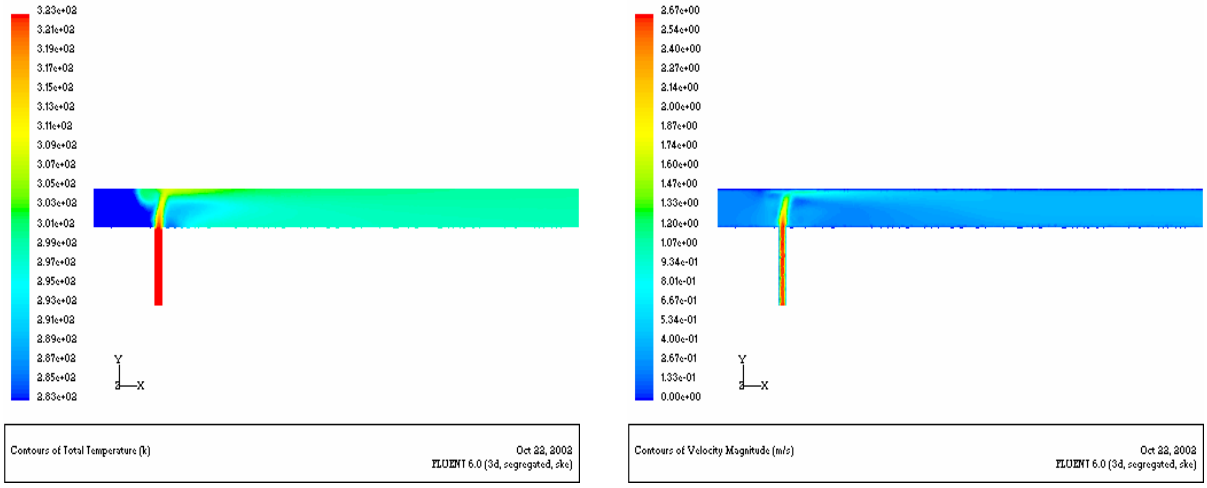

(a) (b)

Figure 7.27: (a) Temperature (K) and (b) Velocity (m/s) contours, U_j/U_m = 11.4, for U_j = 2.63 m/s in 1/4" side-tee velocity.

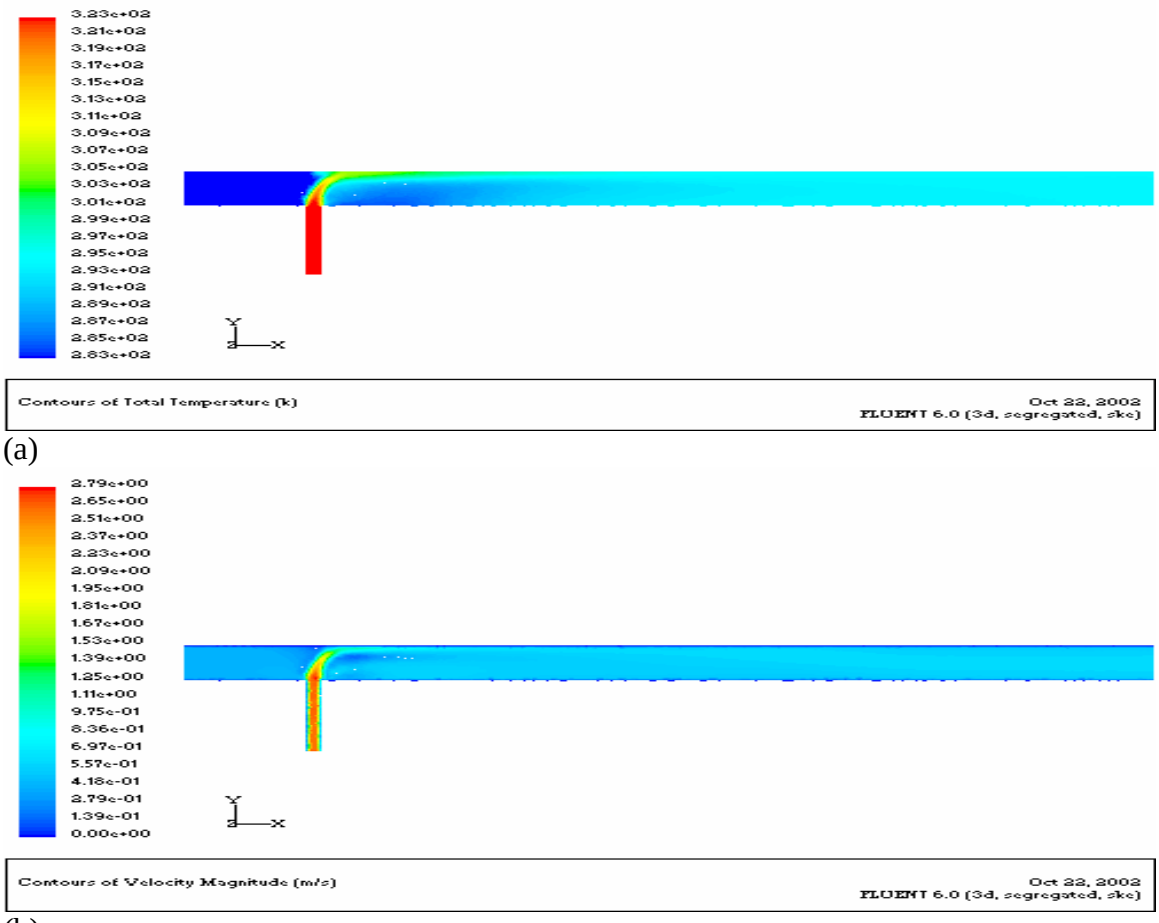

(a)

(b)

Figure 7.28: (a) Temperature (K) and (b) Velocity (m/s) contours, U_j/U_m = 6.5, for U_j = 2.63 m/s in 1/4" side-tee velocity.

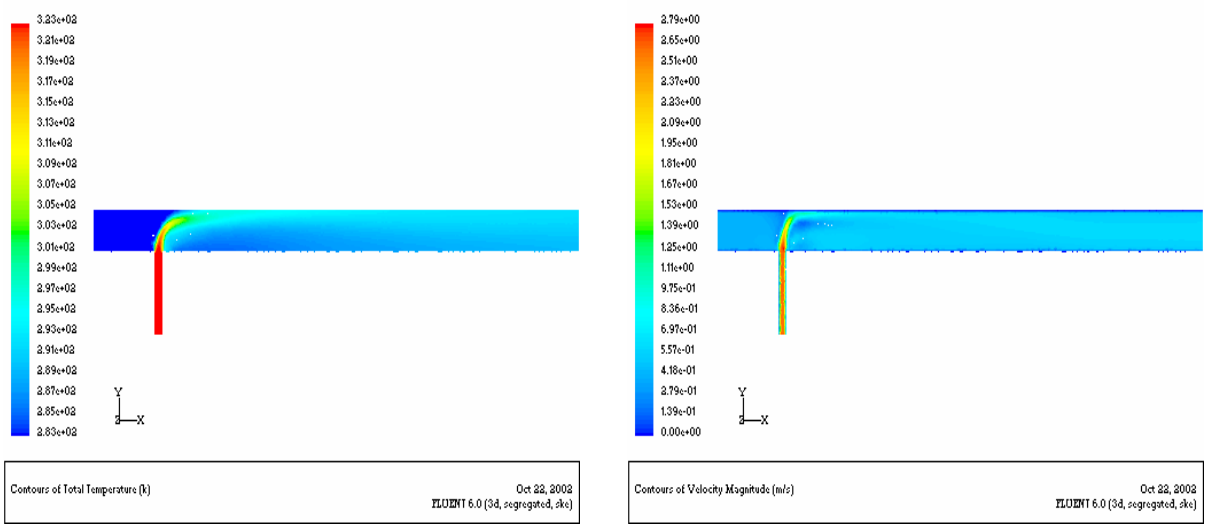

(a) (b)

Figure 7.29: (a) Temperature (K) and (b) Velocity (m/s) contours, U_j/U_m = 4.1, for U_j = 2.63 m/s in 1/4" side-tee velocity.

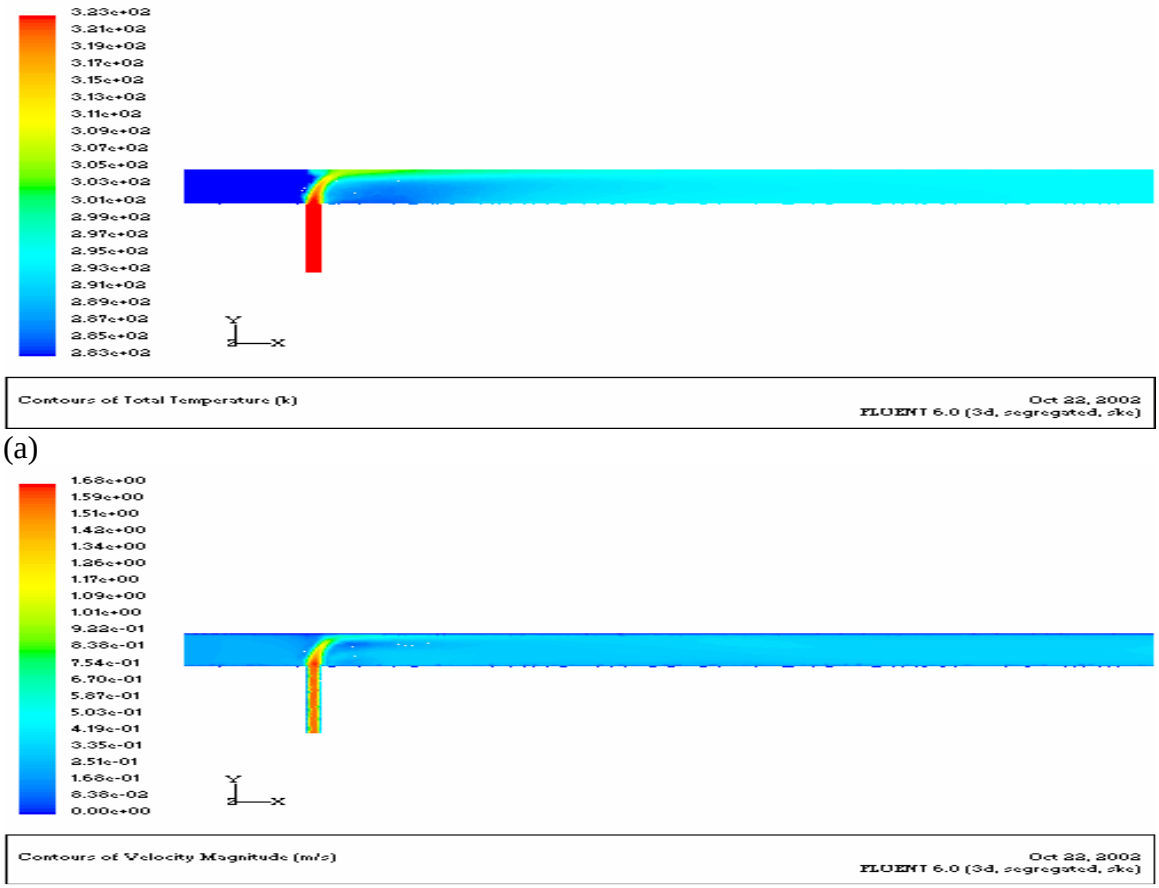

(a)

(b)

Figure 7.30: (a) Temperature (K) and (b) Velocity (m/s) contours, for U_j/U_m = 6.8, and U_j = 1.57 m/s using a 1/4" side-tee.

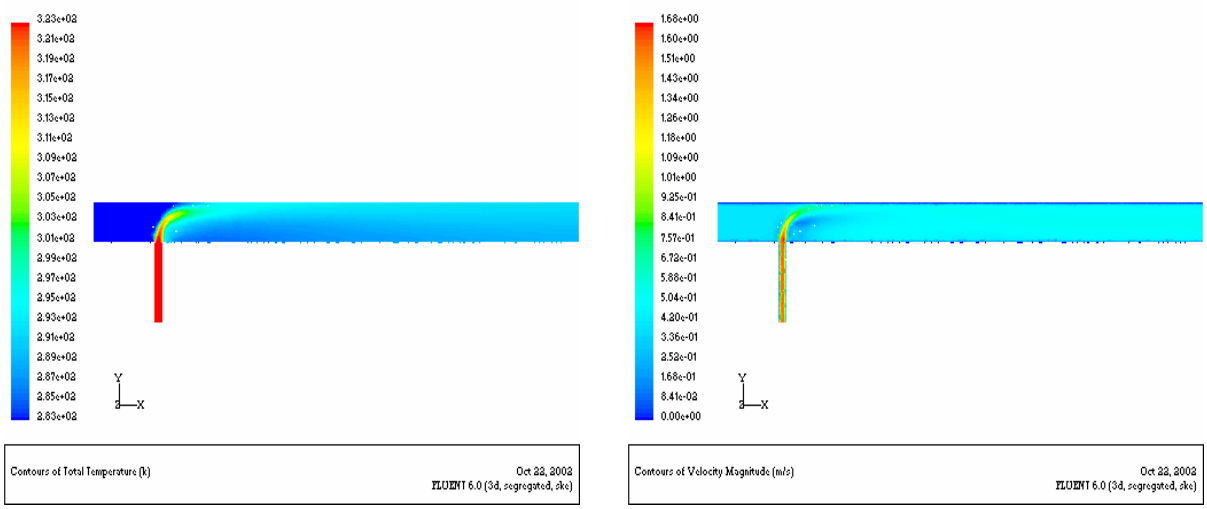

(a) (b)

Figure 7.31: (a) Temperature (K) and (b) Velocity (m/s) contours, for U_j/U_m = 3.9, and U_j = 1.57 m/s using a 1/4" side-tee.

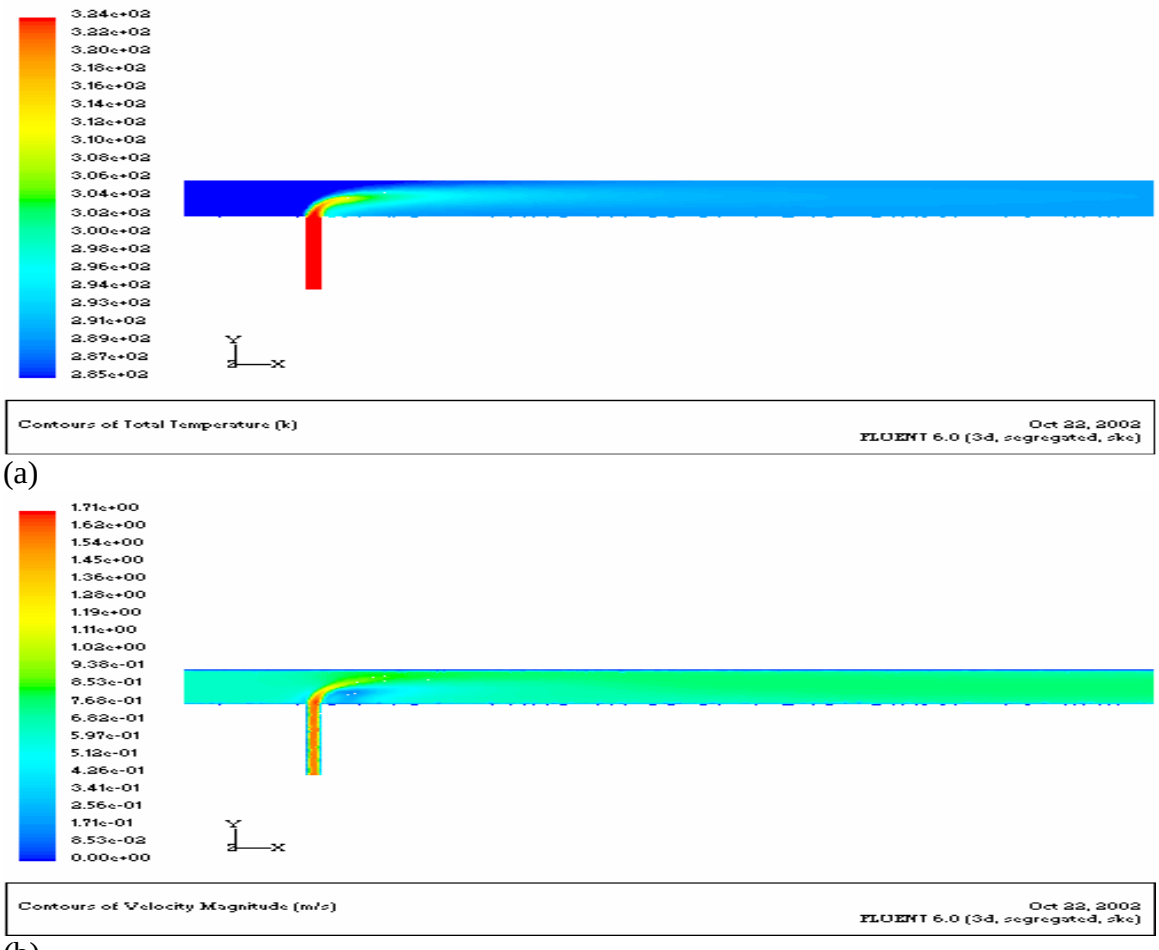

(a)

(b)

Figure 7.32: (a) Temperature (K) and (b) Velocity (m/s) contours, for U_j/U_m = 2.5, and U_j = 1.57 m/s using a 1/4" side-tee.

7.4 Mixing Plots

To gain a better picture of the degree of mixing not only along the centerline of the main pipe but also along off-center lines, temperature is plotted versus position along the centerline and four other off-center lines. These four lines are defined as follows: two in a horizontal plane passing through the pipe axis and two in a, similar vertical plane. Each line is 0.00635 m (1/4”) away from the centerline. In other words, the coordinates of the lines are: z = 0.0, y = ± 0.00635 m and y = 0.0, z = ± 0.00635 m. A large number of points, 73 in total, is chosen along each line in order to obtain the detailed profile of temperature along each line.

Figure 7.33 shows a plot of temperature versus position along these five lines for a case with 1/8” side-tee, U_j/U_m = 23.2 and U_j = 3.94 m/s. This Figure shows that temperature along all five lines converge to the same value at about 9 diameters from the entry of the main pipe or at about 4D downstream from the jet inlet. Figures 7.34 and 7.35 show similar plots for U_j/U_m of 36.4 and 63.8 respectively, for the same geometry. The value of U_j for the last two Figures is 3.94 m/s.

These line plots show a typical mixing lines behavior, i.e., some positions show an overshoot while temperature along certain positions approach the equilibrium temperature slower than others. These lines still do not give full details of mixing in any full cross-sectional plane. This means although the hot and cold fluids become well mixed along the centerline and other nearby lines at a certain pipe length from the jet inlet, there could be other regions of the flow closer to the wall where mixing has not been achieved yet.

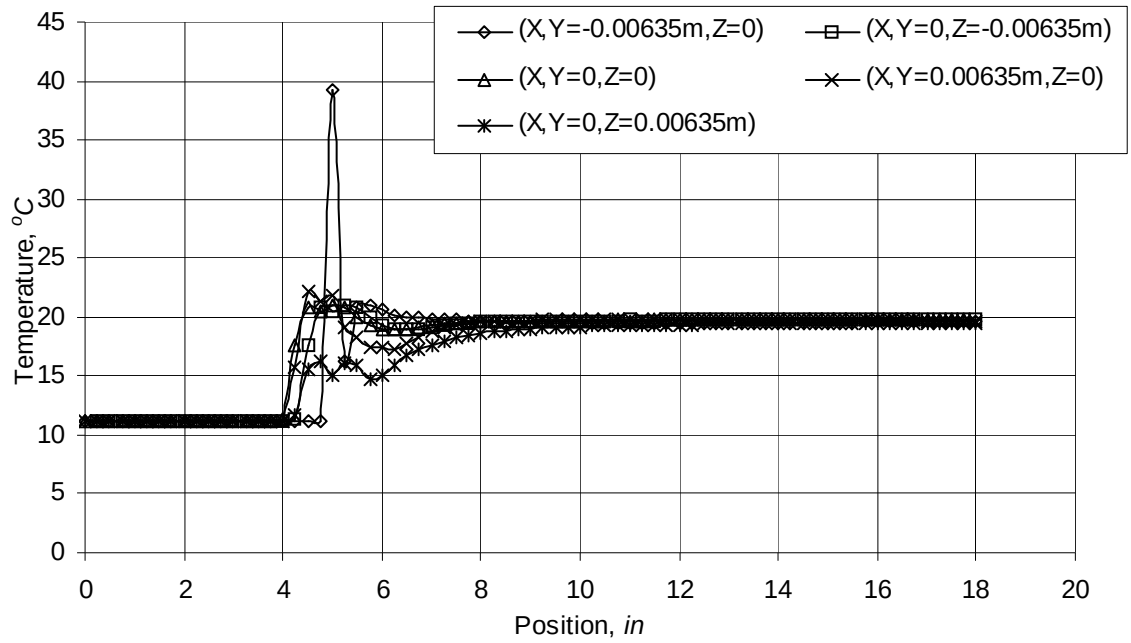

Figure 7.33: Plots of temperature versus position along a centerline and four other axial lines each at 0.00635 m from center. U_j/U_m = 23.2, U_j = 3.94 m/s and a right-angle 1/8" side-tee is used.

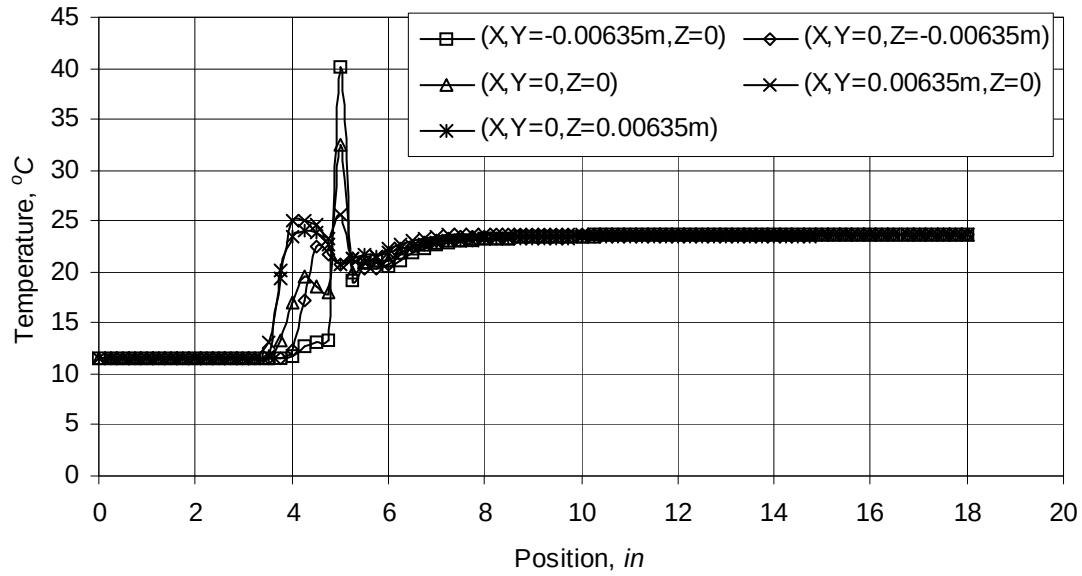

Figure 7.34: Plots of temperature versus position along a centerline and four other axial lines each at 0.00635 m from center. U_j/U_m = 36.4, U_j = 3.94 m/s and a right-angle 1/8" side-tee is used.

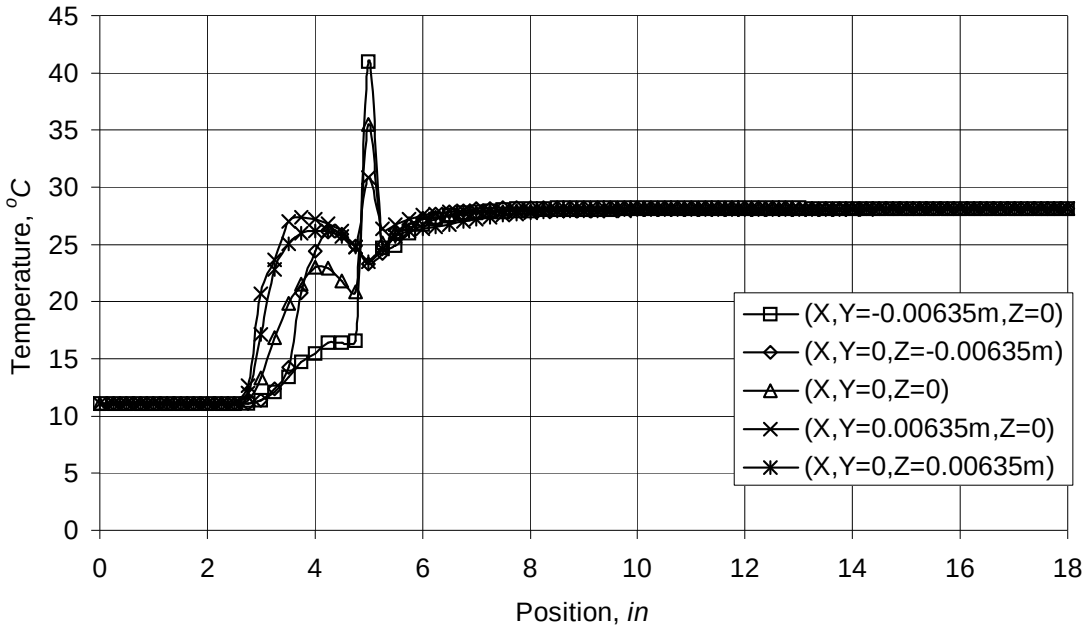

Figure 7.35: Plots of temperature versus position along a centerline and four other axial lines each at 0.00635 m from center. U_j/U_m = 63.8, U_j = 3.94 m/s and a right-angle 1/8" side-tee is used.

To ensure that the desired level of mixing has taken place in a cross-sectional plane, the temperatures across such a plane must be examined and the criterion of mixing must be met everywhere in a cross-sectional plane before one could say that mixing has been achieved at a certain distance downstream of the jet inlet. This topic is discussed in the next section.

7.4.1 Cross-sectional 95% Mixing Completeness

The flow in the main pipe before the jet inlet, is set initially at a certain temperature of about 10^{o}C. The flow through the side-tee is set at a higher of about 50^{o}C. Thus the equilibrium temperature, $\overline{T}$, can be calculated. The 95% mixing is reached when the temperature anywhere across a plane inside the pipe is within the range of $((\overline{T} \pm (\overline{T} - T_{im}) * 0.05)$ where T_{im} is the initial temperature of the fluid in the main pipe, i.e. before the inlet of the side-tee.

The length required for the hot fluid to mix is measured according to the above criterion. The maximum temperature difference between any two points across a cross-sectional area of the pipe should not exceed a certain value, which is a function of the initial temperatures and the flow rates of the fluids in the main- and side-pipes.

Contours of temperatures in selected cross-sectional planes for 1/8" side-tee and U_j/U_m = 23.2, 36.5, and 63.8 are shown in Figures 7.36-7.38. The same temperature scale is used for parts (b) ΔT = 4.2K, (c) ΔT = 1.9K, (d) ΔT = 0.89K and (e) ΔT = 0.7K for each figure at positions 2D, 4D, 7D and 8D respectively along the centerline. This helps to better visualize the degree of mixing.

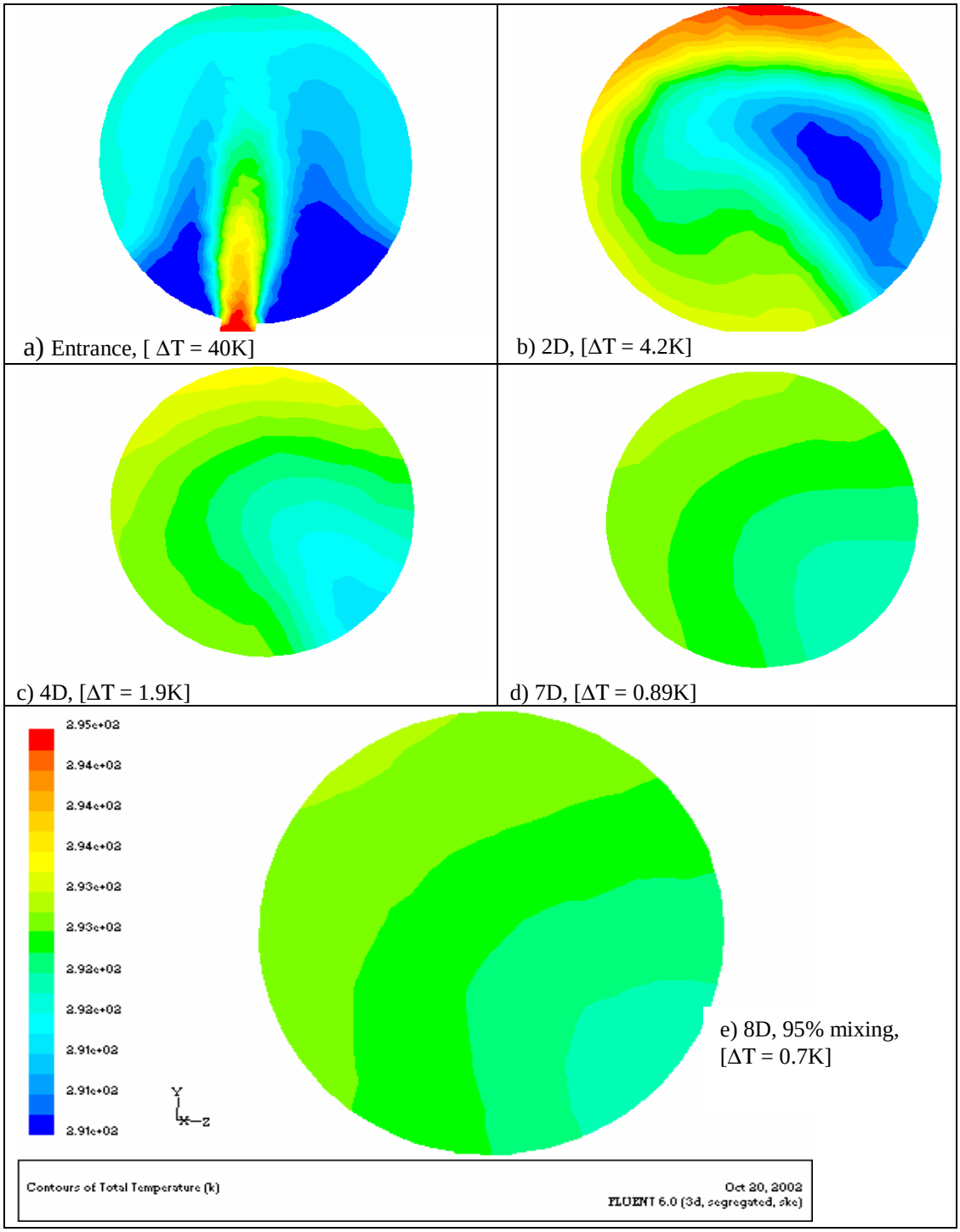

Figure 7.36: Cross sectional view for length required for 95% Mixing for U_j/U_m = 23.2 and for 1/8" right angle side-tee at a) entrance of jet, b) 2D, c) 4D, d) 7D, e) 8D in x-coordinate. Contours in parts b, c, d and e have the same temperature scale of 290.6-294.8K.

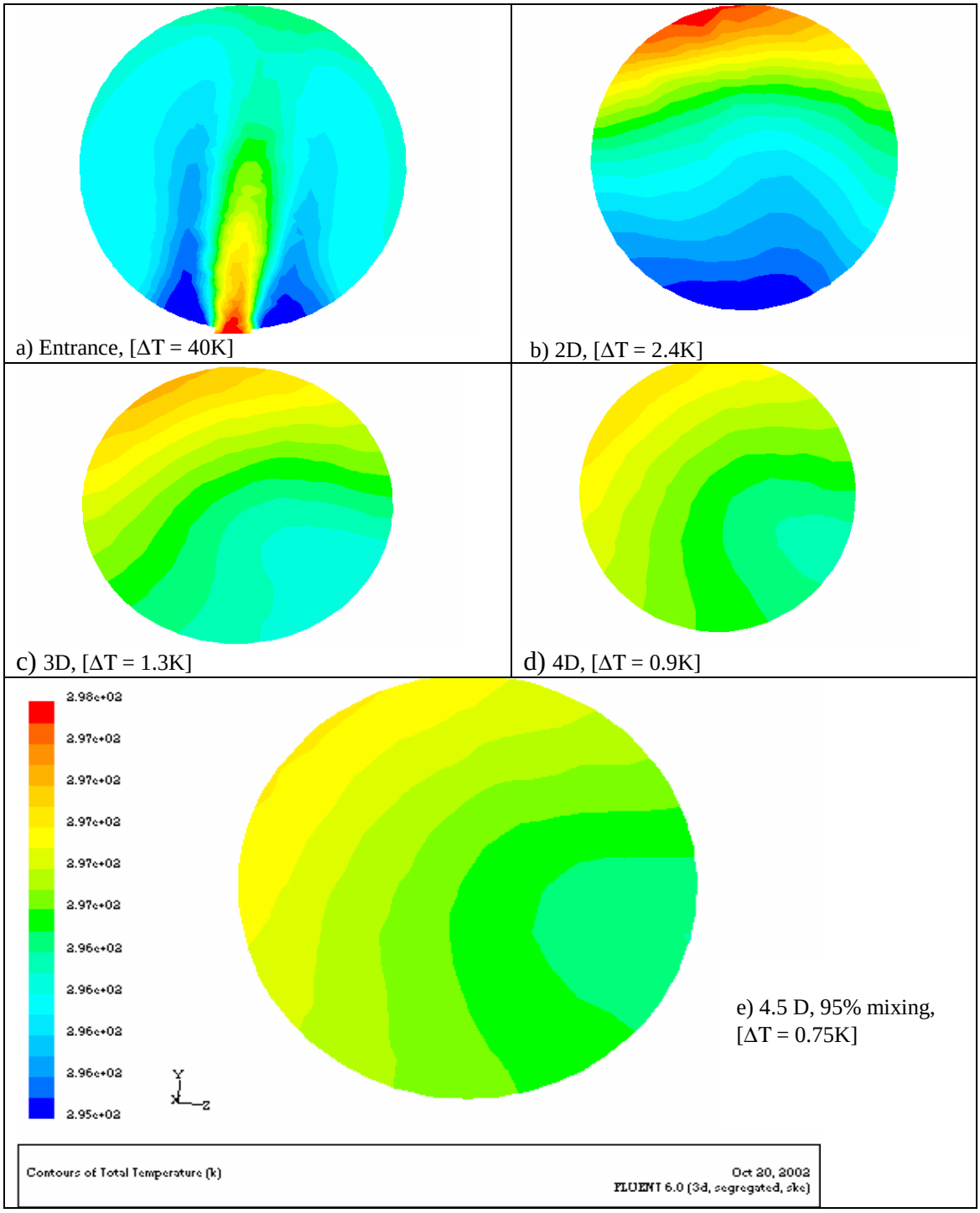

Figure 7.37: Cross sectional view for length required for 95% Mixing for U_j/U_m = 36 and for 1/8" right angle side-tee at a) entrance of jet, b) 2D, c) 3D, d) 4D, e) 4.5D in x-coordinate. Contours in parts b, c, d and e have the same temperature scale of 295.3-297.71K.

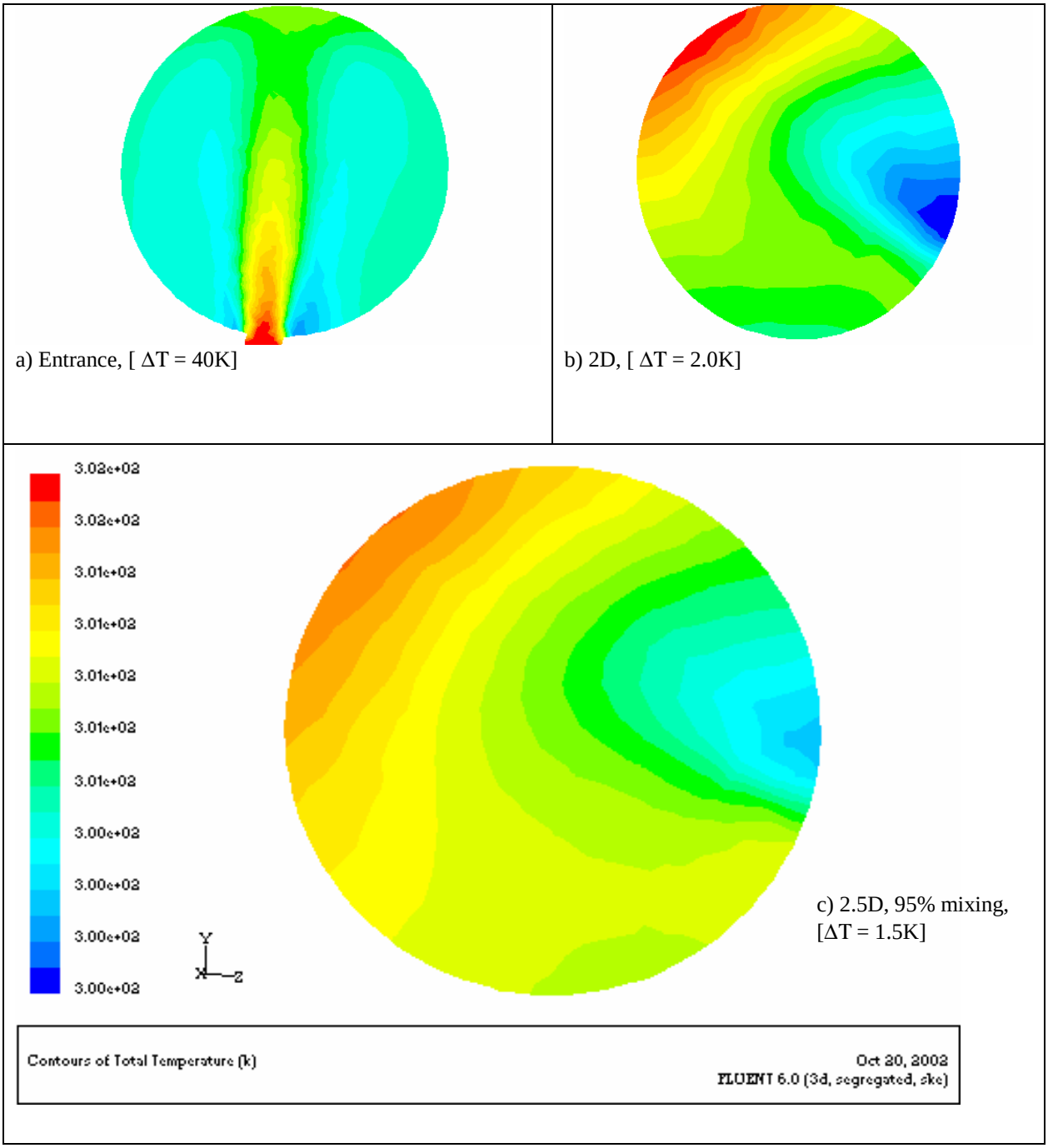

Figure 7.38: Cross sectional view for length required for 95% Mixing for U_j/U_m = 63.8 and for 1/8" right angle side-tee at a) entrance of jet, b) 2D, c) 2.5D in x-coordinate. Contours in parts b and c have same temperature scale of 299.9-301.9K.

The temperature range in cross-sectional planes at intervals of 0.5D is tested until the 95% mixing criterion is met. As the velocity ratio U_j/U_m increases, the pipe length required to achieve 95% mixing decreases. The results deduced from this accurate method agree qualitatively with Figures 7.17-7-19 and 7.21-7.24, which show plots of temperature versus position along the centerline of the main pipe. The pipe length required to achieve 95% mixing for a side-tee diameter of 1/8" and 1/4" and for all velocity ratios are listed in Table 7.3 and 7.4 respectively.

So far, the interest has mainly been concentrated on calculating the pipe length necessary to achieve 95% mixing. However, in many industrial applications, a higher degree of homogeneity is required and more stringent criteria of mixing are applied. Therefore, in certain cases 99% mixing is preferred to 95%. Pipe length required to achieve 99% mixing is calculated using the same method as that used for 95% mixing. For velocity ratios of 63.84 and 45.60, 99% mixing is achieved at a pipe length of 7D and 8D respectively.

For all other velocity ratios, the simulated length after injection of side-fluid (13D) was not enough to achieve 99% mixing. Many chemical industries are more interested in this stringent mixing criteria, i.e. 99% rather than 95%.

These cross-sectional ranges of temperatures are computed for each case to find the length required for 95% mixing. These cross-sectional views are perpendicular to the direction of flow of main fluid in the main pipe in y-z plane along x-coordinate. At entrance temperature, the range is global from cold to hot fluid. A reasonable range is fitted for each case to view the mixed fluid temperature (K) contours to visually decide the mixing degree.

Table 7.3: Length required for 95% mixing for different velocity ratios for 1/8", 90^o, side-tee.

Case	U_j m/s	U_m m/s	U_j/U_m	T_j K	T_m K	T_e K	Length required for 95 % mixing (Diameters of main pipe)
1	14.73	0.63	23.21	284.73	324.59	292.5	7
2	14.73	0.40	36.48	284.61	324.46	296.6	4.5
3	14.73	0.23	63.84	284.08	323.59	301.0	2.5
4	10.52	0.63	16.58	284.19	325.09	291.0	9
5	10.52	0.40	26.06	284.16	324.75	293.5	*7*
6	10.52	0.23	45.60	284.16	325.44	298.1	3
7	6.31	0.63	9.95	284.13	320.85	288.0	13
8	6.31	0.40	15.63	284.26	316.70	289.5	9.5
9	6.31	0.23	27.36	284.69	317.21	292.5	6

Table 7.4: Length required for 95% mixing for different velocity ratios for 1/4", 90^{o}, side-tee.

Case	U_j m/s	U_m m/s	Uj/U_m	T_j K	T_m K	T_e K	Length required for 95 % mixing (Diameter of main pipe)
1	3.94	0.63	6.2	284.0	323.88	295.4	11.5
2	3.94	0.40	9.8	284.0	323.88	298.8	12
3	3.94	0.23	17.1	284.0	323.88	303.5	11
4	2.63	0.63	4.1	284.0	323.88	291.8	13-NC*
5	2.63	0.40	6.5	284.0	323.88	293.2	13
6	2.63	0.23	11.4	284.0	323.88	299.0	9
7	1.57	0.63	2.5	284.0	323.88	286.0	13-NC
8	1.57	0.40	3.9	284.0	323.88	289.8	13-NC
9	1.57	0.23	6.8	284.0	323.88	294.8	11
10	5.75	0.23	25	284.0	323.88	306.5	6
11	3.45	0.23	15	284.0	323.88	301.6	11.5
12	8.0	0.23	34.8	284.0	323.88	309.9	4
13	10.35	0.23	45	284.0	323.88	312.1	2
14	12.65	0.23	55	284.0	323.88	313.5	1
15	14.50	0.23	63	284.0	323.88	314.5	3

*Not Complete, 95% mixing till 13D.

7.5 Length Required for 95% Mixing of 1/8" and 1/4", Right-angle, Side-Tee

The pipe lengths required to achieve 95% mixing have been found as explained in the previous section. These values for 1/8” and 1/4” side-tees are already listed in Tables 7.3 and 7.4 respectively. Figure 7.39 shows plots of length required for 95% mixing versus velocity ratio for constant main- and side-velocities. It can be seen from Figure 7.39 that for $U_j/U_m \leq 45$ the length required for 95% mixing decreases steeply as U_j/U_m increases. For $U_j/U_m > 45$ the length required for 95 % mixing changes very slowly with U_j/U_m. Figures 7.40-7.41 show plots of pipe length required to achieve 95% mixing versus U_j/U_m for all cases. For the case of 1/8” side-tee, the length required for mixing decreases significantly as U_j/U_m increases. For the case of d/D of 1/4, the rate of change is not as steep.

Figure 7.41 shows that at a velocity ratio, U_j/U_m, of 7 the side-jet impinges on the opposite wall and the length of the main pipe required to achieve 95% mixing is large. This is because the jet attaches to the opposite wall and it takes a relatively long distance to reach the center of the pipe. As U_j/U_m increases, the side-jet bounces back more towards the centerline of the main pipe, until it reaches a minimum of about 1D at a value of U_j/U_m of 55. When the value of U_j/U_m is further increased, the jet bends more acutly and it starts to get into the other half of the main pipe, away from the center, thus resulting in an increase in the pipe length required to achieve 95% mixing. The diagram shown in Figure 7.41a further explains this phenomenon.

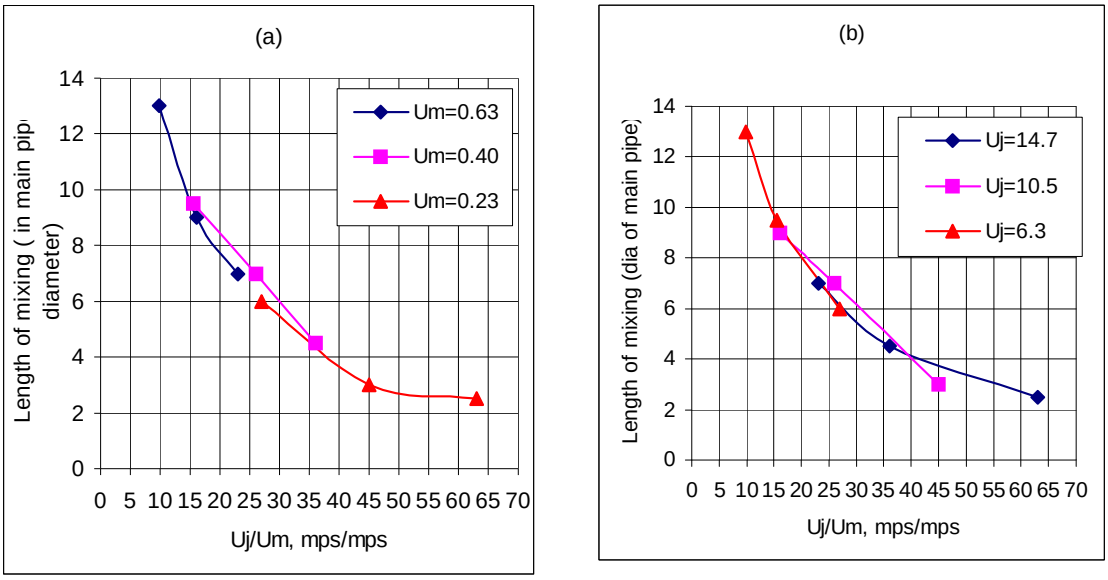

Figure 7.39: Pipe length required to achieve 95% mixing versus U_j/U_m for 1/8" side-tee: a) constant U_m, b) constant U_j

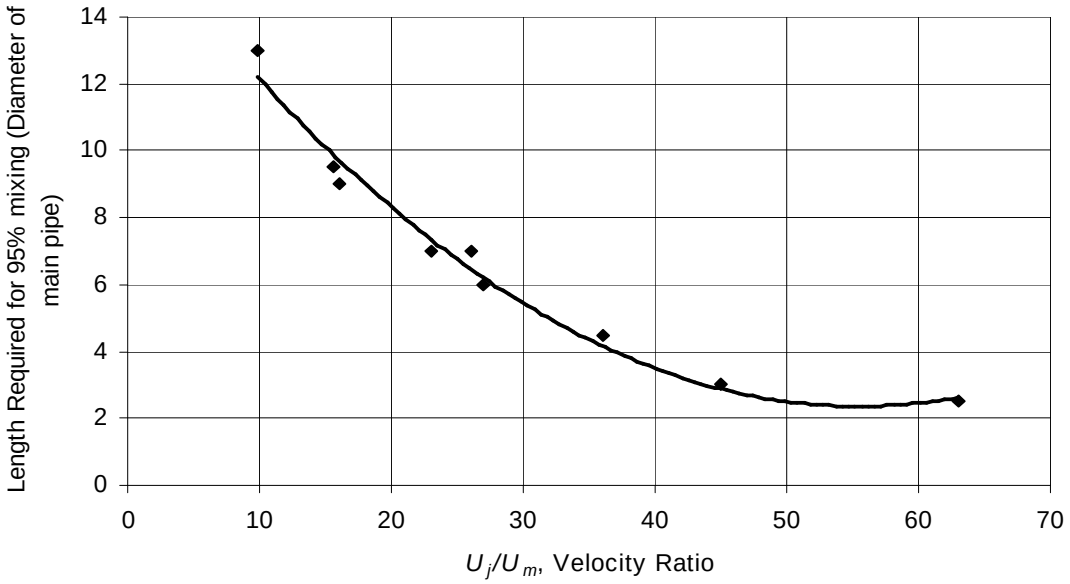

Figure 7.40: Pipe Length required to achieve 95% mixing versus U_j/U_m for all cases of 1/8" right-angle, side-tee.

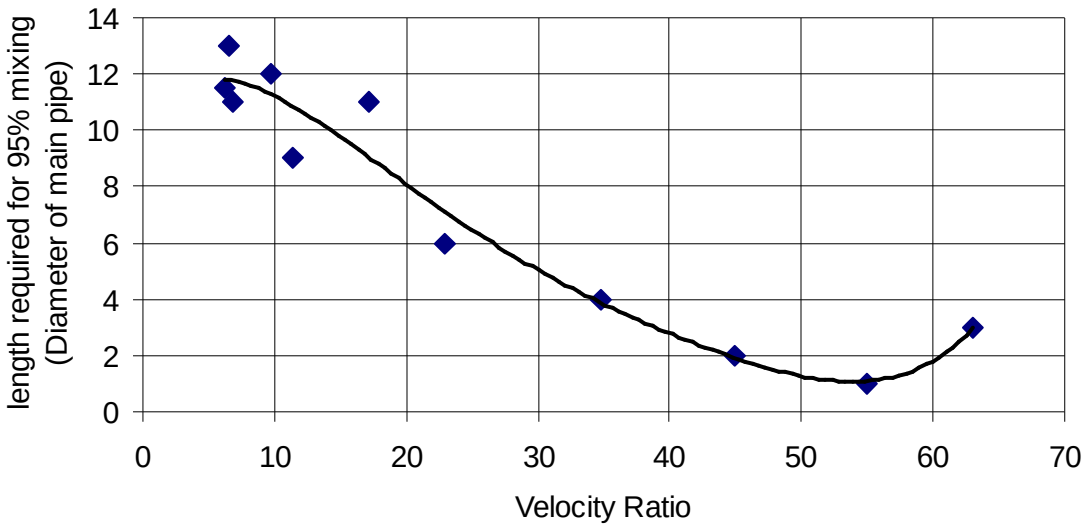

Figure 7.41: Length required for 95% mixing in diameter of main pipe versus U_j/U_m, m/s / m/s, of 95% completely mixed cases for 1/4", 90^o, side-tee.

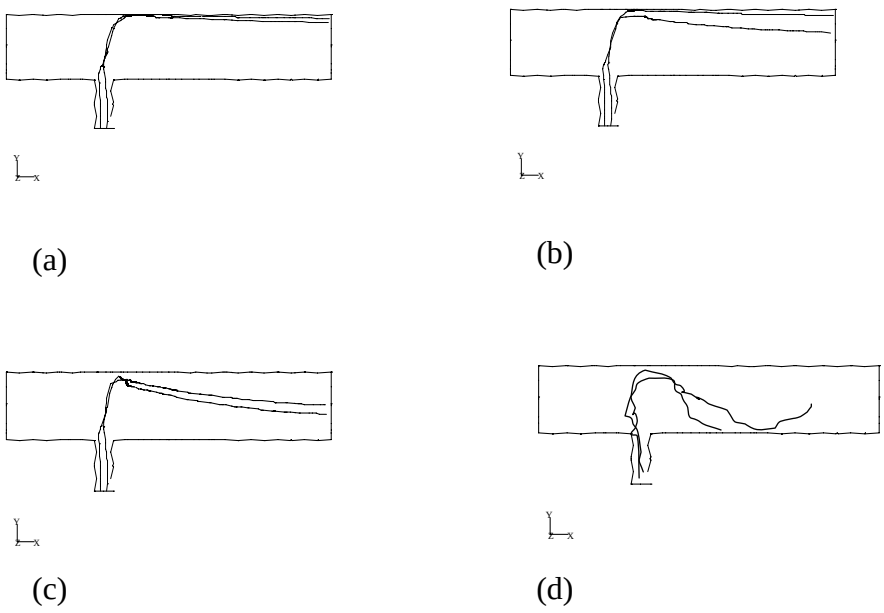

Figure 7.41a: A path line diagram of side-jet bending into main fluid as U_j/U_m is increased (a) low (b) low to medium (c) high (d) Very high

An equilibrium temperature chart corresponding to various velocity ratios is shown in Figure 7.42 for 1/8" and 1/4", 90^{o}, side-tees. This figure shows high value of temperature for high U_j/U_m because U_j is the velocity of the hot stream and U_m is that of the cold stream. If U_j increases, U_j/U_m increases, introducing higher flow rate of hot fluid for mixing with cold stream resulting in higher final mixed temperature.

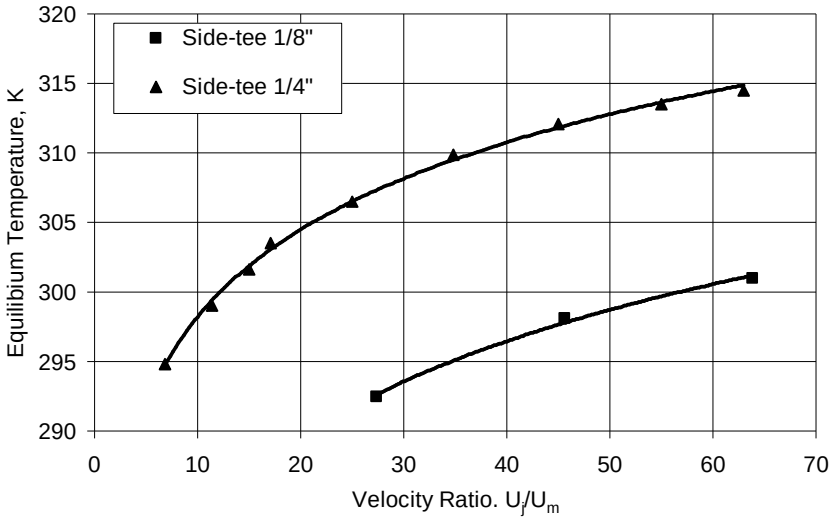

Figure 7.42: Equilibrium temperature in Kelvin (approx.) chart for corresponding velocity ratios for both 1/8 inch and 1/4 inch, 90^o, side-tees for U_m = 0.23 m/s.

7.6 Effect of the Angle of the Tee

Based on experimental and numerical results, it was observed that at certain values of the diameters and velocities ratios, the jet impinges on the opposite wall of the main pipe and a region of backflow is thus created. Some researchers stated that impingement might be desirable in some cases in order to enhance rapid mixing (Feng *et al*., 1999). However in the paper industry, a tracer is often injected at an angle $\theta°(45 \leq \theta° \leq 60)$ to avoid impingement and to minimize pressure pulsation. Schematic diagram of angle injection is shown in Figure 7.43.

The suggestion that a jet impingement results in rapid mixing is a suggestion that may not be necessary to achieve rapid mixing according to the results presented in this study. Numerical simulations of mixing in a pipeline with a 1/4" side-tee at angles of 30^o, 45^o, 60^o and 90^o were carried out using a case where U_j/U_m = 17.1 and U_j = 3.94 m/s maintaining everything else the same for all cases except the jet angle. Figures 7.44-7.46 show the temperature (K) and velocity (m/s) contours for the four angles considered (The 90^o angle has already been discussed).

Results show that out of the four angles considered, the jet impinges at the opposing wall only for an angle of 90^o and to a much lesser extent for an angle of 60^o. Figures 7.44-7.46 show that changing the angle of the side-tee has interesting results on mixing. Figure 7.47 shows the temperature profile along the center of the main pipe for all four cases. This shows that mixing is achieved faster (over a shorter distance) when an angle of 45^o or 60^o is used. Using a 30^o or a 90^o angle resulted in slower mixing. Results are tabulated in Table 7.5.

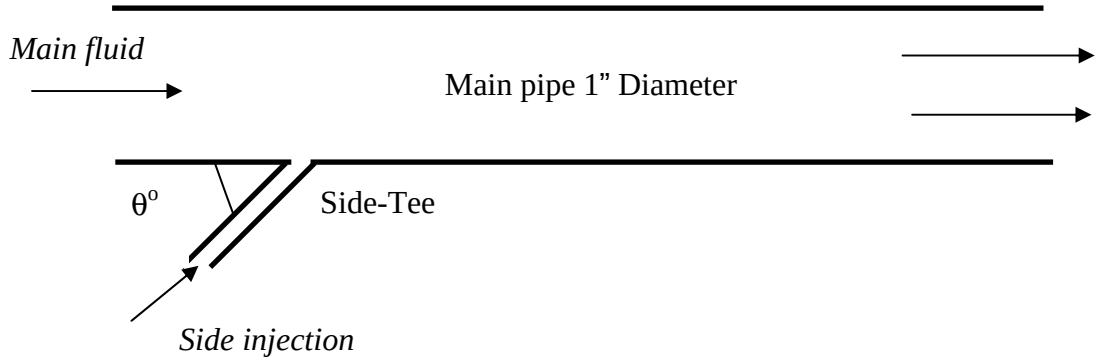

Figure 7.43: Schematic diagram of a side angle-tee

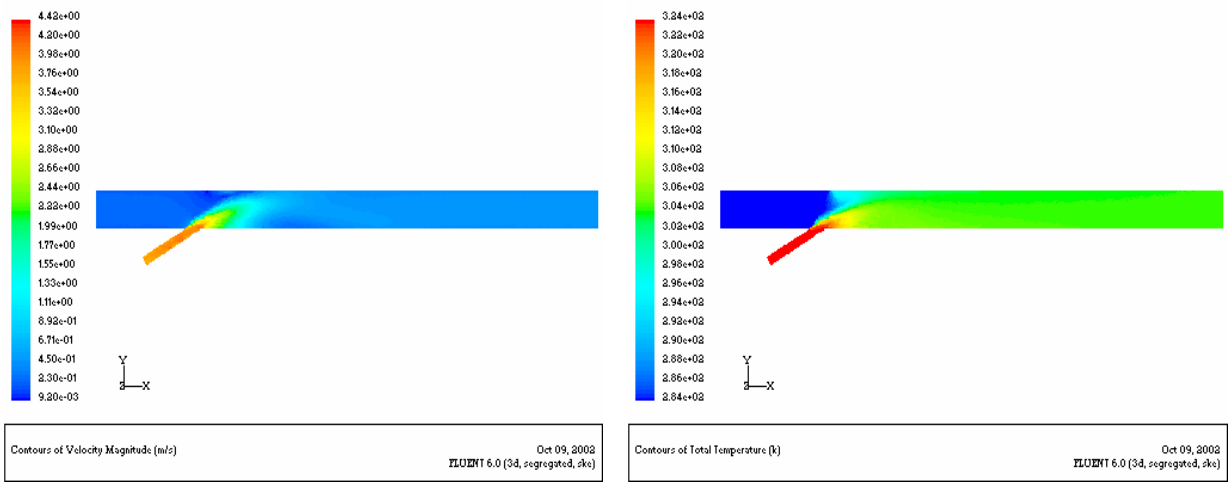

(a) (b)

Figure 7.44: (a) Temperature (K) and (b) Velocity (m/s) contours for U_j/U_m = 17.1 and a 1/4”, 30° side-tee.

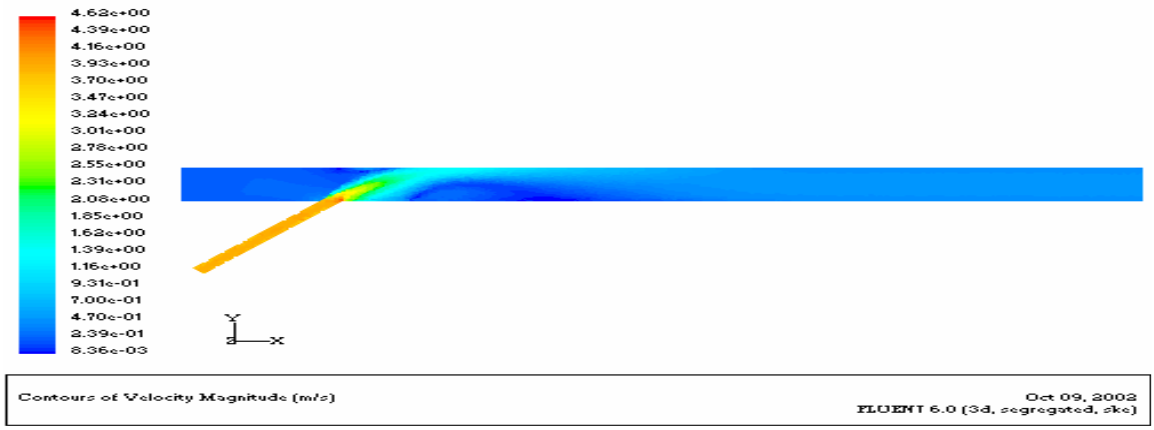

(a)

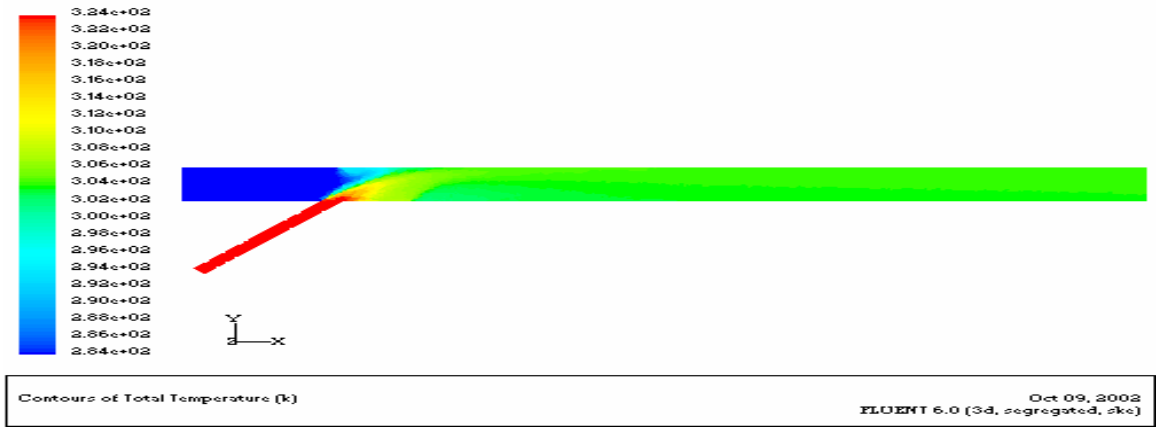

(b)

Figure 7.45: (a) Temperature (K) and (b) Velocity (m/s) contours for U_j/U_m = 17.1 and a 1/4", 45^o side-tee.

(a)

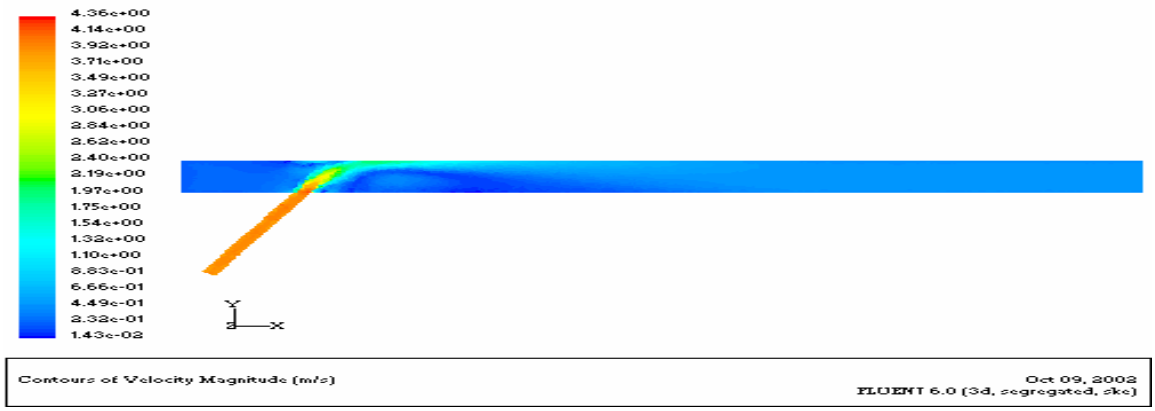

(b)

Figure 7.46: (a)Temperature (K) and (b)Velocity (m/s) contours for U_j/U_m = 17.1 and a 1/4", 60^o side-tee.

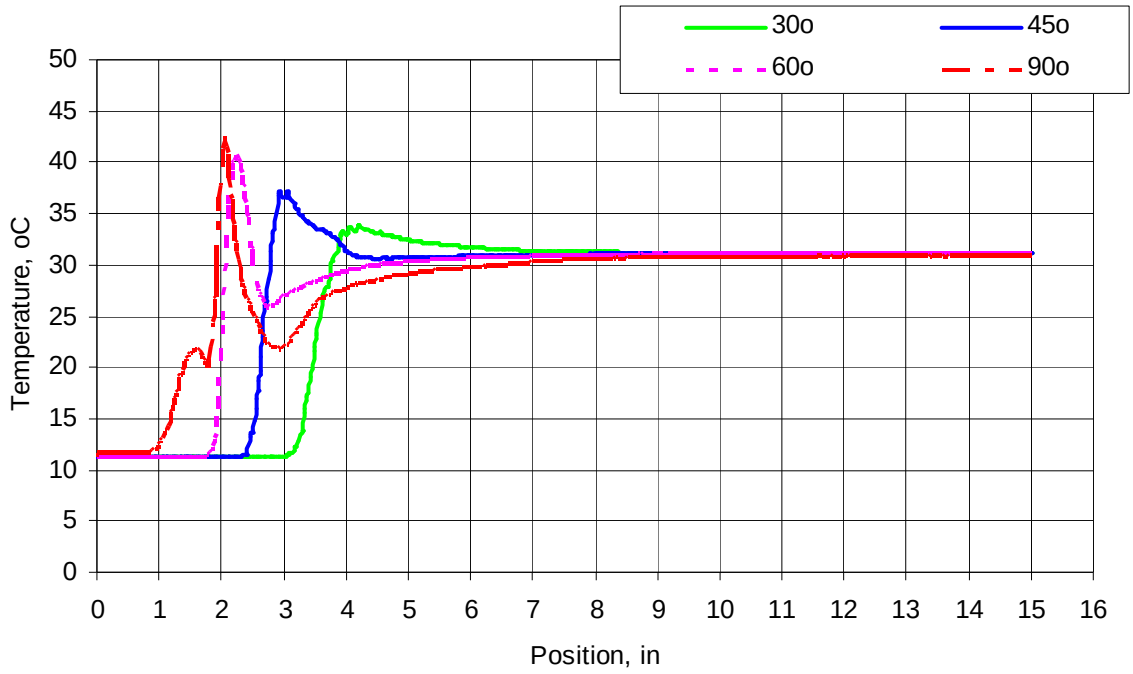

Figure 7.47: Plots of temperature versus position along the centerline of the main pipe, for U_j / U_m = 17.1, for the four angles of 30°, 45°, 60°, and 90°.

Table 7.5: Pipe Length Required for 95% Mixing for Different Angles of Injection

Angle	U_m, m/s	U_j, m/s	U_j/U_m	Mixing Length in main pipe diameter
30	0.23	3.94	17.1	5.5D
45	0.23	3.94	17.1	3.5D
60	0.23	3.94	17.1	4.5D
90	0.23	3.94	17.1	11D

This shows that there is an optimum-tee angle for which the mixing is fastest. An accurate final length required for 95% mixing is calculated by examining differences in temperature in cross-sectional planes downstream of the jet. Figure 7.48 shows the velocity field for the four angles. Significantly, less impingement and back flow are observed as the jet angle is decreased. It should be noted that the upper wall is not showing a free surface, but what looks like a free surface is the velocity vectors scaled up for better clarity.

Figure 7.49 shows a plot of the length of the pipe needed to achieve 95% mixing as a function of the angle of the tee. These results show that the angle of the tee determines whether the jet impinges on the opposite wall and how this affects the length needed to achieve mixing.

Some researchers (Feng *et al.* 1999) stated that the impingement of the side-jet to opposite wall is required in chemical engineering because of high degree of mixedness and for fast occurrence of chemical reactions. This study suggests that mixing can be achieved much more rapidly if the correct angle of the tee is chosen. This is a better option as it delivers mixing without the corrosion problems that may be linked to cases with strong jet impingement on the opposite wall.

A reason for fast occurring reactions may be the excess amount of some reactant over its stoichiometric amount. If one reactant is introduced from side-tee with such a velocity that there is impingement of that reactant on the opposite wall then it may possible for the reaction, to go to completion before 95% mixing of both reactants is reached.

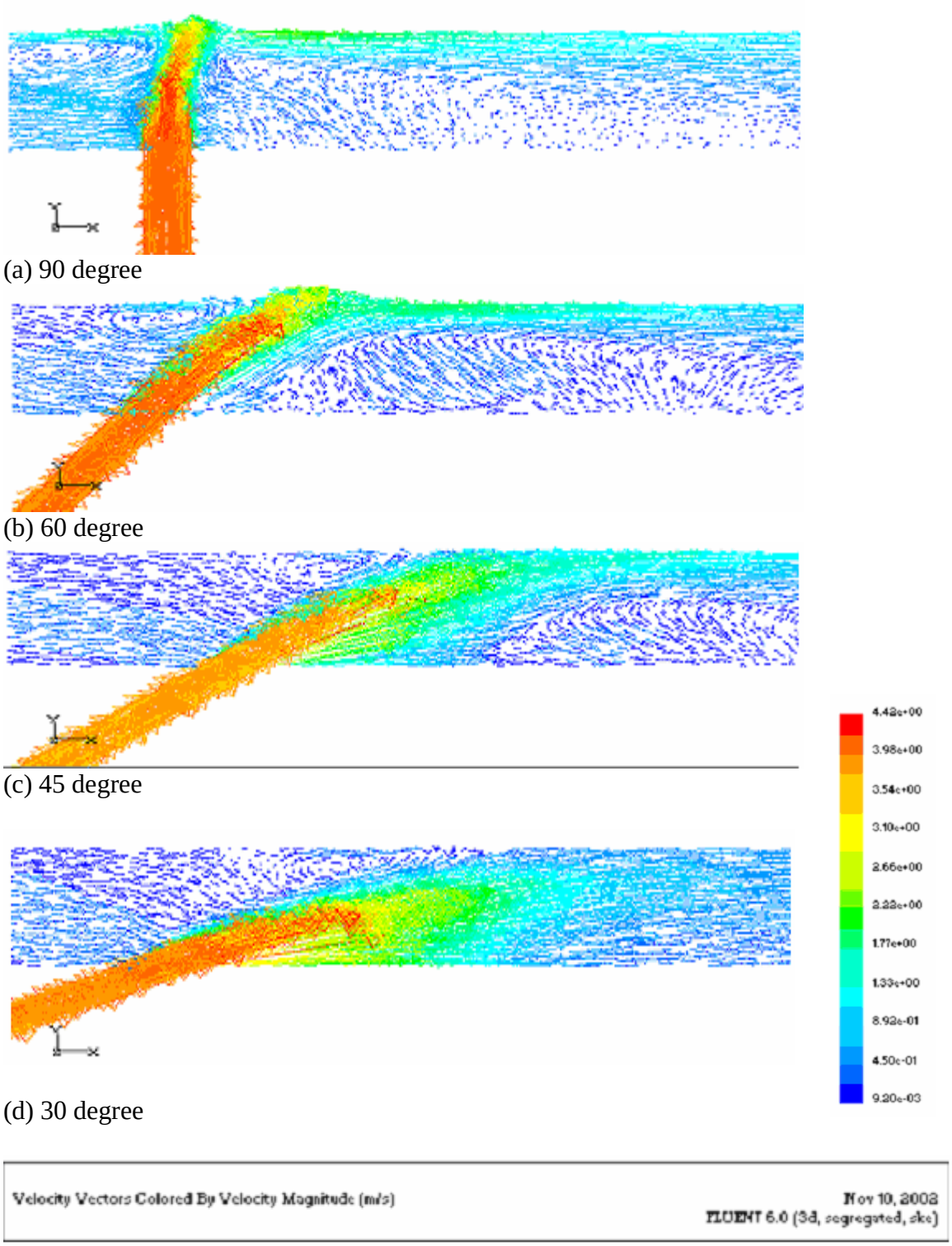

(a) 90 degree

(b) 60 degree

(c) 45 degree

(d) 30 degree

Figure 7.48: Velocity fields of (a) 90^{o} (b) 60^{o} (c) 45^{o} (d) 30^{o} showing clearly, the impingement for 90^{o} and a decrease in impingement as the angle is decreased.

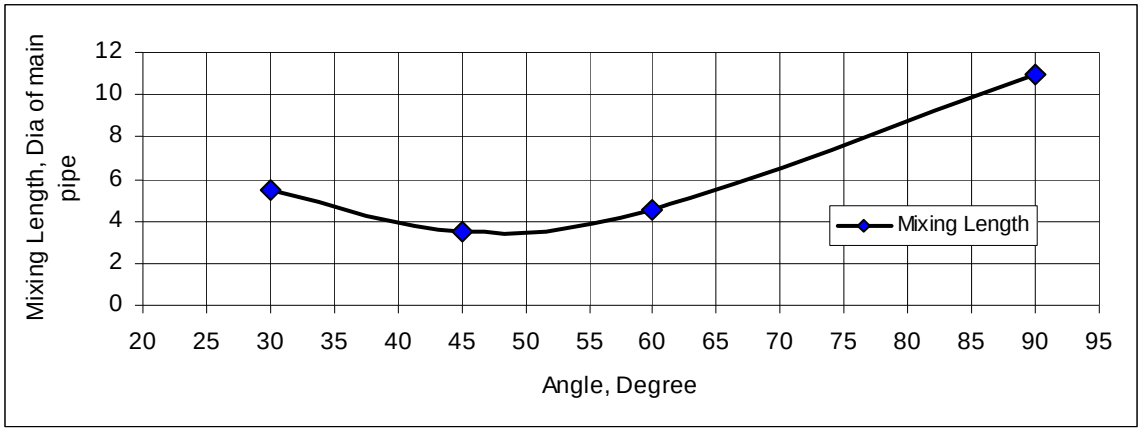

Figure 7.49: Length required for 95% mixing in diameter of main pipe versus angle of side-tee for U_j/U_m = 17.1 and a 1/4" side-tee.

.

7.7 Mixing in Pipeline with Opposite-Tees

Numerical simulations of a pipeline with opposed-tees have been carried out. Some convergence difficulties were experienced when two directly opposite jets were used. This is due mainly to jet-jet interaction which makes it physically unstable. However, with some modifications, converged results were obtained. Three different opposed geometries, 1/4" - 1/4", 1" - 1/4", and 1" - 1" are simulated. Figure 7.50 shows the grid outline of last two geometries. The mesh size used here is the same as that used to simulate the side-tee cases. No refinement has been used unless specified and the results shown in this section are obtained using the k-ε turbulence model. Velocity (m/s) and temperature (K) contours are shown for all these cases.

7.7.1 Opposed 1/4"-1/4" Tee

A geometry consisting of two opposed jets 1/4" in diameter with a 1" main pipe was created. Mixing in this geometry with U_j/U_m = 1.0 (U_j = U_m = 3.94 m/s), and U_j/U_m = 1.07 (U_j = 3.94 m/s), and U_j/U_m = 17.1 (U_j = 3.94 m/s) was simulated. The k-ε model was used and the total number of cell is 135712 tetrahedral cells. Contours of temperature (K) and velocity (m/s) for U_j/U_m = 1.0 are shown in Figure 7.51. Mixing does not take place although the cold and hot streams combine in a centrally oriented mixed stream. Due to direct impingement of the two streams, the jet seems to be dispersed as shown in Figure 7.52. Figure 7.52 shows plots of temperature versus position along three axial lines: one at the center and two at $\pm$ 0.00635 m from the center. All three lines are slow to converge to the equilibrium temperature.

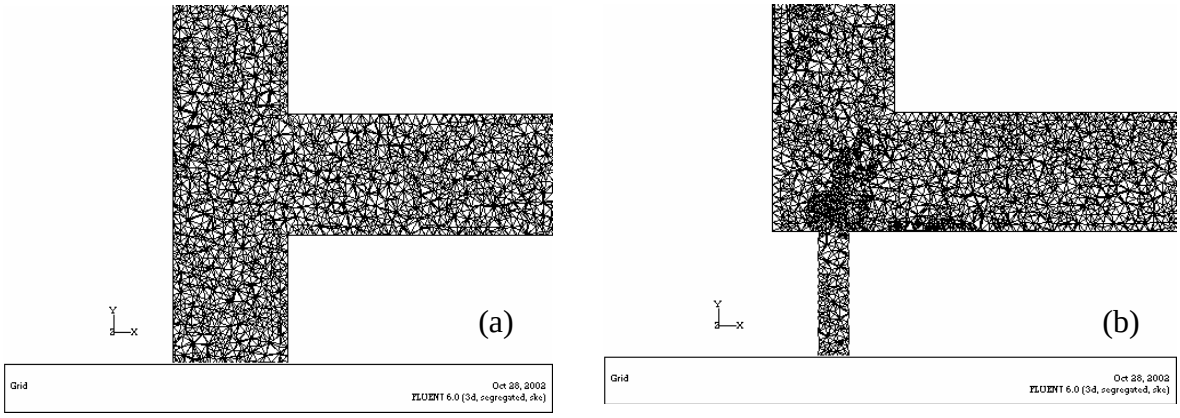

Figure 7.50: Grid outlines of (a) 1”-1” opposed-tee, (b) 1”-1/4” opposed-tee

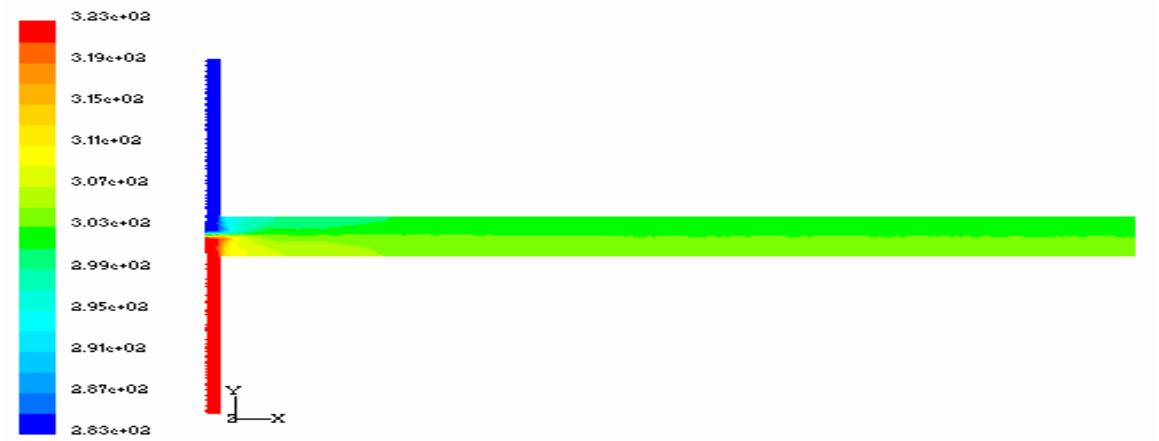

(a)

(b)

Figure 7.51: (a) Temperature (K) and (b) Velocity (m/s) contours for 1/4”-1/4” opposed-tee with inlet velocities 3.94 m/s , having a hot temperature of 323K and a cold stream temperature of 283K.

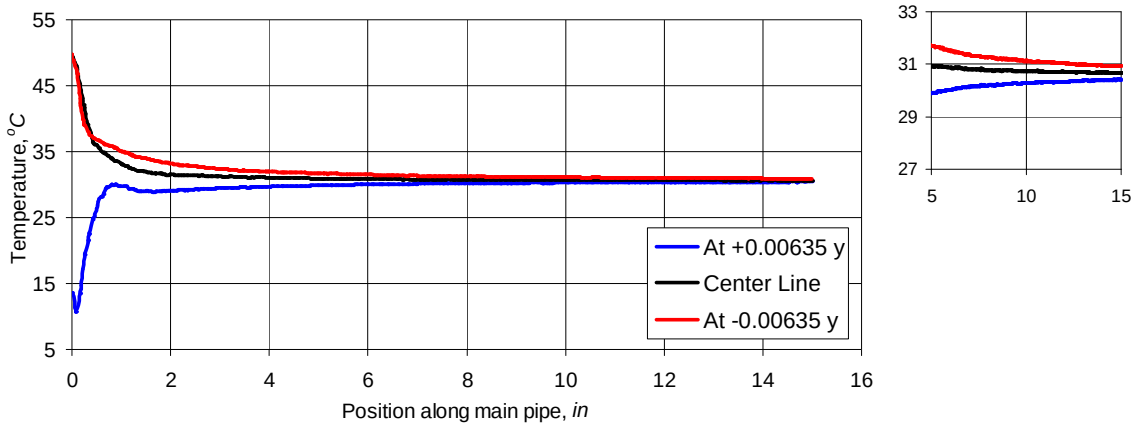

Figure 7.52: 1/4”-1/4” opposed tee with inlet velocities 3.94 m/s down, and 3.69 m/s up main having temperature 323K down, 283K up respectively. At 0.00635 m in negative y-direction and at center of pipe, and at 0.00635 m in positive y-direction.

Figure 7.53 shows the temperature (K) and velocity (m/s) contours for the same geometry for a slightly lower U_m (3.69 m/s compared to 3.94 m/s in the previous case). The trend of mixing is, as expected, very similar to the previous case.

Figure 7.54 shows temperature and velocity (m/s) contours for the same 1/4" - 1/4" opposed-tee for a velocity ratio, U_j/U_m of 17.10 and a hot side-stream velocity, U_j of 3.94 m/s. U_j is the velocity of stream flowing upwards. This stream approaches the upper wall of the main pipe due to its higher velocity. Mixing in this case is faster compared to the previous one, but it is still slower compared to side-tee and much slower than the mixing with side-tee at 45^o for this case.

Figure 7.55 shows line plots of temperature along a centerline of the main pipe and along two lines 0.00635 m above it and below it. All three lines show that the temperature converges towards the equilibrium temperature at about 10D.

Figures 7.53 and 7.54 show that the side-stream facing upwards at high velocity is approaching the upper wall of the main pipe because of higher velocity. Figure 7.55 shows clearly that the hot fluid-stream (facing upwards) has also crossed the centerline of main pipe and started mixing with cold fluid at the entrance of main upper pipe.

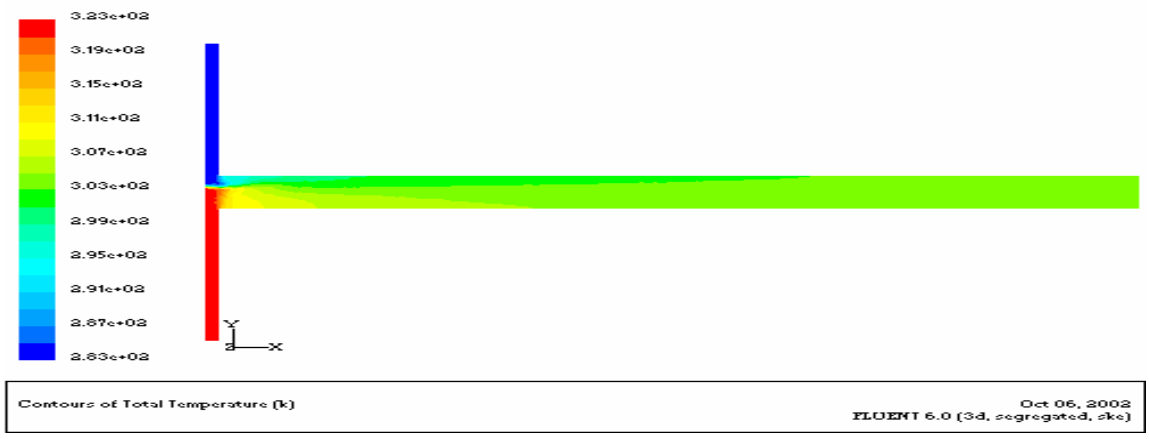

(a)

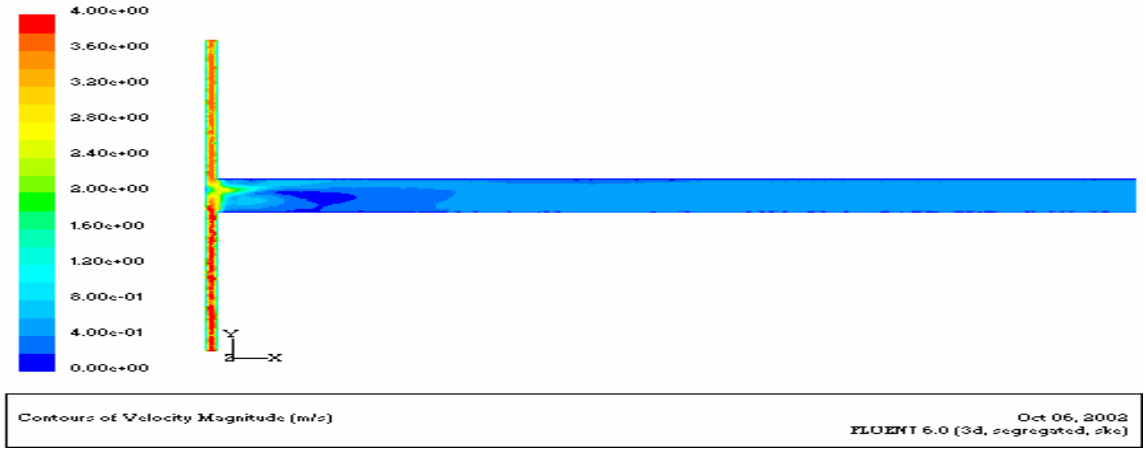

(b)

Figure 7.53: Temperature (K) and Velocity (m/s) contours of case with U_j (3.94 m/s) down , U_m (3.69 m/s) up, (1/4"-1/4" oppose-tee)

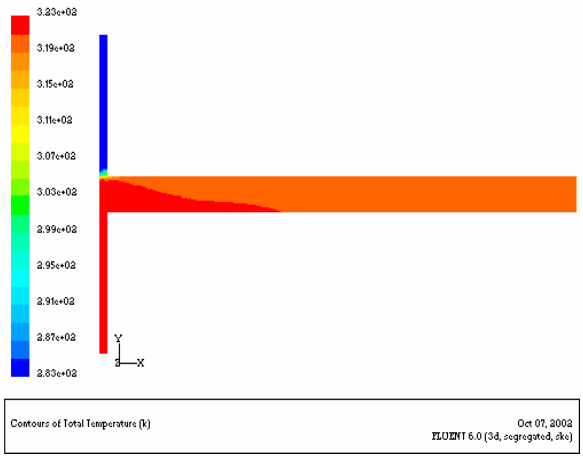

(a)

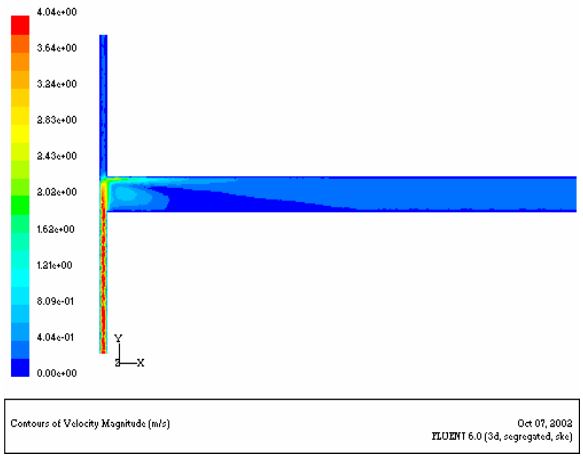

(b)

Figure 7.54: (a)Temperature (K) and (b) Velocity (m/s) contours for U_j/U_m = 17.1, where U_j = 3.94 m/s. (1/4" - 1/4" oppose-tee)

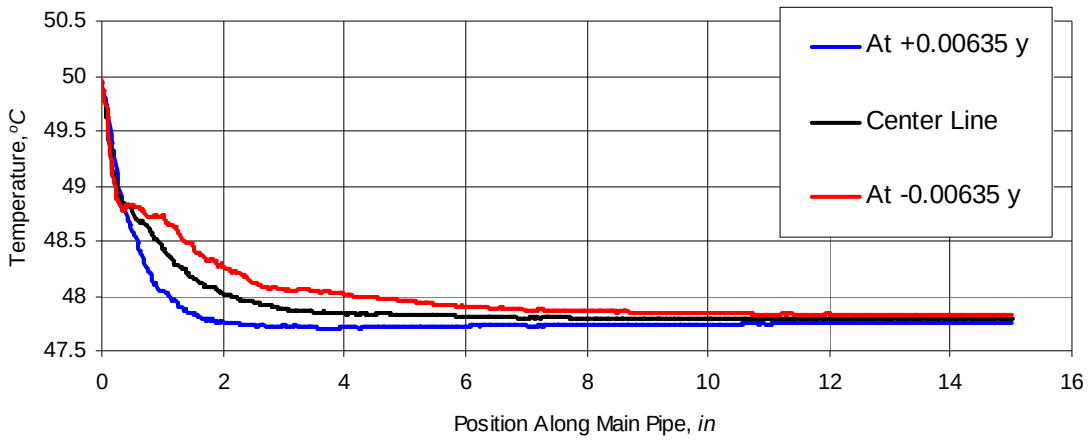

Figure 7.55: Temperature versus position along centerline of main pipe for 1/4"-1/4" opposed-tee for U_j/U_m = 17.1, where Uj = 3.94 m/s, with different temperatures T_j = 323K (down), T_m = 283K (up). At 0.00635m in negative y-direction and at center of pipe, and at 0.00635 m in positive y-direction.

7.7.2 Opposed 1"-1/4", Tee

A new opposed-tee case is simulated. It consists of a 1" main pipe and 1/4" side-tee. Results are shown in Figure 7.56, for U_j/U_m = 17.1, where the two tees are opposed but one side-pipe diameter is much larger than the other one. This Figure shows that mixing takes place in fact faster than when using one, 90^o, side-tee. From 1/4" side entrance, 95% mixing takes place at 5.5D, which is 6D from the left sidewall and 5D from the right side wall of upside main fluid entrance. Figure 7.57 shows the velocity fields for this case. Figure 7.58 shows an opposed-tee, 1"-1/4", with velocity, U_j = 3.94 m/s, and with velocity, U_m = 3.69 m/s (U_j/U_m = 1.1). The velocities are almost the same but it can be seen that upward jet through the 1/4" pipe is bending very early due to higher flow rate of the fluid flowing in the 1" pipe relative to the other flow rate. From Figure 7.56, it can be seen that a significant degree of back mixing has taken place. It is also observed that more back mixing results in a shorter pipe length downstream of the inlet to achieve 95% mixing. This is also observable from 90^o as discussed earlier. For this case (Figures 7.56, 7.57) total path of hot fluid traveling within cold fluid is 9.5D (includes double the length of the back mixing region) with total pipe length 7.5D and the length required for 95% mixing is 5.5D from injection point. This downstream length after injection is concerned and reduction in this length is the main objective. The upstream pipe is already there and as much as possible the upstream length usage is appreciated. This also shows that a geometry, which allows the hot fluid to travel more within cold fluid, will be better for early mixing giving less length required for 95% mixing as discussed in section 7.5.

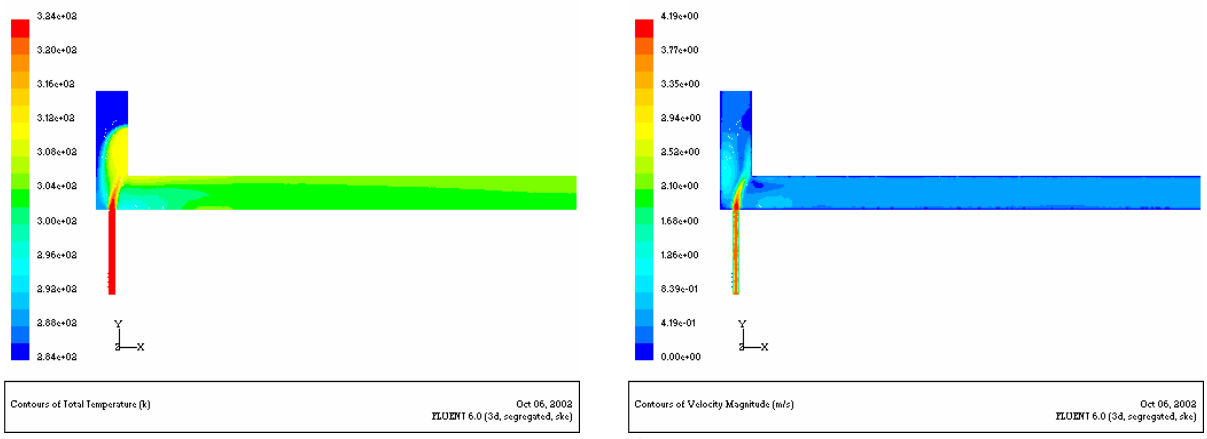

(a) (b)

Figure 7.56: Temperature and Velocity (m/s) contours for 1”- 1/4”, opposed-tee with U_j (323.87K) / U_m (284.21K) = 3.94 m/s / 0.23 m/s = 17.1

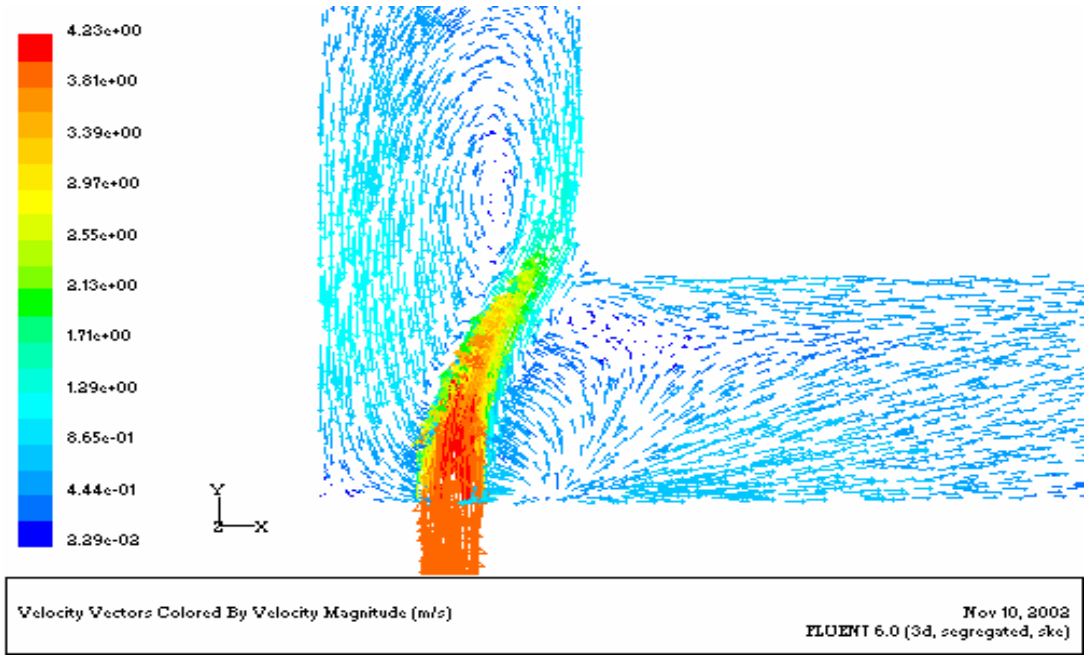

Figure 7.57: Velocity fields for 1”- 1/4”, opposed-tee with U_j (323.87K) / U_m (284.21K) = 3.94 m/s / 0.23 m/s = 17.1

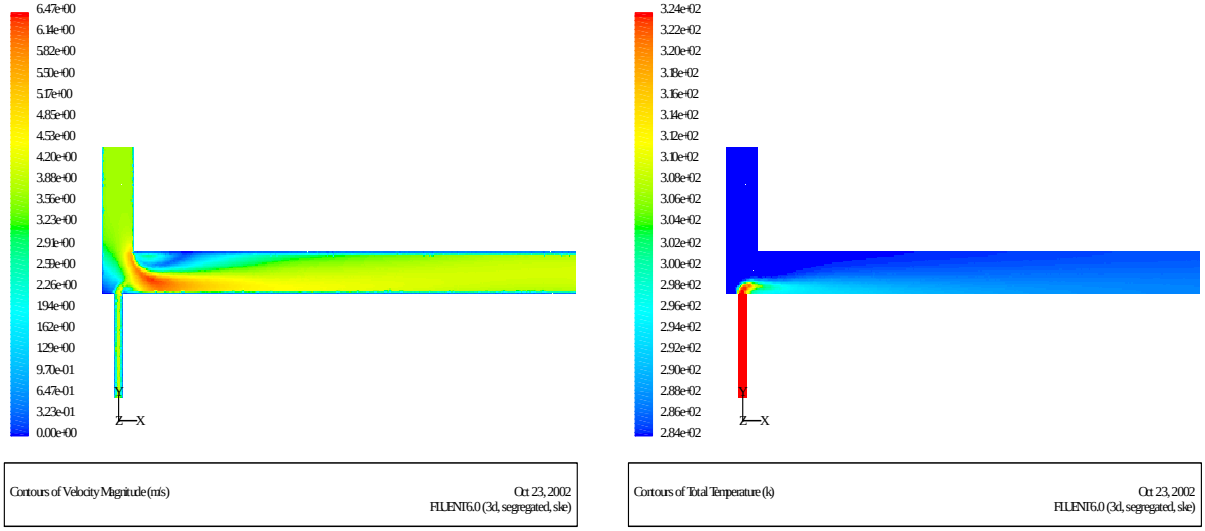

Figure 7.58: Temperature (K) and Velocity (m/s) contours of opposed-tee, 1" - 1/4", U_j = 3.94 m/s, U_m = 3.69 m/s.

7.7.3 Opposed 1" -1", Tee

Following the simulations of 1/4”-1/4” and 1”-1/4” opposed-tees, a 1”-1” opposed-tee is now considered with a main pipe of 1” diameter. Simulations are carried out using this geometry for four different velocity ratios as shown in Table 7.6. The pipe length required for 95% mixing is also listed in the same Table. The fourth case is a base case with velocity ratio, U_j/U_m = 17.1, with U_j = 3.94 m/s. For 1/4”, 90^o side-tee the length required for 95% mixing is 11D and for this opposed-tee, 95% mixing is attained at 10D.

Figures 7.59-7.62 show the Temperature (K) contours and velocity vectors, scaled up by a factor of 10 for clarity and presenting only one in twenty vectors for all four cases. For cases with high U_j/U_m (cases 3 and 4) 95% mixing is achieved in 10 and 14 diameters respectively. For the other 2 cases with lower values of U_j/U_m (2.93 and 1.07) 95% mixing was not achieved in the simulated length of the pipe and therefore, it requires more than 15 diameters. At 14.5 diameters, about 85% mixing has been achieved.

Figures 7.59-7.61 show that the orientation of the combined jet in the horizontal pipe depends directly on the relative values of the two jets. Since the diameter of the both tees is the same, the resulting jet travel along a central direction if $U_j \approx U_m$ (Figure 7.61). As U_j/U_m increases, the jet with higher velocity travels farther towards the opposite wall as shown in Figure 7.61. As U_j/U_m increases further the faster jet tends to impinge on the opposite wall.

Table 7.6: Opposed-tee length required for 95% mixing

Case	U_m, m/s	U_j, m/s	U_j/U_m	Length required for 95% mixing in main pipe diameter
1	3.69	3.94	1.07	14.5D-NC*
2	3.69	10.8	2.93	14.5D-NC*
3	0.40	3.94	9.85	14D
4	0.23	3.94	17.1	10D

*NC: Not Complete 95% mixing

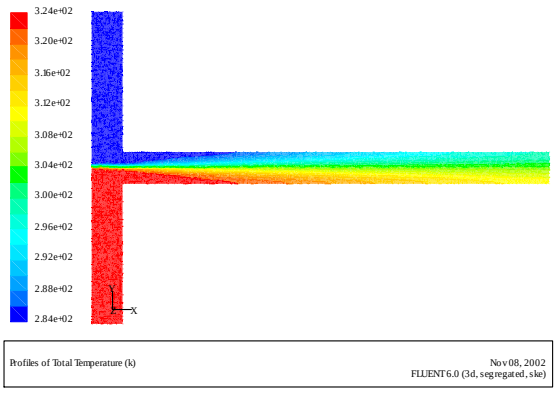

a) Temperature (K) contours

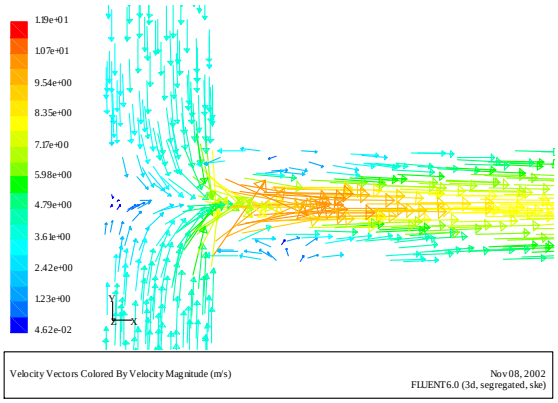

b) Velocity vectors; scaled 10, skipped 20 to clear the view

Figure 7.59: Temperature (K) and Velocity (m/s) contours for U_j = 3.94 m/s, U_m = 3.69 m/s, 95% mixing is not complete till 14.5D from the center of the opposed-tee

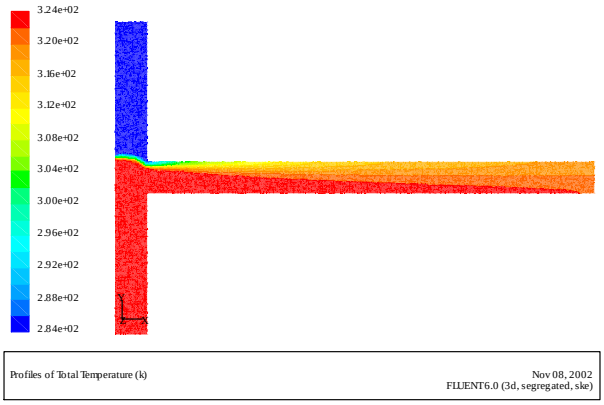

a) Temperature (K) contours

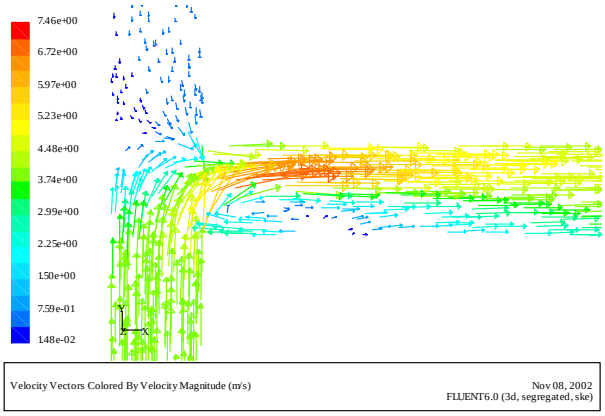

b)Velocity vectors; scaled 10, skipped 20 for a clearer view

Figure 7.60: Temperature (K) and Velocity (m/s) contours for U_j = 3.94 m/s, U_m = 0.40 m/s, 95% mixing completed in 14D from the center of the opposed-tee

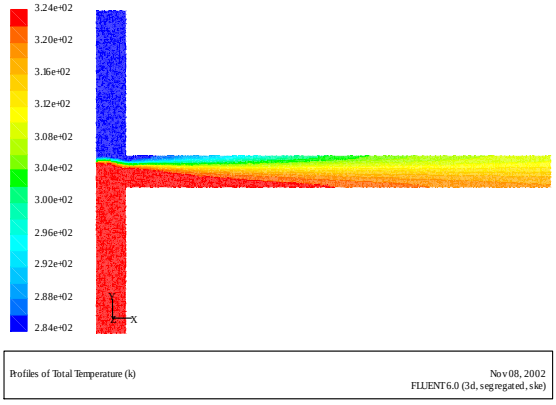

a) Temperature (K) contours

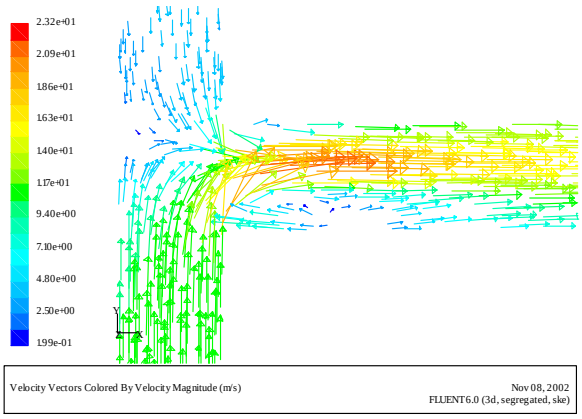

b) Velocity vectors; scaled 10, skipped 20 to clear the view

Figure 7.61: Temperature (K) and Velocity (m/s) contours for U_j = 10.8 m/s, U_m = 3.69 m/s, 95% mixing is not complete till 14.5D from the center of the opposed-tee

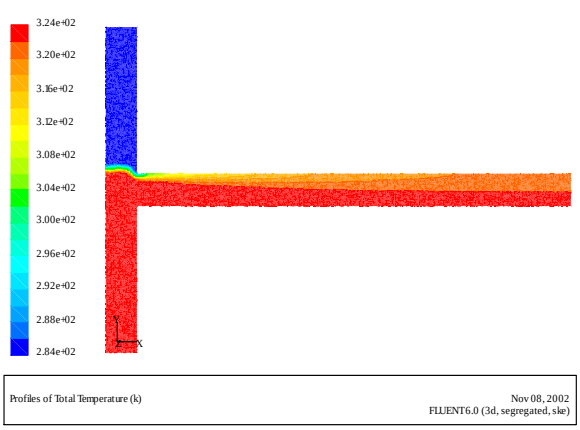

a) Temperature (K) contours

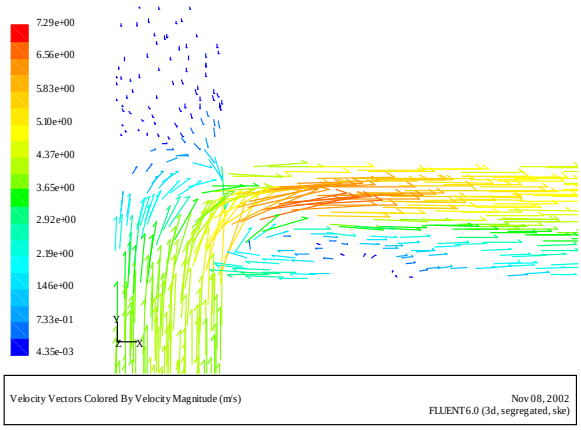

b) Velocity vectors; scaled 10, skipped 20 to clear the view

Figure 7.62: Temperature (K) and Velocity (m/s) contours for U_j = 3.94 m/s and U_m = 0.23 m/s, 95% mixing completed in 10 D from the center of the opposed-tee.

7.8 Scale Up

In this section, various scaling-up criteria of one base case are tested numerically. A base case of 1/4", 90^o side-tee and 1" main pipe with an U_j/U_m of 45.6 and U_m of 0.23 m/s is chosen. A geometric scale-up factor of 4 is chosen, i.e. a 60" long main pipe of 4" diameter and a side-tee of 1" are considered with side-injection at 8". The question of interest is what flow conditions are required in order to obtain the same mixing performance.

Three cases are considered. In the first case, the velocities are kept constant which means the values of Reynolds number have been increased by a factor of four. In the second case the flow rate are kept constant which means that the values of Reynolds number have been reduced by a factor of 4. In the third case Reynolds number are kept constant which means that the flow rate for larger diameter are increased by a factor of 4 while keeping U_j/U_m constant. It should be noted that U_j/U_m is kept constant for all three cases. Data for these 3 cases are shown in Tables 7.7-7.9, and results are presented in Table 7.10.

It can be clearly seen from Table 7.10 that the length required for 95% mixing for the 1"-1/4" and 4"-1" cases are almost identical. However, a significant difference in the values of the length required for 99% mixing was observed.

The scaling up criteria used in these runs consists of (i) using a geometric factor for scaling up the side and main diameters and (ii) keeping the velocity ratio, U_j/U_m, constant.

Table 7.7: Comparison of data for 1”-1/4” and 4”-1” cases keeping the velocities constant.

Velocity Kept Constant	Velocity *m/s*	*Q*, Flow rates *lpm*	Base *Re*	Base Diameter *in*	Scale-up Diameter	New Flow rates, *lpm*	New *Re*
Main	0.23	7.01	5842.0	1	4	111.8	23368.0
Jet	10.52	19.99	66802.0	0.25	1	319.8	267208.0
Ratio, Jet/main	45.7	2.9	11.4	0.25	0.25	2.9	11.4

Table 7.8: Comparison of 1”-1/4” and 4”-1” cases keeping the flow rates constant

Flow Rate kept Constant	*Q*, Flow rates *lpm*	Velocity m/s	Base *Re*	Diameter *in*	Scale-up Diameter	New Velocity m/s	New *Re*
Main	7.01	0.23	5842.0	1	4	0.0144	1464.1
Jet	19.99	10.52	66802.0	0.25	1	0.6575	16700.8
Ratio, Jet/main	2.9	45.7	5.7	0.25	0.25	45.6	11.4

Table 7.9: Comparison of 1”-1/4” and 4”-1” cases keeping Reynolds number constant

Flow Rate kept Constant	*Re*, Reynold Number	Old Q, Flow rates *lpm*	Velocity m/s	Diameter *in*	Scale-up Diameter	New Flow rate, *lpm*	New Velocity m/s
Main	5842.0	7.01	0.23	1	4	28	0.06
Jet	66802.0	19.99	10.52	0.25	1	80	2.63
Ratio, Jet/main	5.7	2.9	45.7	0.25	0.25	2.9	45.7

Table 7.10: Comparison of length required for 95% and 99% mixing for 1”-1/4” and 4”-1” cases keeping Velocity, Flow rate, and Reynolds number constant with base case

Case, D_m - d_j	Re_{mixed}	U_j / U_m	Length required, from entrance of side-jet, for			
			95% mixing		99% mixing	
			inches	Diameters of main pipe	inches	Diameters of main pipe
1”-1/4” Base Case	22542.5	45.7	3	3 D_m	11	11 D_m
4”-1”, Velocity constant	90170	45.7	9	2.25 D_m	27	6.75 D_m
4”-1”, Flow rate constant	5639.3	45.7	9	2.25 D_m	27	6.75 D_m
4”-1”, Reynold number constant	22542.5	45.7	9	2.25 D_m	27	6.75 D_m

For larger diameters, it was noticed that 99% mixing was achieved faster than in smaller diameters. This shows that there may be a larger diameter scale up factor exists for which length required for 95% mixing and 99% mixing criteria become very close. In industry, those diameters will be better to use for side injection mixing.

7.9 Jet Temperatures along Main Pipe after Injection

For each simulation case, the side-stream was at a temperature higher than that of the main stream. The Jet enters and expands in the main fluid as shown in Figure 7.63 for a velocity-ratio of 2.5. Mixing is ultimately achieved when the jet expands to engulf the whole pipe circumference.

Figure 7.64 shows the path lines of particles injected with the side-jet for U_j/U_m = 17.10 with U_j = 3.94 m/s for 1/4" side-tee in 3D, x-y-z plane colored by the temperature in Kelvin. The path of the side-jet is shown in Figures 7.65-7.67 for 1/4" side-tee, choosing the maximum temperature of side-stream within the main fluid. Temperature is decreasing as the path increasing due to mixing with cold main water. For higher velocity ratios, the side-jet temperature is also higher than for lower velocity ratios.

From Figure 7.65, for velocity ratio of 6.2 more fluctuations are observed than for velocity ratios of 17.1 and 9.7. These fluctuations are clearer in Figure 7.66 for a lower velocity ratio of 4.1. Figure 7.67 highlights this phenomenon further for velocity ratio of 2.5, the fluctuations show that for a weak side-jet, the cooler main fluid tries to dominate and the fluctuations are created by turbulence. Figure 7.68 and 7.69 show plots of turbulent dissipation rate, ε , m^2/s^3, and turbulent kinetic energy, k, m^2/s^2 respectively along the centerline for U_j/U_m of 17.1 and 2.5 for 1/4" side-tee.

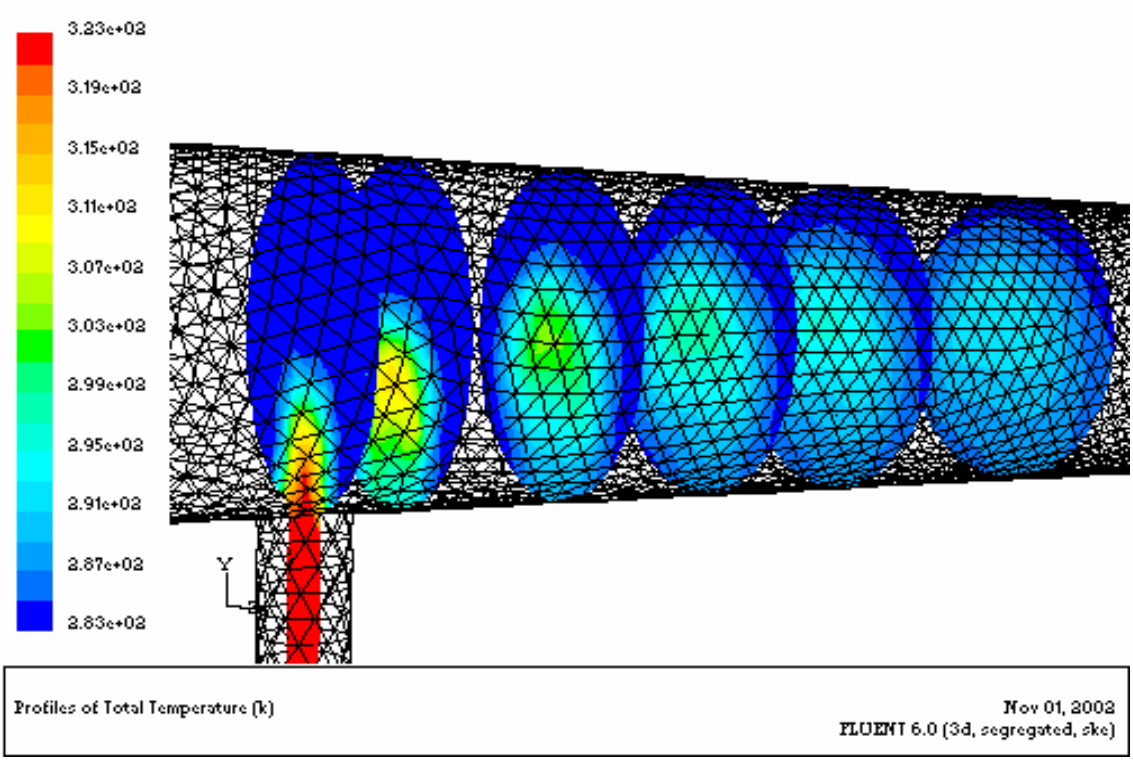

Figure 7.63 : The expansion and bending towards the center of the main pipe of a jet entering the main fluid for a 1/4" side-tee with a 1" main pipe for a velocity ratio = 2.5.

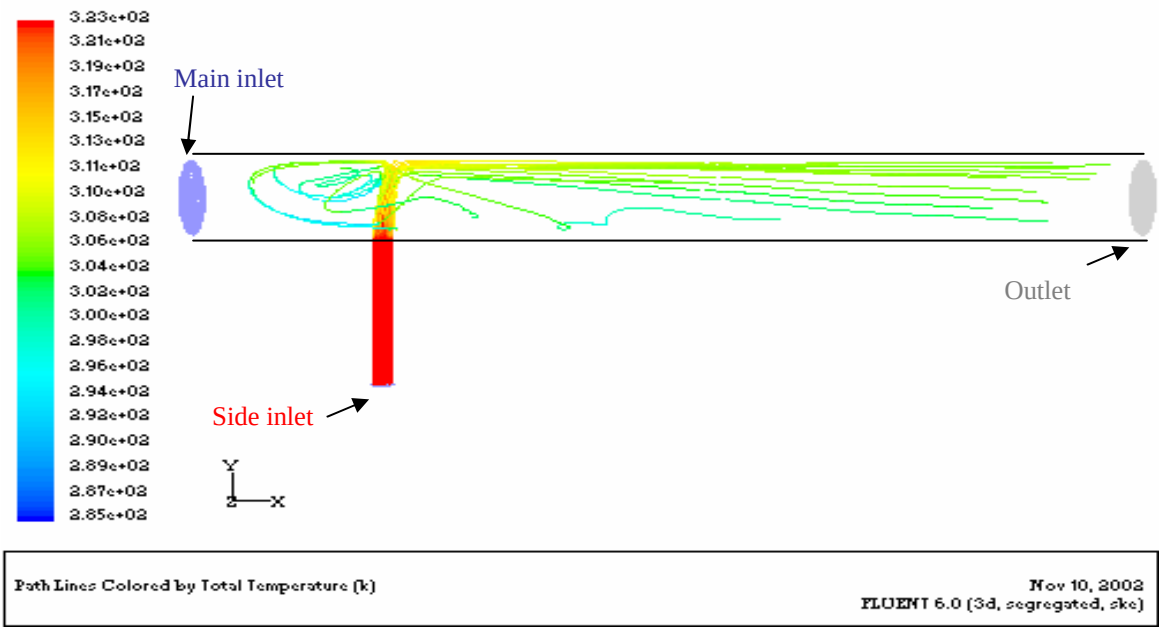

Figure 7.64: Path lines for U_j/U_m = 17.1 for 1/4" side-tee, U_j = 3.94 m/s

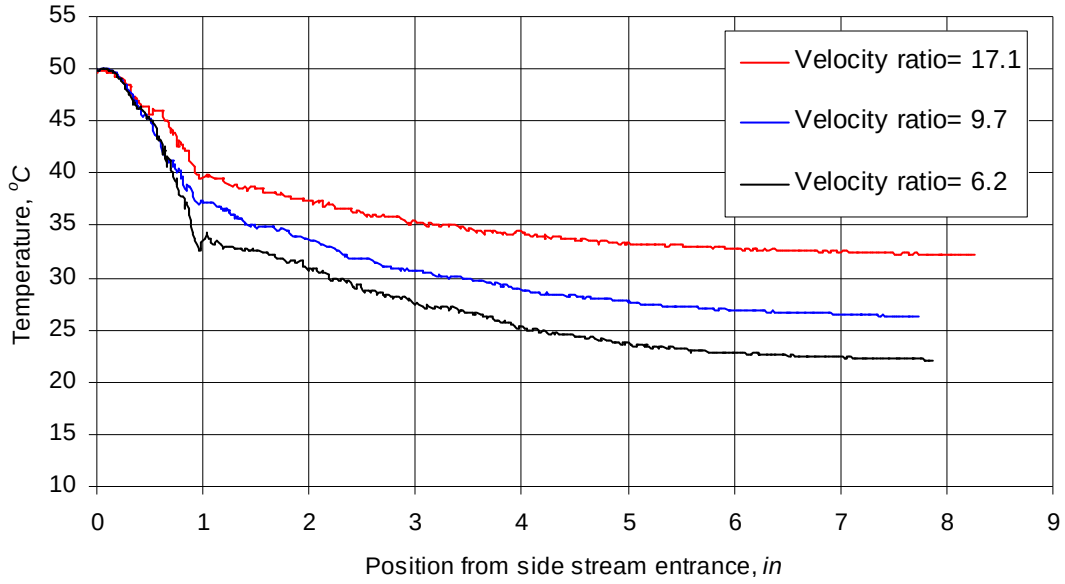

Figure 7.65: Side-jet path-line temperature plots for U_j/U_m = 17.1, 9.7, 6.2, for 1/4" tee, U_j = 3.94 m/s from entrance along motion of jet

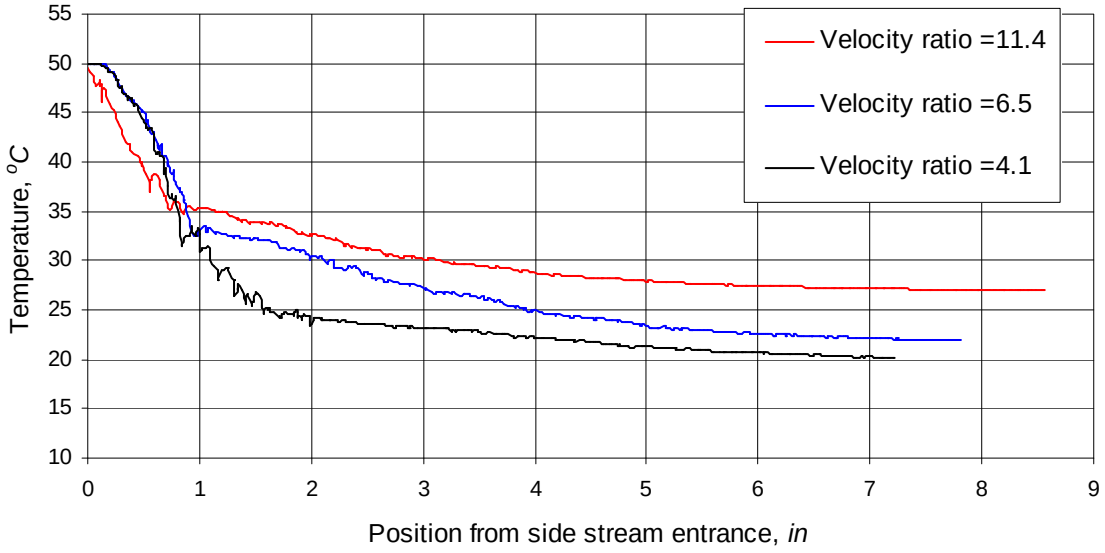

Figure 7.66: Side-jet path-line temperature plots for U_j/U_m = 11.4, 6.5, 4.1, for 1/4" tee, U_j = 2.63 m/s from entrance along motion of jet

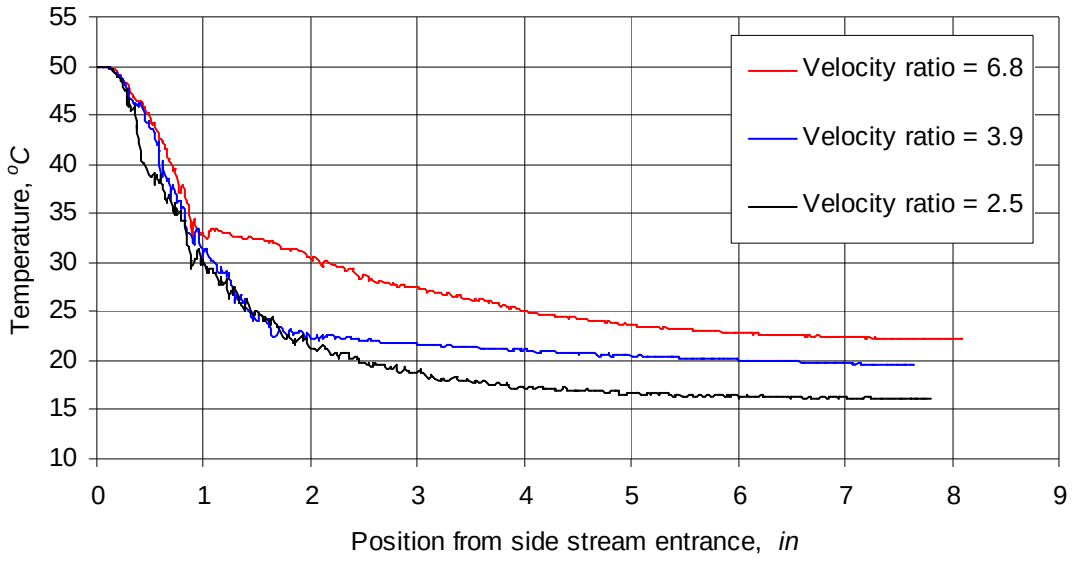

Figure 7.67: Side-jet path-line temperature plots for U_j/U_m = 6.8, 3.9, 2.5, for 1/4" tee, U_j = 1.57 m/s from entrance along motion of jet

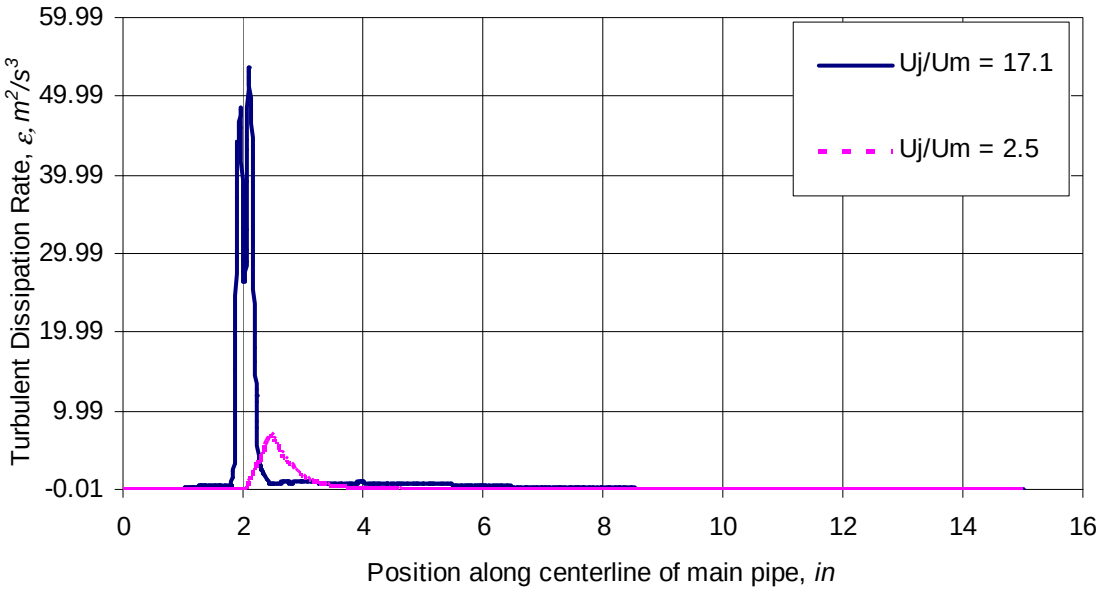

Figure 7.68: Plots of turbulent dissipation rate, ε, m^2/s^3, along the centerline for U_j/U_m of 17.1 and 2.5

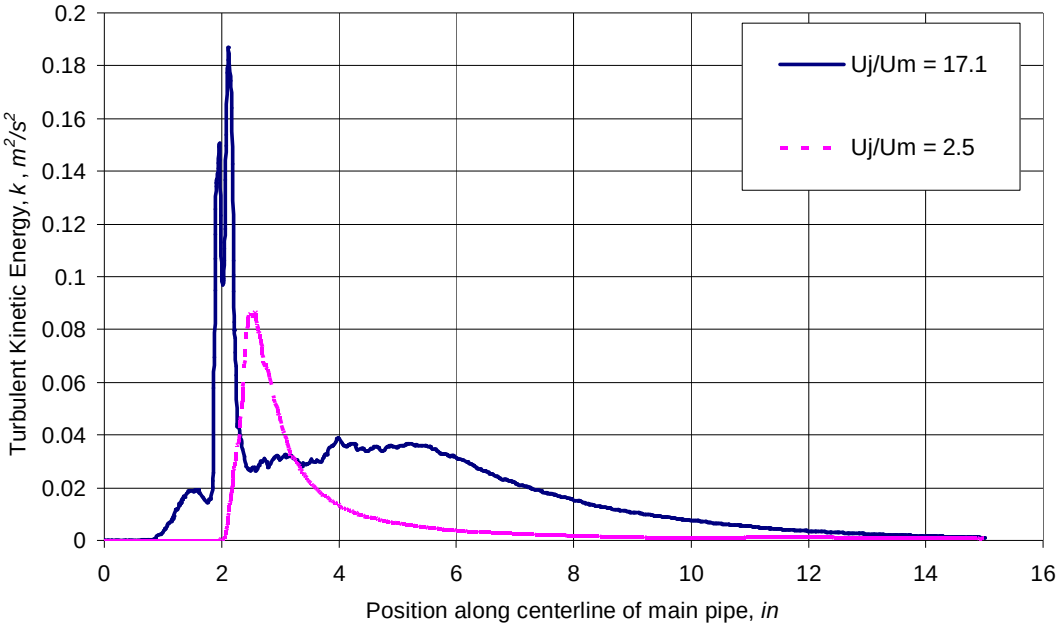

Figure 7.69: Plots of turbulent kinetic energy, k, m^2/s^2, along the centerline for U_j/U_m of 17.1 and 2.5

7.10 Multiple-Tees

Simulation of a multiple-tee geometry has also been carried out. Figure 7.70 shows the grid displaying the four side-tees with a main pipe inlet and outlet. A 1” main pipe and side-jet of 1/4” are considered. Cases with different velocities were simulated as shown in Table 7.11. A mesh size of 3 mm is taken in order to reduce the computational time. Temperature is taken for main- and side-streams as 283 K and 323 K respectively. Three cases are studied for side velocities of 3.94 m/s and 1.313 m/s with main 0.23 m/s and 0.92 m/s as shown in Table 7.11. Cross-sectional views are provided in the next few Figures to show the exact length required for 95% mixing for case two.

Contours of temperature (K) and velocity (m/s) are shown for each case in Figures 7.71-7.73. Velocity vectors are also shown to gain an idea about the flow. Figure 7.71 shows the temperature (K) and velocity (m/s) contours, and velocity vectors for case one. A z-coordinate view shows that streams bend towards the center of the pipe and no back mixing. Velocity vectors describe the straight flow of the jets towards each other and the bending inside of pipe and mixing with each other. Figure 7.72 shows contours of temperature (K) and velocity (m/s) and velocity vectors for a lower main velocity. Cross-sectional views are taken to show where the 95% mixing is taking place.

Figure 7.73 shows temperature (K), velocity (m/s) contours, and velocity vectors for the base case: dividing the side velocity 3.94 m/s into four side-tees (i.e. each jet velocity is 1.313 m/s) with 0.23 m/s main pipe fluid velocity.

Table 7.11: Velocities of main and side fluids for multiple-tees used in simulation

Case	Main Fluid		Side Fluid Velocity, m/s				Temperature of Side Fluid
	Velocity, m/s	Temperature, K	Side 01	Side 02	Side 03	Side 04	
1	0.92	283	3.94	3.94	3.94	3.94	323
2	0.23	283	3.94	3.94	3.94	3.94	323
3	0.23	283	1.313	1.313	1.313	1.313	323

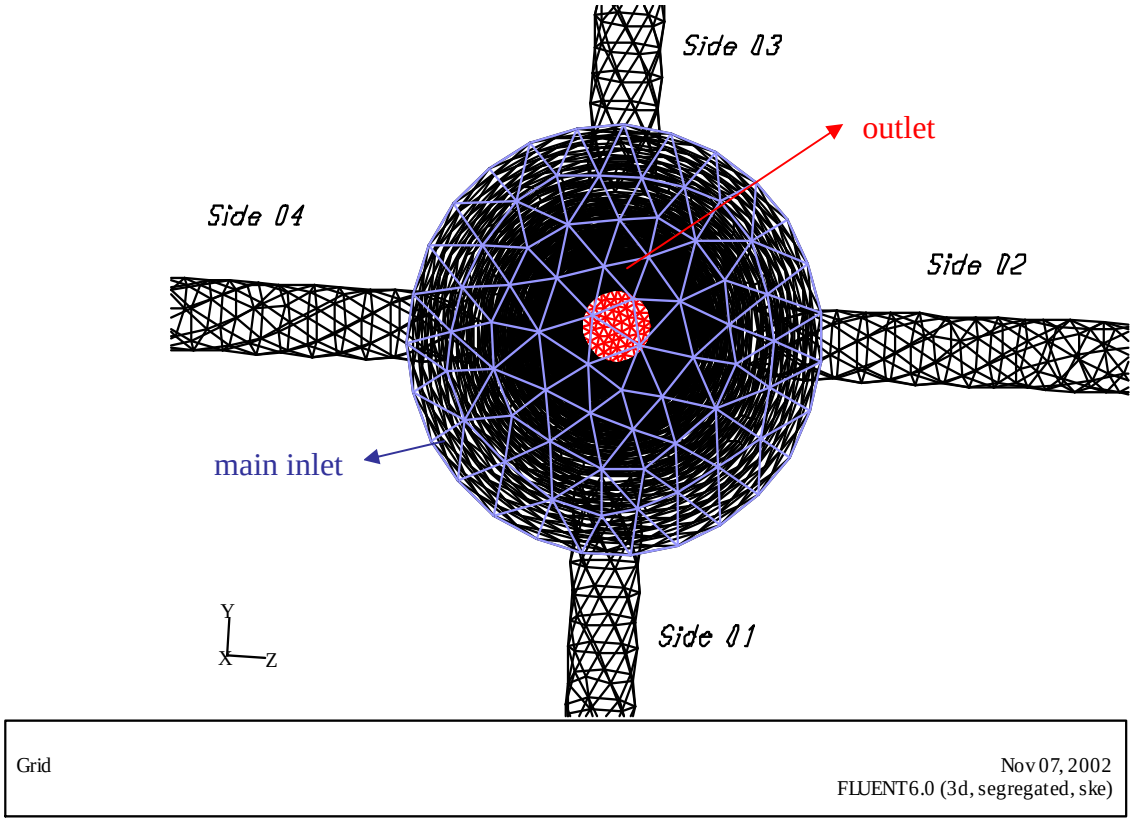

Figure 7.70: Grid display of multiple-tee showing the four side jet and the main pipe with an inlet and an outlet of the main pipe.

The above results, show that for a side-stream divided into four equal flow rates (case 3), the length required for 95% mixing is very short. It has already been tabulated in section 7.5 that for a side velocity of 3.94 m/s and main velocity of 0.23 m/s, velocity ratio 17.10, length required for 95% mixing is 11D (Table 7.4).

It was shown earlier in section 7.6 and Table 7.5 that by keeping everything the same and changing the side-tee angle from 90^o to 45^o, the length required for 95% mixing changed from 11D to 3.5D. Now for the same case if the side-stream is divided into 4 equal streams and injected at 90% into the main-stream, the length required for 95% mixing is 3.5D. For an opposed-tee (section 7.7.2), the length required for 95%, mixing for the same case was shown to be 5.5D

A comparison of the length required for 95% mixing for these different geometries is given in Table 7.13. Comparing 45^o side-tee injection and multiple-tees mixing length, it may be decided that angle 45^o tee may be preferable due to less fabrication work otherwise both are doing almost the same mixing for velocity ratio of 17.10. It can also be seen from Table 7.12 that keeping everything same except using multiple-tees, as in case 2, instead of 1 side-tee 95% mixing is achieved faster. So multiple-tee arrangement may be used where large amount of fluids are to be mixed and higher velocities are to be avoided.

Opposed-tee could also give efficient mixing, and it may be a means to avoid jet impingement on walls. It can be seen from the contours already shown that when the same case for 90^o, 1/4", side-tee with 1" main pipe is simulated for 1"-1/4" opposed-tee, the back-mixing zone is transferred to main-stream coming from the opposite side impinging on the main fluid and avoiding the wall.

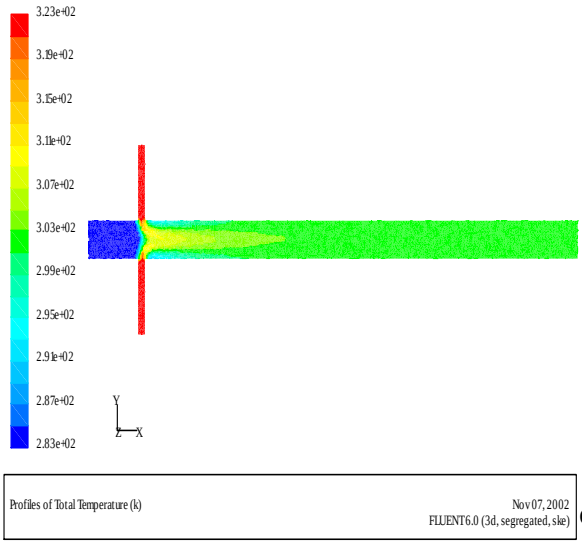

a) Temperature (K) contours in a central z-plane.

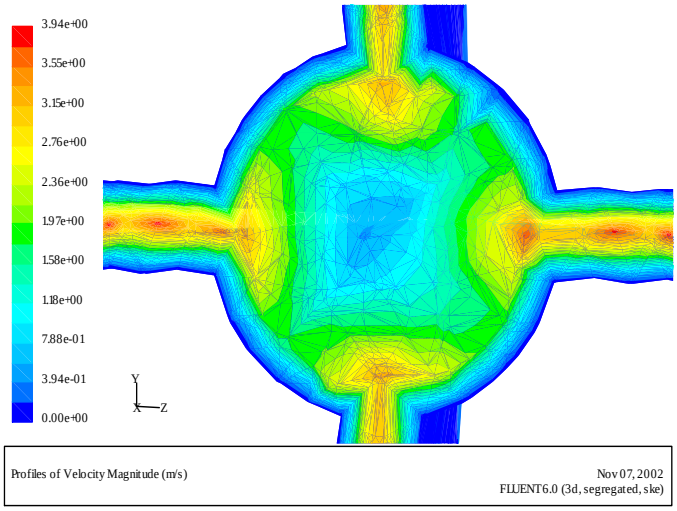

c) Velocity (m/s) contours in an x-plane passing through the incoming jets.

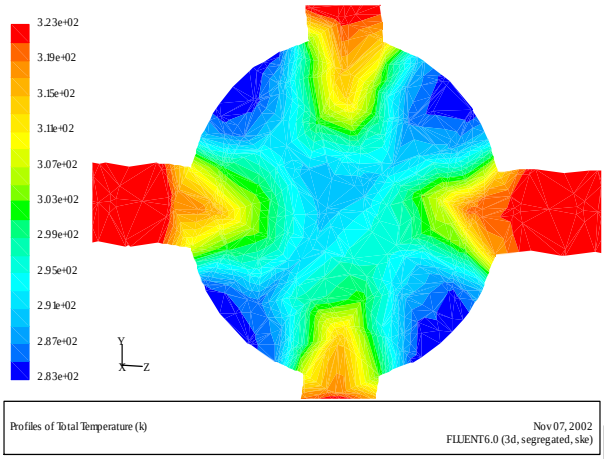

b) Temperature (K) contours in an x-plane passing through the incoming jets.

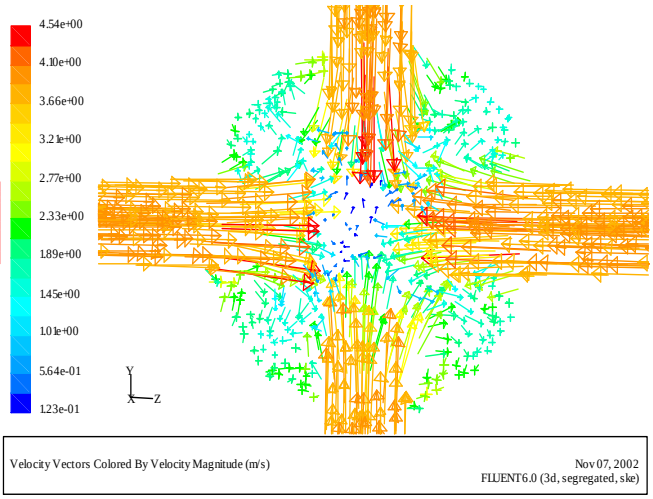

d) Velocity vectors scaled up by a factor 2 in an x-plane.

Figure 7.71: Temperature (K) and Velocity (m/s) contours and velocity vectors for case one.

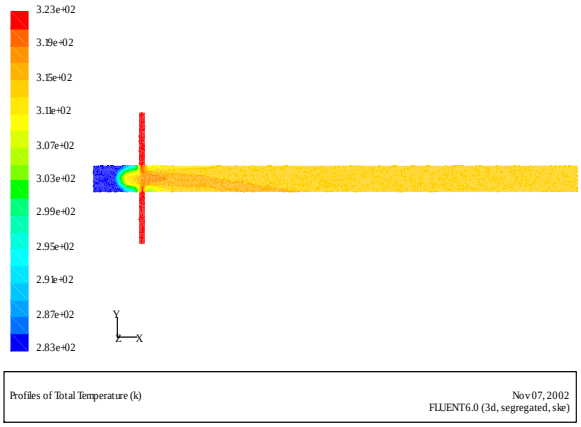

a) Temperature (K) contours in a central z-plane.

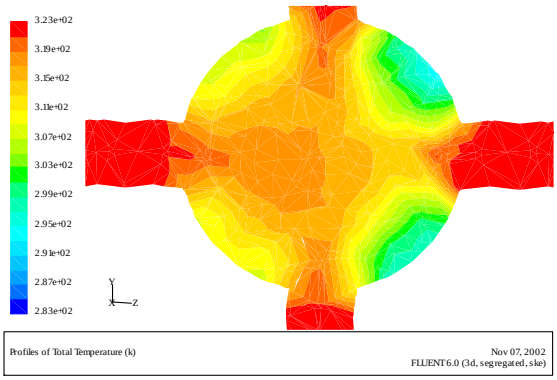

b) Temperature (K) contours in an x-plane passing through the side jets.

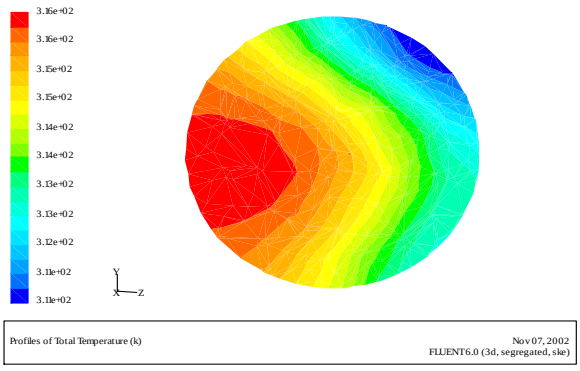

c) Temperature (K) contours at 2D. The range is from 310.9 to 316.4K ($\Delta T = 5.5$).

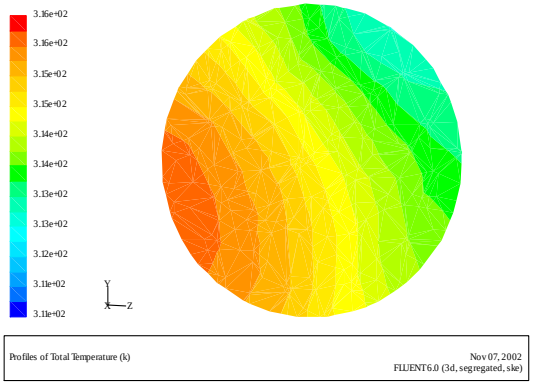

d) Temperature (K) contours showing 95% mixing attained at 4D for temperature range from 312.8 to 316.0K drawn for temperature scaled as above

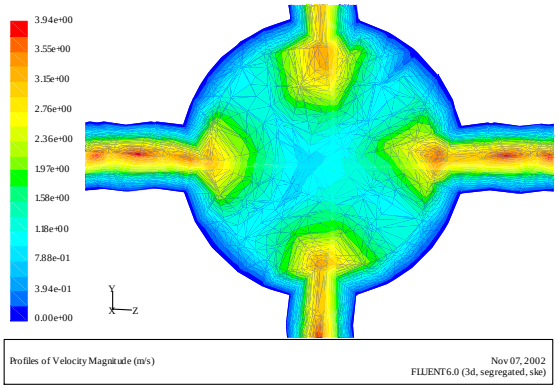

e) Velocity (m/s) contours in an x-plane passing through the side jets

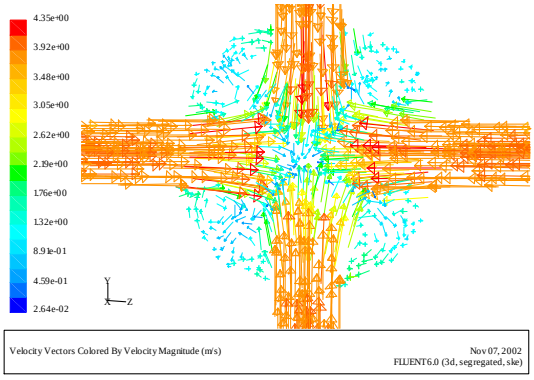

f) Velocity vectors scaled by a factor of 2 at the entrance of the jets.

Figure 7.72: Temperature (K) and Velocity (m/s) contours and velocity vectors for case two showing 95% mixing at 4D.

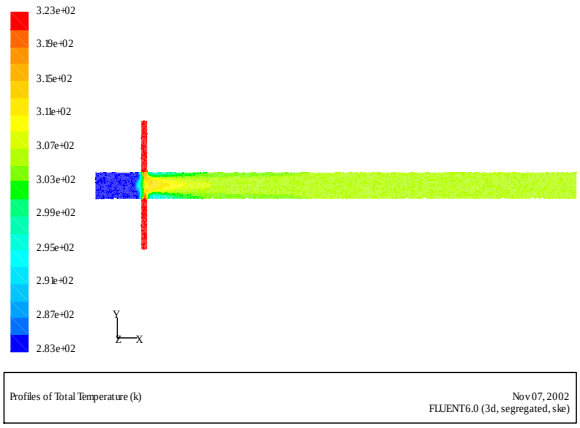

a) Temperature (K) contours in a central z-plane.

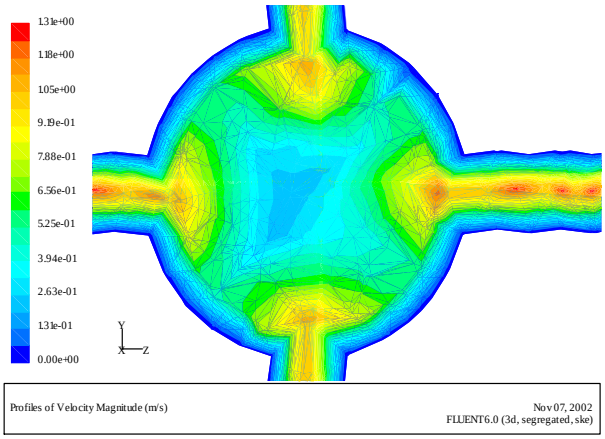

c) Velocity in an x-plane passing through the side jets

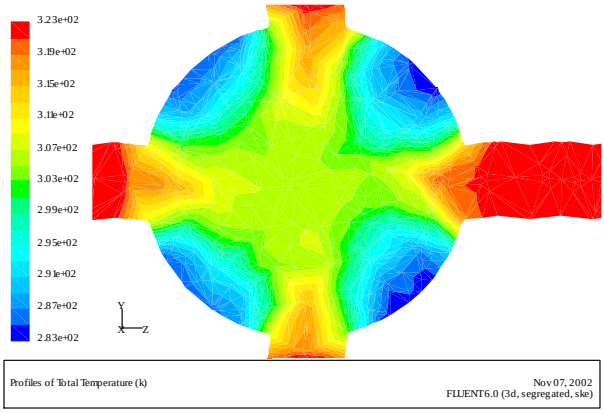

b) Temperature (K) contours in an x-plane passing through the side jets

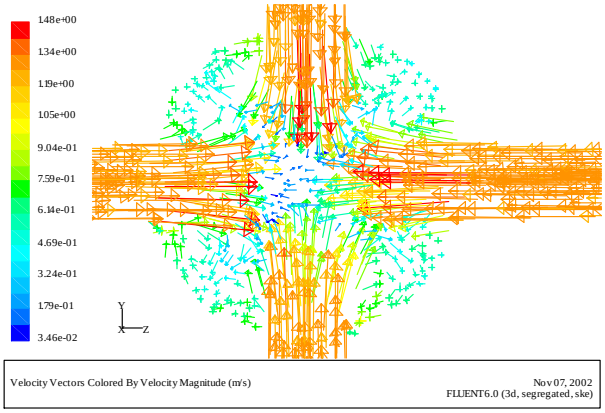

d) Velocity vectors scaled by a factor of 2 at the entrance of the jets.

Figure 7.73: Temperature (K) and Velocity (m/s) contours and velocity vectors for case three.

Table 7.12: Side to main velocity ratios with mixing length in diameter of main pipe.

Case	Main velocity m/s	Side Velocity m/s	Side to main velocity ratio				Mixing Length in main pipe diameters
			01	02	03	04	
1	0.92	3.94	4.283	4.283	4.283	4.283	4.0D
2	0.23	3.94	17.130	17.130	17.130	17.130	4.5D
3	0.23	1.313	5.709	5.709	5.709	5.709	3.5D

Table 7.13: Comparison of length required for 95% mixing for different geometries

Case	Main velocity, m/s	Side velocity, m/s	Length Required for 95% mixing in main pipe diameter
Right-angle, side 1/4” tee with 1” main	0.23	3.94	11D
45^{o} injected side 1/4” tee with 1” main	0.23	3.94	3D
Opposed 1”-1/4” tee	0.23	3.94	5.5D
Four multiple 1/4” tees with 1” main	0.23	1.313 each	3.5D

CHAPTER EIGHT

CONCLUSIONS AND RECOMMENDATIONS

8.1 Conclusions

In the present study, numerical and experimental investigations of mixing in pipelines with side-, opposed-, and multiple-tees were carried out. The temperature of the mixing streams were chosen in such a way which allowed the use of temperature as a measured variable to quantify mixing.

Good agreement between experimental and numerical results is observed especially when the final temperatures and the distance required to achieve 95% mixing are considered. Some differences are observed in the values of temperature in the vicinity of the jet incoming through the side-tee. This could be due to the more complex nature of the flow and the position of the thermocouple. A small difference in position may results in a significant difference in the value of temperature. A better agreement in this regime was obtained by using RSM turbulence model instead of the k-ε model. Finally, the results obtained in a consolidated form can be represented as:

1) The designed experimental facility responded excellently to data generation.
2) The general-purpose three-dimensional computational fluid dynamics package FLUENT 6.0 with unstructured tetrahedral grid optimally refined for a

temperature gradient of 0.001 successfully calculated the axial centerline temperatures.

3) Theoretical and experimental axial centerline temperature-profiles are in good agreement. This provided a sound basis to numerically establish the desired level of mixing, 95% in the present case.

4) Temperature predictions for 95% mixing based both on RSM and k-ε model remained more or less same. RSM, however, gave a better estimate of temperatures in the vicinity of the jet.

5) Simulated results showed that the centerline temperature-profile did not vary much when the constant fluid properties as used presently were made a function of the temperature, thus validating the usage of constant fluid properties.

6) It was observed that the length required for 95% mixing decreased with increasing velocity ratio U_j/U_m for both 1/8" and 1/4" side-tees. This decrease was more steep for the 1/8" case.

7) As U_j/U_m increases, for 90^o side-tee, the jet first hits the opposite wall and with further increase in the velocity ratio, back mixing starts occurring.

8) Excellent matching between the theoretical and experimental results establishes numerical scheme as potential tool to study the physics of mixing for various configurations of side-tee.

9) Numerical simulation of mixing in 1/4" main pipe shows that amongst the four angles 30^o, 45^o, 60^o, and 90^o side-jet entry, an optimum angle exists depending on velocity ratio U_j/U_m. For example, for velocity ratio 17.1, 45^o was found to be optimum of the four angles. It can be proposed that whenever the combined

effect of U_j/U_m and angle of side jet indicate that the probability of hitting the opposite wall is minimum, that would be the optimum combination of U_j/U_m and θ.

10) Based on observation 9, it can be conjectured that with much back mixing the best results are when that has the lower probability of hitting the opposite wall. It shall be noted that lowest angle slides along the wall, which is the worst condition.

11) An interesting observation is that for velocity ratio of 3.94 m/s / 0.23 m/s = 17.1, when the configuration of main pipe was changed to form opposite-tee arrangement, the mixing was distinctly found to be better than for 90^o side-tee arrangement.

12) Another interesting observation was found that when the mass flow rate was divided into four equal symmetric jets of same side entry diameter, the length required for 95% mixing was reduced to almost one third that of 90^o side-tee.

8.2 Recommendations

1) It is highly recommended that industry should not use 90^o tees for pipeline mixing for higher side velocities to avoid impingement resulting in corrosion and other problems. Other upstream angles > 95^o may also be investigated. An industrial criterion of 99% mixing should also be studied.
2) It is also recommended that experiments should be done for angle-tee and opposed-tee to compare the numerical results. Experiments may be done for the same side-tee model, which has been validated, introducing some reaction using suitable experimental setup.
3) Different non-reactive fluids may also be evaluated in the same manner.
4) For all the above mentioned cases, simulation work may be done using the model, which we have already validated. Two phase mixing of same or different fluid may also be investigated.
5) In a distillation column, phase separation takes place, so instead of mixing this tee can be investigated for phase separation to cut the cost of design and installation of the distillation column.
6) For higher velocity ratios, impingement and back mixing effects on reaction may be studied. Opposed-tee and multiple-tees may be the best geometries for some chemical reactions. Investigations should be done in this area. More detailed study of angle injection for different fluids and for different phases may result in some useful findings for the industry.

7) Heat transfer investigation through the walls may also be done for same side-tee model especially where the impingement is taking place.

8) A geometry is shown in Figure 8.1 with three opening **A**, **B**, and **C**, of diameters D_α, D_β, and D_γ respectively, forming three angles with each other as α, β, and γ respectively. Using any of two for inlet and third one as out let, for different diameters with different velocity ratios for different angles, a comprehensive study of optimum length required for mixing may be done.

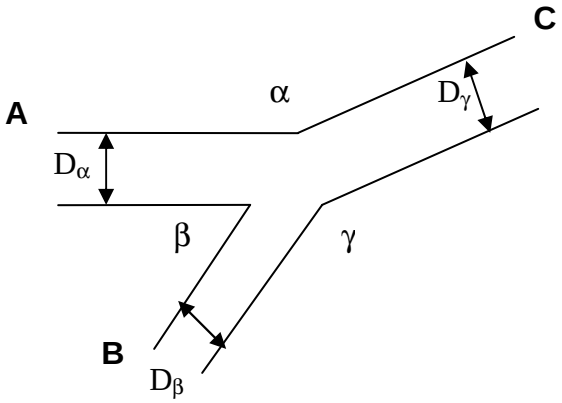

Figure 8.1: A general side injection arrangement, a side-Y.

9) Numerical prediction for various configurations and combinations of jet entry should be comprehensively studied with the view to identify a recognizable, rational and logical parameter based on physics of flow and mixing.

10) Investigations and studies of mixing of highly viscous fluids using tees may also be done.

11) Gravity effects on mixing by changing the direction of injection point of side-tee to main pipe may also be studied.

12) Off centering the side-tee from main pipe, introducing swirls to main flow, may also be investigated experimentally and numerically.

13) Multiple angle-tees may also reduce the length required for mixing. This may also be checked.

NOMENCLATURE

A	Area (m ^{2}, ft ^{2})
$\boldsymbol{A}$	Surface area vector (m ^{2}, ft ^{2})
A_f	Area of Face f (m ^{2}, ft ^{2})
A, B, C	Opening of pipe of various or equal diameters
$\vec{a}$	Acceleration (m/s ^{2}, ft/s ^{2})
C	Concentration (mass/volume, moles/volume)
$\overline{C}$	Mean Tracer Concentration (mass/volume, moles/volume)
C_μ	0.09, Constant for k-ε model
$C_{1\varepsilon}$	1.44, Constant for k-ε model
$C_{2\varepsilon}$	1.92, Constant for k-ε model
C_D	Drag coefficient, defined different ways (dimensionless)
c_p, c_v	Heat capacity at constant pressure, volume (J/kg-K, Btu/lb $_m$- ^{o}F)
d, d_m	Diameter of side-tee (cm, in)
D, D_j	Diameter main-pipe(cm, in)
D_α, D_β, D_γ	Diameter of pipe(cm, in)
Di	Diffusivity of phase i, (m ^{2}/s, ft ^{2}/s)
D_{ij}, D	Mass diffusion coefficient (m ^{2}/s, ft ^{2}/s)
E	Total energy, activation energy (J, kJ, cal, Btu)
f	Mixture fraction (dimensionless)
F	Force vector (N, lb $_f$)
F_D	Drag force (N, lb $_f$)
$\vec{g}$	Gravitational acceleration (m/s ^{2}, ft/s ^{2}); standard values = 9.80665 m/s ^{2}, 32.1740 ft/s ^{2}
G_k	The generation of turbulent kinetic energy due to the mean velocity gradients. (m ^{2}/s ^{2}, ft ^{2}/s ^{2})
G_b	The generation of turbulent kinetic energy due to buoyancy, (m ^{2}/s ^{2}, ft ^{2}/s ^{2})
H	Total enthalpy (energy/mass, energy/mole)
h	Heat transfer coefficient (W/m ^{2}-K, Btu/ft ^{2}-h- ^{o}F)

h	Species enthalpy; h^0, standard state enthalpy of formation (energy/mass, energy/mole)
I	Identity matrix,
J	Mass flux; diffusion flux (kg/m ^{2}-s, lb $_m$/ft ^{2}-s)
j	Representing Jet (side tee) when used as subscript
K	Equilibrium constant = forward rate constant/backward rate constant (units vary)
k	Turbulent kinetic energy (m ^{2}/s ^{2}, ft ^{2}/s ^{2})
k	Kinetic energy per unit mass (J/kg, Btu/lb $_m$)
k	Thermal conductivity (W/m-K, Btu/ft-h- ^{o}F)
k, k_c	Mass transfer coefficient (units vary); also K, K_c
LRF95%M	Length Required for 95% Mixing (in, Diameter of main pipe)
LDA	Laser Doppler Anemometry
LES	Large Eddy Simulation
LIF	Laser Induced Fluorescence
m	Representing main fluid when used as subscript
m	Mass (g, kg, lb $_m$)
m_i	Mass per unit volume entering phase i from all sources (g /cm^3, kg/m^3, lb $_m$/ ft^3)
$\dot{m}$	Mass flow rate (kg/s, lb $_m$/s)
M_w	Molecular weight (kg/kgmol, lb $_m$/lb $_m$mol)
p	Pressure (Pa, atm, mm Hg, lb $_f$/ft ^{2})
PDA	Phase Doppler Anemometry
Pe	Peclet number $\equiv$ Re x Pr for heat transfer, and $\equiv$ Re x Sc for mass transfer (dimensionless)
PISO	Pressure Implicit with Splitting of Operators
PIV	Particle Image Velocimetry
Pr	Prandtl number $\equiv$ratio of momentum diffusivity to thermal diffusivity (dimensionless)
Q	Flow rate (lpm)
Q_j	Jet side-tee flow rate (lpm)
Q_m	Main-fluid flow rate (lpm)
q	Heat flux (W/m ^{2}, Btu/ft ^{2}-h)

R_i	volume fraction of phase *i*
R	Gas-law constant (8.31447 x 10^3 J/kgmol-K, 1.98588 Btu/lb $_m$mol- ^{o}F)
r	Radius (m, ft)
Re	Reynolds number ≡ ratio of inertial forces to viscous forces (dimensionless)
RNG	Renormalization Group
RSM	Reynolds Stress Model
Sc	Schmidt number ≡ ratio of momentum diffusivity to mass diffusivity (dimensionless)
SIMPLE	Semi Implicit Method for Pressure Linked Equations
SIMPLER	SIMPLE Revised
SIMPLEC	SIMPLE Consistent
S_ϕ	Source rate of ϕ per unit volume
$S_{\phi i}$	Source rate of ϕ_i per unit volume
T	Temperature (K, ^{o}C, ^{o}R, ^{o}F)
T_j	Jet side-stream Temperature (K, ^{o}C, ^{o}R, ^{o}F)
T_m	Main-fluid temperature (K, ^{o}C, ^{o}R, ^{o}F)
$T_{e,}$ $\overline{T}$	Equilibrium Temperature (K, ^{o}C, ^{o}R, ^{o}F)
T_{im}	Initial Temperature of main stream before mixing (K, ^{o}C, ^{o}R, ^{o}F)
t	Time (s)
U	Free-stream velocity (m/s, ft/s)
U_i	velocity vector of phase i
U_j	Jet (side-stream) velocity (m/s, ft/s)
U_m	main fluid(main-stream) velocity (m/s, ft/s)
u, v, w	Velocity magnitude (m/s, ft/s); also written with directional subscripts (e.g., v_x, v_y, v_z, $v_{r,}$ v_θ)
V	Volume (m ^{3}, ft ^{3})
X	Mole fraction (dimensionless)
Y	Mass fraction (dimensionless)
Y_M	The contribution of the fluctuating dilatation in compressible turbulence to the overall dissipation rate.
α	Volume fraction (dimensionless)

$\alpha, \beta, \gamma, \theta$	Angle, degree
Δ	Change in variable, final - initial
ε	Turbulent dissipation rate (m^2/s^3, ft^2/s^3)
ε	Void fraction (dimensionless)
η	Effectiveness factor (dimensionless)
μ	Dynamic viscosity (cP, Pa-s, lb_m/ft-s, kg/m-s)
μ_{eff}	Effective viscosity (cP, Pa-s, lb_m/ft-s, kg/m-s)
μ_i	Turbulent viscosity (cP, Pa-s, lb_m/ft-s, kg/m-s)
ν	Kinematic viscosity (m^2/s, ft^2/s)
ρ	Density (kg/m^3, lb_m/ft^3)
τ	Stress tensor
ρ_i	Density of phase *i* (kg/m^3, lb_m/ft^3)
σ_k	turbulent Prandtl numbers for *k* (dimensionless)
σ_ε	Turbulent Prandtl numbers for ε.(dimensionless)
ϕi	Any conserved property of phase *i*
Γ_ϕ	Diffusion coefficient of ϕ in phase *i*
Γ_{ϕ_i}	Exchange coefficient of ϕ in phase *i*
ω	Specific dissipation rate (s^{-1})

REFERENCES

Andreopoulos, J., "Heat Transfer Measurements in a Heated Jet-Pipe Flow Issuing into a Cold Cross Stream", *Phys. Fluids*, **26**, 3201, 1983.

Angst, W., J. R. Bourne, and R. N. Sharma, "Mixing and Fast Chemical Reaction-IV - The Dimensions of the Reaction Zone", *Chem. Eng. Sci*., **37**(4), 1982.

Angst, W., J. R. Bourne, and R. N. Sharma, "Mixing and Fast Chemical Reactions-V Influence of Diffusion with Reaction Zone on Selectivity", *Chem. Eng. Sci*., **37**(8), 1982.

Avalosse, Th. and M. J. Crochet, "Finite-Element Simulation of Mixing: 1. Two-Dimensional Flow in Periodic Geometry", *AIChE J*., **43**(3), 577-587, 1997.

Azzopardi, B. J., D. A. Colman and D. Nicholson, "Plant application of a t-junction as a partial phase separator", *Trans IChemE,* **80** (A), 87-96, 2002.

Baldyga, J. and W. Orciuch, "Barium sulphate precipitation in a pipe -an experimental study and CFD modelling", *Chem. Eng. Sci.*, **56**, 2435-2444, 2001.

Baldyga, J. and W. Orciuch, "Closure problem for precipitation", *Transactions of the Institution of Chemical Engineers"* **75**(A), 160-170, 1997.

Baldyga, J., J. R. Bourne (Fellow), B. Dubuisj, A. W. Etchells, R. V. Gholap and B. Zimmermann, "Jet reactor scale-up for mixing-controlled reactions", *Trans IChemE*, **73** (A), 497-502, 1995.

Bourne, J. R., G. Schwarz, and R. N. Sharma, "A New Method for Studying Diffusive Mixing in a Tubular Reactor", Proc. Fourth European Conf. on Mixing, Netherlands, 1982.

Brodkey, R. S., Ed., Turbulence in Mixing Operation, Academic Press, NY (1975).

Chilton, T. H., and R. P. Genereaux, "The mixing of gases for reactions," *AIChE J. Trans.*, **25**, 103 ,1930.

Chyu M.K., Y. Hsing, V. Natarajan, J. S. Chiou, " Effect of perpendicular flow entry on convective heat/mass transfer from pin-fin arrays", *Trans. ASME, J. of Heat Transfer*, **121**, 668-674 , 1999.

Cozewith, C. and M. Busko, "Design Co-relations for Mixing Tees", *Ind. Eng. Chem. Res.*, **28**, 1521-1530, 1989.

Cozewith, C., G. Ver Strate, T. J. Dalton, J. W. Frederick, and P.R. Ponzi, " Computer Simulation of Tee Mixers for Non-reactive and Reactive Flows", *Ind. Eng. Chem. Res.*, **30**, 270-275, 1991.

Crabb, D., D. Durao, and J. H. Whitelaw, "A Round Jet Normal to a Cross Flow", *J. Fluids Eng.,* **103**, 103, 1981.

Devahastin, S. and A. S. Mujumdar, "A numerical study of flow and mixing characterististics of laminar confined impinging streams", *Chem. Eng. J.*, **85,** 215-223, 2002

Epstein. M. and J. P. Burelbach, "Vertical mixing above a steady circular source of buoyancy", *Intl. J. of Heat and Mass Transfer*, **44**, 525-536, 2001.

Etchells, A.W. and D. G. R Short, "Pipeline Mixing - A user's View Part I - Turbulent Blending", Proc. of the BHRA, *6th European Conf. on Mixing*, Italy, 24-26th May, 1988.

Feng, Z., X. Wang, and L.J. Forney, "Single jet mixing at arbitrary angle in turbulent tube flow", *Transactions of the ASME,* **121,** 762-746, 1999.

Fischer, H. B., E. J. List, R. C. Y Koh, J. Imberger, N. H. Brooks, “Mixing in Inland and Coastal Waters”, pp 346, Academic Press, NY (1979).

Fitzgerald, S. D. and E. R. Holley, “Jet Injection for Optimum Mixing in Pipe Flow,” Research Report No. 144, Water Resources Center, Univ. of Illinois, URBANA, Il ,1979.

Fitzgerald, S. D. and E. R. Holley, “Jet Injection for Optimum Mixing in Pipe Flow,” *J. Hydraul. Div. ASCE,* **107** (HY 10), 1179, 1981.

Forney, L. J. and G. E. Gray, “Optimum Design of a Tee Mixer for Fast Reactions”, *AIChE J.*, **31(**11), 1773-1776, 1990.

Forney, L. J. and L. A. Monclova, “Numerical Simulation of Pipeline Tee Mixers: Comparison with Data”, Industrial Mixing Technology: Chemical and Biological Applications, E. L. Gaden, G. B. Tatterson, R. V. Calabrese, and W. R. Penney, pp 141-143, Academic Press, NY, 1994.

Forney, L. J., and T. C. Kwon, “Efficient Single Jet Mixing in Turbulent Tube Flow”, *AIChE J.*, **25(**4), 623-630, 1979.

Forney, L. J., and H. C., Lee, “Optimum Dimensions for Pipeline Mixing at a T-Junction”, *AIChE J.*, **28(**6), 980-987, 1982.

Forney, L. J., and L. A. Oakes, “Slow Second-Order Reactions in a Deflected Buoyant Jet”, *AIChE J.*, **30**(1), 30-37, 1984.

Forney, L. J., Encyclopedia of Fluid Mechanics, Vol. II, Ch. 25, N. P. Cheremisinoff, Gulf Publishing Co., Houston ,1986.

Ger, A. M. and E. R. Holley, “Comparison of Single-Point Injection in Pipe Flow”, *J. Hydraul. Div. ASCE*, **102** (HY 6), 731, 1976.

Gosman, A. D. and R. Simitovic, “An Experimental Study of Confined Jet Mixing”, Chem. Eng. Sci., **41**, 1853, 1986.

Gosman, A. D., “Developments in Industrial Computational Fluid Dynamics”, *Trans I Chem E*, **76(**Pt A), 53-161, 1998.

Gouldin, F. C., “Role of Turbulent Fluctuations in NO Formations,” *Comb. Sci. Tech.*, **9,** 17, 1974.

Gray, J. B., Mixing: Theory and Practice, III, J.B. Gray and V. W. Uhl, Academic Press , 1986.

Guilkey, J. E., P. A. McMurty and J. C. Klewicki “Effect of Inlet Conditions on Scalar Statistics in Pipe Mixing”, *AIChE J.*, **43**(8), 1947-1955, 1997.

Gyenis, J., J. Arva and L. Nemeth, “ Steady State Particle Flow in Mixer Tubes equiped with Motionless Mixer Elements”, Industrial Mixing Technology: Chemical and Biological Applications, E. L. Gaden, G. B. Tatterson, R. V. Calabrese, and W. R. Penney, pp 144-156, Academic Press, NY, 1994.

Hansen L., J. E. Guilkey, P. A. MacMurtry. and J. C. Klewicki, “The Use of Photoactivable Fluorophores in the Study of Turbulent Pipe Mixing: Effect of Inlet Geometry”, *Meas. Sci. Technol.*, **II**, pp1235-1250, 2000.

Hansen, L. J. and J. C. Klewicki, “Effect of Initial Conditions on Turbulent Pipe Mixing”, *ASME Fluids Engineering Div., Fluids Eng. Div.*, **244**, 297-300, 1997.

Howes, T and P. J. Shardlow, "Simulation of Mixing in Unsteady Flow Through a Periodically Obstructed Channel", *Chem. Eng. Sci.*, .**52**(7), 1215-1255, 1997.

Johnson, D. A. and P. E. Wood, "Self -Sustained oscillations in impinging jets in an enclosure" *The Can. J. Chem. Eng.*, **78,** 867-875, 2000.

Khokhar, Z. H., H. D. Zughbi, and R. N. Sharma, "Mixing in Pipeline with Side-Tees", *Accepted for 6th Saudi Engineering Conference*, 17-19th December 2002.

King, R., ed., "Fluid Mechanics of Mixing: Modelling, Operations and Experimental Techniques", Kluwer Academic Publishers, DorDrecht, 1992.

Kresta, S. M. and P. E. Wood, "Prediction of Three-dimensional Turbulent Flow in Stirred Tanks", *AIChE J.*, **37**, 448-460, 1991.

Lam, K. M. and L. P. Xia, "Experimental Simulation of a Vertical Round Jet Issuing into an Unsteady Cross-Flow", *J. Hyd. Eng*., 369-379, 2001.

Lin. C. H. and E. E. O'Brien, "Turbulent Shear Flow Mixing and Rapid Chemical Reactions: an Analogy," *J. Fluid Mech*., **64**, 195, 1974.

Liou, T. M., C. C. Liao, S. H. Chen, and H. M. Lin, "Study on Side-Jet Injection near a Duct Entry with Various Injection Angles", *Trans. ASME*, **121**, 580, 1999.

Maruyama, T., T. Mizushina, and S. Hayashigushi, "Optimum Jet Mixing in Turbulent Pipe Flow", *Int. Chem., Eng.*, **23**, 707, 1983.

Maruyama, T., T. Mizushina, and F. Watanabe, "Turbulent Mixing of Two Fluid Streams at an Oblique Branch, "*Int. J. Chem. Eng.*, **22**(2), 287, 1982.

Maruyama, T., S. Suzuki, and T. Mizushina, “Pipeline Mixing Between Two Fluid Streams Meeting at a T-Junction”, *Int. J. Chem. Eng.*, **21**, 205, 1981.

McKelvey, K. N., H. N. Yieh, S. Zakanycz, and R. S. Brodkey, “Turbulent Motion, Mixing and Kinetics and Chemical Reactor Configuration,” *AIChE J.*, **21**, 1165, 1975.

Middleman, S., ‘Fundamentals of Polymer Processing’, McGraw-Hill Book Co. New York, 1977.

Morchain J., C. Maranges and C. Fonade, “CFD modeling of a two phase jet aerator under influence of a crossflow”, *Wat. Res.*, **34**(13), 3460-3472, 2000.

Morton-Jones, D. H., Polymer Processing, Chapman and Hall, London, 1989.

Moussa, Z., J. Trischka, and S. Eskinazi, “The near Field in the Mixing of a round Jet with a Cross Stream”, *J. Fluid Mech.*, **80,** 49, 1977.

Oldshue, J. Y., Fluid Mixing Tech., McGraw-Hill Publications Co., NY, 1983.

Ottino, J. M., “The Kinematics of Mixing: Stretching, Chaos and Transport”, Cambridge University Press, Cambridge, 1990.

Pan, G. and H. Meng, “Experimental Study of Turbulent Mixing in a Tee Mixer Using PIV and PLIF”, *AIChE J.* **47,** 2653, 2001.

Patankar, S. V., Spalding, “DBA Calculation Procedure for Heat, Mass and Momentum Transfer in Three-Dimensional Parabolic Flows”,. *Int. J. Heat Mass Trans.*, **15**, 1787-1806, 1972.

Patterson, G. K., “Turbulence in Mixing Operations”, Academic Press, NY, 1975.

Patwardhan, A. W., CFD modelling of jet mixed tanks, *Chem. Eng. Sci.*, **57**, 1307. 2002

Rajaratnam, N., Turbulent Jets, Elsevier Scientific Pub. Co., Washington, 1976.

Reed, R. D. and B. C. Narayan, "Mixing Fluids under Turbulent Flow Conditions", *Chem. Eng.*, **86**, 131, 1979.

Seo W. I., H. S. Kim, D. Yu, and D. S. Kim, "Performance of Tee diffusers in shallow water with crossflow", *J. of Hydraulics Engineering*, **127**(1), 53-61, 2001.

Sharma R. N. and S. V. Patankar, "Numerical Computations of Wall-Jet Flows", *Int. J. of Heat and Mass Transfer*, **25**(11), 1982.

Shiau L. D., and T. S. Lu, "Interactive effects of particle mixing and segregation on the performance characteristics of a fluidized bed crystallizer", *Ind. Eng. Chem. Res.*, **40**, 707-713, 2001.

Simpson, L. L., "Turbulence and Industrial Mixing," *Chem. Eng. Prog.*, **70**, 77 (1974).

Singh, M., and H. L. Toor, "Characteristics of jet mixers-effect of number of jets and Reynolds numbers," *AIChE J.*, **20**, 1224, 1974.

Souvaliotis, A., S. C. Jana, and J. M. Ottino, "Potentialities and Limitations of Mixing Simulations", *AIChE J.*, **41**(7), 1605-1621, 1995.

Sroka, L. M. and L. J. Forney, "Fluid Mixing in a 90° Pipeline Elbow", *Ind. Eng. Chem. Res.*, **28**(6), 850-856, 1989.

Sroka, L. M. and L. J. Forney, "Fluid Mixing with a Pipeline Tee: Theory and experiment". *AIChE J.*, **35**(3), 406-414, 1989.

Tosun, G., "A Study of Micromixing in Tee Mixers", *Ind. Eng. Chem. Res.*, **26**, 1184-1193, 1987.

Weber, L. J., E. D. Schumate, N. Mawer, “Experiments on Flow at a 90° Open-Channel Junction”. *J. Hyd. Eng*., **127**, 340, 2001.

Winter, D. D., “Turbulent Jet in a Turbulent Pipe Flow,” *M.S. Thesis*, Univ. of Illinois at Urbana-Champaign, 1975.

Yao, W., K. Takahashi, and K. Koyama, “Theoretical Tool for Optimum Design of Mixer, and Visualisation and Quantification of Mixing Performance”, *J. Chem. Eng. Jap.*, **31(**22), 220-227, 1998.

Yuan L. L. and R. L. Street, “Large-eddy simulations of a round jet in cross flow”, *J. Fluid Mech.*, **379**, 71-104, 1999.

Zughbi, H. D. and M. A. Rakib, Z. H. Khokhar, “Investigations of Mixing in a Fluid Jet Agitated Large Tank”, Submitted to *Ind. Chem. & Eng. Res.* (September 2001).

Zughbi, H.D. and M. A. Rakib, “Investigation of Mixing in Fluid Jet Agitated Tank”, *Chem. Eng. Comm.*, **189** (9), pp 1038-1057, 2002.

Zughbi, H.D. and M. A. Rakib, “Mixing in a Fluid Jet Agitated Tank: Effects of Jet Angle and Position” *Chem. Eng. Sci.* (Submitted in April 2001), Sent to reviewers, June 2001.

Zughbi, H.D. and M.P. Schwarz, “Numerical Simulation of Liquid Flow in the Maxhutte Pilot Converter (III) Mixing Time Calculations”, CSIRO, *Mineral and Process Engineering Communication*, MIE 225, 1987.

Zughbi, H.D., Z. H. Khokhar, and R. N. Sharma, “Mixing in Pipeline with Side- and Opposed-tee”, *AIChE* conference, November 2002, Indianapolis, USA.

APPENDICES

PUBLICATIONS

A: Zughbi, H. D., **Khokhar, Z. H.**, and Sharma, R. N., "Mixing in Pipeline with Side and Opposed Tee", paper 177e, AIChE annual conference: November 3-8, 2002, Indianapolis, USA. [Speaker: Zughbi, H. D.]

B: **Khokhar, Z. H.**, Zughbi, H. D., and Sharma, R. N., "Mixing in Pipeline with Side-Tees", *Paper 3-04-021, The 6th Saudi Engineering Conference, KFUPM,* December 14-17, 2002, Dhahran, KSA. [Speaker: Khokhar, Z. H.]

C: **Khokhar, Z. H.**, Zughbi, H. D and Sadique S., "Effects of Jet Arrangement on Mixing in Pipelines with Side-Tees ", Accepted for ICCBPE Conference 27-29th August 2003, Sabah, Malaysia.

D: Zughbi, H. D., **Khokhar, Z. H.**, Ahmed I. and Rakib, M. A., "Optimization of mixing Equipments using CFD", Accepted for PETROTECH Conference, 29th September-1st October 2003, Manama, Bahrain.

A: AIChE Annual Conference, USA

Zughbi, H. D., **Khokhar, Z. H.**, and Sharma, R. N., "Mixing in Pipeline with Side and Opposed Tee", paper 177c, AIChE annual conference: November 3-8, 2002, Indianapolis, USA. [Speaker: Zughbi, H. D.]

AIChE

Technical Program Menu

[177e] - Mixing Pipelines with Side- and Opposed-Tees

Presented at: [177] - Industrial Mixing and Scale down
For schedule information click here
Author Information:

Habib D Zughbi *(speaker)*
King Fahd University of
Petroleum & Minerals
KFUPM, Box 124
Dhahran, 31261
Saudi Arabia
Phone: 966 3 860 4729
Fax: 966 3 860 4234
Email:
szughbi@hn.ozemail.com.au

Abstract:

MIXING IN PIPELINES WITH SIDE- AND OPPOSED-TEES

Habib Zughbi1*, Zahid Khokhar1, and Rajendra Sharma1

1Department of Chemical Engineering,
King Fahd University of Petroleum & Minerals,
Dhahran, 31261, Saudi Arabia

*Corresponding author: Habib Zughbi, email:
hdzughbi@kfupm.edu.sa

ABSTRACT

Numerical and experimental investigations are of mixing in pipelines with side- and opposed-tees are carried out. Water at a given temperature, usually about 10 °C, flows in a main pipe while water at a higher temperature, usually about 45 ℃, flows through the tee. Temperat ure is measured experimentally to quantify the degree of mixedness. Numerically, the field of temperature is calculated and then compared with experimental results to validate the models.

The computational fluid dynamics (CFD) package FLUENT is used to solve the governing equations, namely the equations of continuity, motion and energy. Experimental estimates of the pipe length required to achieve 95% mixing is compared with predictions of the numerical model. Good agreement is observed over a relatively wide range of Reynolds number. Close agreement is harder to obtain for the temperature profile of the impinging jet.

The numerical model is thoroughly tested before final comparisons are made with experimental results. The mesh size is first tested and a relatively very small mesh size (before refinement, a total of about 170000 cells for a 15 in piece of 1 in pipe) is chosen. The mesh is then refined especially at the zones of high temperature and/or velocity gradients. This mesh refinement improved the results. Different lengths of the section of the pipe before the tee are also tested and a length of 5 diameters is found enough for the flow to be fully developed. The k-e turbulence model has been widely used in previous mixing studies. This model and the Reynolds stress model (RSM) are used in the present study. The two models gave similar results as far as the pipe length required to achieve 95% mixing, however, the temperature and velocity profiles in the jet zone were better predicted using the RSM model. The computational time required to achieve convergence with RSM is three times that required while using the k-e model The dependence of physical properties, density, viscosity and heat capacity, of the fluid on temperature is found not to have a significant effect on the final results.

With all the numerical enhancements, good agreement between the experimental and numerical lengths of pipe required to achieve 95% mixing. The numerical predictions were in general slightly more than the experimental values. The agreement between the numerical and experimental temperature profile of the impinging jet was good but grid refinement was needed to achieve that.

At some jet velocity to main velocity ratios (Uj/Um) it was found that the jet impinges quite strongly at the opposing wall and there was a certain degree of backward

movement at the impingement location. This could have a negative effect, including corrosion, in some industrial injection operations. It was found that by changing the angle of the jet to 45 degrees, the impingement and the backward flow was eliminated while the pipe length required for 95% mixing did not show any significant increase.

The pipe length required to achieve 95% mixing is found to be a function of Uj/Um and the ratio of pipe to jet diameters. A number of scale-up cases were simulated using the pipe diameter, velocity and the liquid flow rates as scale-up criteria.

For opposed jets, a number of arrangements were examined. For a standard opposing jets where the two streams are injected normal to each other and the main flow is at 90 degrees to each of the jets, it was found that numerical convergence was hard to obtain. This is expected due to the jet-jet interaction at high Reynolds numbers. Some modifications including the staggering of the two jets made it easier for the solution to converge.

Key words: Mixing, pipeline, side-tee, opposed-t

Contact Information:

Meetings Department
American Institute of Chemical Engineers
3 Park Ave, New York, N.Y., 10016-5991, U.S.A.
Tel: (212) 591-7338 Fax: (212) 591-8894
E-mail: meetmail@aiche.org

B: The 6th Saudi Engineering Conference, KSA

Khokhar, Z. H., Zughbi, H. D., and Sharma, R. N., "Mixing in Pipeline with Side-Tees", *Paper 3-04-021, The 6th Saudi Engineering Conference, KFUPM,* December 14-17, 2002, Dhahran, KSA. [Speaker: Khokhar, Z. H.]

The 6th Saudi Engineering Conference, KFUPM, Dhahran, December 2002 Vol. 2. 171

MIXING IN PIPELINES WITH SIDE-TEES

Zahid Khokhar[1], Habib D. Zughbi[2], and Rajendra Sharma[3]

1: Graduate student, Department of Chemical Engineering, KFUPM, Dhahran, 31261
2. Assistant Professor, Department of Chemical Engineering, KFUPM
3. Professor, Department of Chemical Engineering, KFUPM

E-mail: hdzughbi@kfupm.edu.sa

ABSTRACT

Numerical and experimental investigations of mixing in pipelines with side-tees are carried out to determine the quality of mixing in such pipelines. Temperature is measured experimentally to quantify the degree of mixedness. Numerically, the temperature field is calculated and then compared with experimental results to validate the models.

The computational fluid dynamics (CFD) package FLUENT is used to solve the governing equations, namely the equations of continuity, motion and energy. Numerical results showed good agreement with experimental results. The mesh size is selected do that the numerical solution is independent of mesh size. Turbulence is modelled using the standard k-ε model and the more involved Reynolds stress model. The pipe length required for achieving 95% mixing is found to be a function of the ratio of the velocities of the side and main streams.

Keywords: *Mixing, pipeline, side-tee, opposed-tee, numerical simulation*

الملخص

تم إجراء بحوث عددية ومعملية للخلط في أنابيب مزودة بأنابيب جانبية وذلك لتقييم نوعية الخلط في هذه الأنابيب وطول الانبوب اللازم لتحقيق ٩٥% من الخلط. وقيست الحرارة معملياً لتحديد درجة الخلط، وتم حلّ حقل الحرارة عددياً ثم قورنت قيم الحرارة العددية بالقيم المعملية وذلك للتأكد من فعالية ودقة النموذج العددي. استعمل برنامج متعدد الأهداف لديناميكا الموائع العددية FLUENT لحل المعادلات الرياضية التي تتحكم بانتقال المادة والطاقة وسريان الموائع.

وفي البحث الحالي تم استعمال السائل ذاته في الانبوب الرئيسي والانبوب الجانبي. وقد أظهرت النتائج العددية تطابقاً جيداً مع النتائج المعملية ووجد أن طول الأنبوب اللازم لتحقيق ٩٥% من الخلط يعتمد على نسبة سرعة السائل في الانبوب الجانبي والانبوب الرئيسي

1. INTRODUCTION

Mixing problems, such as the design and scale-up of a mixer and quantification of mixing, have been traditionally tackled by developing empirical design equations mainly due to the complexity of the fluid dynamics of mixing. Although this approach has proven to be satisfactory for many applications, it is rather limited because it neglects the complexity of flow in most mixing applications.

Applications where pipeline mixing with tees is used include low viscosity mixing such as wastewater treatment and blending of some oils (injection of additives) and petrochemical products. Other applications include blending of fuel gas, and mixing of feed streams for catalytic reactors. A tee is formed by two pipe sections joined at a right angle to each other. One stream passes straight through the tee while the other enters perpendicularly at one side as shown in Figure 1. This flow arrangement is known as the side-tee. However other flow arrangements may be used, such as having the two opposing streams entering co-axially and leave through a pipe, which is perpendicular to the entering direction. This is known as the opposed-tee. A review of various flow arrangements is presented by Gray (1986). A survey of the literature shows that simulation using CFD of pipeline mixing with tees have been carried out by Cozewith et al. (1991) and Forney and Monclova (1994).

The main interest in this paper concentrates around the side-tee shown in Figure 1. For all designs of pipe tees, mixing takes place in shorter distances compared with distances required for mixing in a pipe with undisturbed turbulent flow. Reviews of pipeline mixing with tees has been presented by (Simpson, 1974), (Gray, 1986) and (Forney, 1986).

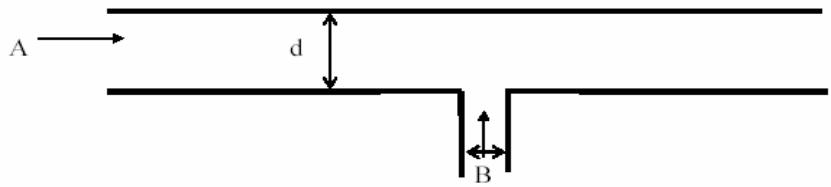

Figure 1: A schematic diagram of a pipeline side tee

The flows generated by a tee mixer have been studied by (Moussa et al., 1977) and (Crabb et al., 1981). Cozewith et al.(1991) simulated tee mixing characteristics with and without a reaction for a tee with d/D = 0.188 over the range of side stream/main stream velocity ratios from 1.2 to 6.5. A three-dimensional model was constructed and the k-ε model was used to model turbulence. Literature recommends and uses the k-ε model especially for non-circulating flows. Cozewith et al. (1991) compared their numerical results with the experimental results of Cozewith and Busko (1989) and got reasonable agreement for concentration trajectory for x/D > 0.7. Concentration trajectory is defined as the locus of

Top

maximum concentration. Other comparisons also showed qualitative agreement between experimental and numerical results.

Forney and Monclova (1994) simulated pipeline side-tee mixing quality with the commercially available fluid flow package PHOENICS. The $k-\varepsilon$ model was used to model turbulence. They compared numerical results with the experimental results of Sroka and Forney (1989) and obtained reasonable agreement.

Both of the above numerical models solved the conservation equations for mass and momentum in primitive variables for steady turbulent flow of a single-phase fluid with an inert tracer introduced at the injection point. Both models also used a mixing criteria based on the standard deviation of the component mixed and the mean value of the tracer over the pipe cross sectional area $\overline{C}$. The use of CFD, despite the two above-mentioned papers, has still a lot to offer in analyzing and understanding mixing at pipeline tees. Simulation of variations of tees mixers and opposed flow tee have not been reported in literature.

2. MODEL EQUATIONS

The differential equations representing mass, momentum and energy conservation can be written in the general form:

$$\frac{\delta\left(R_i \rho_i \phi_i\right)}{\delta t} + div\left(R_i \rho_i U_i \phi_i - R_i \Gamma_{\phi_i} grad \phi_i \right) = R_i S\phi_i$$

Transient Convection Diffusion Source

Where R_i is the volume fraction of phase i, ϕ_i, is any conserved property of phase i, U_i, is velocity vector of phase i, Γ_{ϕ_i} is the exchange coefficient of ϕ in phase i, S_{ϕ_i}, is the source rate of ϕ_i. Thus, the continuity equation for phase i becomes:

$$div\left(R_i\, \rho_i\, U_i - R_i\, D_i\, grad\, R_i\right) = m_i$$

where D_i, is the diffusivity of phase i, m_i, is mass per unit volume entering phase i, and ρ_i is the density of phase i. The conservation of momentum for variable ϕ_i becomes:

$$div\left(R_i\, \rho_i\, U_i\, \phi_i - R_i\, \mu_{eff}\, grad\, \phi_i\right) = R_i\, S_{\phi_i}$$

where μ_{eff} is the effective viscosity and S_{ϕ_i} is the source of ϕ_i per unit volume

Top

3. THE EXPERIMENTAL APPARATUS

An experimental apparatus was built to quantify mixing in a pipeline with a side-tee. Temperature is used as the measured variable. Hot water is injected from the side tee and is mixed with the same liquid flowing in the main pipe at a lower temperature. A one-inch main pipe is shown in Figure 2. This Figure shows a schematic diagram of the experimental apparatus. A ¼ inch side-tee is also shown. Eight thermocouples are inserted at various positions of the main pipe in order to measure the temperature of the flow. These thermocouples are connected via an OMEGA data-logging card to a PC as shown. Flow through the side passes through a heater that can raise the temperature of the side stream significantly above that of the main stream.

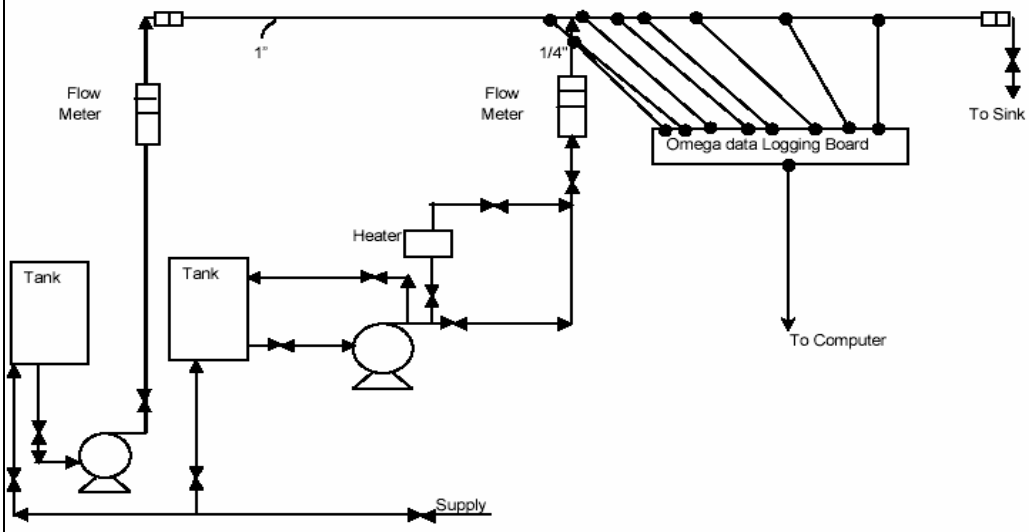

Figure 2: A schematic diagram of the experimental rig used to investigate mixing a pipeline with a side-tee

4. THE NUMERICAL MODEL

Flow in pipeline is simulated by solving the mass and momentum conservation equations. The degree of mixedness is investigated by solving for the energy equation and by monitoring the temperature at various positions along the flow. The general-purpose three-dimensional computational fluid dynamics package FLUENT is used to solve the governing equations. This allows the investigation of a range of conditions and geometries quite efficiently once a general model has been established and validated against experimental results.

Top

A basic three-dimensional numerical model representing a 15 in section of a main pipe with a side-tee located at 2 in from the front end of the pipe has been constructed. The grid is shown in Figure 3. An unstructured tetrahedral grid was chosen. To test the dependence of the numerical solution on the grid size and to also test different models to simulate turbulence, one case with Q_j of 7 lit/min and Q_m of 9 lit/min has been chosen.

In this study, the pipe length required to achieve 95% mixing is numerically and experimentally determined. This is the length from the jet inlet to the location along the pipe centreline where the value of the measured quantity anywhere in the pipe is less than 5% of the step input. The step input is defined as the difference between the initial value and the final mean value. In this study, the 95% mixing is defined and used to quantify mixing. Distinction should be made between mixing length and blending length. Blending length is when the flow through the side pipe (hot fluid) is started exactly at the same time as the flow through the main pipe. Other papers may refer to mixing length, which is defined in a similar way except the flow through the side-tee is started not when the flow in the main pipe starts but after the flow reaches steady state.

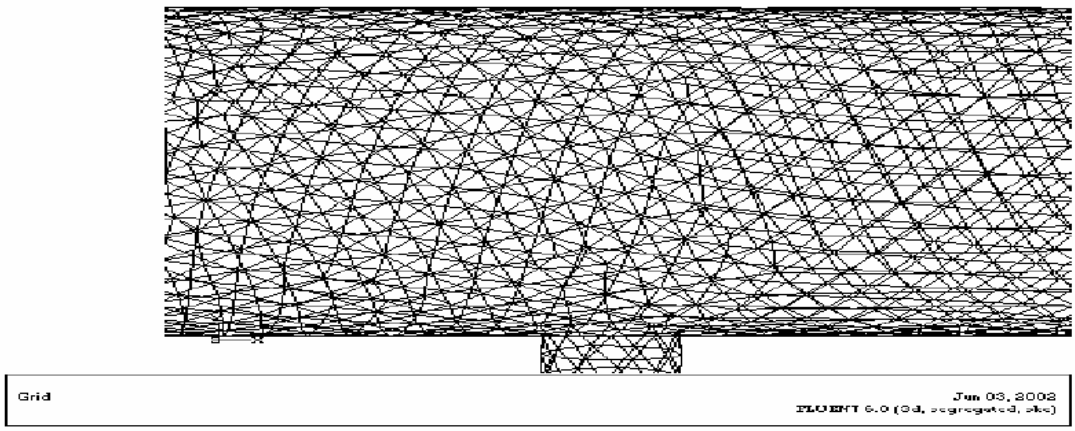

Figure 3: The computational grid of a piece of main pipeline with a side tee used in these simulations

In terms of a concentration tracer, m can be defined as:

$$m = \left| \frac{c - \overline{c}}{\overline{c}} \right| < 0.05$$

Where $\overline{c}$ is the equilibrium concentration and c is the concentration at any monitoring point at any time. When the above condition is met at all monitoring points in a cross sectional plane of the main pipe, it can then be said that concentration at any point of the pipe after that length has reached 95% or more of the equilibrium concentration. For this case the initial value of m before the addition of the tracer is considered to be 0.

Top

In the present study, the flow in the main pipe before the jet inlet is set initially at a certain temperature. The flow through the side-tee is set at a higher but know temperature. Thus the equilibrium temperature, $\overline{T}$, can be calculated. The 95% blending is reached when the temperature anywhere across a plane inside the pipe is within the range of $((\overline{T} \pm (\overline{T} - T_{im}) * 0.05)$ where T_{im} is the initial temperature of the fluid in the main pipe, i.e. before the inlet of the side tee. The length required for the hot fluid to blend is then measured according to this criterion that means that the maximum temperature difference between any two points across a cross sectional area of the pipe should not exceed a certain value which is a function of the initial temperatures and the flow rates of the fluids in the main and side pipes.

5. RESULTS

5.1. Numerical Results and Validation of Numerical Model

Numerical and experimental results are presented in this paper. Figures 4 and 5 show the velocity and temperature contours in a plane along the pipe axis for a velocity ratio (U_j/U_m) of 17.1.

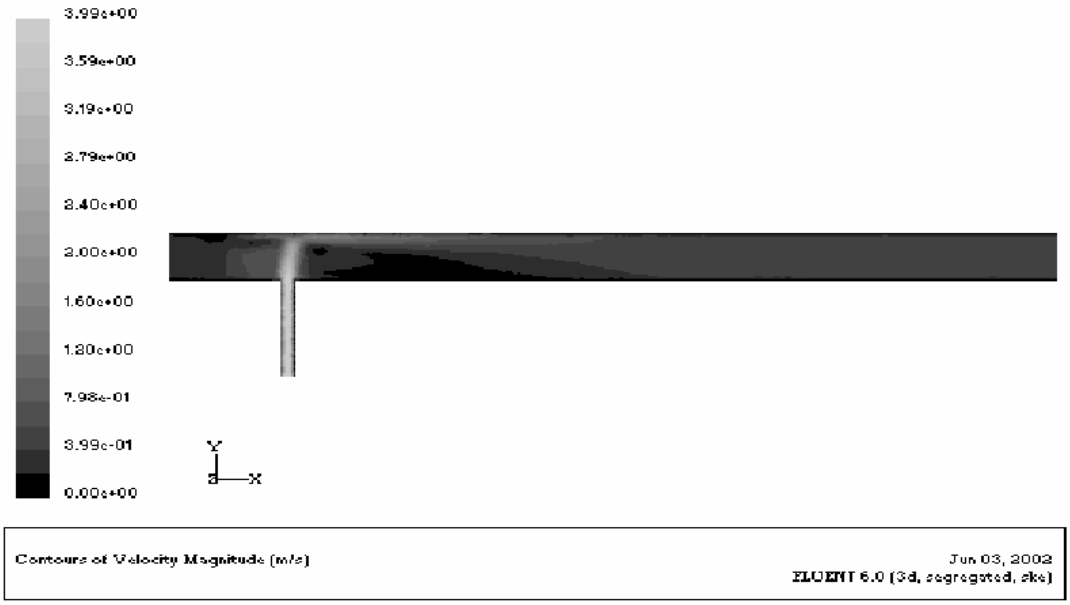

Figure 4: Velocity contours in a plane passing through the centreline for a mesh size of 2

Top

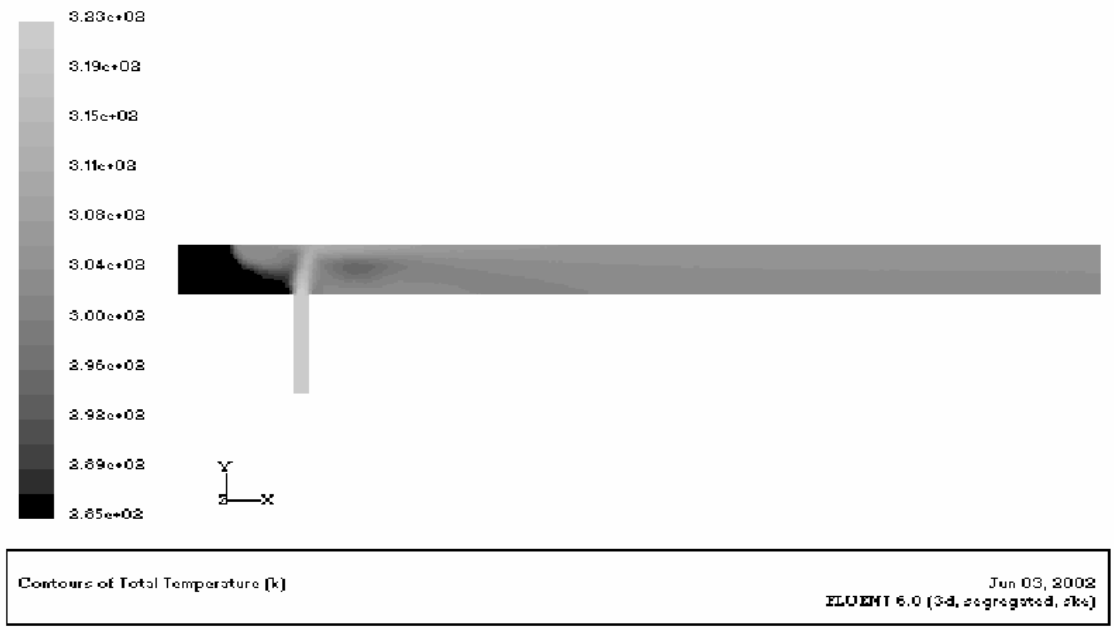

Figure 5: Temperature contours in a plane passing through the centreline for a mesh size of 2

A mesh size of 2 is used and turbulence is modelled using Reynolds Stress Model (RSM) or the k-ε. Model. Figure 4 shows clearly that the jet impinges on the opposite wall of the pipe. Figure 5 shows that the distance for 95% mixing to be achieved is about 9 inches. In order to analyze the results quantitatively, values of temperature versus location along the pipe axis are plotted. In order to validate the numerical model, these numerical values are compared with experimental values measured at exactly the same locations.

Figure 6 shows a plot of experimental and numerical values of temperature versus location along the main pipe axis. Good overall agreement is observed between numerical and experimental results especially regarding the distance required to achieve 95% mixing. Some differences are observed in the vicinity of the jet coming through the side-tee. The final (equilibrium) temperatures and the distance required for 95% mixing are almost identical. The difference in the value of temperature in the vicinity of the jet can be explained by the high sensitivity of temperature to the location of the thermocouple. A difference of a couple of mm could result in a significant difference in temperature.

The side jet impinges on the opposite wall of the pipe and this creates a region of backflow. This region could be significant and it could explain some problems faced by some process industries. These problems are corrosion related and could be due to this zone of low velocity.

Top

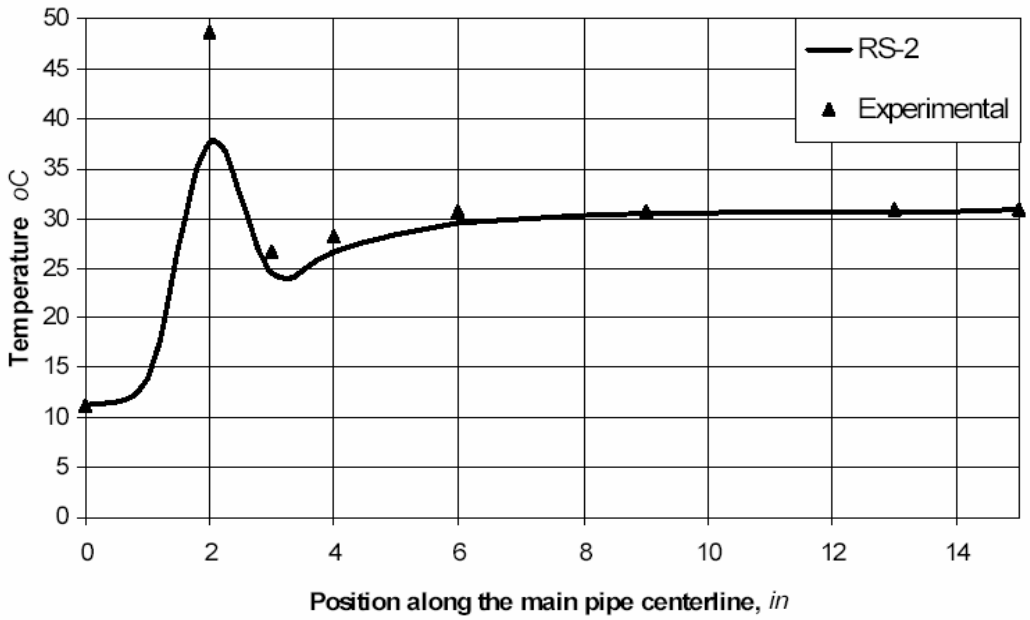

Figure 6: Simulated and experimental temp vs. position along a centreline for the same case of mesh size 2

5.2. Dependence of Solution on Grid Size

In order to quantitatively compare results with different mesh sizes, a plot of temperature versus position along a centreline of the main pipe is shown in Figure 7. Mesh sizes of 4, 3 and 2 have been tested. The number of cells used in each case is shown in Table 1.

Table 1: Number of cells for mesh sizes of 2, 3 and 4

Mesh Size	2	3	4
Number of cells	162367	56463	18610

Figure 7 shows a comparison of the temperature versus location along a centreline for mesh sizes of 2 and 3. It is clear that the solution changes with a mesh size, although the difference between solutions of mesh size of 3 and 2 is not very significant. The number of cells for a mesh size of 2 is relatively very high, however, since the solution still shows some change a mesh size of 1 was attempted. This attempt could not be completed, because the time required to perform the meshing of the computational domain is prohibitively excessive. A mesh size of 2 was used for all the main runs in this study.

Top

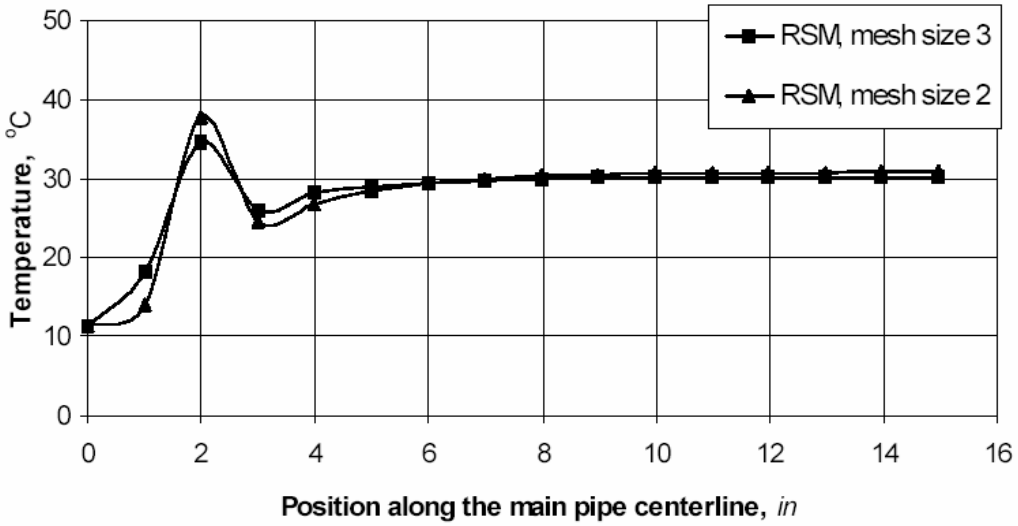

Figure 7: Comparison of temperature versus location along a centreline for mesh sizes of 2 and 3.

5.3. Dependence of Solution on Turbulence Model

Plots of the temperature versus location along the centreline of the main pipe obtained using the k-ε model and the Reynold Stress Model (RSM) are shown in Figure 8. It is noted that the mixing length required to produce 95% mixedness is exactly the same for both cases. However, differences are observed in the vicinity of the jet where high turbulence intensity is observed.

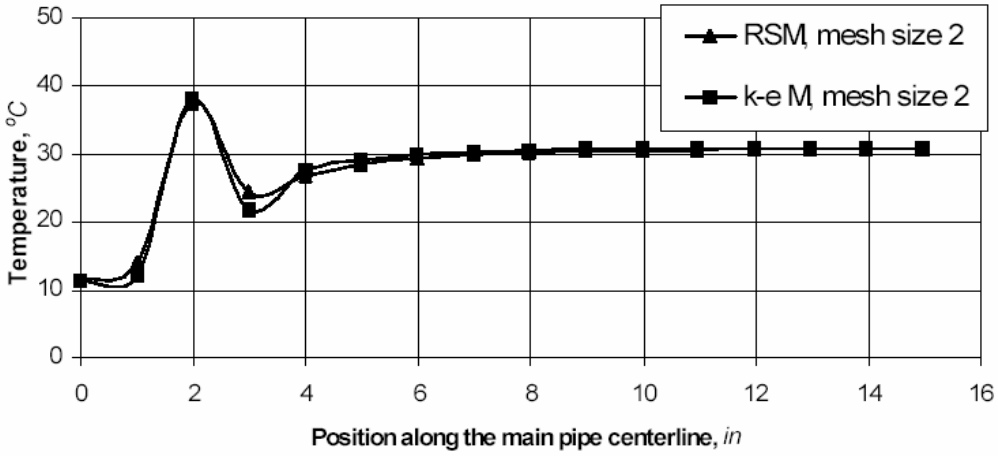

Figure 8: Plots of temperature versus location along the centre line of the main pipe for cases with k-ε and RSM

Top

The time required for the above case to converge was 8 hours when the RSM model is used compared to 3 hours only needed for convergence when the k-ε model is used. Since the jet impingement area is of interest in this work, the RSM model is used despite it being computationally more expensive.

5.4. Experimental Results

Experimental runs have been carried out with water flow rates through the main pipe and the side tee as 7.02, 12.28 and 19.30 liters/min and water flow rate through the side pipe of 7.5, 5.0 and 3.0 liters/min. Details of these runs together with the corresponding values of the velocity in the side stream U_j, velocity in the main pipe, U_m, ratio of U_j/U_m, values of Reynolds number in the side pipe and main pipe before and after the tee are given in Table 2.

Figure 9 shows plots of the temperature measured by the thermocouples versus the location along the centreline of the main pipeline for the three cases with U_m of 7.02 lit/min. From the Figure, the pipe lengths required for 95% mixing of hot and cold fluids can be deduced. These values and other values for the remaining six cases are summarized in Table 3.

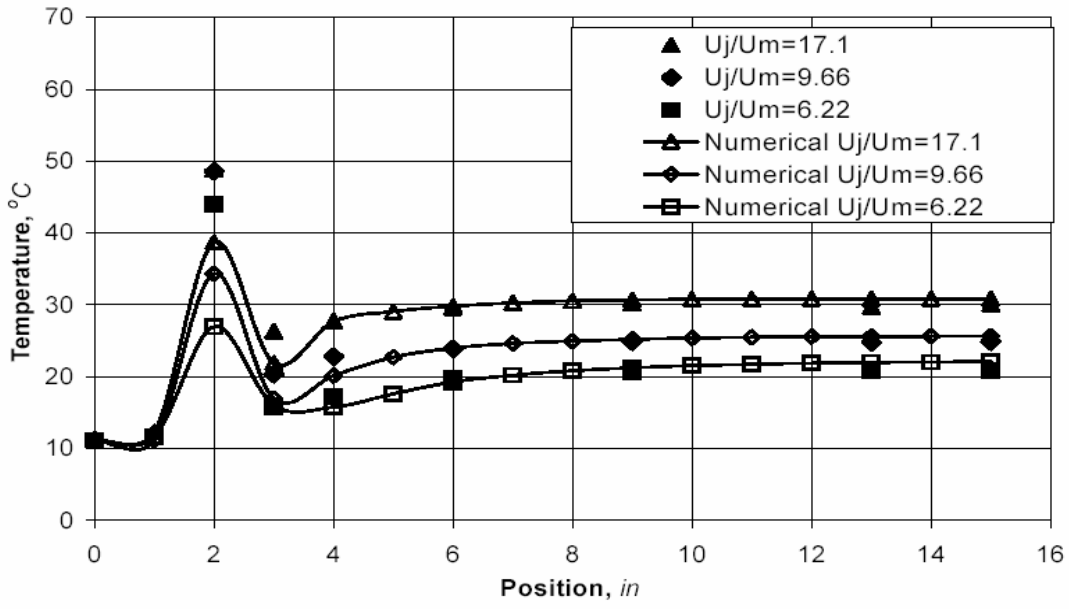

Figure 9: Experimental and simulation, using k-ε model, values of temperature versus location along the centreline of the main pipe for cases with Q_m of 7.02, 12.28 and 19.3 lit/min and Q_j of 7.5, lit/min

Top

Table 2: Values of variables for certain experimental runs

Q_j lit/min	Q_m lit/min	V_j m/s	V_m m/s	U_j/U	Re_j	Re_m	R_m (after the tee)	Distance required for 95% mixing (diameters)
7.5	7.02	3.9471	0.23082	17.10	250637.7	16122.9	22390.3	9
7.5	12.28	3.9471	0.40394	9.77	250637.7	10260.0	16475.3	11
7.5	19.30	3.9471	0.63476	6.22	250637.7	5862.9	12130.9	13

Table 3: Comparison of experimental and numerical results

Q_j lit/min	Q_m lit/min	U_j/U_m	Distance (experimental) required for 95% mixing (diameters)	Distance (numerical) required for 95% mixing (diameters)
7.5	7.02	6.22	13	13
7.5	12.28	9.77	11	11
7.5	19.30	17.10	9	9

6. COCLUSIONS

Mixing in pipelines with side-tees has been experiemntally and numerically investigated. Temperature is measured and used to quantify mixing. Good agreement between experimental and numerical results is observed especially when the final temperatures and the distance required to achieve 95% mixing are considered. Some differences are iobserved in the values of teperature in the vicinity of the jet incoming through the side-tee. This could be due to the high sensisitivity of such value to the position of the the thermocouple. A small difference in position results in a significant difference in the value of temperature. The mesh size was chosen such that the solution is made independent of the mesh size. The Reynolds Stress Model (RSM) and the k-ε model were used to account for turbulence and gave similar results except in the vicinity of the jet impingement region. Results showed that the pipe length required to achieve 95% mixing depends on the ration of Uj/Um.

Top

REFERENCES

1. Cozewith, C. and Busko, M., 1989, "Design Co-relations for Mixing Tees", *Industrial and Engineering Chemistry Research*, 28, pp. 1521-1530.
2. Cozewith, C., Ver Strate, G., Dalton, T. J., Frederick, J. W. and Ponzi, P.R., 1991, " Computer Simulation of Tee Mixers for Non-reactive and reactive Flows", *Industrial and Engineering Chemistry Research,* 30, pp. 270-275.
3. Crabb, D., Durao, D., and Whitelaw, J.H., 1981, "A Round Jet Normal to a Cross Flow", *Journal of Fluids Engineering*, 103, pp. 143-151.
4. Forney, L.J., 1986, Encyclopaedia of Fluid Mechanics, Vol. II, Ch. 25, N. P. Cheremisinoff, ed., Gulf Publishing Co., Houston USA.
5. Forney, L.J. and Monclova, L.A., 1994, "Numerical Simulation of Pipeline Tee Mixers: Comparison with Data", Industrial Mixing Technology: Chemical and Biological Applications, Gaden, E.L., Tatterson, G.B.Calabrese, R.V. and Penney, W.R., eds., pp. 141-143.
6. Gray, J. B., 1986, Mixing: Theory and Practice, Ch. 13, Vol. III, J.B. Gray and V. W. Uhl, eds., Academic Press, USA.
7. Moussa, Z., Trischka, J. and Eskinazi, S., 1977, "The Near Field in the Mixing of a round Jet with a Cross Stream", J*ournal of Fluid Mechanics*, 80 pp. 49-58.
8. Ottino, J. M., 1990, "The Kinematics of Mixing: Stretching, Chaos and Transport", Cambridge University Press, Cambridge, UK.
9. Simpson, L. L., *Chem. Eng. Prog.,* 70, 77 (1974)
10. Sroka, L. M. and Forney, L. J., 1989, "Fluid Mixing with a Pipeline Tee: Theory and experiment". Journal of the American Institute of Chemical Engineers, 35(3) pp. 212-218.
11. Sroka, L. M. and Forney, L. J., 1989, "Fluid Mixing in a 90° Pipeline Elbow", *Industrial and Engineering Chemistry Research,* 28(6), pp. 850-856.
12. Yao, W., Takahashi, K. and Koyama, K., 1998, " Theoretical Tool for Optimum Design of Mixer, and Visualisation and Quantification of Mixing Performance", *Journal of Chemical Engineering of Japan*, 31(22), pp. 220-227.

Top

C: ICCBPE Conference, Malaysia

Khokhar, Z. H., Zughbi, H. D and Sadique S., "Effects of Jet Arrangement on Mixing in Pipelines with Side-Tees ", Accepted for ICCBPE Conference 27-29th August 2003, Sabah, Malaysia.

Effects of Jet Arrangement on Mixing in Pipelines with Side-Tees

Zahid H. Khokhar Habib D. Zughbi[1] Shad Siddiqui
Department of Chemical Engineering, King Fahd University of Petroleum & Minerals, Dhahran, 31261, Saudi Arabia
Tel: +966 3 860 4729, Fax: +966 3 860 4234, [1]Corrsponding author. Email: hdzughbi@kfupm.edu.sa

Abstract

Mixing is an important operation in many chemical processes including blending, dispersing and emulsifying. Numerical and experimental investigations of mixing in pipelines with side-tees were carried out to optimize mixing in such pipelines. A side jet of 1/8 inch in diameter is connected to a 1 inch main pipe. The tip of the jet protrudes to the centerline of the main pipe. Temperature was measured experimentally to quantify the degree of mixing. Numerically, the field of temperature was calculated and then compared with experimental results to validate the models. The length of the main pipe downstream of the jet inlet required to achieve 95% mixing was determined.

Numerical results showed good agreement with experimental results. The pipe length required for achieving 95% mixing is a strong function of the ratio of the side-stream to main-stream. The angle of the jet has a significant effect on mixing length. Mixing depends on the flow patterns created by the jet impingement. These patterns depend on the degree of penetration of the jet in the main flow stream.

Keywords: Mixing, Pipeline, Side-Tee, Jet, Computational Fluid Dynamics

Introduction

Mixing is an important operation in many oil, chemical, and petrochemical industries. It plays a significant and often a controlling role in unit operations. Mixing can be achieved by mechanical mixers such as stirred tanks, static mixers, and fluid jet agitated tanks or in pipelines with side- and opposed-tees. This paper is concerned with mixing in pipelines with tees.

A pipe tee is a simple device for mixing two fluid streams. A tee is formed by two pipe sections joined traditionally at a right angle to each other. A side-tee is also commonly built so that it is flush with the main pipe and not protruding inside it. In this study the effects of angles other than 90° and the effects of a protruding side jet are investigated. A 90° protruding-tee considered in this study is shown in Figure 1. Figure 2 shows a protruding-tee at an angle less than 90°.

Previous researchers investigated mixing in pipelines with side-, opposed- and multiple-tees. Experimental investigation of mixing in pipelines with side-tees was first investigated by Chilton and Generaux [1]. Reed and Narayan [2] quantified the degree of mixing of air-carbon dioxide streams in pipeline mixers. They found that mixing can be achieved in a few diameters with normal side-tee arrangements. Brodkey [3] presented a general review of turbulent mixing in chemically reactive flows.

Other reviews of the mechanics of jet behaviour of various kinds were presented by Rajatanam [4] and Fisher [5]. Forney and Kwon [6], Forney and Lee [7], Forney [8], Feng, Wang and Forney [9], and Maruyama, Suzuki and Mizushina [10] studied the jet injection of fluid into a pipeline over the first twelve diameters from the injection point and the objective of these studies was to establish optimum conditions for pipeline mixing. The experimental data were limited and the results were frequently inconclusive. A review of mixing in pipelines was presented by Gray [11].

Computer simulation of turbulent flow phenomena has been successfully applied to many industrial applications. Patterson [12] described the principles of applying mathematical models to various mixing operations. More recently, the advances in CFD software and computer power raised the possibility of determining the performance of pipeline mixing with tees by simulation rather than by experiments. A survey of the literature shows that simulation using CFD of pipeline mixing with tees has been carried out by Cozewith, Ver Strate, Dalton, Frederick, and Ponzi [13], Forney and Monclova [14] and Zughbi, Khokhar and Sharma [15] and Khokhar [16]. CFD is nowadays extensively used in many applications including investigations of mixing.

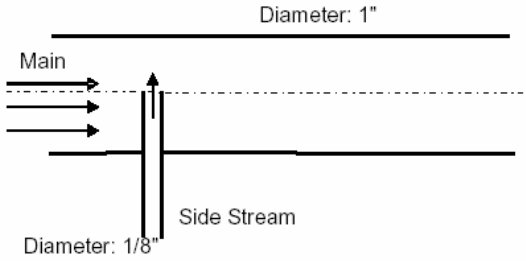

Figure 1: A schematic diagram of a protruding 90° side-tee.

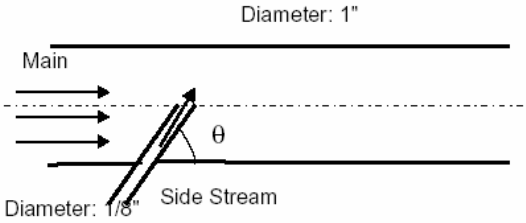

Figure 2: A schematic diagram of a protruding angle-side-tee.

Approach and methods

An experimental set-up consisting of a one inch diameter main pipe and a side-tee of 1/8 of an inch in diameter is attached to the main pipe as shown in Figure 3. A photograph of the experimental set-up is shown in Figure 4. The jet is protruding to the center of the main pipe. Cool water at a temperature of about 10 °C is injected in the main pipe while warm water, at about 50 °C, is injected in the side-tee. Seven thermocouples are inserted at various places as shown in Figure 3 in order to measure the temperature. The temperatures were logged in using an Omega data logging card. The tips of the thermocouples are aligned with the axis of the main pipe.

This mixing system is governed by the equations of conservation of mass, momentum and energy. This means that this mixing system can be resolved by solving the equations of continuity, Navier-Stokes and energy over the whole domain. The boundary conditions are simply a constant velocity condition for both the main and side inlets, a constant pressure condition for the outlet and no slip boundary condition at all the walls of both the side- and main-pipes. These equations are solved using a commercial three-dimensional, general purpose computational fluid dynamics (CFD) package, FLUENT, version 6.0.12. A SIMPLE based algorithm is used to solve the pressure-velocity equations and then the equation of energy is solved sequentially.

The 95% mixing is reached when the temperature anywhere in the flow inside the pipe is within the range of $(\overline{T} \pm (\overline{T} - T_{in}) * 0.05)$ where T_{in} is the initial temperature of the fluid in the main pipe, i.e. before the inlet of the side-tee and $\overline{T}$ is the equilibrium temperature. The length required for the injected fluid to mix is then measured according to this criterion, that means the maximum temperature difference between any two points across a cross sectional area of the pipe should not exceed a certain value which is a function of the initial temperatures and the flow rates of the fluids in the main and side pipes.

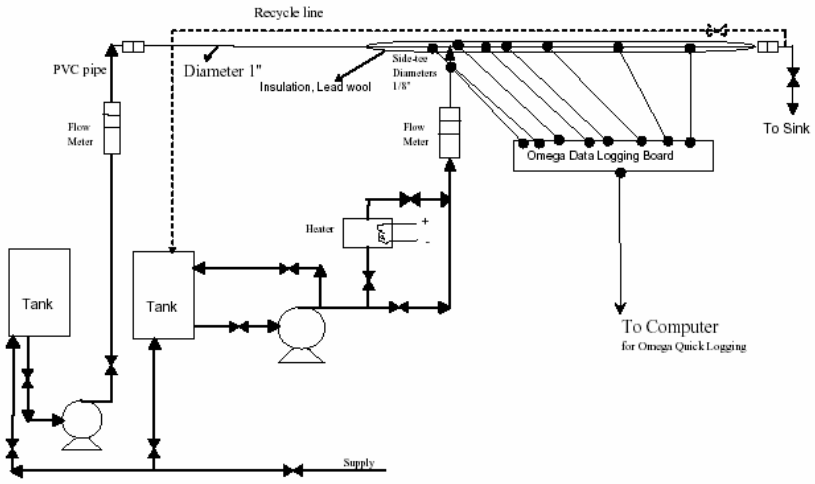

Figure 3: A schematic diagram of the experimental set-up used in the present study.

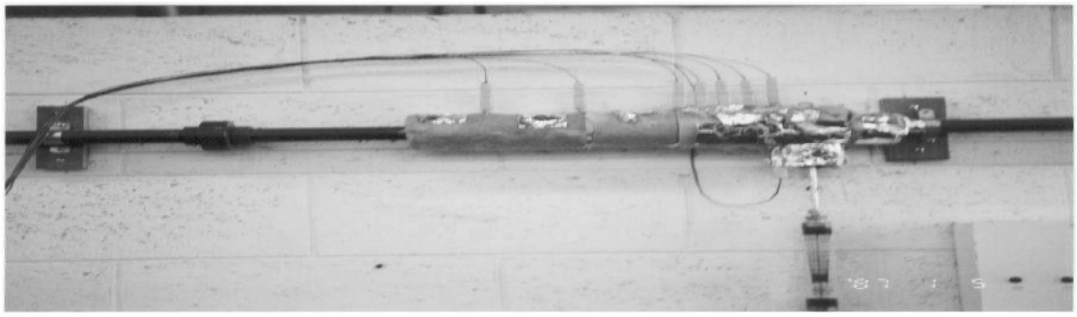

Figure 4: A view of the tee set-up showing the main and side pipes and the thermocouples.

Results

Experimental and numerical results of mixing in a pipeline with a side-tee protruding inside the main pipe up to the center-line are shown in Figures 5-7. These results show the values of measured temperatures along a centerline of the main-pipe as a function of the position from the location of the side-tee. These Figures show good agreement between experimental and numerical results of temperature versus location along a central line. These results are mainly used to validate the numerical model. Mixing lengths cannot be always deduced from such plots because although the temperature along a central line may reach the equilibrium value, the temperature somewhere away from the center may still be away from the equilibrium value. Therefore in order to measure the mixing length properly many temperatures have to be measured at the same plane. Alternatively, the mixing length is determined numerically by ensuring that all temperatures at a plane fall within the criterion discussed earlier.

In this paper nine cases were considered for various values of U_j/U_m for the side-tee at 90°. Jet velocities of 14.73, 10.52 and 6.31 m/s were considered. For each of these values, three cases were obtained by using a main velocity of 0.63, 0.40 and 0.23 m/s. These results are listed in Table 1. A plot of mixing length versus U_j/U_m is shown in Figure 8. This shows clearly that for the same tee arrangement, mixing length decreases as U_j/U_m increases.

The effect of the tee angle was also investigated. Angles of 45° and 135° in addition to the base case of 90° were considered. Three cases of velocity ratios equal to 27.6, 45.6 and 63.84 are selected. These results are shown in Table 2 and are plotted in Figure 9. Included also in this Figure are data for a flush side-tee from Khokhar [16]. A comparison of these plots show that a protruding tee gives shorter 95% mixing length compared to a flush side-tee. It is also observed that the plots show dependence not only on the velocity ratio but also on the initial velocity of the main stream. For a protruding side-tee the plots show that for the same main velocity, the pipe length required to achieve 95% mixing in a pipeline with a protruding side-tee decreases as the velocity ratio increases.

This Figure shows that for high velocity ratios, namely 45.6 and 63.84, the shortest pipe length to achieve 95% mixing is obtained when a 90° protruding side-jet is used. For the lower velocity ratio of 27.36, a limited change in the value of mixing length is observed as the angle of the tee is changed.

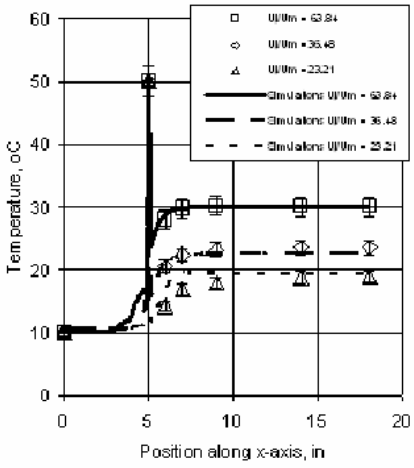

Figure 5: Comparison of Experimental and simulation results for U_j/U = 63.84, 36.48, and 23.21 for U_j = 14.73 m/s

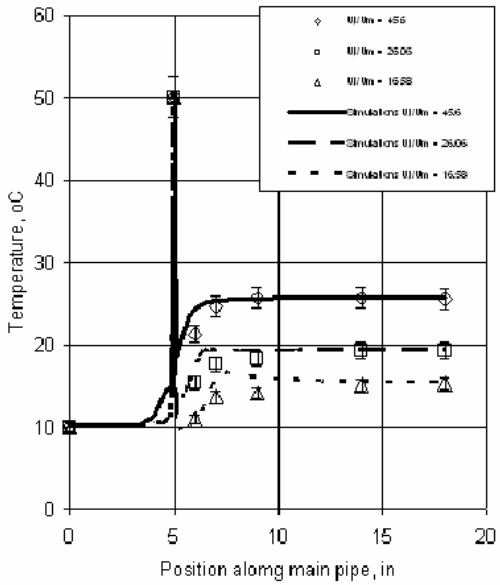

Figure 6: Comparison of the experimental and simulation results for U_j/U_m = 45.6, 26.06, and 16.58 for U_j = 10.52 m/s.

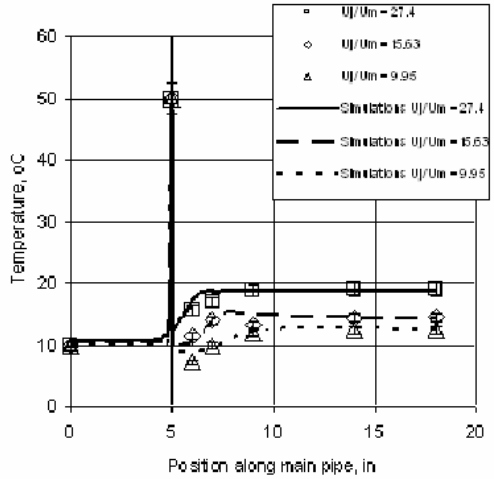

Figure 7: Comparison of experimental and simulation results for U_j/U = 27.4, 15.63, and 9.95 for U_j = 6.31 m/s.

Discussion

Results show that the pipe length required to achieve 95% mixing in a pipeline with a protruding side-tee is a function of the velocity ratio U_j/U_m and possibly of U_m. For a constant U_m, as the ratio increases, the mixing length decreases. A main factor that determines the length needed to achieve 95% mixing is the flow patterns in the pipeline with side-tees. Khokhar [16] and Zughbi, Khokhar and Sharma [15] showed that factors that contribute to make the side jet travels along the center of the main pipe will lead to achieving mixing within a shorter distance. For a flush side-tee, injecting at an angle other than 90° resulted in significant reduction in the length of the pipe required to achieve 95% mixing. This is totally different from what was observed in this study. This could be explained by the fact that because of the jet protrudes to the centreline of the main pipe, injecting at 45° or 135° does not contribute to centering of the jet. 90° produced best mixing results because the jet impinged hardest on the opposite wall and the side fluid bounced back pretty quickly for efficient mixing. Although protruding tees proved to be efficient for mixing, using such tees is likely to result in much harder impingement and consequently possible erosion and other problems associated with the portion of the side jet inside the main pipe.

Results also show that the angle of the protruding-tee plays a significant role in determining the 95% mixing length. For an angle of 45°, changing the velocity from 27.36 to 63.84 resulted in very little change in the mixing length. This length was about 5 main pipe diameters. For an angle of 90° the velocity ratio has a significant impact on the mixing length. A similar effect was observed for an angle of 135°.

The best arrangement for mixing is one which has a high velocity ratio and a jet as close as possible to the centre of the main pipe. Such an arrangement enhances the entrainment of the main or slow moving fluid by the jet or fast moving fluid. For a protruding side-tee to the center of the main pipe, centering the jet is much more difficult compared with a jet from a flush tee. For every class of tees, flush tees, protruding tees etc. there exists an optimum injection-angle which results in the shortest mixing length. This is not a simple matter to decide because it depends on the flow patterns which in turn are a function of geometry and tee-arrangement.

Table 1: Velocity ratios of side stream velocity (U_j, m/s) to main stream velocity (U_m, m/s) for a geometry of 1/8" protruding side-tee (90°) with 1" main pipe.

Case For side 1/8"	U_m, main velocity, m/s	U_j, Side velocity, m/s	U_j/U_m	Length Required for 95 % Mixing
1	0.63	14.73	23.21	2.5
2	0.40	14.73	36.48	2.5
3	0.23	14.73	63.84	1
4	0.63	10.52	16.58	5
5	0.40	10.52	26.06	2
6	0.23	10.52	45.60	1.5
7	0.63	6.31	9.95	13
8	0.40	6.31	15.63	6
9	0.23	6.31	27.4	5.5

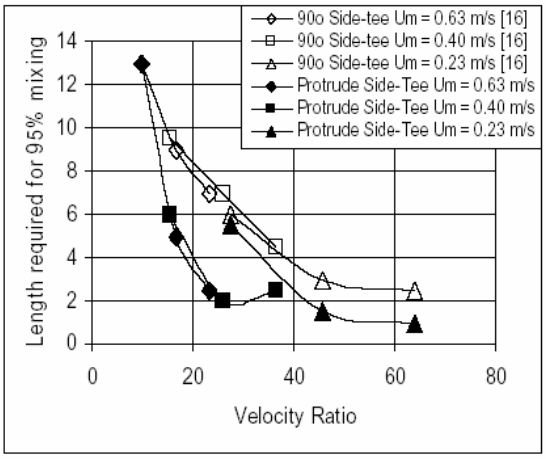

Figure 8: Pipe length required for 95% mixing versus values of velocity ratio U_j/U_m

Conclusions

Mixing in a pipeline with side-tee protruding inside the main pipe was experimentally and numerically investigated. Good agreement was observed between the experimental and numerical results. It was found that 95% mixing can be achieved in a distance much shorter than the recommended 7 to 10 main pipe diameters depending on the ratio of the jet to main velocities. The velocity ratio was found to have significant effects on the pipe length required to achieve 95% mixing. Protruding tees were found to be more efficient mixers than flush tees. The optimum angle for such a jet arrangement is found to be 90°. This is different from the optimum angle of flush side-tees. Protruding tees resulted in shorter mixing lengths when compared to flush tees over a wide range of velocity ratios.

Table 2: Velocity ratios of side stream velocity (U_j, m/s) to mainstream velocity (U_m, m/s) for a geometry of 1/8" protruding side-tee with 1" main pipe.

Angle / U_j/U_m	45 Degree	90 Degree	135 Degree
27.36	5	5.5	6.5
45.60	5.5	1.5	2
63.84	5	1	4

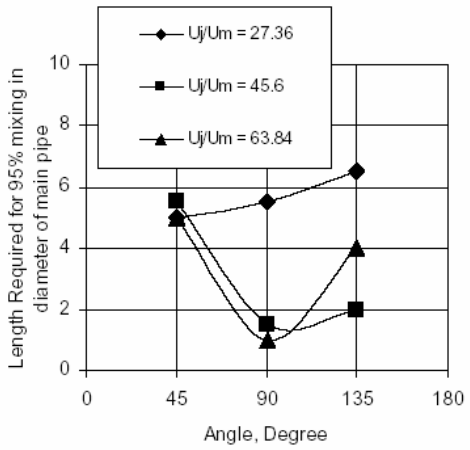

Figure 9: Pipe lengths required for 95% mixing for various values of velocity ratio U_j/U_m

Acknowledgments

The authors would like to acknowledge the support of KFUPM during the course of this work. The authors would also like to acknowledge Dr. R. N. Sharma for his contribution to discussions of some aspects of this work.

References

[1] Chilton, T. H.; and Genereaux, R. P. 1930. The mixing of gases for reactions. *American Institute of Chemical Engineers Journal Transaction* 25: 103-110.

[2] Reed, R. D.; and Narayan, B. C. 1979. Mixing Fluids under Turbulent Flow Conditions. *Chemical Engineering* 86: 131-140.

[3] Brodkey, R. S. edition 1975. *Turbulence in Mixing Operation*, New York: Academic Press.

[4] Rajaratnam, N. 1976. *Turbulent Jets*. Washington: Elsevier Scientific Pub. Co.

[5] Fischer, H. B.; List E. J.; Koh R. C. Y.; Imberger, J.; Brook N. H. 1979. *Mixing in Inland and Coastal Waters,* New York: Academic Press.

[6] Forney, L. J.; and Kwon, T. C. 1979. Efficient Single Jet Mixing in Turbulent Tube Flow. *American Institute of Chemical Engineers Journal Transaction* 25(4): 623-630.

[7] Forney, L. J.; and Lee, H. C. 1982. Optimum Dimensions for Pipeline Mixing at a T-Junction. *American Institute of Chemical Engineers Journal Transaction* 28(6): 980-987.

[8] Forney, L. J. 1986 *Encyclopedia of Fluid Mechanics*. Vol. II, Ch. 25: N. P. Cheremisinoff Houston: Gulf Publishing Co.

[9] Feng, Z.; Wang, X.; and Forney, L. J. 1999. Single Jet Mixing at Arbitrary Angle in Turbulent Tube Flow. *Transaction ASME*: 121: 762.

[10] Maruyama, T.; Mizushina, T.; and Watanabe, F. 1982. Turbulent Mixing of Two Fluid Streams at an Oblique Branch. *International Journal of Chemical Engineering* 22(2): 287.

[11] Gray, J. B. 1986. *Mixing: Theory and Practice*, Ch. 13, Vol. III, J.B. Gray and V. W. Uhl, eds., USA: Academic Press.

[12] Patterson, G. K. 1975. *Turbulence in Mixing Operations.* New York: Academic Press.

[13] Cozewith, C.; Ver Strate, G.; Dalton, T. J.; Frederick, J. W.; and Ponzi, P. R. 1991. Computer Simulation of Tee Mixers for Non-Reactive and Reactive Flows. *Industrial Engineering Chemical Research* 30: 270.

[14] Forney, L. J.; and Monclova, L. A. 1994. Numerical Simulation of Pipeline Tee Mixers: Comparison with Data. *Industrial Mixing Technology: Chemical and Biological Applications.* E. L. Gaden, G. B. Tatterson, R. V. Calabrese, and W. R. Penney, New York: Academic Press. 141-143.

[15] Zughbi, H. D.; Khokhar, Z. H.; and Sharma, R. N., 2002. Numerical and Experimental Investigations of Mixing at side and Opposed-Tees. American Institute of Chemical Engineers 2002 Annual Conf. Indianapolis, USA.

[16] Khokhar, Z. H. 2002. Investigations of Mixing in Pipelines with Side-, Opposed- and Multiple-Tees. M.S. thesis, Dept. of Chemical Engineering, King Fahd University of Petroleum & Minerals.

D: PETROTECH Conference, Bahrain

Zughbi, H. D., **Khokhar, Z. H.**, Ahmed I. and Rakib, M. A., "Optimization of mixing Equipments using CFD", Accepted for PETROTECH Conference, 29th September-1st October 2003, Manama, Bahrain.

OPTIMIZATION OF MIXING EQUIPMENT USING COMPUTATIONAL FLUI DYNAMICS

Habib Daoud Zughbi*, Zahid Hafeez Khokhar, Iqtedar Ahmad

Department of Chemical Engineering, King Fahd University of Petroleum & Minerals, Dhahran, Saudi Arabia.
*Corresponding Author, hdzughbi@kfupm.du.sa

Mohammad Abdur Rakib
Department of Chemical Engineering, King Saud University of Petroleum & Minerals, Riyadh, Saudi Arabia.

ABSTRACT
This paper is concerned with using computational Fluid dynamics (CFD) in optimizing the design of mixers, namely fluid jet agitated tanks and pipelines with tees.
Experimental data of mixing in fluid jet agitated tanks and pipelines are used to validate separate CFD models. These CFD models are then used to carry out parametric runs in order to optimize the design of mixing equipment.
For a fluid jet agitated tank, mixing time is found to be a function of Reynolds number and the angle, position and number of the incoming jets. Flow asymmetry was also studied and found to have a significant effect on mixing.
For mixing in pipelines, the angle of the jet is found to have a significant effect on pipe length required to achieve 95% mixing. This length is also found to be a function of the ratio of the jet to the main pipe velocity.

1. INTRODUCTION
Mixing is a common operation in the oil, chemical and petrochemical industries. In some cases, mixing can play a controlling role and an optimum design is necessary for successful and efficient operations. Mixing is used in blending, dispersing, emulsifying, suspending and enhancing heat and mass transfer. Mixing can be achieved using stirred vessels, static mixers, fluid jet agitation or pipelines with tees. This paper is concerned with optimum design of mixers of the last two types.
Traditionally, design and operations of mixers have been carried out using empirical equations. These equations are highly specific and seldom contribute to the development of theory. More recently, computational fluid dynamics (CFD) has been increasingly used to obtain better understanding of the mixing process and consequently CFD is now being used for more efficient design and operation of mixers.
Mixing using fluid jet agitated tanks is widely used in many industries especially in blending operations. It has many advantages over the traditional stirred tank mixing including less structural changes, more economic operation and easier maintenance.
Clodrey 1978 recommended that jets be injected along the diagonal of tanks (longest dimension). This means, for an aspect ratio (tank diameter/liquid height) of 1, a 45° jet injection angle should be used for best mixing results. As mixing takes place due to the entrainment of the unmixed liquid by the jet at its boundaries, a 45° injection for an aspect ratio of 1 is thought to give the longest jet length and consequently the shortest

mixing time. Many researchers including Lane and Rice 1982 and Okita and Oyama 1983 have used the Coldrey design. Harnby et al. 1997 also recommended this concept in their textbook. Zughbi and Rakib 2003 found that this concept is not necessarily true.

Zughbi and Rakib 2000, 2002 have shown that CFD predictions agree well with the experimental results of Lane and Rice 1982. Mixing in a fluid jet agitated tank was also studied by many researchers including Fox and Gex 1956, Fosset and Prosser 1949 Maruyama et al. 1982, Grenville and Tilton 1996, Perona et al. 1998, Patwardhan 2001, Jayanti 2001, and Zughbi, Khokhar and Rakib 2003 and Ahmad 2003.

Mixing in a fluid jet agitated tank is further optimized by Ahmad 2003, who investigated mixing in a geometry that is more commonly used in the industry. Experimental and numerical investigations of mixing in such a vessel were carried out. The location of the pump suction was chosen using CFD. The time required to achieve 95% mixing in such geometry was found to be a little longer than that in the geometry of Lane and Rice 1982. In this paper, an asymmetric jet is also investigated and its effects on mixing time are reported.

For pipelines with tees, the more common practice in industry is to use 90^o tees. In this paper, this concept is closely investigated and found not to be always justified. The mixing length required to achieve 95% mixing was found to be a strong function of U_j/U_m. The mixing length was reduced as the U_j/U_m was increased.

There have been many papers published dealing with mixing in pipelines. Gray 1986 presented a full review of mixing in pipelines. Cozewith and co-workers 1989, 1991, Forney 1986, Sroka and Forney 1989a, 1989b, Forney and Monclova 1994, Zughbi, Khokhar and Sharma 2002 and Khokhar 2002 also investigated mixing in pipelines with tees.

2. MODEL EQUATIONS

Flow in pipelines and in fluid jet agitated tanks is simulated by solving the differential equations representing mass, momentum and energy conservation. These equations can be written in the general form:

$$\frac{\delta\left(R_i \rho_i \phi_i\right)}{\delta t} + div\left(R_i \rho_i U_i \phi_i - R_i \Gamma_{\phi_i} grad \phi_i \right) = R_i S\phi_i$$

Transient Convection Diffusion Source

Where R_i is the volume fraction of phase i, ϕ_i , is any conserved property of phase i, U_i, is velocity vector of phase i, $\Gamma\phi i$ is the exchange coefficient of ϕ in phase i, $S_{\phi i}$, is the source rate of ϕ_i. Thus, the continuity equation for phase i becomes:

$$div\left(R_i\, \rho_i\, U_i - R_i\, D_i\, grad\, R_i\right) = m_i$$

where D_i , is the diffusivity of phase i, mi , is mass per unit volume entering phase i, and ρ_i is the density of phase i. The conservation of momentum for variable ϕi becomes:

$$div\left(R_i\, \rho_i\, U_i\, \phi_i - R_i\, \mu_{eff}\ grad\, \phi_i \right) = R_i\, S_{\phi_i}$$

where μ_{eff} is the effective viscosity.

The general-purpose three-dimensional computational fluid dynamics package FLUENT is used to solve the governing equations. This allows the investigation of a range of

conditions and geometries quite efficiently once a general model has been established and validated against experimental results.
In the numerical as well as the experimental sections of this study, mixing is quantified by estimating the 95% mixing time or length. This is defined as the time or length needed for the value of the measured quantity anywhere in the mixer to be less than 5% of the step input. This can be expressed as:

$$m = \left| \frac{c - \bar{c}}{\bar{c}} \right| \langle 0.05$$

Where $\bar{c}$ is the equilibrium concentration and c is the concentration at any monitoring point at any time. When the above condition is met at all monitoring points within the tank, it can then be said that concentration at any point within the tank has reached 95% or more of the equilibrium concentration. For this case the initial value of m before the addition of the tracer is considered to be 0. If temperature is the measured variable, the 95% mixing is reached when the temperature anywhere inside the tank is within the range of $((\bar{T} \pm (\bar{T} - 300) * 0.05)$. For mixing in pipelines, a similar criterion is applied in order to find the pipe length required to achieve 95% mixing.

3. THE EXPERIMENTAL APPARATUS

Figure 1a shows the experimental set-up used by Lane and Rice 1982. This geometry has been simulated by Zughbi and Rakib 2002. An experimental apparatus was built to quantify mixing in a fluid jet agitated tank as shown schematically in Figure 1b. Conductivity was used as the measured variable. Two Orion conductivity meters were used to measure the mixing inside the tank. Two variations of this geometry were built. The first one is referred to as a symmetric case where the jet enters towards the center of the tank. The second variation is referred to as the asymmetric case and the jet enters not in a plane passing through the tank center but at an angle to that plane.
The pump-around was simulated by adding a momentum source to the fluid in the pipe near the outlet. This is similar to a pump. The velocity at the jet inlet is read from the model. The jet Reynolds number, R_{ej}, is then calculated as $R_{ej}=\rho D_j V_j/\mu$ where D_j is the diameter of the jet and V_j is the velocity at the jet inlet.
For simulation studies of mixing in jet agitated tanks, the temperature was used as an alternative for a mass less tracer that travels with the local fluid velocity. Accordingly, density and viscosity were considered not to vary with temperature in the range considered. Thus, the flow field was not affected by the change in temperature. Another experimental apparatus was built to quantify mixing in a pipeline with a side-tee. A pipeline with a side-tee is schematically shown in Figure 1c.
Temperature is used as the measured variable. Hot water was injected from the side tee and was mixed with the same liquid flowing in the main pipe at a lower temperature. Eight thermocouples are inserted at various positions of the main pipe in order to measure the temperature of the flow. These thermocouples are connected via an OMEGA data-logging card to a PC. Flow through the side-tee passes through a heater that can raise the temperature of the side stream significantly above that of the main stream. In the simulation studies of mixing in pipelines, the dependence of the physical properties of water on temperature was taken into consideration.

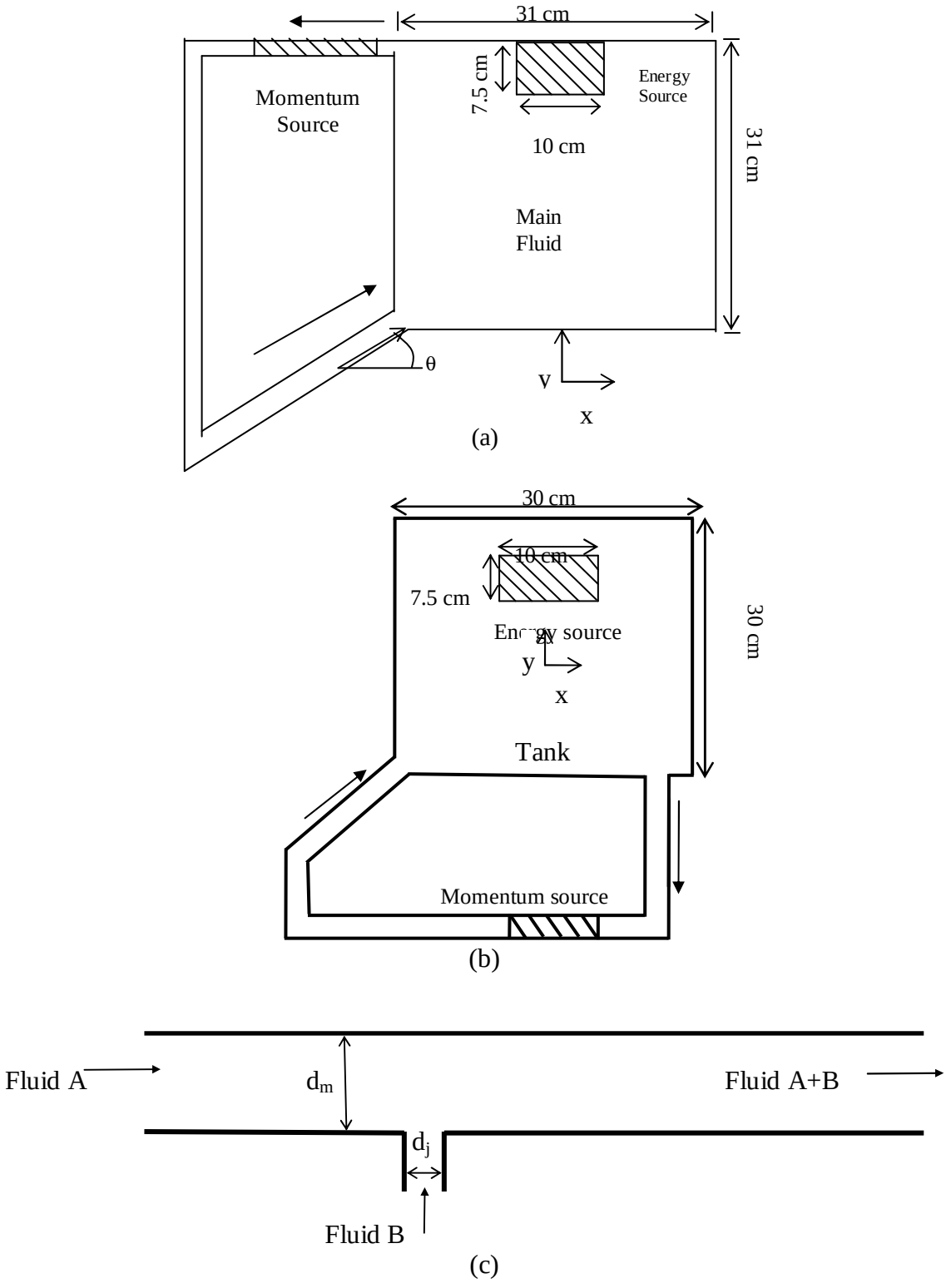

Figure 1: A schematics diagram of (a) A fluid jet agitated tank with a pump-around as that used by Lane and Rice, (b) A fluid jet agitated tank as that used by Zughbi and Ahmad, (c) A pipeline with side-tee used by Zughbi and Khokhar

4. RESULTS

The CFD model of mixing in a fluid jet agitated tank for the geometry shown in Figure 1a is first validated against the experimental data of Lane and Rice 1982. The comparison is shown in Figure 2a and a good agreement was observed over a wide range of Reynolds numbers. The results show that the numerical model is consistently over-predicting by a few percent. The numerical and experimental results were fitted well by the correlation of Grenville and Tilton 1996 while the correlation of Fosset and Prosser 1949 predicted longer mixing times over the whole turbulent range of Reynolds number considered.Figure 2b shows a comparison of simulation results of the geometry shown in Figure 1b and the corresponding experimental results. The agreement is also excellent. It should be noted that there is a certain degree of data scatter in experimental mixing results. This is similar to that shown by Lane and Rice 1982, Perona et al. 1996, Cozewith et al. 1989, 1991.

Figure 2c shows a comparison of numerical and experimental results of temperature along a centerline for mixing in a pipeline with a side-tee.

The agreement is excellent following the refinement of the CFD model including mesh size and local refinement (grid adaption), dependence of physical properties on temperature and the turbulence model used.

It was found that the mixing time and mixing length depend on: (a) the angle of jet injection, i.e. the angle at which the jet enters the tank or the main pipe, (b) Reynolds number or the ratio of the jet velocity to the main stream velocity and (c) the number of jets.

4.1 Effects of the Jet Injection Angle

The concept of injecting the jet along the diagonal of a tank put forward by Coldrey 1978 was found not to be always true. The flow patterns were found to have a significant effect on determining the mixing time or length. For the fluid jet agitated tank, the jet angle had a significant effect as shown in Figure 3a. It was found that an angle of 30° gives the shortest mixing time and not 45° as previously thought by Coldrey 1978, Okita and Oyama 1983 and Harnby et al. 1997. Figure 3b shows the effects of the angle of injection on mixing time for the bottom pump-around. An angle of about 25° gave the best mixing time. Figure 3c shows how the pipe length required to achieve 95% mixing changes with the angle of injection. The commonly used 90° did not give the best results. The optimum angle was found to be 45°.

Experimental and numerical investigations of mixing in fluid jet agitated tanks and in pipelines with side- and opposed-tees have shown that the flow patterns play a major role in determining the time and/or mixing length required to achieve 95% mixing. The generally used angle of 90^o for side or opposed tees and 45^o for liquid jet injections are not the optimum angles. For jet agitated tanks considered in this study a jet angle of 25^o-30^o was found to be the optimum angle for an aspect ratio of 1. For mixing in pipeline with tees, a tee angle of 45^o was found to the optimum.

4.2 Effects of Asymmetry

The effects of asymmetry on mixing time in a fluid jet agitated tank have been investigated. Instead of a jet injected towards the center of the tank, a jet making a side angle with a plane passing through the center of the tank and the outlet is used. This asymmetry is found to reduce the mixing time. Results are shown in Figure 4.

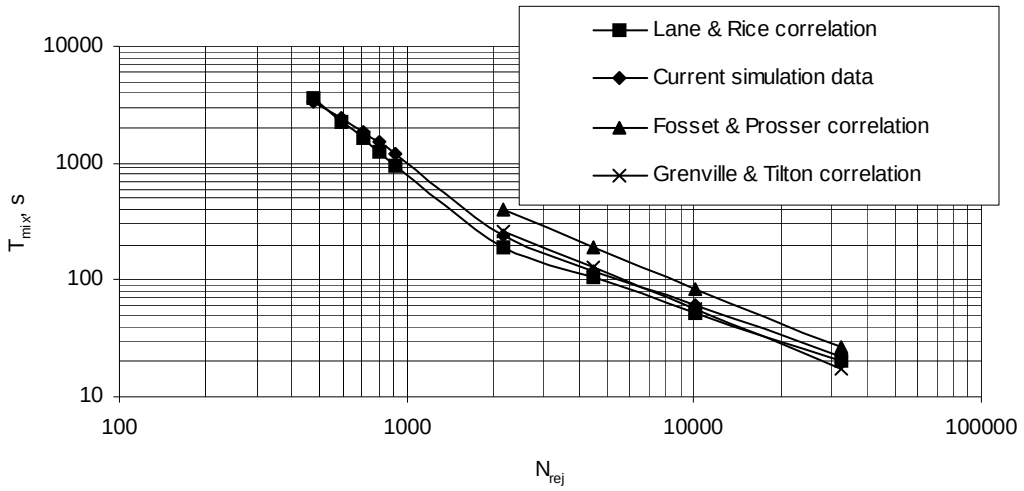

(a)

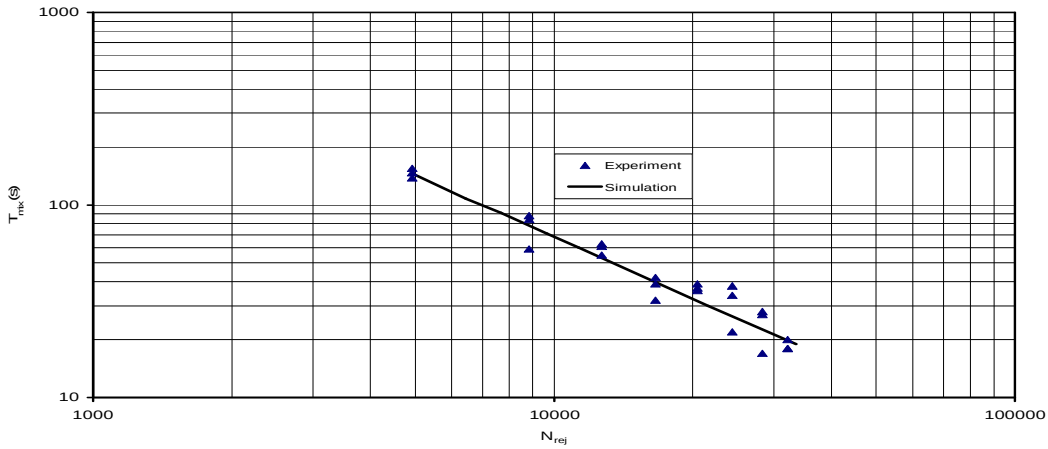

(b)

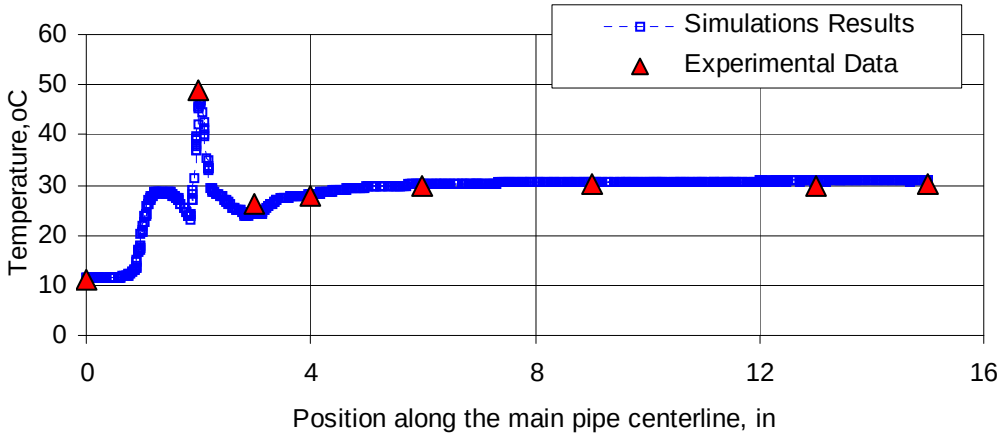

(c)

Figure 2: Comparison of numerical and experimental results for (a) Lane and Rice experimental and current numerical results, (b) current experimental and numerical results for geometry shown in Figure 1b and (c) current numerical and experimental results for geometry shown in Figure 1c.

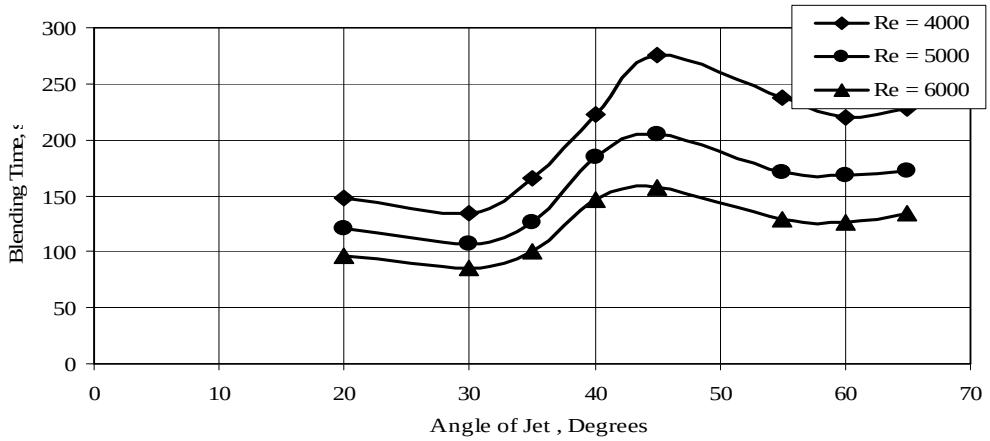

(a)

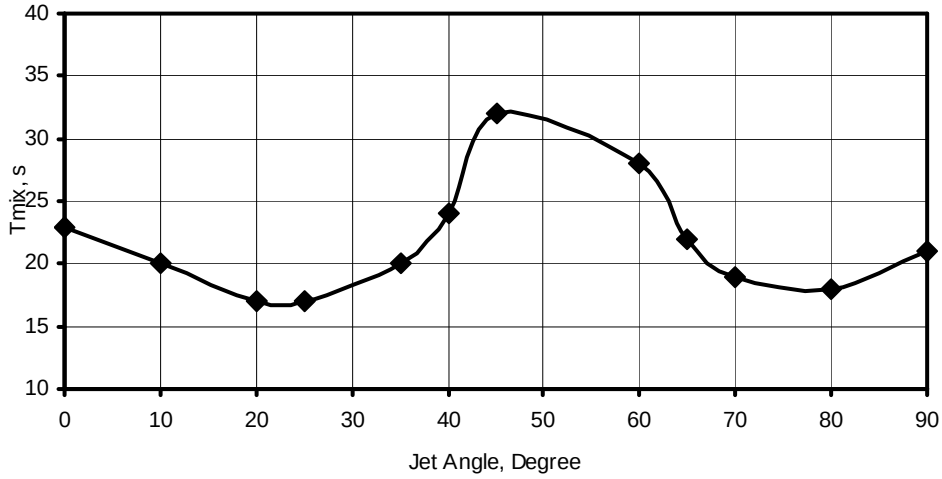

(b)

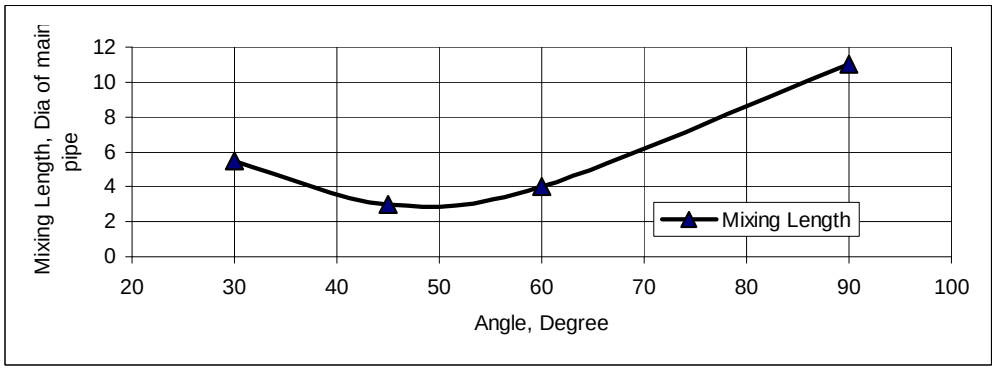

(c)

Figure 3: The effects of angle of injection on (a) mixing time in a side pump-around geometry, (b) mixing time in a bottom pump around geometry for jet Reynolds number of 34000 and (c) mixing length in a pipe line with a side-tee.

These results are for a case where an asymmetric jet is injected at a side angle of 15^o and an up angle of 45^o. A side angle is defined as the angle that the jet makes with a normal plane passing through the tank center and the outlet. An up angle is defined as the angle that the jet makes with the horizontal bottom plane of the tank. This asymmetric jet is found to reduce the mixing time by about 30% compared to the symmetric jet having same up angle but a side angle of 0^o.

4.1 Effects of Reynolds Number and the Ratio of Velocities

The 95% mixing time in a fluid jet agitated tank is a function of the jet Reynolds number as shown in Figure 2a and 2b. As the jet Reynolds number increases, the mixing time decreases, with the dependence being steeper in the laminar region as shown in Figure 2a. Results showed that the pipe length required to achieve 95% mixing depends on the ratio of U_j/U_m as shown in Figure 5. Results also showed that for high values of U_j/U_m, the jet impinges on the opposite wall of the pipe resulting in regions of low velocity which may lead to some corrosion/erosion related problems. The injection at an angle other than 90^o not only decreases mixing length but it helps avoid problems due to the jet impingement on the opposite pipe wall.

4.2 Effects of the Number of Jets

The number of jets affect the mixing time in jet agitated mixing tanks and the pipe length required to achieve 95% mixing in pipelines with tees. However, adding a second jet resulted in achieving an improvement of about 30 to 60% and not 100% as one would have expected.

5 CONCLUSIONS

Computational fluid dynamics models for mixing in a fluid jet agitated tank and in pipeline with side-tees have been constructed and validated against own and published experimental data. Results showed that the 95% mixing time in a fluid jet agitated tank depends on the angle of the jet. An up angle of 30° is found to be the optimum for a side pump-around. For a bottom pump around the optimum angle is found to be 25°. The jet asymmetry was also found to influence the mixing time. A jet side angle of 15° was found to give shorter mixing time. In summary, CFD is a powerful tool to design jet mixers and the shortest mixing time is obtained for a jet up angle of 45° and a side-angle of 15°.

For mixing in pipelines with tees, the industrially commonly used 90° jet angle should be avoided as it results in poor mixing and hard impingement on the opposite wall. This impingement may cause erosion. It was found that the shortest mixing length is obtained if an angle of 45^o is used.

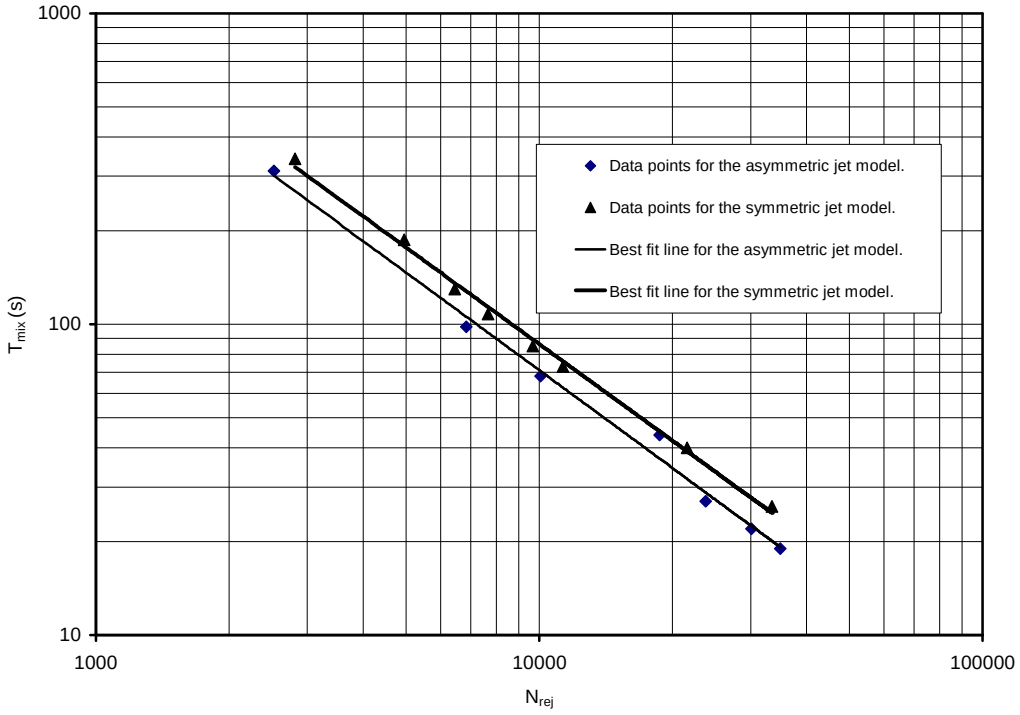

Figure 4: Effects of jet asymmetry on mixing time in a fluid jet agitated tank.

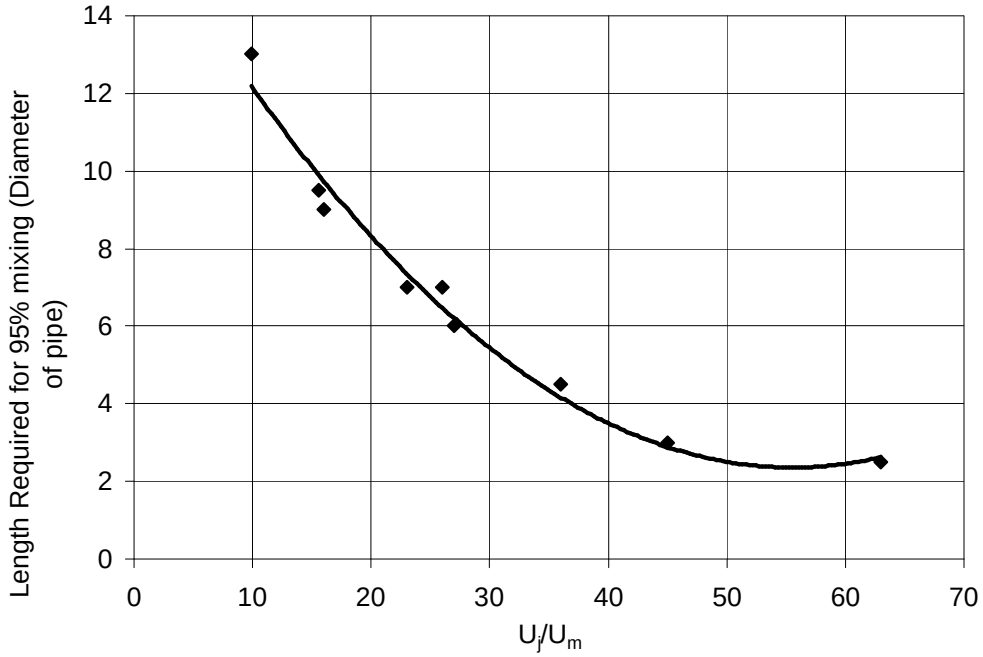

Figure 5: Effects of the jet to main velocity ratio on pipe length required to achieve 95% mixing in a pipeline with a side-tee.

Acknowledgement

The authors are grateful for the support of King Fahd University of Petroleum & Minerals during the course of this work and the preparation of this paper. Parts of this work have been funded by KFUPM projects SABIC/2000-09 and CHE/MIX/253.

References

Ahmad, I. 2003. Effects of Geometry and Flow Asymmetry on Mixing in Fluid Jet Agitated Tanks M. Sc. Thesis. King Fahd University of Petroleum & Minerals.

Coldrey, P. W. 1978. Jet Mixing. Paper to Industrial Chemical Engineering Course. University of Bradford.

Cozewith, C. and M. Busko 1989. Design Co-relations for Mixing Tees. Industrial and Engineering Chemistry Research. 28, pp. 1521-1530.

Cozewith, C, G. Ver Strate, T. J. Dalton, J. W. Frederick and P.R Ponzi 1991. Computer Simulation of Tee Mixers for Non-reactive and reactive Flows. Industrial and Engineering Chemistry Research. 30 pp. 270-275.

Fossett, H. and L. E. Prosser 1949. The application of free jets to the mixing of fluids in bulk. Journal of Institute of Mechanical Engineers, 160, 224-232.

Forney, L. J., 1986, Encyclopedia of Fluid Mechanics, Vol. II, Ch. 25, N. P. Cheremisinoff, ed., Gulf Publishing Co., Houston USA.

Forney, L. J. and L. A. Monclova 1994. Numerical Simulation of Pipeline Tee Mixers: Comparison with Data, Industrial Mixing Technology: Chemical and Biological Applications, Gaden, E. L., G. B Tatterson, R. V Calabrese, and W. R Penney, eds. pp. 141-143.

Fox, E. A., and V. E. Gex 1956. Single phase blending of liquids, American Institute of Chemical Engineering Journal 2, 539-544.

Gray, J. B., 1986. Mixing: Theory and Practice, Ch. 13, Vol. III, J.B. Gray and V. W. Uhl, eds., Academic Press USA.

Grenville, R. K. and J. N. Tilton 1996. A new theory improves the correlation of blend time data from turbulent jet mixed vessels. Transactions of Industrial Chemical Engineering. 74A 390-396.

Harnby, N., M. F. Edwards and A. W. Nienow 1997. Mixing in the Process Industries 2nd ed. Butterowrth-Heinman.

Jayanti, S. 2001. Hydrodynamics of Jet Mixing in Vessels. Chemical Engineering Science 56, 193-210.

Khokhar, Z. H., H. D. Zughbi and R. N. Sharma 2002. Mixing in Pipeline with Side-Tees. 6th Saudi Engineering Conference 17-19th December.

Khokhar, Z. H. 2002. Investigations of Mixing in Pipelines with Side-, Opposed and Multiple-Tees M. Sc. Thesis. King Fahd University of Petroleum & Minerals.

Lane, A. G. C. and P. Rice 1982. An investigation of liquid jet mixing employing an inclined side-entry jet. Transactions of Industrial Chemical Engineering. 60, 171-176.

Maruyama, T., Y. Ban and T. Mizushina 1982. Jet mixing of fluids in tanks. Journal of Chemical Engineering of Japan. 15, 342-348.

Okita, N. and Y. Oyama 1983. Mixing characteristics in jet mixing. Japan Chemical Engineering 31 (9), 92-101.

Patwardhan, A. W. 2002. CFD modeling of jet mixed tanks. Chemical Engineering Science 57, 1307-1318.

Perona, J. J., T. D. Hylton, E. L. Youngblood and R. L. Cummins 1998. Jet Mixing of Liquids in Long Horizontal Cylindrical Tanks. Industrial Engineering and Chemical Research. 38, 1478-1482.

Rakib, M.A. 2000. Numerical investigations of mixing in fluid jet agitated tank, M. Sc. Thesis, King Fahd University of Petroleum & Minerals.

Sroka, L. M. and L. J. Forney 1989. Fluid Mixing with a Pipeline Tee: Theory and experiment. Journal of the American Institute of Chemical Engineers. 35-3 pp. 212-218.

Sroka, L. M. and L. J. Forney 1989. Fluid Mixing in a 90° Pipeline Elbow. Industrial and Engineering Chemistry Research, 28(6) pp. 850-856.

Zughbi, H. D. and M. A. Rakib, 2000. Investigation of Mixing in a Fluid Jet Agitated Tank. AIChE Annual Meeting. Los Angeles, USA.

Zughbi, H. D. and M. A. Rakib 2002. M. A. Simulation of Mixing in a Fluid Jet Agitated Tank, Chemical Engineering Communications, 189 (7) pp. 225-234.

Zughbi, H. D., Z. H. Khokhar and R. N. Sharma 2002. Numerical and experimental Investigations of Mixing in Pipelines with side- and opposed-tees, AIChE Annual Meeting, Indianapolis, USA Nov. 3-7.

Zughbi, H. D., Z. H. Khokhar and R. N. Sharma 2003. Numerical and Experimental Investigations of Mixing in Pipelines with side- and opposed-tees. Submitted to Industrial and Engineering Chemistry Research.

Zughbi, H. D., Z. H. Khokhar and M. A. Rakib 2003. Numerical Investigations of Mixing in a Large Horizontal Fluid Jet Agitated Tank. Submitted to Industrial and Engineering Chemistry Research.

VITA

Name: Zahid Hafeez Khokhar
Date & Place of Birth: January 27, 1974 & Sargodha, Pakistan
Religion: ISLAM
Permanent Address: P-2420, St. 19, Farooqabad, Faisalabad-38060, PAKISTAN
Nationality: Pakistani

Education Qualification:

M.S. Chemical Engineering, (Nov 2002)
King Fahd University of Petroleum & Minerals, Dhahran, Saudi Arabia
Post Graduate Computer Orientation Course, (Dec 1998)
Computer Training Centre, UGC-Campus, H-8, Islamabad, Pakistan
B.Sc. Chemical Engineering, (Jan 1998)
University of Engineering & Technology, GT Road, Lahore, Pakistan

Professional Experience:

Lecturer (May 1998-June 1998)
University of Engineering & Technology, Peshawar, Pakistan
Post Graduate Fellow (July1998-Dec 1998)
Computer Training Centre, UGC-Campus, H-8, Islamabad, Pakistan
Assistant Engineer (Jan 1999-August 2000)
CTC, A Government Research Organization, Islamabad, Pakistan
Research Assistant (Sep 2000-date)
Chemical Engineering Department, KFUPM, Dhahran, Saudi Arabia